



Terms and Conditions of Use of Digitised Theses from Trinity College Library Dublin

Copyright statement

All material supplied by Trinity College Library is protected by copyright (under the Copyright and Related Rights Act, 2000 as amended) and other relevant Intellectual Property Rights. By accessing and using a Digitised Thesis from Trinity College Library you acknowledge that all Intellectual Property Rights in any Works supplied are the sole and exclusive property of the copyright and/or other IPR holder. Specific copyright holders may not be explicitly identified. Use of materials from other sources within a thesis should not be construed as a claim over them.

A non-exclusive, non-transferable licence is hereby granted to those using or reproducing, in whole or in part, the material for valid purposes, providing the copyright owners are acknowledged using the normal conventions. Where specific permission to use material is required, this is identified and such permission must be sought from the copyright holder or agency cited.

Liability statement

By using a Digitised Thesis, I accept that Trinity College Dublin bears no legal responsibility for the accuracy, legality or comprehensiveness of materials contained within the thesis, and that Trinity College Dublin accepts no liability for indirect, consequential, or incidental, damages or losses arising from use of the thesis for whatever reason. Information located in a thesis may be subject to specific use constraints, details of which may not be explicitly described. It is the responsibility of potential and actual users to be aware of such constraints and to abide by them. By making use of material from a digitised thesis, you accept these copyright and disclaimer provisions. Where it is brought to the attention of Trinity College Library that there may be a breach of copyright or other restraint, it is the policy to withdraw or take down access to a thesis while the issue is being resolved.

Access Agreement

By using a Digitised Thesis from Trinity College Library you are bound by the following Terms & Conditions. Please read them carefully.

I have read and I understand the following statement: All material supplied via a Digitised Thesis from Trinity College Library is protected by copyright and other intellectual property rights, and duplication or sale of all or part of any of a thesis is not permitted, except that material may be duplicated by you for your research use or for educational purposes in electronic or print form providing the copyright owners are acknowledged using the normal conventions. You must obtain permission for any other use. Electronic or print copies may not be offered, whether for sale or otherwise to anyone. This copy has been supplied on the understanding that it is copyright material and that no quotation from the thesis may be published without proper acknowledgement.

*A characterisation of cyclooxygenase activity in
synaptic transmission and plasticity in the
Hippocampus*



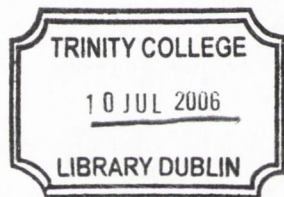
by

Thelma R. Cowley

A dissertation submitted for the degree of Doctor of Philosophy of the University of
Dublin, Trinity College, Dublin 2, Ireland.

This research was conducted in the Department of Psychology, Trinity College Institute
of Neuroscience.

October 2005

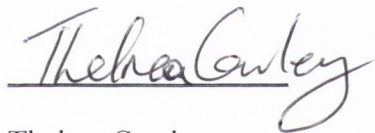


THESIS
7971

Declaration

I declare that this work has not been submitted previously as an exercise for a degree at this or any other university and that it is entirely my own work. The Trinity College Library may lend or copy this thesis without restriction.

Signed

A handwritten signature in cursive script that reads "Thelma Cowley". The signature is written in black ink and is positioned above a horizontal line.

Thelma Cowley

Acknowledgements

Since the conception of the idea behind this thesis, Shane O'Mara has been a constant pillar of support, inspiration and guidance. I would like to thank him sincerely for the opportunity to do this research and for making it such an enjoyable and life-changing experience.

Without the great friends I made during the past few years, and their ability to laugh even at the most stressful times, when everything seemed to be going wrong, my experience of research would not have been so enjoyable and satisfying. The biggest of thanks go to my fellow groupies Sinéad Mullally, Bríana Fahey, Maeve Mangaoang, Oliviero Gobbo, Richard Roche, Jorge Brotons and Sally Barlow. I will always treasure our time together.

Also, I would like to thank the following people for their technical expertise and time: Sean Commins, Frank Maher, Aileen Lynch, Darren Martin, Amy Hennigan and Charlotte Callaghan.

Ardent gratitude is owed to my parents, Richard and Colette, for the constant love and support they gave me throughout my education. I owe everything I have achieved to them. Thank you to the rest of my family – Richie, Aisling, Shane, Alan, Anne & Paul – who were always there with encouraging words and an ear to bend.

Keeping me on an even keel, and supporting me throughout the ups and downs was not always easy and so I am eternally indebted to my darling Rod. Thank you.

Finally, to old friends who even in my continued absence I know will always be there.

Summary

We used *in vivo* electrophysiological techniques to investigate the role played by cyclooxygenase (COX) enzymatic activity in synaptic transmission and plasticity. The use of selective pharmacological antagonists for the COX-1 and COX-2 isoforms enabled us to differentiate the functions of these two very similar enzymes in the dentate gyrus of the hippocampal formation, using a model of memory storage – long-term potentiation (LTP). This is a process whereby repeated firing of neurons by tetanic stimulation results in an increase in synaptic efficacy and a change in synaptic weights. It is this change in synaptic weight that is postulated to underlie memory storage. We have shown that exogenous replacement of a metabolite of COX activity, PGE₂, directly into the hippocampus was sufficient to reverse the effects of the antagonism.

We employed immunological techniques – ELISA and western blot analysis – to investigate the effects of both the antagonists and the replacement strategies on cellular protein changes. We looked at the effects of LTP induction on brain derived neurotrophic factor (BDNF) a protein implicated in both the storage of long-term memory and the induction and endurance of LTP, and how COX inhibition affected it. Finally, we examined the changes as a result of exogenous replacement of PGE₂ on intracellular phosphorylation cascades (ERK-phosphorylation) and the signal transduced to the nucleus (c-Fos protein expression), known to be associated with LTP induction and maintenance.

Abbreviations

γ -HLA γ -homolinolenic acid
15-PGDH 15-hydroxyprostaglandin dehydrogenase

A

AA Arachidonic acid
AD Alzheimer’s disease
2-AG Arachidonoyl glycerol
AMPA Alpha-amino-3-hydroxy-5-methyl-4-isoxazolepropionic acid
ANOVA Analysis of variance
AP-1 Activating protein-1
ATP Adenosine triphosphate
BDNF Brain derived neurotrophic factor

B

bpAP back propagating action potential
BSA Bovine serum albumin
BSCI Broad spectrum COX inhibition
CA1-4 Cornus ammon regions 1-4 (subregions of the hippocampus)

C

Ca²⁺ Calcium ion
CaBP Calcium binding protein
CaMKII Calcium-dependent calmodulin kinase II
cAMP Cyclic adenosine monophosphate
cAMP cyclic-andeylate mono-phosphate
CBI Cannibanoid receptor 1
COX Cyclooxygenase
 -1 -1
 -2 -2
 -3 -3
cPLA₂ Cytosolic phosphalipase A₂
CRE c-AMP response element
CREB c-AMP response element binding protein
CXB Celecoxib (Celebrex®)
DAG Diacylglycerol

D

DG Dentate gyrus
DGK Diacylglycerol –kinase
DGLA Dihomo- γ -linolenic acid
DMSO Dimethyl sulfoxide
DNA Dioxyribonucleic acid
DRG Dorsal root ganglion neurons

DSI Depolarisation-induced suppression of inhibition

E

EC Entorhinal cortex
ECL Electrochemiluminescence
ECS Electroconvulsive shock
ELISA Enzyme linked immunosorbent assay
EP Prostaglandin receptors of the E-series
EPA Edicosapentanoic acid
ER Endoplasmic reticulum
ERK Extracellular response kinase

F

fEPSP Field excitatory postsynaptic potential

G

GABA Gamma-amino butyric acid
GDP Guanine diphosphate
GIP Guanine triphosphate
GIT Gastrointestinal tract
GPCR G-protein coupled receptor
GR Glucocorticoid receptor
GST Glutathione S-transferase

H

HFS High frequency stimulation

I

I κ B Inhibitory protein κ B
i.p. Intraperitoneal
I/O Input/output
IC50 Concentration required to inhibit 50% of receptors
IEG Immediate early gene
IP₃ Inositol triphosphate
IPSP Inhibitory postsynaptic potential
ir Immunoreactivity
ISI Interstimulus interval

K

K⁺ Potassium ion

L

LFS Low frequency stimulation
LOX Lipoxygenase
LPP Lateral perforant path

LPS	Lipopolysaccharide
LTP	Long term potentiation
MAPK	Mitogen activated protein kinase

M

mEPSP	Miniature excitatory post synaptic potential
Mg ²⁺	Magnesium ions
MPGES2	Microsomal prostaglandin E synthase-2
MPP	Medial perforant path
MRI	Magnetic resonance imaging
mRNA	messenger ribo nucleic acid
MTL	Medial temporal lobe
MTT	Multiple-trace theory
Na ⁺	Sodium ion

N

NaCl	Sodium chloride
NDGA	Nordihydroguaiaretic acid
NFκB	Nuclear factor κB
NMDA	N-methyl-D-aspartate
NMJ	Neuromuscular junction
NO	Nitric oxide
NSAID	Non-steroidal anti-inflammatory drug
NT	Neurotransmitter
NT-3	Neurotrophin-3

P

PA	Phosphatidic acid
pAb	polyclonal antibody
PAF	Platelet activating factor
PG	Prostaglandin
D ₂	D ₂
E ₂	E ₂
F ₂	F ₂
G ₂	G ₂
H ₂	H ₂
I ₂	I ₂
PG	Prostaglandin
DS	D Synthase
ES	E Synthase
FS	F Synthase
GS	G Synthase
HS	H Synthase
IS	I Synthase
PI3K	Phosphatidylinositol 3-kinase
PIP ₂	Phosphatidylinositol bisphosphate
PLA ₂	Phospholipase A ₂
PLC	Phospholipase C

PLD	Phospholipase D
PPD	Paired-pulse depression
PPI	Paired pulse index
PPR	Paired pulse ratio
PSA	Pop-spike amplitude
PTP	Post tetanic potentiation
PUFA	Polyunsaturated fatty acid
PV	Parvalbumin

R

RIA	Radioimmunoassay
Rmax	Maximum response

S

SDS	Sodium dodecyl sulphate
SEM	Standard error of the mean
SIE	c-Sis inducible element
St. Dev.	Standard deviation
STP	Short-term potentiation

T

$t_{1/2}$	half-life
TBS	Tris-buffered saline
TrkB	Tyrosine kinase receptor B
TTX	Tetrodotoxin
TXA ₂	Thromboxane A ₂
TXS	Thromboxane synthase

V

V	Voltage
VGCC	Voltage gated calcium channels

Table of Contents

Table of Contents.....	1
List of figures and Graphs	4
Chapter 1 Literature review.....	9
1.1 Introduction.....	11
1.1.1 The hippocampus.....	11
1.1.2 BDNF and synaptic plasticity	26
1.1.3 Synaptic lipid signalling	29
1.1.4 ERK and intracellular signalling.....	45
1.1.5 Transcription factors	47
1.1.6 Objectives of this thesis	49
Chapter 2 Cyclooxygenase: baseline synaptic transmission and short-term plasticity	50
2.1 Introduction.....	52
2.2 Materials & methods.....	56
2.2.1 Animals.....	56
2.2.2 Materials	56
2.2.3 Pharmacological treatment schedules.....	56
2.2.4 Surgery.....	57
2.2.5 Input/output curves	58
2.2.6 Paired-pulse protocol	58
2.2.7 Bradford assay	59
2.2.8 BDNF ELISA	59
2.2.9 Analysis and statistics.....	60
2.3 Results.....	62
2.3.1 Input/output curves	62
2.3.2 Paired-pulse ratio	69
2.3.3 BDNF concentration.....	71
2.4 Discussion.....	74
Chapter 3 The selective inhibition of COX-2 but not COX-1 blocks the induction of long-term potentiation.....	78
3.1 Introduction.....	80
3.2 Materials & methods.....	82

3.2.1	Materials	82
3.2.2	Animals.....	82
3.2.3	Pharmacological treatment schedules	82
3.2.4	Surgery.....	83
3.2.5	Long-term potentiation protocol.....	83
3.2.6	Bradford assay	83
3.2.7	BDNF ELISA	83
3.2.8	Corticosterone measurement.....	83
3.2.9	Statistics.....	84
3.3	Results.....	85
3.3.1	Selective inhibition of the COXs and the effects on LTP & BDNF.....	85
3.3.2	COX-2 inhibition and baseline synaptic transmission at constant current ..	94
3.3.3	The effects of COX-2 inhibition on the maintenance of LTP and BDNF concentration in DG.....	96
3.4	Discussion.....	101
3.4.1	Isoform specificity and the block of LTP	101
3.4.2	The maintenance of LTP is not affected by COX-2 inhibition, although the concentration of BDNF is	104
Chapter 4	Exogenous PGE ₂ alleviates the block of LTP	106
4.1	Introduction.....	108
4.1.1	PGE ₂ and central effects	108
4.1.2	Intracellular signalling and LTP	111
4.2	Materials & methods.....	114
4.2.1	Materials	114
4.2.2	Surgery.....	114
4.2.3	Pharmacological treatment schedules.....	115
4.2.4	Stimulation and data acquisition.....	116
4.2.5	Western blotting.....	116
4.2.6	Statistics.....	117
4.3	Results.....	118
4.3.1	Input/output curves	118
4.3.2	Paired-pulse ratio	122
4.3.3	Occlusion of the COX-2-dependent block of LTP by intrahippocampal injection of PGE ₂	124

4.4	Discussion.....	140
4.4.1	Baseline synaptic transmission, PPR and PGE ₂	140
4.4.2	Occlusion of the block of LTP by intrahippocampal injection of PGE ₂ ...	142
Chapter 5	Summary & conclusions.....	145
5.1	Introduction.....	147
5.2	Summary of results.....	147
5.2.1	Chapter II: Baseline synaptic transmission and short-term plasticity.....	147
5.2.2	Chapter III: Cyclooxygenase and synaptic plasticity.....	148
5.2.3	Chapter IV: Exogenous PGE ₂ alleviates the block of LTP.....	149
5.3	Discussion & conclusions.....	151
5.3.1	COX-2 inhibition and LTP induction: effects on BDNF.....	151
5.3.2	COX-2 inhibition and exogenous PGE ₂	152
5.3.3	COX, PGE ₂ & memory.....	154
5.3.4	COX and neuroinflammation.....	155
References.....		157
Appendix 1.....		181
Appendix 2.....		183

List of figures and Graphs

Figure 1.1 A schematic diagram of the medial temporal lobe system showing its basic circuits. DG, dentate gyrus; S, subiculum. Taken from {Squire, 2004 #4}.	13
Figure 1.2 The upper left drawing shows a transparent rat brain with the position of the right (grey) and left (white) hippocampi shown and the right drawing show the appearance of the cross section of the left hippocampus. The lower diagram shows a transverse slice of the hippocampus and clear divisions of the hippocampal formation substructures. Slices of this orientation preserve much of the essential circuitry of the hippocampus.	15
Figure 1.3 Taxonomy of memory systems showing the brain structures and connections thought to be important (taken from {Milner, 1998 #1}).	17
Figure 1.4 Increased Ca^{2+} entry as a result of NMDAR activation is not sufficient to maintain the expression of LTP. CaMKII phosphorylation results in the AMPAR conductance, subunit composition and increased expression at silent synapses (see text for details). Adjusted from {Lynch, 2004 #295}	23
Figure 1.5 Overview of the experimental strategies used to investigate the role of BDNF-TrkB signalling in synaptic plasticity, in vitro and in vivo.	27
Figure 1.6a) Generic structure of phospholipids. Note the central glycerol molecule around which are attached two asymmetric fatty acid groups and a phosphate group. The filled in oval represents a small hydrophilic molecule such as ethanolamine, choline, serine or the less common inositol. b) The structure of phosphatidylinositol bisphosphate (PIP_2). Note the brackets indicating the potential signalling moieties after cleavage by phospholipase.	30
Figure 1.7 Representative autoradiographs showing COX-2 mRNA hybridization in animals sacrificed after A) saline injection, and B) 0.5 h after systemic LPS administration. A) Clearly shows that COX-2 mRNA is expressed at basal level in the hippocampal formation and B) shows its rapid induction in response to an inflammatory challenge. {Quan, 1998 #75}	34
Figure 1.8 The arachidonic acid cascade showing the classic prostanoid structure of the cyclopentane ring and the two side-chains; note the presence of two double bonds on the side-chains of all of these prostanoid originating due to their formation from arachidonic acid.	36
Figure 1.9 The arachidonic acid cascade: arachidonic acid metabolites are called eicosanoids (chequered boxes). The thick arrows highlight the cyclooxygenase pathway and resultant prostanoids. Dotted lines represent inhibition. Adapted from Sales & Jabbour 2003 {Sales, 2003 #36}	41
Figure 1.10 Activation of the MAP-kinase cascade in response to NMDA and growth factor receptor activation; taken from {Platenik, 2000 #4}	46

Figure 1.11 Link between NMDA receptor, MAP-kinase cascade and <i>c-Fos</i> transcription {Kovacs, 1998 #1}.....	48
Figure 2.1 Chemical structures of Sc560 and celecoxib. Note the overall the structures are very similar except for the presence of a bulkier sulphonamide group (circled) on the celecoxib molecule that causes steric hindrance and prevents binding to the COX-1 isoform {Smith, 1998 #239}.....	54
Figure 2.2 The upper diagram shows a representation of the hippocampal trisynaptic loop and the regions where the stimulating and recording electrodes were aimed. The lower diagram depicts the set up used to stimulate record and amplify evoked responses in the anaesthetised rat.	57
Figure 2.3 A typical field EPSP from stimulation of the medial perforant path recording in the dentate gyrus. The grey lines show how measurement of fEPSP slope, population spike amplitude (PSA) and amplitude of the fEPSP were made. All future analyses are based on these measurements.	58
Figure 2.4 Input/output curves for the slope of fEPSP at each stimulus intensity applied: A) within the range 0-5000 μ A, B) expanding the early part of the graph to show the range 0-1000 μ A in more detail (CTRL v Sc560 * $p < 0.05$, ** $p < 0.01$).	64
Figure 2.5 Population spike amplitude for current intensities ranging from A) 0-5000 μ A and B) 0-1000 μ A, for the three treatment groups vehicle, celecoxib and Sc560: # $p < 0.05$ Sc560 v CTRL, * $p < 0.05$ CXB v CTRL.	66
Figure 2.6 E-S curve showing the pattern of cell firing relative to cell depolarisation. The E-S curve for the control animals is shifted to the left relative to either COX-1 or COX-2 inhibitor treated animals implying that less depolarisation is required for the cell to fire i.e. they may be more excitable relative to the COX-1 and COX-2 inhibited animals.	68
Figure 2.7 The paired-pulse ratio: A) representative fEPSPs for control and celecoxib treated rats for 10, 100 and 1000ms ISIs spanning all three phases of depression. B) Depicts the ratio of the slope of fEPSP2/fEPSP1 at various inter-stimulus intervals (ISI) within the range 10-1000ms; ratios < 1 imply depression and > 1 imply facilitation. Pre-treatment with celecoxib diminishes the degree of depression seen in the controls at 10ms ISI [evident in both A) and B)], but not at any other time latency.	70
Figure 2.8 Input/output experiment: the percentage of BDNF relative to unstimulated control tissue in the dentate gyri \pm SEM. There are no significant differences between any of the conditions demonstrating that neither the administration of celecoxib nor Sc560, nor implanting electrodes and at 0.05Hz stimulating had any effect on BDNF concentration.....	72
Figure 2.9 Paired-pulse experiment: BDNF concentration after paired-pulse stimulation. Although there was no individual effect of drug or stimulation on BDNF concentration in the dentate gyrus, there is a significant interaction of celecoxib treatment and stimulation ($p < 0.05$).....	73

Figure 3.1 Effect of selective COX-1 and COX-2 inhibition on long-term potentiation. Selective COX-2 inhibition was obtained using celecoxib (CXB) and COX-1 with Sc560.	88
Figure 3.2 Representative non-averaged recordings from individual celecoxib and vehicle treated rats. Results are expressed as the percent change of the fEPSP slope relative to baseline for all stimuli. Note the impairment of a post-tetanic potentiation in the celecoxib (35mg/kg) treated animal.	89
Figure 3.3 The block of LTP depends on the dose of celecoxib given to the rats. Either CXB low dose (28mg/kg) or CXB high dose (35mg/kg) was administered 30mins prior to anaesthesia.	90
Figure 3.4 Percentage of animals with $\geq 20\%$ increase in fEPSP slope and/or amplitude after 25-30 minutes post HFS. A binomial test showed that the proportion of animals with LTP was greatly reduced by celecoxib treatment but not by Sc560.....	91
Figure 3.5 BDNF concentration was measured in the dentate gyrus of both stimulated and unstimulated hemispheres of each animal by ELISA and these concentrations are expressed as a percentage of the average untetanised, vehicle-treated control. Significantly more BDNF was measured in the celecoxib treated (35mg/kg) animals than in the controls or Sc560 treated animals bilaterally.....	92
Figure 3.6 Significantly more BDNF was measured in the animals treated with the higher concentration of celecoxib (35mg/kg) compared to the lower dose of 28mg/kg. Concentrations are expressed as a percentage of the BDNF concentration in the untetanised hemisphere of the vehicle-treated animals.	93
Figure 3.7 Blood plasma corticosterone was measured using radioimmunoassay as a control to ensure that celecoxib treatment (35mg/kg) did not affect the corticosterone levels and thus impair LTP induction.	94
Figure 3.8 Recording made during the administration of celecoxib (CXB) or its vehicle remained constant up to an hour after administration when maximal concentrations of CXB are reported to be reached in the brain.	95
Figure 3.9 The injection of celecoxib (35mg/kg) 20 minutes after the induction of LTP did not alter the maintenance phase of the LTP up to 90 minutes after its induction i.e. 70mins after the administration of celecoxib.....	97
Figure 3.10 The concentration of BDNF, measured 90 minutes after LTP was induced by HFS, was dramatically decreased by injecting celecoxib (35mg/kg) 20 minutes after HFS even though there was no effect on the degree of LTP. Concentrations are expressed as a percentage of the BDNF concentration in the unstimulated hemisphere of the vehicle treated animals.	99
Figure 3.11 Blood plasma corticosterone was measured using radioimmunoassay as a control to ensure that celecoxib treatment (35mg/kg) did not affect the corticosterone levels and thus impair LTP induction.	100

Figure 4.1 Schematic diagram of the intracellular signalling pathways involved in NMDA-mediated induction of <i>c-Fos</i> transcription in dentate gyrus neurons (adapted from {Lerea, 1995 #9}).	111
Figure 4.2 Metabolic degradation of PGE ₁ in the rat plasma and tissue homogenate {Nakano, 1972 #6}.	112
Figure 4.3 Diagram showing the simultaneous electrode-cannula system used to record fEPSP while injecting PGE ₂ .	116
Figure 4.5 The change in fEPSP slope as a result of intra-hippocampal injection of PGE ₂ across a range of stimulus intensities: A) 0-5000μA, and B) 0-1000μA.	119
Figure 4.6 PGE ₂ intra-hippocampal injection had no effect on input/output curves, recorded before and after the injection. The above graphs shows the change in PSA (pop spike amplitude) from pre-to-post PGE ₂ in the range A) 0-5000μA, and B) 0-1000μA.	120
Figure 4.7 E-S curves for current intensities ranging from 0-5000μA, measured in systemic celecoxib treated animals, pre- and post-PGE ₂ (66μM) (fig. B) or its vehicle (0.5%DMSO/saline) (fig. A) injected locally into the hippocampus. The curves are not obviously altered as a result of the injection process (fig. A) nor as a result of applying PGE ₂ to the tissue (fig. B).	121
Figure 4.8 Effects of PGE ₂ on the paired-pulse ratio in celecoxib treated animals. PGE ₂ failed to restore the depression seen in the non-celecoxib treated animals (cf. Chapter II). A) Representative fEPSPs at 10, 250 and 1000ms. B) PPR calculated as slope fEPSP ₂ /fEPSP ₁ ±SEM.	123
Figure 4.9 Baseline recording before, during and after the intrahippocampal injection of PGE ₂ or its vehicle (0.1% DMSO/saline). All animals were treated with celecoxib 30mins prior to anaesthesia. The fEPSPs of the PGE ₂ animals were significantly smaller than were those of the controls, immediately after injection and up ten minutes later. There was no observable difference by fifteen minutes after the end of injection.	125
Figure 4.10 Exogenous replacement of PGE ₂ prior to HFS assuages the deficit of LTP seen with COX-2 inhibition. Both groups were treated with celecoxib prior to anaesthesia and either PGE ₂ or its vehicle (0.1% DMSO) was injected into the hippocampus 15mins prior to HFS.	127
Figure 4.11 Protein expression measured in ipsi- and contralateral dentate gyri, 1 hour after the induction of LTP. All rats were injected i.p. with celecoxib prior to anaesthesia and then with either 1μl vehicle (0.1% DMSO) or PGE ₂ ipsilateral to LTP induction, 15mins prior to HFS.	129
Figure 4.12 There was no significant difference in total-ERK concentration observed one hour after the application of HFS, in response to PGE ₂ injection.	130

Figure 4.13 A significant increase in ERK phosphorylation was observed one hour after HFS in response to PGE2 injection relative to the untetanised hemisphere. This increase was not seen in the control group.	131
Figure 4.14 c-Fos protein was seen to be significantly upregulated only in the tetanised-PGE2 treated animals relative to the contralateral untetanised hemisphere.	132
Figure 4.15 A significant positive correlation exists between the amount of phosphorylated ERK and the amount of c-fos present in the tetanised (fig A: $r=0.625$; $n=12$; $p<0.05$) and untetanised (fig B: $r=0.581$; $n=12$; $p<0.05$) tissue irrespective of whether it is control or PGE2 treated.	133
Figure 4.16 Long-term potentiation was successfully induced when PGE2 (132 μ M) was exogenously replaced by intrahippocampal injection. Both groups were treated with celecoxib prior to anaesthesia and again four hours later (one $t_{1/2}$) to maintain the block of cyclooxygenase-2.	135
Figure 4.17 Representative blots from western analysis of dentate gyrus tissue three hours after HFS in the presence of intrahippocampal PGE2 or its vehicle control or the respective naïve hemispheres.	136
Figure 4.18 Densitometric analysis revealed no significant difference in the quantity of ERK-2, as a measure of total-ERK, three hours after HFS in response to PGE2 injection while subjected to COX-2 antagonism with celecoxib (CXB).	137
Figure 4.19 Densitometric analysis shows no significant difference in the quantity of c-Fos protein present in dentate gyrus three hours after HFS in response to PGE2 intrahippocampal injection. All animals were injected with celecoxib prior to anaesthesia.	138
Figure 4.20 A very strong and highly significant correlation exists between the concentration of c-fos and total-ERK concentration in both tetanised (fig A: $r=0.847$, $n=12$, $p<0.001$) and untetanised (fig B: $r=0.869$, $n=12$, $p<0.0001$) hemispheres.	139
Figure 5.1 A hypothetical model for the regulation of COX2 during varying degrees of stimulation and inhibition {Shaw, 2001 #58}.	156
Figure 5.2 Taken from {Chen, 2005 #159}	154

Chapter 1 Literature review

Chapter 1	Literature review.....	9
1.1	Introduction.....	11
1.1.1	The hippocampus.....	11
1.1.1.1	Synaptic architecture of the hippocampus.....	11
1.1.1.2	The hippocampus and memory.....	16
1.1.1.3	LTP and its underlying mechanisms.....	21
1.1.1.4	The intracellular mechanisms involved in LTP.....	22
1.1.1.5	The evidence for an LTP-based memory mechanism.....	24
1.1.2	BDNF and synaptic plasticity.....	26
1.1.3	Synaptic lipid signalling.....	29
1.1.3.1	The arachidonic acid cascade and eicosanoids.....	31
1.1.3.2	Cyclooxygenase.....	33
1.1.3.3	Prostaglandins.....	37
1.1.3.4	Pharmacology of COX inhibitors.....	42
1.1.4	ERK and intracellular signalling.....	45
1.1.5	Transcription factors.....	47
1.1.6	Objectives of this thesis.....	49

1.1 Introduction

"I have lost myself." – the poignant self-description given by the world's first Alzheimers patient documented by Alois Alzheimer, M.D in 1906, and thus the centenary of the first described case of AD (Alzheimer disease) is almost upon us.

In this thesis, we are going to investigate certain key signalling events and signalling molecules that participate in synaptic transmission and synaptic plasticity. These signalling molecules (cyclooxygenase 1 and 2: COX-1 and COX-2) are also believed to play a role in the neuropathology underlying AD. Up until recently, the commonly held perception of the COX isoforms was that COX-1 was involved in physiological function while COX-2 is responsible for pathology. The aim of this thesis is to add to the understanding of the non-pathological activity and functions of synaptic lipid modulators with the ultimate aim to add to the picture of neuroinflammation in the CNS. The following literature review will discuss some of the functions of the hippocampus with regard to memory, LTP as a model of a memory mechanism and molecular alterations associated with it. Furthermore, it will review the current understanding of synaptic lipid signalling with particular attention to cyclooxygenase and the arachidonic acid cascade.

1.1.1 The hippocampus

1.1.1.1 Synaptic architecture of the hippocampus

The hippocampus is a cylindrical structure located in the medial temporal lobe (MTL) forming a semicircle around the thalamus. It is so called because of the resemblance of its cross section to a seahorse, the literal translation of 'hippocampus' from Greek. The connectivity, physiology and anatomy of this highly organised structure have been thoroughly studied and characterised in detail due to evidence of its participation in mnemonic functioning in animals and humans. The hippocampus proper is defined as the regions CA1-CA4 (CA coming from Cornu Ammonus meaning the rams horn, referring to its shape) with CA1 and CA3 comprising its majority, this combined with the dentate gyrus (DG), the subiculum, and the entorhinal cortex (EC), make up the hippocampal formation, as shown in Figure 1.1. The EC is a major source of sensory input to the hippocampus and in turn it receives major inputs from the extrahippocampal structures, the

parahippocampus and the perirhinal cortex. It was thought that the latter structures simply relayed information from the neocortex to the hippocampus; lesion studies have shown that damage to these structures results in memory deficits almost as severe as hippocampal lesions (Zola-Morgan, Squire, D.G., & Suzuki, 1989). Thus these cortices form a hierarchy of processing increasing in complexity from neocortex to hippocampus, with the final abstracted information returning to its origin in the neocortex for storage as long-term memory (Lavenex & Amaral, 2000).

Connections and circuitry of the hippocampus

At its most basic the circuitry of the hippocampus can be described as a trisynaptic loop; perforant path neurons originating in the EC synapse with the granule cells of the DG, these granule cells synapse with CA3 pyramidal neurons via their axons called ‘mossy fibers’; next the axons of the CA3 pyramidal cells – called schaffer collaterals – synapse with CA1 pyramidal neurons. This simple trisynaptic circuit is present in all transverse slices along the longitudinal axis of the hippocampus as shown in the picture of the slice in Figure 1.2. The hippocampal region receives its main inputs from the entorhinal cortex via the alvear and perforant pathways; the dentate gyrus and CA3 inputs originate in layer II and the CA1 and subiculum via layer III, of the EC, a six-layer cortex. The perforant pathway can be divided into medial and lateral, evolving from the medial and lateral EC, the lateral EC receiving projections from the olfactory bulb and amygdala, for example, and medial EC receiving projections from the presubiculum (T. H. Brown & Zador, 1990). The medial and lateral perforant pathways not only receive different information but they also show different electrophysiological and intracellular signalling properties (Asztely, Kokaia, Olofsson, Ortengren, & Lindvall, 2000; Doyere, Srebro, & Laroche, 1997). As is evident in Figure 1.1, in addition to the trisynaptic loop discussed, each region can send projections not only to its neighbouring region but also to one or even two regions later in the sequence, with the exception of the DG which only projects to the CA3. To close the loop, CA1 projects strongly to the EC via the subicular complex and weakly directly to the EC (T. H. Brown & Zador, 1990).

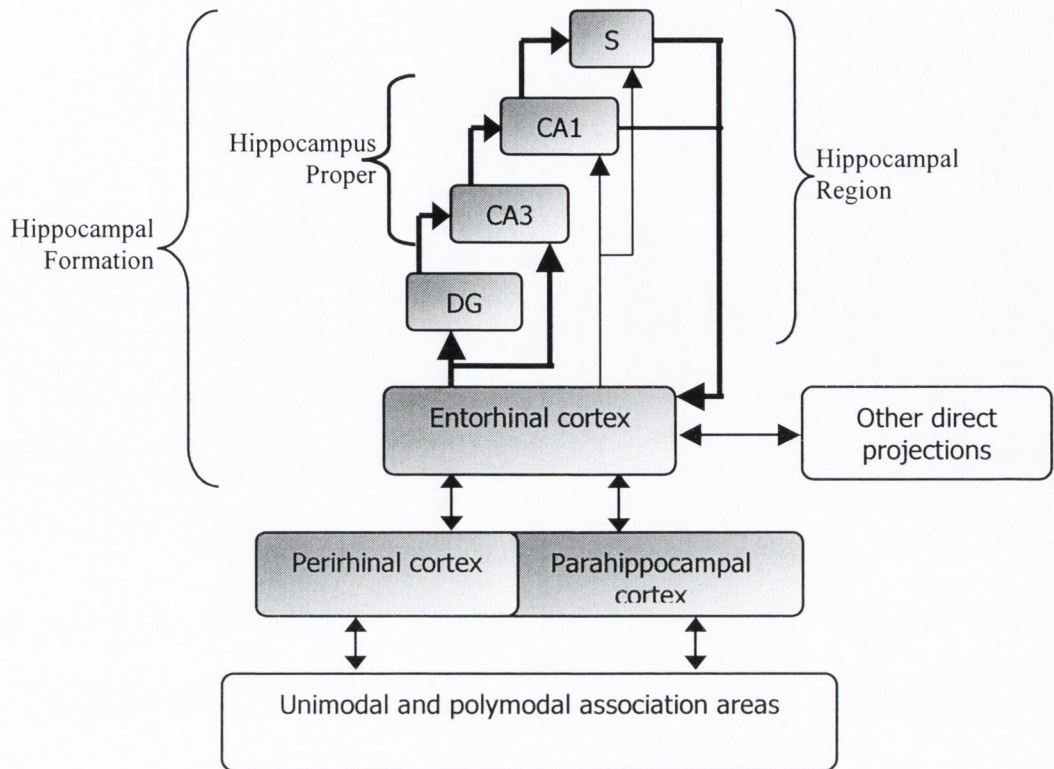
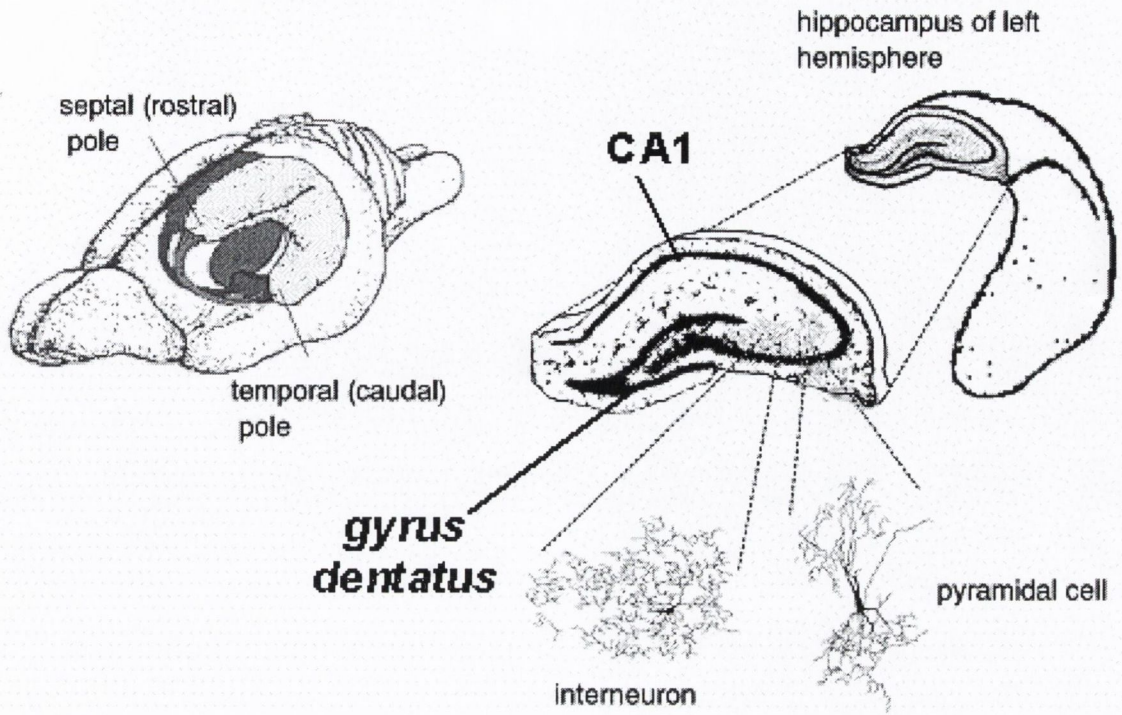


Figure 1.1 A schematic diagram of the medial temporal lobe system showing its basic circuits. DG, dentate gyrus; S, subiculum. Taken from (Squire, Stark, & Clark, 2004).

The perirhinal and the parahippocampal cortices receive convergent inputs from both unimodal and polymodal association cortices, which in turn supply the EC with almost two thirds of its neocortical inputs (Insausti, Amaral, & Cowan, 1987). The perirhinal cortex receives mainly visual object information compared to the parahippocampus, which receives mainly visuospatial information (Lavenex & Amaral, 2000), as well as the information from the auditory association cortex. Cortices involved in somatosensory processing project to both perirhinal and parahippocampal cortices. Thus the perirhinal and parahippocampal cortices are the second level in the hierarchy of the neocortical-hippocampal information-processing loop (Lavenex & Amaral, 2000).

While the fundamental intrinsic connectivity of the hippocampus repeats itself along its longitudinal axis the extrinsic, afferent and efferent connections change suggesting that the dorsal and ventral parts of the hippocampus may have individual functions (Bannerman et al., 2004; M. B. Moser & Moser, 1998). Lesion studies by the Mosers and colleagues, both by aspiration and neurotoxins (which spare nerve fibres and blood supply as compared to aspiration), of the septal pole of the dorsal hippocampus showed acute watermaze

impairment while ventrally-lesioned animals learned the watermaze normally (E. Moser, Moser, & Andersen, 1993; M. B. Moser, Moser, Forrest, Andersen, & Morris, 1995). In a very recent study, it was also shown that excitotoxic, fibre-sparing lesion of the dorsal but not the ventral part of the EC resulted in impairment in spatial memory recall, while the ventral lesion reduced avoidance of the open arms of the plus maze agreeing with the hypothesis of a modular organisation of the EC (Steffenach, Witter, Moser, & Moser, 2005). In conclusion, the hippocampus is functionally heterogeneous with distinct modules located in the transverse as well as the longitudinal plane.



Hippocampus

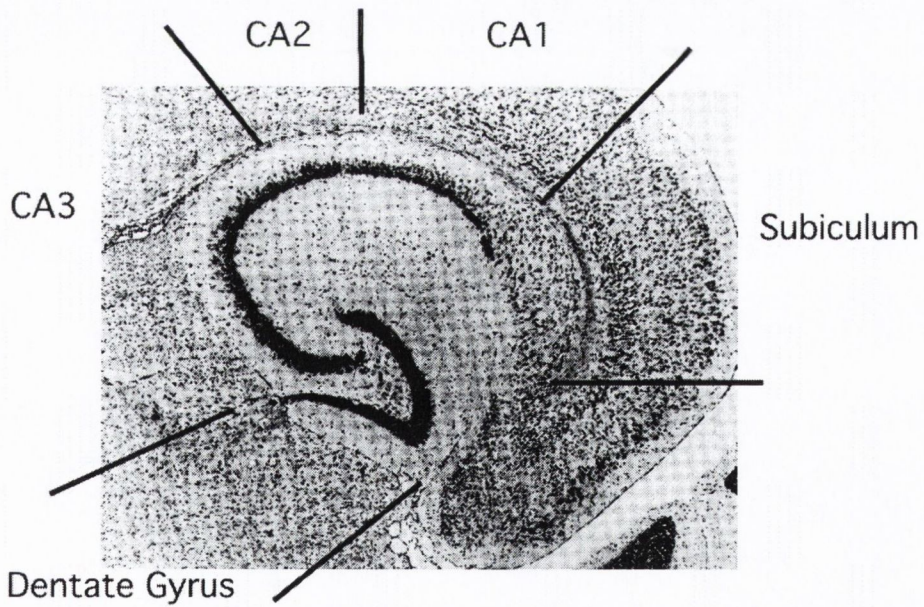


Figure 1.2 The upper left drawing shows a transparent rat brain with the position of the right (grey) and left (white) hippocampi shown and the right drawing show the appearance of the cross section of the left hippocampus. The lower diagram shows a transverse slice of the hippocampus and clear divisions of the hippocampal formation substructures. Slices of this orientation preserve much of the essential circuitry of the hippocampus.

1.1.1.2 The hippocampus and memory

The first insight into the function of the hippocampus was gleaned in tragic circumstances whereby a young man suffering intractable epilepsy in 1953 underwent a bilateral removal of an apple-sized portion of both medial temporal lobes incorporating the hippocampus and amygdala. H.M.'s IQ remained above average after the surgery but he suffers severe anterograde amnesia (Scoville & Milner, 1957). He is capable of learning new procedural memories including puzzles but is incapable of remembering new people, conversations or facts. Magnetic resonance imaging (MRI) confirmed the precise structures lesioned in H.M.'s brain and found they concurred with the view that lesions of the hippocampus and neighbouring cortices resulted in global and enduring amnesia (Corkin, Amaral, Gonzalez, Johnson, & Hyman, 1997). H.M.'s amnesia is so profound it has become the yardstick for judging the degree of other amnesias. Examination by Brenda Milner and Wilder Penfield (Penfield & Milner, 1958) of similar patients, who had undergone hippocampal lesions, revealed a lack of memory for recent events, in sharp contrast to their retention of memories prior to surgery and their overall intelligence. These observations were groundbreaking since they distinguished intelligence from memory and furthermore confirmed the division of memory into distinct systems (a concept proposed as early as the 19th century), namely *declarative* (memory of facts and events; also termed explicit and is expressed by word) and *non-declarative* (habit; also called implicit and is expressed by action) memory. Figure 1.3 shows these divisions of memory and the associated brain regions thought to be important in each (Milner, Squire, & Kandel, 1998); note the division of declarative memory into episodic (autobiographical memories associated with a time and place) and semantic (worldly knowledge, facts).

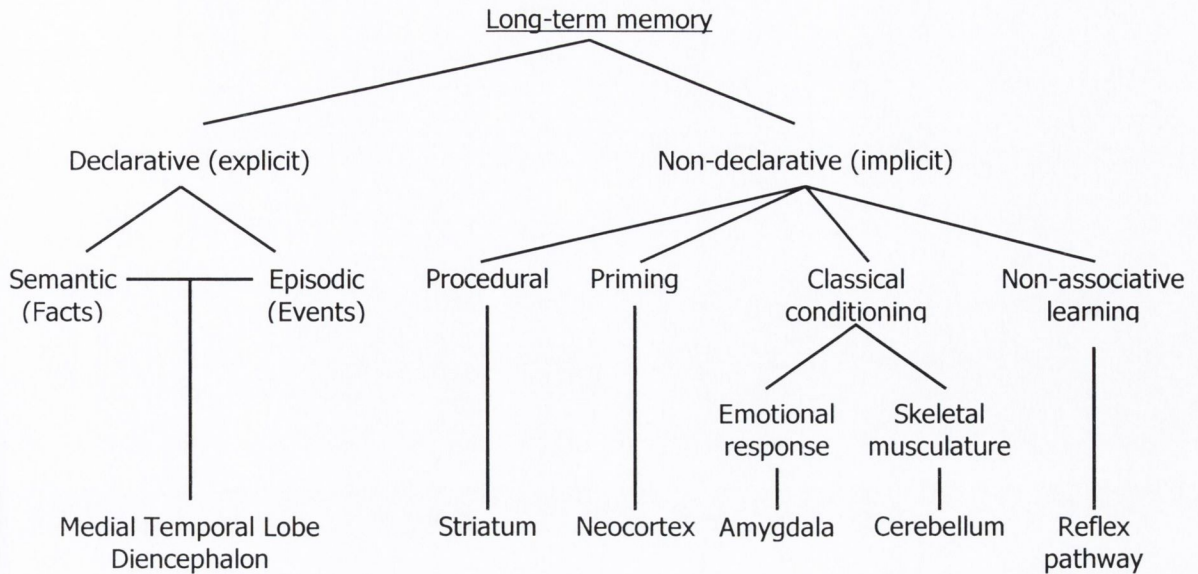


Figure 1.3 Taxonomy of memory systems showing the brain structures and connections thought to be important; taken from (Milner et al., 1998).

Since H.M.'s lesion incorporates neighbouring cortices and not solely the hippocampus proper, further studies were required to investigate exactly what structure was required for what function. Systematic animal lesion studies were performed with behaviour tests to determine the ensuing losses, defining the hippocampal region and the adjacent entorhinal, perirhinal and parahippocampal cortices as important for declarative memory; the amygdala, while not necessary for declarative memory, was found to modulate it (Zola S.M., 2000). Moreover, the greater the lesioned area of the MTL the worse the amnesia. Monkeys with large lesions in, equivalent to those in amnesic patients, resulted in similar patterns of memory loss, being both multimodal and long lasting. Several theories have been proposed as to the role of the hippocampus in formation and retrieval of long term declarative memory, based on the fact that the hippocampus is the final point of convergence within the medial temporal lobe (Lavenex & Amaral, 2000), the plastic nature of its synapses being able to undergo facilitation and depression (Bliss & Collingridge, 1993), and the connectivity between it and the neocortex (Lavenex & Amaral, 2000), the final resting place of long term memories (Fuster, 1997). While the formation of new declarative memories is profoundly affected in H.M., he also shows temporally graded retrograde amnesia – that is memories immediately prior to surgery were more disrupted than older more “consolidated” memories – and it is this impairment in the retrieval of memories which is most ardently debated in relation to the hippocampus. Two of the main

theories of medial temporal lobe function will be considered further: Classic Consolidation Theory and Multiple Memory Trace theory.

Classic consolidation theory

According to the consolidation theory of memory a “fixation” process occurs whereby newly formed memories become stabilized and permanent over a period of time, becoming intertwined with older memories. This theory has been bandied about since the early 20th Century but was only associated with the medial temporal lobe and declarative memory in the latter half of the century; for review see (Shimamura, 2002; Squire et al., 2004). Many theories of learning have been based on this consolidation theory being used to explain the coincidence of anterograde and retrograde amnesia as a result of hippocampal damage. The most popular of these theories is that put forward by Squire (Squire, 1992; Squire & Alvarez, 1995) proposing that the MTL associates inputs from different cortical regions leading to a strengthening of the signal and an increased probability of retrieval, akin to LTP (below). Over time, this strengthening of hippocampal-cortical connections results in cortical-cortical connection independent of the hippocampus and the MTL for retrieval of the memory. This theory encompasses consolidation of both episodic and semantic memories and goes some way to explaining the anterograde and temporally graded retrograde amnesia observed with MTL damage.

Multiple memory trace

Some debate has been on-going regarding the extent of the retrograde amnesia, and its temporal gradation associated with MTL damage. Nadel and Moscovitch (1998), on reviewing studies of retrograde amnesia, found that the existing consolidation theories failed to account for long-lasting, non-graded retrograde amnesia and thus proposed an alternative Multiple-Trace Theory (MTT) (Moscovitch & Nadel, 1998; Moscovitch et al., 2005). While they accepted that the hippocampus rapidly associates cortical representations making them more likely to be reactivated, they contradicted the opinion that memories eventually became independent of the hippocampus, i.e. they are always dependent on cortical-hippocampal connections. The proposed alternative involved the laying down of a new trace every time a memory is reactivated and the more traces the stronger the memory, meaning that the more a memory was revisited the less susceptible it

becomes to disruption. These traces are said to be long lasting and widely distributed throughout the hippocampus. A distinction is made between storage and retrieval of episodic and semantic memory, suggesting that eventually, semantic memories are exclusively represented in the cortex (conforming to the classic model of consolidation) while episodic memories will always depend on the MTL. To account for the complex nature of episodic memory they considered that distinct regions of the MTL might contribute differently to the composition of a memory and damage to an area would result in loss of that aspect of the memory. This implies the greater the size and gravity of the damage to the MTL the more traces of a memory are destroyed (as seen in the lesion studies), implying that newer memories (with fewer traces) are more susceptible to amnesia, a plausible explanation for a gradient in amnesia.

While these are two of the most popular theories of MTL function they are by no means the only ones. The classic consolidation theory states that over a period of time a memory becomes stable and hippocampal independent. This tenet has been contradicted by the observations that reactivation of a consolidated memory followed by an amnesia inducing procedure (e.g. electroconvulsive therapy (ECT), hypoxia, hypothermia) or a memory modulator can render this memory labile and susceptible to disruption or facilitation (Sara, 2000). Misanin et al in 1968 showed that ECT after reactivation of a consolidated memory resulted in retrograde amnesia – reviewed by (Miller & Matzel, 2000) – and DeVietti et al in 1977 showed that electrical stimulation of the mesencephalic reticular formation applied after reactivation of a trial-conditioned fear response improved the memory; for review see (Sara, 2000). This ability to reactivate and alter a memory (either to augment it, eliminate it or change it in some way) has been termed reconsolidation. Systematic, well-controlled experiments by Nader et al. showed that protein synthesis was required for “reconsolidation” of memories (Nader, Schafe, & Le Doux, 2000). Thus reconsolidation does not come under the remit of consolidation theories and so starts a new era of debate.

Synaptic plasticity and excitability

The turn of the twentieth century saw a revolution in how the brain was viewed. Ramon y Cajal demonstrated that the brain is not just a syncytium, but is divided into discrete nerve cells. Sherrington added to this by proposing the ‘synapse’ as the point of communication between two nerve cells with both excitatory and inhibitory properties (Cooper, 2005).

Donald Hebb in 1949, proposed a ‘dual trace mechanism’ of memory whereby an unstable *dynamic storage* would become a stable *structural storage*, that is, synaptic plasticity was responsible for memory storage.

“Let us assume then that the persistence or repetition of a reverberatory activity tends to induce lasting cellular changes that add to its stability...When an axon of cell A is near enough to excite cell B and repeatedly or persistently takes part in firing it, some growth process or metabolic change takes place in one or both cells so that A’s efficiency as one of the cells firing B is increased.” (Hebb, 1949)

This succinctly put postulate has a particular ramification, that in order for a memory to be stored the neuronal signal must have the properties of input specificity, associativity and cooperativity. Input specificity implies that plasticity can result only in the cells that “take part in firing”. “A’s efficiency as one of the cells firing B” alludes to the property of associativity whereby a weak input could result in plasticity when it is coactive with a strong input and the phrase “repeatedly or persistently take part in firing” implies cooperativity, that is a threshold of activation is essential. The first tangible evidence for such a mechanism in memory did not materialise for many years.

Given the insights into the potential role of the MTL and the hippocampus in long-term memory, the relative simplicity of the hippocampal architecture and the proposal of a neuronal basis for information processing and memory storage, Tim Bliss and Terje Lomo purposely set about to discover a neuronal memory mechanism. The 1973 paper that resulted was the first paper to show ‘long-lasting potentiation’ in the hippocampal formation as a result of a single tetanus and to make the association with a potential memory mechanism (Bliss & Lomo, 1973). The repeated firing of the cells by tetanic stimulation resulting in increased synaptic efficacy mirroring exactly Hebb’s postulate and the three implicit characteristics: associativity, cooperativity and input specificity (Bliss & Collingridge, 1993). Prior to this, observations of facilitation or post tetanic potentiation (PTP) of a response were merely a curiosity, a means to extend the length of a recording when the response was shrinking due to exhaustion, only lasting minutes; for reviews see (Andersen, 2003; Craver, 2003). In the thirty years since the discovery of LTP, definitive evidence for a memory storage mechanism similar to that of LTP is still lacking. In the following review the focus will be on hippocampal LTP.

1.1.1.3 LTP and its underlying mechanisms

The crucial event in the induction of LTP is an increase in intracellular calcium concentration ($[Ca^{2+}]_i$); calcium sequestration blocks LTP induction (G. Lynch, Larson, Kelso, Barrionuevo, & Schottler, 1983) and postsynaptic calcium injection induces LTP (Malenka, Kauer, Zucker, & Nicoll, 1988). Several different routes have been proposed to modulate $[Ca^{2+}]_i$, entry through ionotropic glutamate receptors in particular NMDA, entry through voltage gated calcium channels (VGCC) and release from intracellular stores.

There are two types of LTP, NMDA-dependent (Collingridge, Kehl, & McLennan, 1983) and NMDA-independent. The former is the main type of LTP in the hippocampus occurring at all synapses in the hippocampus, with the exception of the mossy fibre-CA3 where due to the relative sparseness of NMDARs, NMDA-independent LTP is induced. NMDA-dependent LTP requires the interaction of glutamate with postsynaptic NMDA receptors, which upon activation allows Ca^{2+} ions enter the cell. However, the NMDARs are a family of ligand gated ion channels that are also voltage dependent, that is to say, in order for the ion channel to become activated and permeable to Ca^{2+} ions the cell must be depolarised first. This is due to a magnesium ion (Mg^{2+}), which at resting membrane potential blocks the ion channel (Nowak, Bregestovski, Ascher, Herbert, & Prochiantz, 1984). Thus, the property of cooperativity is expressed in the requirement for the NMDAR to simultaneously have glutamate bound and the cell to be depolarised in order for the ion channel to open. Furthermore, NMDARs act as coincidence detectors between pre- and postsynaptic activity, exhibiting the property of associativity: repeated depolarisation of the presynaptic neuron with the release of glutamate results in fast depolarisation of the postsynaptic neuron via the AMPA receptor resulting in the relief of the Mg^{2+} -block with subsequent slow NMDAR depolarisation. Furthermore, the dendritic spines have been proposed to localise and concentrate the increase in $[Ca^{2+}]_i$, the narrow neck prevents the Ca^{2+} ions from diffusing away from calcium-sensitive proteins located in the postsynaptic densities (Zador, Koch, & Brown, 1990) – for a review of spine function in long-term plasticity read (Segal, 2005) – for instance Ca^{2+} /calmodulin-dependent kinase (CaMKII). This local increase in $[Ca^{2+}]_i$ accounts for the property of input specificity of LTP.

As mentioned, the mossy fibre-CA3 synapses display a form of LTP insensitive to NMDAR inhibition. Similarly, blocking Ca^{2+} entry into the postsynaptic cell has no effect

on LTP. Thus this form of LTP is mediated by influx of Ca^{2+} into the presynaptic cell with a resultant increase in the probability of glutamate release; for review see (Nicoll & Malenka, 1995). LTP at these synapses is non-hebbian in that they do not show associativity and cooperativity, since its induction only depends on presynaptic events.

1.1.1.4 The intracellular mechanisms involved in LTP

So far the induction process involved in LTP has been discussed but what is involved in maintaining this increase in efficacy of the cell for long periods of time, even up to days and weeks? Hebb described “some growth process or metabolic change”; one possibility is the transcription of new proteins needed to maintain the cell. Indeed, experiments have been done which showed that inhibition of new protein synthesis impedes the maintenance of LTP (Krug, Lossner, & Otto, 1984; Stanton & Sarvey, 1984). For pedagogical reasons LTP has been divided into phases – induction, early (E-) and late (L-) LTP – such that E-LTP is protein synthesis independent and L-LTP is protein synthesis dependent. Other work has shown morphological changes such as increases in synaptic area (Desmond & Levy, 1988), spine number and spine area (Fifkova & Vanharraveld, 1977) after LTP induction. The question begs: what are the intracellular processes that lead to E-LTP with subsequent L-LTP and the protein synthesis and structural changes downstream of Ca^{2+} influx?

An important finding was that inhibition of Ca^{2+} /calmodulin-dependent protein kinase II (CaMKII) impaired the induction of LTP (Malenka et al., 1989; Malinow, Schulman, & Tsien, 1989). Similarly, transgenic mice lacking the α -subunit of the CaMKII exhibit markedly impaired LTP (Silva, Stevens, Tonegawa, & Wang, 1992). This deficit was also evident in tests of spatial learning (Silva, Paylor, Wehner, & Tonegawa, 1992) showing a causative link between LTP and learning mechanisms; for review see (M. A. Lynch, 2004). An important characteristic of CaMKII is that when it is autophosphorylated at Thr²⁸⁶ its activity is no longer dependent on Ca^{2+} /calmodulin, thus acting to prolong the response of the cell to the increase in $[\text{Ca}^{2+}]_i$ long after the increase has dissipated (Malenka & Nicoll, 1999). But what are the functional consequences of CaMKII activation?

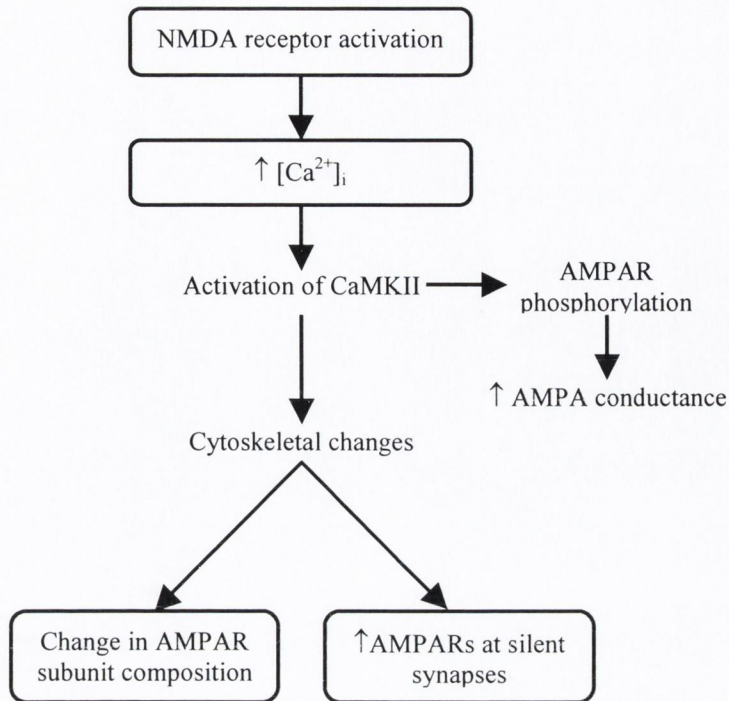


Figure 1.4 Increased Ca^{2+} entry as a result of NMDAR activation is not sufficient to maintain the expression of LTP. CaMKII phosphorylation results in the AMPAR conductance, subunit composition and increased expression at silent synapses (see text for details). Adjusted from (M. A. Lynch, 2004).

It has been shown that a large proportion of synapses in the hippocampus lack AMPAR but not NMDAR and given the voltage dependent nature of NMDAR these synapses are unable to respond to glutamate binding, consequently, they have been termed ‘silent synapses’. It has been shown that CaMKII phosphorylates target proteins involved in AMPAR vesicular trafficking into the membrane, thus activating the synapse (Rongo, 2002). This activation of silent synapses is consistent with the decrease in the number of failures after minimal stimulation, observed after LTP induction. As demonstrated in Figure 1.4 the activation of CaMKII can alter AMPAR in three distinct ways: as discussed above it can increase trafficking of AMPAR to the synapse with activation of silent synapses, secondly, phosphorylation of the GluR1 subunit of the AMPAR results in increased conductance and thirdly, it can modulate in an activity dependent manner the subunit composition of AMPARs at the synapse; for comprehensive review see (Rongo, 2002). These alterations in AMPAR function by CaMKII have been proposed as a mechanism for the expression of LTP, suggesting a predominant postsynaptic locus.

CaMKII is not the only kinase activated by LTP induction, for example the cAMP-dependent protein kinase PKA, PKC and ERK are also activated. ERK will be discussed below and in Chapter IV in relation to LTP and *c-Fos* expression.

1.1.1.5 The evidence for an LTP-based memory mechanism

Obvious caveats accompany the proposal for an LTP-based model of how the brain stores memory, the most obvious being the unnatural levels of stimulation employed by Bliss and Lømo to achieve successful LTP. This problem was surmounted with the execution of LTP induction with a pattern of stimulation, which mimics brain activity recorded in animals during exploration, called theta. Another protocol with lower thresholds of activation involves the presynaptic stimulation with postsynaptic back propagating action potentials (bpAP) (Magee & Johnston, 1997); when a cell fires an action potential travels down the axon but also antidromically towards the dendrites, resulting in Na⁺ channel opening and a lowering of the threshold for further depolarisation and a ensuing facilitation. A second mismatch considers the longevity of the increased responsiveness observed with LTP (days-week) compared to long-term memory (months-years/ life-long). Some explanations have been put forward to account for the relative brevity of LTP: one group showed that CA1 LTP could be reversed in awake rats by allowing them to explore a novel environment (Xu, Anwyl, & Rowan, 1998); also, resetting of homeostasis after LTP induction could also account for decrement in LTP (Martin & Morris, 2002). Thirdly, are structural changes observed as a result of L-LTP also observed in memory storage?

Different approaches have been used to investigate LTP as a mechanism for learning and memory:

- *Correlation of the ability to induce LTP with the ability to learn.*

Most of the evidence, favourable or not, comes from correlative data regarding LTP induction and memory, e.g. NMDA receptor blockade by intraventricular injection blocks both LTP induction and memory acquisition in the watermaze (Morris, Anderson, Lynch, & Baudry, 1986) or the dual impairment in LTP and memory in the CaMKII mutant mice (Silva, Paylor et al., 1992; Silva, Stevens et al., 1992). As pointed out by Edvard Moser, there are obvious problems with such an approach, most notably that the proteins investigated are abundant in the hippocampus and are likely to

have more than one function, even non-mnemonic functions (E. I. Moser & Moser, 1999).

- *Test the effect of LTP induction on learning and vice versa.*

If one used the premise that memory is a function of changes in synaptic-efficacy then it follows that saturation with LTP would impair new memory formation. McNaughton et al (1986) used this tactic investigating whether saturation of LTP in the main afferent to the hippocampus – the perforant pathway – would result in spatial memory impairment in rats. The authors successfully demonstrated that the formation of new spatial memory was impaired while well-established memories remained intact, thus arguing in favour of consolidation of memory in the hippocampus (McNaughton, Barnes, Rao, Baldwin, & Rasmussen, 1986). However, attempts to replicate these findings by McNaughton et al. and several different groups failed. The Mosers tested whether these failed attempts at replication were a result of insufficient saturation, by inducing LTP by a ‘cross-bundle stimulation’ protocol involving simultaneous stimulation of both the medial and lateral perforant path in one hemisphere and removal of hippocampus and dentate gyrus in the other. Rats were unable to learn the watermaze only if the LTP could be potentiated maximally (E. I. Moser & Moser, 1999). A further study in the Mosers’ lab showed an impaired recall in animals that were subjected to LTP after training in a watermaze task only when the LTP resulted in changes in synaptic weights (Brun, Ytterbo, Morris, Moser, & Moser, 2001).

In one particular study of the effects of learning on LTP induced over a range of stimulus intensities were studied (Jeffery, 1995). The author found that as the intensity was increased the magnitude of LTP decreased and this decrease was negatively correlated with learning impairment, i.e. poor learners showed more LTP at high stimulus intensities, thus warning that LTP studied at single intensities may miss important characteristic of the relationship between learning and LTP.

- *The ability to detect structural changes associated with LTP after memory acquisition.*

Given that a mnemonic process is likely to potentiate only a minute fraction of the synaptic connections available, as suggested by neural network models (Martin & Morris, 2002), the detection of changes could prove difficult. Moser (1995) showed increases in the size of fEPSPs recorded in the rat dentate gyrus during exploratory

training, which decayed by between 15-20 minutes, however, subsequent investigations implicated brain temperature, motor activity and arousal as factors affecting this result. With sufficient controls for the above factors the two effects were successfully dissociated and the potentiation endured (E. I. Moser, 1995).

Even given all the pros and cons associated with an LTP-based model of memory formation and the tentative and mostly circumstantial evidence at this time, in its favour it is not unwise to assume that such a process is feasible.

1.1.2 BDNF and synaptic plasticity

The discovery of the neurotrophins is a classic tale of systematic experimentation and pure luck (Levi-Montalcini, 1987). Over fifty years ago it was discovered that a diffusible constituent of the mouse sarcoma tumour was responsible for the accelerated growth of cultured neurons and that this same compound was present in snake venom. It was the purification of this compound, from the venom, that introduced nerve growth factor (NGF) to the scientific world. Since then a whole family of neurotrophic factors has been characterised including brain-derived neurotrophic factor (BDNF) (Barde, Edgar, & Thoenen, 1982), neurotrophin-3 (NT-3) (Hohn, Leibrock, Bailey, & Barde, 1990), and NT-4/5 (Hallbook, Ibanez, & Persson, 1991) which share a common core protein structure (showing that they are phylogenetically related) and individual moieties which confer receptor specificity. These are secretory proteins, which bind to their associated receptors, all bind to p75 and then individually; NGF binds TrkA, BDNF and NT-4/5 bind TrkB and NT-3 binds TrkC. Activation of the Trk receptors by ligand binding involves receptor dimerisation and autophosphorylation resulting in tyrosine kinase activity. This kinase activity can, in turn, set in motion other signalling cascades, e.g. MAPK, PI3K (phosphatidylinositol 3-kinase) and PLC- γ (phospholipase- γ) which transduce the signal to the nucleus ultimately resulting in gene transcription; reviewed by (Lu, 2003a). They have all been shown to be crucial in regulating the survival and differentiation of neurons during development. Further to their role in development, a rapidly growing body of literature has implicated these neurotrophic factors in neuronal structure and function throughout life; for reviews see (E. J. Huang & Reichardt, 2001). Most relevantly, BDNF has been implicated in synaptic plasticity; the first evidence of this enhanced synaptic efficacy came just over 10 years ago with the discovery that exogenously applied BDNF potentiated the response

at the *Xenopus* neuromuscular junction (Lohof, Ip, & Poo, 1993). Thus, a dichotomy exists in the function of BDNF on cells; acute administration modulates synaptic transmission by opening of ion channels etc. acting within seconds or minutes, whereas chronic exposure over a period of days or hours results in cell survival and differentiation. This review will focus on BDNF and synaptic plasticity in the hippocampus.

Shortly after the demonstration of BDNF-induced potentiation in the *Xenopus* NMJ, BDNF – along with NT-3 and NT-4/5 – was shown to facilitate synaptic transmission in the mammalian hippocampus *in vitro* (Lessmann, Gottmann, & Heumann, 1994); (Kang & Schumann, 1995); (Levine, Dreyfus, Black, & Plummer, 1995). Since this revelation innumerable papers with a wide range of experimental approaches have been published, as outlined in Figure 1.5; for a thorough review see (Bramham & Messaoudi, 2005). The most exciting finding was that BDNF did not just induce potentiation *in vitro* it also potentiated responses in the dentate gyrus effectively, when injected directly into the hippocampus of the anaesthetised rat (Messaoudi, Bardsen, Srebro, & Bramham, 1998).

In addition to its ability to facilitate synaptic transmission, BDNF was shown to be required for the induction of activity dependent LTP since hippocampal LTP was significantly impaired in BDNF knockout (KO) mice (Korte et al., 1995). This deficit in BDNF-KO mice could be reversed by its replacement with recombinant BDNF (Patterson et al., 1996).

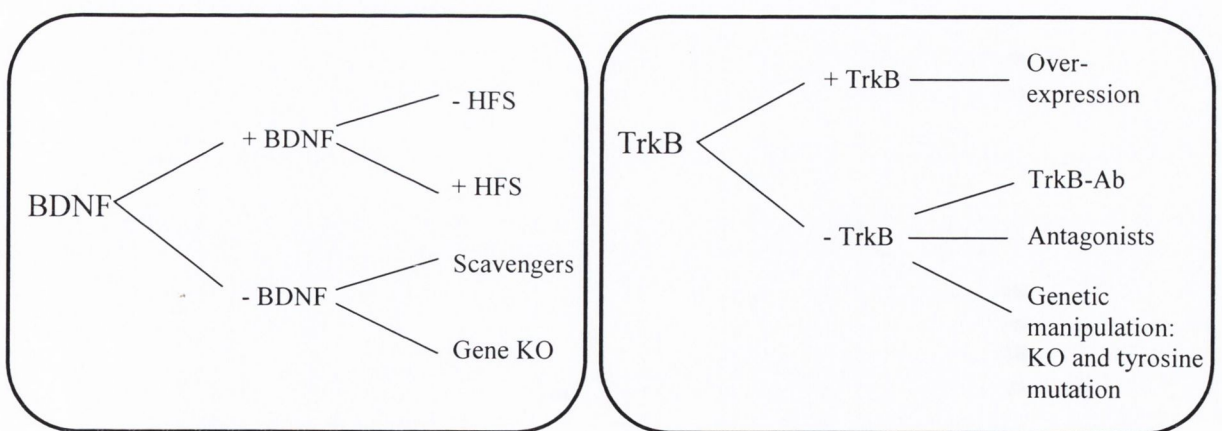


Figure 1.5 Overview of the experimental strategies used to investigate the role of BDNF-TrkB signalling in synaptic plasticity, *in vitro* and *in vivo*.

Increased BDNF mRNA and protein expression associated with LTP-induction (Bramham, Southard, Sarvey, Herkenham, & Brady, 1996; Gooney & Lynch, 2001; Morimoto, Sato,

Sato, Yamada, & Hayabara, 1998) and learning (Kesslak, So, Choi, Cotman, & Gomez-Pinilla, 1998) have been reported in the dentate gyrus of the hippocampus. BDNF is an immediate early gene although its expression lags behind that of other IEGs (e.g. *c-Fos*) and this has been proposed as a possible switch between E-LTP and L-LTP (Lu, 2003a). Instantaneous and transient secretion of BDNF in response to HFS, more effectively than LFS (low frequency stimulation), has been reported in cultured neurons, suggesting a potential modulatory effect of BDNF at active synapses, in agreement with a model Hebbian-synapse (Balkowiec & Katz, 2002; Gartner & Staiger, 2002). Parallel changes in Trk-phosphorylation in LTP and spatial learning have been reported, with associated increases in downstream ERK-phosphorylation (Gooney, Shaw, Kelly, O'Mara, & Lynch, 2002).

BDNF has been shown to be necessary for the maturation and stabilization of synapses during development, and the activation of silent synapses, increasing both the frequency and amplitude of AMPA mediated miniature excitatory postsynaptic currents (mEPSC). A change in mEPSC frequency reflects the number of vesicles being spontaneously released presynaptically, and an increase in amplitude suggests a postsynaptic increase in sensitivity or number of receptors. Thus, BDNF can act pre- and postsynaptically, facilitating synapse maturation and activation. However, this research was performed in immature cells but it does suggest a potential mechanism for BDNF in the maintenance of LTP; for review see (Vicario-Abejon, Owens, McKay, & Segal, 2002).

A further level of complexity can be added to the role of BDNF in LTP. Neurotrophins are secreted as precursors e.g. pro-BDNF, and are transformed into the mature form, mBDNF, by proteolytic cleavage of the “pro” region. The pro and mature forms of neurotrophins can elicit different functions by interacting with different receptors e.g. pro-BDNF shows a higher affinity for p75 receptor, whereas mBDNF has a higher affinity for the TrkB receptor. These receptors signal via different intracellular cascades, TrkB by tyrosine kinase and p75 by increased NF- κ B and c-jun N-terminal kinase activities (Lu, 2003b). Pro-BDNF can be cleaved by plasmin at hippocampal synapses; plasmin activity is controlled by tissue plasminogen activator, which has been implicated in late-phase LTP and learning and memory (Pang et al., 2004).

1.1.3 Synaptic lipid signalling

Cells of the nervous system (neurons, astrocytes and other glia) have some of the largest surface areas of membranes of all cells given their highly networked and branched nature with dendrites and dendritic spines. These membranes at their most basic level are composed of phospholipids and polyunsaturated fatty acids (PUFA). A growing area of interest is the function of discrete reservoirs of phospholipids which, when released upon stimulation by receptor activation, membrane depolarisation, ion channel activation etc., act as second messengers contributing to neuronal cell differentiation, restructuring, protection and repair (Bazan, 2003). However, unlike classical second messengers these lipid signals have the added ability to diffuse across membranes and act intercellularly binding to high-affinity receptors on neighbouring cells. Some of these bioactive phospholipids, PUFA and their metabolites – with particular reference to arachidonic acid – with respect to synaptic signalling, memory and long-term potentiation will be discussed in detail.

As stated previously the nervous system is made up of a vast surface area of membrane and 50% of these membranes are lipids (i.e. the lipid bi-layer). A large proportion of these lipids are phospholipids (others include cholesterol and glycolipids) that can function as mediators and modulators within and without the cell (Alberts et al., 1994b). Phospholipids consist of a hydrophilic polar head and a hydrophobic tail (Figure 1.6a) which when cleaved by lipase enzymes release bioactive molecules. Phospholipids are centred on a glycerol molecule with three attached groups – two fatty acids and a phosphate group. The fatty acid groups are comprised of long chains of carbon bonds, which vary in length and the degree of saturation (i.e. the number of double bonds), for example oleate has 18 carbons and 1 double bond whereas arachidonate has a 20-carbon chain and four double bonds. The fatty acid chains in the phospholipid determines the fluidity of a membrane – double bonds add kinks to the carbon chain thus taking up more space and the two chains can be asymmetric varying in length and saturation. In the nervous system membranes were formerly divided according to fluidity, e.g. oligodendrocytes are rigid and grey matter more fluid. The negatively charged phosphate group can have several different neutral groups attached e.g. glycine, choline, inositol or the negatively charged serine. The negative charge on the latter, serine, is vital for protein kinase C (PKC) activation where it bind in the presence of elevated intracellular calcium and diacylglycerol (DAG) (see

below). The highest concentration of PKC is found in the brain and when activated it phosphorylates ion channels changing neuronal excitability, it initiates kinase cascades and it phosphorylates I κ B liberating NF κ B, both resulting in gene transcription.

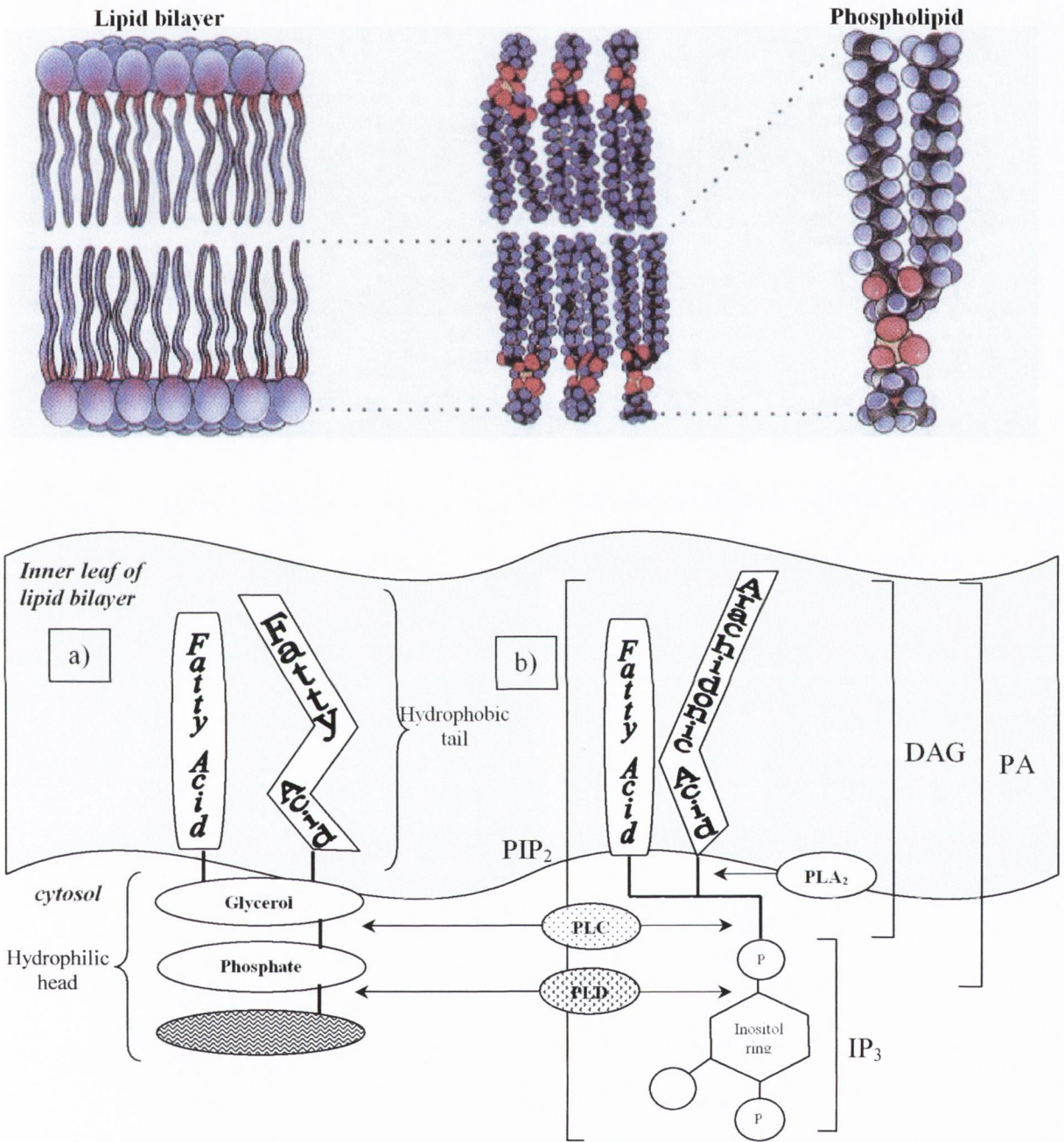


Figure 1.6a) Generic structure of phospholipids. Note the central glycerol molecule around which are attached two asymmetric fatty acid groups and a phosphate group. The filled in oval represents a small hydrophilic molecule such as ethanolamine, choline, serine or the less common inositol. b) The structure of phosphatidylinositol bisphosphate (PIP₂). Note the brackets indicating the potential signalling moieties after cleavage by phospholipase.

Inositol phospholipids, although sparse, are very important in signal transduction, in particular phosphatidylinositol 4,5, biphosphate (PIP₂) (Figure 1.6b). When a g-protein-coupled receptor (GPCR) (e.g. metabotropic glutamate receptor) is stimulated by the binding of its ligand, a chain of events involving phospholipase C_β activation (an inositide-specific lipase) results in liberation of inositol triphosphate (IP₃) and DAG from PIP₂ within seconds. IP₃ liberates Ca²⁺ from intracellular stores in the endoplasmic reticulum (ER) by binding to IP₃-gated Ca²⁺-channels. DAG, as mentioned before, can activate PKC in tandem with the Ca²⁺ released by IP₃ resulting in down-stream gene transcription. DAG can be further cleaved by PLA₂ to generate arachidonic acid. DAG from PIP₂ is rapidly metabolised by DAG-kinase (DGK) back to phosphatidic acid (PA) conferring a very short lifespan of activity. However, DAG can also be generated from another phospholipid phosphatidylcholine (PC) through the action of another phospholipase, PLD, resulting in a different fatty acid composition than PIP₂ generated DAG and since this is more slowly metabolised it is thought to be more involved in cell proliferation and differentiation (Alberts et al., 1994a). It has been shown that mice deficient in the enzyme DGK ϵ , which regenerates PIP₂ from DAG, show a lower accumulation of PIP₂ and free arachidonic acid, and an attenuated LTP (Rodriguez de Turco et al., 2001).

1.1.3.1 The arachidonic acid cascade and eicosanoids

Arachidonic acid (AA) is released from phospholipids by receptor activation of one of three possible phospholipase enzymes (Figure 1.6b): PLA₂ directly from the phospholipid, and PLC and D indirectly from DAG (as previously mentioned) and PA respectively. The binding of glutamate to both ionotropic and metabotropic receptors has been shown to activate PLA₂ resulting in AA release (Dumuis, Pin, Oomagari, Sebben, & Bockaert, 1990; Dumuis, Sebben, Haynes, Pin, & Bockaert, 1988). Upon release arachidonic acid can act inside the cell, can diffuse through the membrane or it can be metabolised into eicosanoids which have a diverse spectrum of actions throughout the body.

AA has been shown to modulate the release of glutamate from synapses (Dickie, Stevens, & Davies, 1994; McGahon & Lynch, 1996), and is suggested to act as a retrograde signal in long-term potentiation (Cunha, Almeida, & Ribeiro, 2000; Piomelli, Shapiro, Feinmark, & Schwartz, 1987). However, O'Dell et al. proposed NO as the retrograde signal and not AA (O'Dell, Hawkins, Kandel, & Arancio, 1991). AA has been also reported to

differentially modulate the reuptake of glutamate by excitatory amino acid transporters (EAAT) depending on the type of EAAT present (Zerangue, Arriza, Amara, & Kavanaugh, 1995).

Arachidonic acid can be metabolised by a number of different enzymes resulting in a family of metabolites called eicosanoids; they include prostaglandins, thromboxanes, leukotrienes and hydroxyeicosatetraenoic acid (HETE) compounds. Prostaglandins and thromboxanes are derived from initial metabolism by COX and are generally termed prostanoids, whereas leukotrienes and HETEs result from metabolism by the numerous lipoxygenase enzymes (LOX pathway), as shown in Figure 1.7.

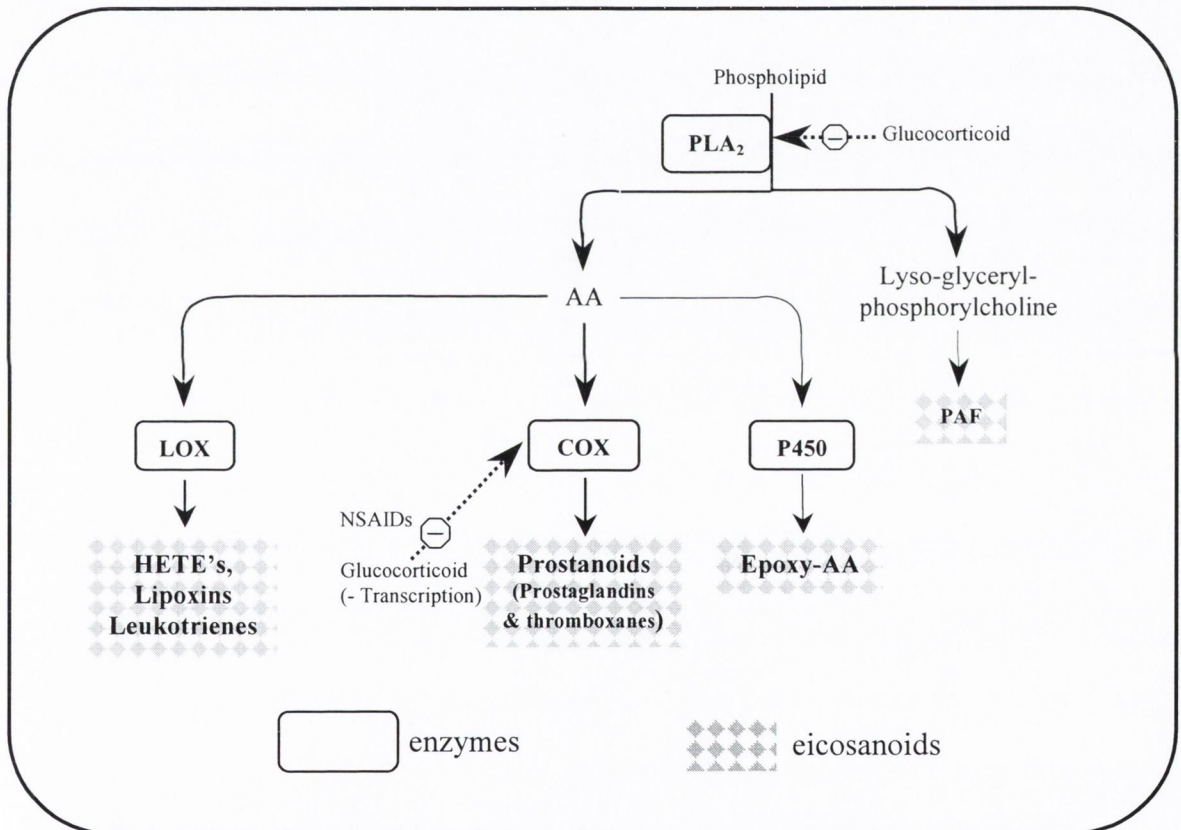


Figure 1.7 Arachidonic acid upon release is metabolised either by the COX family or the lipoxygenase (LOX) family of enzymes or to a lesser extent cytochrome P450.

1.1.3.2 Cyclooxygenase

Cyclooxygenase was first discovered in the 1970's when a breakthrough was made into the mechanism of action of aspirin (which has been used for over 100 years for analgesic and antipyretic qualities) (Vane, 1971). Cyclooxygenase produces prostaglandins (PG) in two steps by the biotransformation of AA. The first step generates PGG₂, an unstable intermediate, which is then rapidly converted into PGH₂ by the same enzyme in a peroxidase reaction. In 1991, it was reported that more than one isoform of COX existed and that the isolated protein (COX-2) had 60% amino acid sequence homology with COX-1 (D.A. Kujubu, Fletcher, Varnum, Lim, & Herschman, 1991; Xie, Chipman, Robertson, Erikson, & Simmons, 1991). More recently, COX-3 has been cloned along with other partial transcripts of the COX-1 gene (Chandrasekharan et al., 2002).

Cyclooxygenase	Gene of origin	Expression Characteristic	Function	Antagonists
COX-1	COX-1	Constitutively expressed	Involved in organ pain, platelet activation	Aspirin, indomethacin, ibuprofen, Sc58560
COX-3	COX-1	Constitutively expressed, particularly highly in brain	Possibly involved in sensing pain; little involvement in inflammation	Highly sensitive to acetaminophen; also inhibited by some NSAIDs
PCOX-1a	COX-1	Not known	Not known	Not known
PCOX-1b	COX-1	Not known	Not known	Not known
COX-2	COX-2	Induced by growth factors, neurotransmitters, inflammatory cytokines, oxidative stress, injury, inflammation, oxygen deprivation to the brain, seizure & neurodegeneration. Constitutively expressed in brain, kidney and other organs.	Inducible COX-2 causes inflammatory pain & fever; constitutive COX-2 is involved in synaptic plasticity	NSAIDs, selective Cox-2 inhibitors: celecoxib, rofecoxib, NS398, nimesulide etc. Curcumin (curry powder extract)

Table 1.1 Individual cyclooxygenase isoforms, genetics, expression, function and pharmacological antagonists; adjusted from (Bazan & Flower, 2002).

The genes for COX-1 and -2 are found on different chromosomes, come under separate regulation (Kraemer, Meade, & DeWitt, 1992; D. A. Kujubu, Reddy, Fletcher, & Herschman, 1993) and have different intracellular compartmentalisation (Morita et al., 1995). COX-1 is constitutively expressed in most tissues (Kaufmann, Andreasson, Isakson, & Worley, 1997); the rate-limiting step in its production of PGs is the release of AA from the lipid membrane (Kaufmann et al., 1997). The kinetics of its activity are co-operative in nature in that it requires the presence of a second molecule (feedback activation by

hydroperoxide) to hasten its rate of activity (W. Chen, Pawelek, & Kulmacz, 1999; Swinney, Mak, Barnett, & Ramesha, 1997). COX-2, on the other hand, is undetectable in non-neuronal tissue except under appropriate stimulation when it is upregulated 10-80 fold (Masferrer et al., 1994) and displays saturable kinetics. The expression of the COX-2 protein is tightly controlled at the transcription/translation level and thus its own concentration limits the production of PGs. In contrast to expression patterns in non-neuronal tissue, COX-2 is detectable at basal levels in the brain, in particular in the neocortex, hippocampus, amygdala and limbic cortices (Kaufmann, Worley, Pegg, Bremer, & Isakson, 1996; Yamagata, Andreasson, Kaufmann, Barnes, & Worley, 1993). Furthermore, COX-2 immunoreactivity (ir) has been localised to dendrites and dendritic spines - structures involved in synaptic signalling - on excitatory neurons (Kaufmann et al., 1996). Since PGs are lipid soluble they have the ability to diffuse across membranes to act intracellularly, or on neighbouring cells as 1st messengers (Shimizu & Wolfe, 1990; J. H. Williams, Errington, Lynch, & Bliss, 1989), in this way it is possible that the PGH₂ produced in response to COX-2 upregulation may act as a signal for neuronal activity. COX-2 and PGE₂ receptor binding share a similar pattern of distribution. Regions with relatively high density of PGE₂ binding are rich in neuronal cell bodies or synapses (as seen in the entorhinal cortex, and the molecular layer of the dentate gyrus and subiculum) (Matsumura et al., 1992).

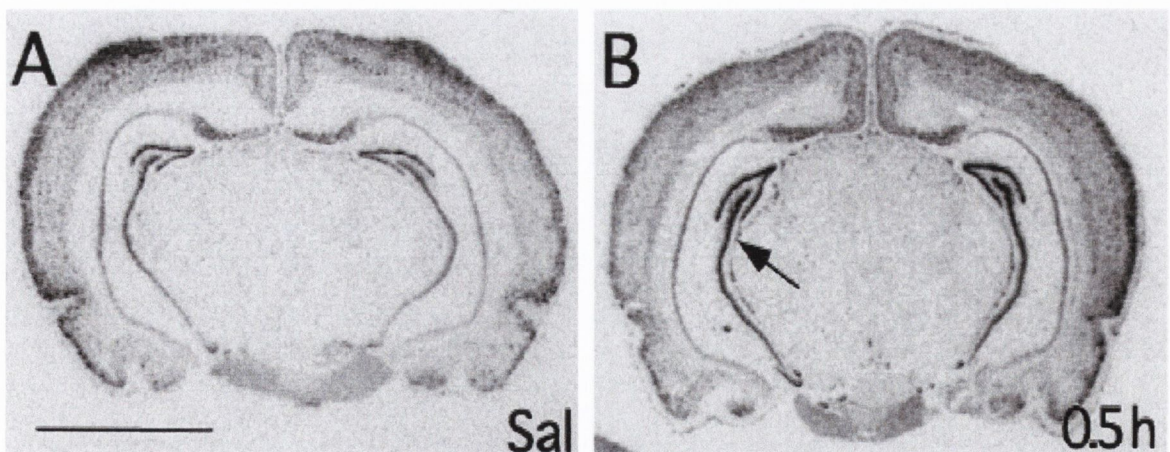


Figure 1.8 Representative autoradiographs showing COX-2 mRNA hybridization in animals sacrificed after A) saline injection, and B) 0.5 h after systemic LPS administration. A) Clearly shows that COX-2 mRNA is expressed at basal level in the hippocampal formation and B) shows its rapid induction in response to an inflammatory challenge (Quan, Whiteside, & Herkenham, 1998).

It has previously been shown that high frequency induced NMDA-dependent LTP augments COX-2 mRNA and protein levels, and the blockade of this increase by the NMDA-receptor antagonist MK801 suggests it is NMDA-receptor dependent (Yamagata et al., 1993). Similar COX-2 mRNA increases were observed with MECS, a synthetic activator of synapses, and acute stress induced by forced cold swim, a natural stimulus (Yamagata et al., 1993). Williams & Bliss showed that Ca^{2+} -induced LTP could be blocked with NDGA, an antagonist of both lipoxygenase and PLA2 demonstrating that arachidonic acid metabolites were involved in synaptic plasticity (J. H. Williams & Bliss, 1989). A more recent *in vitro* study showed that selective COX-2 inhibitors reduced postsynaptic membrane excitability and LTP induction, and that exogenous PGE2 reversed these effects (C. Chen, Magee, & Bazan, 2002). Broad-spectrum COX inhibitors (BSCI) impair passive avoidance memory in chicks and prevent the subsequent learning-induced PG release (Holscher, 1995a), and selective COX-2 inhibition impairs memory acquisition and consolidation in the hidden platform task in the watermaze (Rall, Mach, & Dash, 2003; Teather, Packard, & Bazan, 2002).

Shaw et al. showed that BSCI impaired acquisition of the watermaze task and LTP induction, and that these deficits were associated with a decrease in BDNF concentration. Furthermore, they showed that subjecting the animals to exercise increase BDNF concentrations and this was sufficient to reverse the BSCI induced impairments (Shaw, Commins, & O'Mara, 2003), giving circumstantial evidence of a link between COX and BDNF in learning processes. PGE₂, the main bi-product of COX activity, has also been shown to stimulate neurotrophin production, BDNF and NGF for example, in embryonic rat hippocampal co-culture of neurons and glia, and astrocytes in mouse (Friedman et al., 1990; Toyomoto et al., 2004). Elevated levels of PGE₂ and BDNF were reported in association with partial status epilepticus in rat hippocampus, furthermore BSCI with flurbiprofen abated these increases (Ajmone-Cat et al., 2006). All of the above evidence indicates an involvement of COX-2 activity and its products in signal transmission, synaptic plasticity and learning and memory, and an association between COX activity and BDNF production.

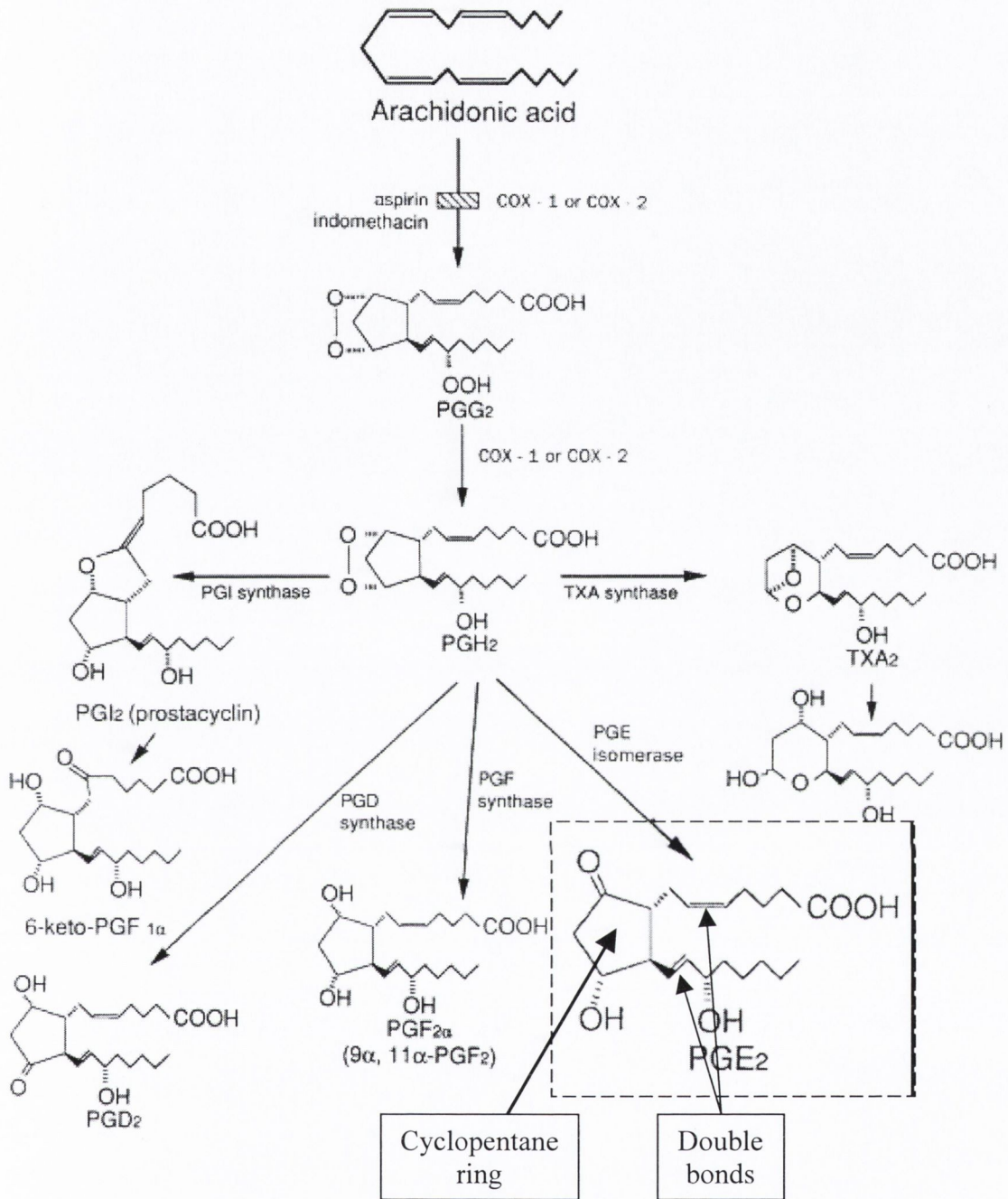


Figure 1.9 The arachidonic acid cascade showing the classic prostanoid structure of the cyclopentane ring and the two side-chains; note the presence of two double bonds on the side-chains of all of these prostanoid originating due to their formation from arachidonic acid.

The main function of cyclooxygenase is the synthesis of prostanoids – which consist of prostaglandins and thromboxanes – from arachidonic acid, a C-20 unsaturated fatty acid liberated from membrane fatty acids in response to many pathological and physiological stimuli. There are five main bioactive prostanoids: PGD₂, PGE₂, PGF_{2α}, PGI₂ and thromboxane A₂ (TXA₂). The basic structure of the prostanoids consists of a cyclopentane ring and two side chains α and ω as evident in Figure 1.9. The nomenclature of the

prostanoids is based on modifications to these structures; they are labelled A-I for possible changes to the ring structure (A, B, and C are thought not to exist endogenously) and subscripted 1-3 for the number of double bonds in the side chains. The precursor molecules determine the number of double bonds, series 1,2 and 3 being synthesised from γ -homolinolenic acid (γ HLA), AA and eicosapentanoic acid (EPA) respectively. COX-2 but not COX-1 can metabolise dihomo- γ -linolenic acid (DGLA) (a metabolite of γ HLA) to produce series one prostaglandins, e.g. PGE₁ which has been shown to have anti-inflammatory properties compared to PGE₂. Since COX-2 can generate both pro- and anti-inflammatory prostanoids, it is the relative abundance and the release of the lipid precursor in the membrane that determine the physiological outcome. As arachidonic acid is the most abundant of the three precursors it follows that so too are the series 2 prostanoids, however it has been shown that dietary and chemical manipulations of precursor composition of membranes can decrease pathogenic inflammation in conditions such as Alzheimer's disease and arthritis. Being derived from phospholipids, prostanoids are highly lipid soluble and can diffuse easily through membranes, (e.g. the nuclear envelope, brain parenchyma, blood vessel endothelium), however carrier-mediated reuptake leads to their very rapid catabolism and inactivation by 'prostaglandin specific' enzymes, limiting their diffusion, and thus they act as autacoids. They are not found preformed in tissue but are synthesised *de novo*, the initial rate limiting step being the release of the relevant phospholipid precursor from the membrane, thus they have very short half-lives ($t_{1/2}$) and are typically present for <1min in tissue. The estimated $t_{1/2}$ of PGE₂ is less than 15 seconds.

1.1.3.3 Prostaglandins

The word prostaglandin comes from the misconception that a component of semen reported to cause uterine smooth muscle contractions, was a product of the prostate gland. It was later discovered that these "prostaglandins" were ubiquitously found in the body and that they had many and varied actions from smooth muscle contraction and relaxation, stimulation and inhibition of neurotransmitter release, febrile response and sleep induction to name but a few. Furthermore, this diversity of activity could be found even within one specific prostaglandin. For example, PGE₂ can cause blood vessel dilation but constriction of the trachea. This led to the postulation that there were multiple prostaglandin receptors and that activity was determined by the distribution of the specific receptors.

Approximately 20 types and splice variants of prostanoid receptor have been cloned and characterised: DP, EP₁₋₄, FP, IP and TP for prostanoids PGD₂, PGE₂, PGF_{2α}, PGI₂ and TXA₂ (Table 1.2) respectively amongst others. To further complicate matters each prostanoid can bind to prostanoid receptors other than their namesake, but with a lesser affinity. The type of prostanoid released by a cell and its subsequent function in the tissue is dictated by the ratio of 1) lipid precursor in the membranes, 2) the presence of specific synthases, 3) the class of prostanoid receptor and splice variant present, and 4) the g-protein coupled to the intracellular C-terminal domain and consequent signalling pathway. This leads to hugely diverse functions of prostanoids in tissues and require tight regulation and the net effect of their actions depending on the balance of their opposing affects.

Prostanoid synthases and metabolic enzymes

As shown in Figure 1.10 the initial steps in the metabolism of AA into prostanoids is performed by cyclooxygenase resulting in the unstable intermediary molecule PGH₂. Synthesis of specific prostanoids from this precursor involves a family of secondary enzymes called synthases (e.g. PGDS, TxS, PGES etc.). The first of these synthases was identified in 1999 by Jakobsson et al., who reported that a human microsomal glutathione-S-transferase (GST)-1-like 1 superfamily had the ability to convert PGH₂ to PGE₂ (Jakobsson, Thoren, Morgenstern, & Samuelsson, 1999). This protein was located only in the membrane fraction and not the cytosolic fraction of *E. Coli* and is now called membrane-bound prostaglandin E synthase-1 (mPGES-1). Since then, multiple types of prostanoid synthase have been described as evident from Figure 1.10. With respect to PGE₂ synthesis there are five main types classified: mPGES-1, cytosolic (c)PGES, mPGES-2 and μ class of glutathione S-transferase (GST). mPGES-1 couples favourably with COX-2 – compared to COX-1 – to convert AA into PGE₂. Importantly, mPGES-1 can be inhibited with the COX-2 inhibitor NS398 with an IC₅₀ approximately two orders of magnitude higher. cPGES in contrast couples with COX-1 and mPGES-2 can be coupled to both COX-1 and -2 (as reviewed by (Murakami & Kudo, 2004).

In the periphery the half-life ($t_{1/2}$) of prostanoids is of the order of seconds; PGE₂ is so rapidly degraded that direct measurement is not possible to determine its half-life and so is estimated as being less than 15 seconds. The presence of the enzyme 15-

hydroxyprostaglandin dehydrogenase (15-PGDH) is the rate-limiting enzyme in the degradation of prostaglandins (Bygdeman, 2003).

Prostanoid receptor classification

The prostanoid receptors all belong to family A, group V of G-protein coupled receptors (GPCRs). These receptors consist of seven transmembrane domains, responsible for the specificity of ligand binding, and an internal C-terminal domain thought to determine the intracellular signalling pathway, agonist binding induced phosphorylation, desensitisation and internalisation. The group five GPCRs in general signal via stimulation of phospholipase C (PLC), generating DAG & IP₃ or inhibition of adenylyl cyclase and a resultant decrease in cAMP. Furthermore, different splice variant of the C-terminals of each receptor can result in alterations in the above characteristics; as can be seen from Table 1.2 the splice variants of the intracellular C-terminus of the EP₃ receptor interact with G_s, G_i or G_q which either stimulate or inhibit adenylyl cyclase or activate PLC, respectively (for reviews see (Breyer, Bagdassarian, Myers, & Breyer, 2001; Hata & Breyer, 2004; Narumiya, Sugimoto, & Ushikubi, 1999)).

Until very recently, there was virtually no information regarding the cellular localisation, temporal expression pattern of the individual isoforms of the EP receptor in the hippocampus, except for two papers reporting that EP₄ mRNA was practically absent (Takadera, Shiraishi, & Ohyashiki, 2004; Zhang & Rivest, 1999). A comprehensive profile of EP-receptor expression and regulation showed heterogeneous expression throughout the hippocampus – mainly in neurons both pre- and postsynaptically, but also in astrocytes – with differential expression in response to neuronal activity including LTP induction (Zhu et al., 2005). Expression of EP₁ and EP₂ in the cytoplasm and nucleus suggest they may regulate gene expression. Co-localization of EP_{1,2} and EP₃ with synaptophysin, a pre-synaptic protein, in hippocampal cultured cells, suggests these EPs receptors are presynaptic, while EP₃ double-immunostaining with PSD-95 is indicative of postsynaptic expression. EP₂ and EP₄ were upregulated in response to HFS-LTP in both the perforant path and Shaffer collateral, as measured at four hours suggesting their importance in LTP (Zhu et al., 2005).

Type	Subtype	Isoform	G Protein	Second Messenger
DP			G _s	cAMP ↑
EP	EP ₁		Unidentified	[Ca ²⁺] _i ↑
	EP ₂		G _s	cAMP ↑
	EP ₄		G _s	cAMP ↑
	EP ₃	EP _{3A}	G _i	cAMP ↓
		EP _{3B}	G _s	cAMP ↑
		EP _{3C}	G _s	cAMP ↑
		EP _{3D}	G _i , G _s , G _q	cAMP ↓, cAMP ↑, PI response
FP			G _q	PI response
IP			G _s , G _q	cAMP ↑, PI response
TP	TP _α		G _q , G _i	PI response, cAMP ↓
	TP _β		G _q , G _s	PI response, cAMP ↑

Table 1.2 Signal transduction of prostanoid receptors. PI, phosphatidylinositol; ↑, increase; ↓ decrease. Taken from Narumiya et al 1999 (Narumiya et al., 1999).

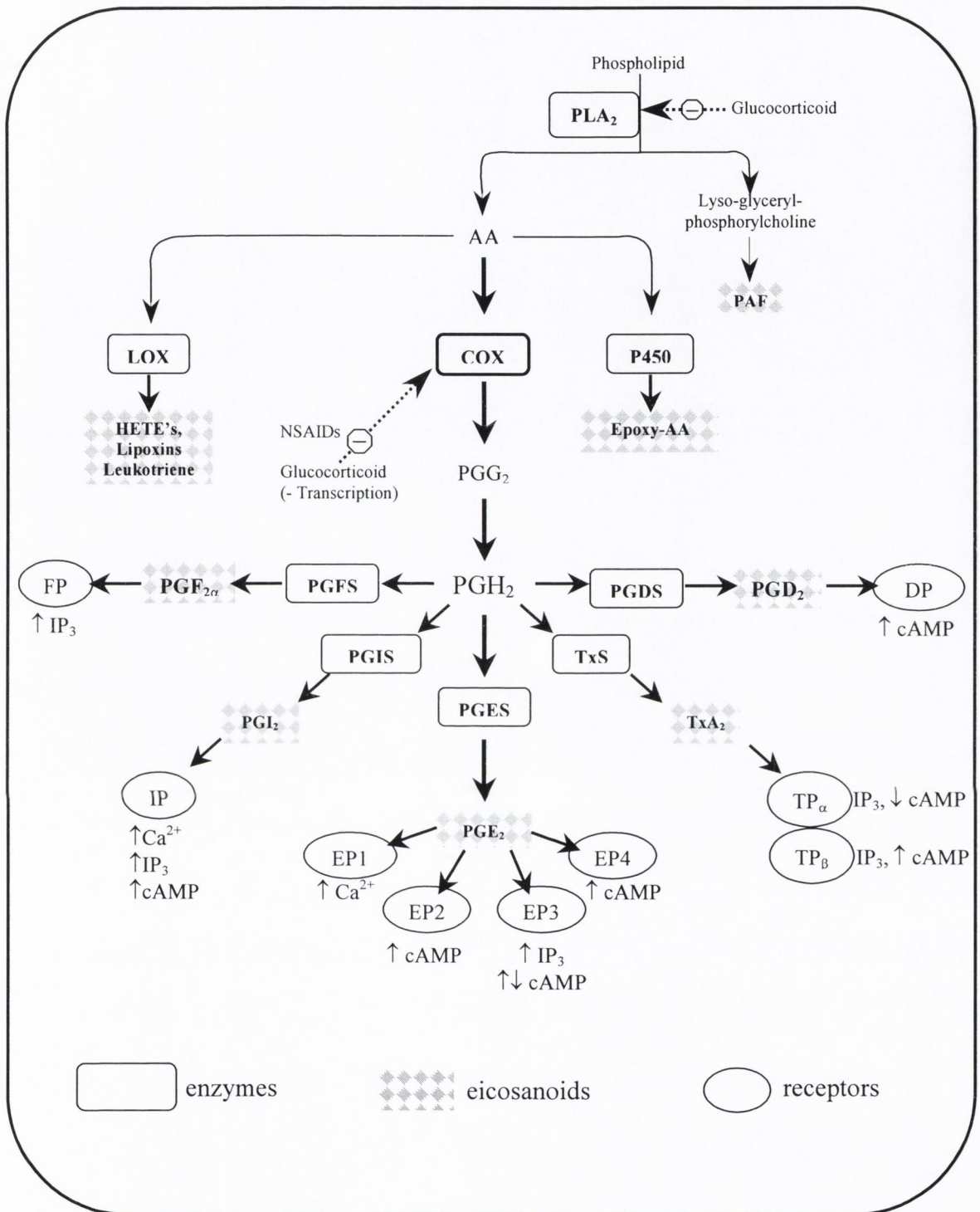


Figure 1.10 The arachidonic acid cascade: arachidonic acid metabolites are called eicosanoids (chequered boxes). The thick arrows highlight the cyclooxygenase pathway and resultant prostanoids. Dotted lines represent inhibition. Adapted from (Sales & Jabbour, 2003).

1.1.3.4 Pharmacology of COX inhibitors

As mentioned aspirin has been used for the treatment of inflammation, pyrexia and pain for over 100 years, and only in the 1970s was COX discovered as its site of action (Vane, 1971). Aspirin belongs to a family of drugs termed Non-Steroidal Anti-Inflammatory Drugs (NSAIDs), which includes other household names such as acetaminophen (paracetamol) and ibuprofen. The COX-1 isoform is constitutively expressed in almost every cell and tissue types compared to COX-2, which is highly inducible in response to inflammatory signals, but is also constitutively expressed at low levels in restricted cell and tissue types. Thus, the use of NSAIDs can prevent the formation of prostanoids required for physiological functions, as well as those responsible for inflammation. Prolonged use of aspirin can cause dyspepsia and, more seriously, ulceration and bleeding of the gastrointestinal tract (GIT) due to its inhibition of the COX-1 isoform, resulting in the secretion of excess acid and the loss of protective prostaglandins from the GIT. NSAIDs can also cause decreased renal blood circulation due to a loss of prostaglandins responsible for renal blood vessel dilatation. This can lead to renal insufficiencies, water retention, hypertension and some times kidney failure, especially in patients with reduced renal function. A loss of PGE₂-induced smooth muscle dilatation, and an overflow of AA-metabolism from the inhibited COX pathway to the LOX pathway (cf. Figure 1.7) can result in bronchoconstriction and trigger asthmatic events; reviewed by (Dannhardt & Kiefer, 2001). Thus, since the discovery of more than one isoform of COX, boundless research and money has been ploughed into designing new NSAIDs with isoform specificity and hence less side effects.

Specificity of a COX antagonist is conferred by swapping two bulky isoleucine residues at positions 434 and 523 in COX-1 for valine residues in COX-2, resulting in an enlarged binding site and exposing an additional side-pocket in the COX-2 enzyme, access to which is required for COX-2 selectivity. These structural differences are genetically encoded.

The current classification of COX inhibitors was introduced by Kurumbail (Kurumbail et al., 1996) and is based on the interaction of the drugs with the enzyme protein structure:

- 1) ***Irreversible inhibitors of COX-1 or COX-2.*** Aspirin covalently binds to and irreversibly acetylates a serine residue preventing AA from accessing the enzymes catalytic site.

- 2) **Reversible, competitive inhibitors of COX-1 and COX-2.** These are a group of drugs that compete with AA for the catalytic site e.g. ibuprofen, piroxicam or mefenamic acid.
- 3) **Slow, time-dependent, reversible inhibitors of COX-1 and COX-2.** These compounds form ionic bonds with the arginine residue of the enzyme reducing the flexibility of the protein e.g. indomethacin and flurbiprofen.
- 4) **Slow, time-dependent, irreversible inhibitors of COX-2.** The irreversible binding of COX-2 by celecoxib and rofecoxib increases with time, but they are also weak competitive inhibitors of COX-1.

COX-2 antagonists are a heterogeneous group in that they belong to different structural classes:

- 1) Diaryl- or aryl-heteroaryl-ethers: nimesulide, NS-398, flosulide, L-745337.
- 2) Vicinal diaryl heterocycles: celecoxib, rofecoxib, SC-57666, DuP-697.
- 3) Known NSAIDs modified to improve COX-2 selectivity: meloxicam, etodolac.
- 4) Antioxidant compounds.
- 5) 1,2-Diarylethylene derivatives

These different structures determine important characteristics such as isozyme specificity, lipophilicity and solubility (celecoxib is not soluble in aqueous solution and so is only administered orally and not parenterally). The ratio of IC_{50} (the molar concentration of an antagonist, which produces 50% of the maximum possible inhibitory response for that antagonist) for COX-1/COX-2 is generally used to show isozyme specificity, however a number of different assays had been used to determine the IC_{50} values. This lead to very different values for the same drug in different assay systems e.g. indomethacin ranged from a 14-fold more selective COX-1 to only 2-fold (Dannhardt & Kiefer, 2001). Another example would be the similar affinity of celecoxib for COX-1 and COX-2 when measured without prior incubation, however there is a slower, time-dependent process, which contributes more to the selectivity for COX-2 (Gierse, Koboldt, Walker, Seibert, & Isakson, 1999). Warner et al. (1999) systematically tested over 40 known COX inhibitors using a standard assay and compared the effects of these drugs on COX-1 when 80% of the COX-2 isoform was inhibited (c.f. Figure 1.11) (Warner et al., 1999).

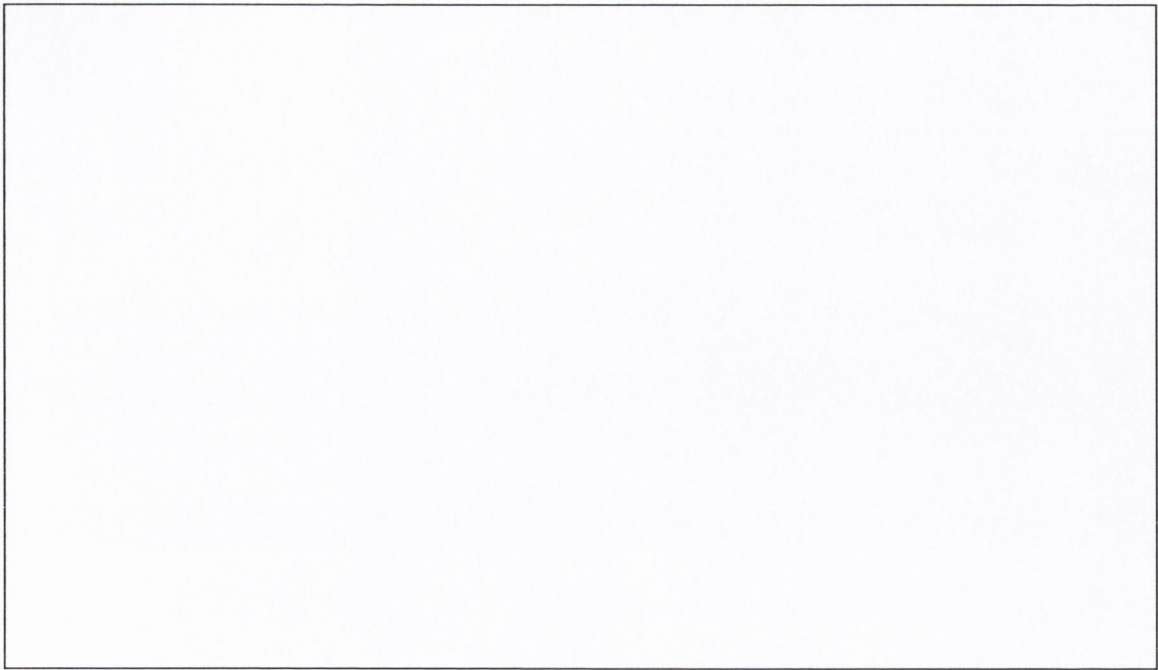


Figure 1.11 Analysis of the percent inhibition of COX-1 seen when COX-2 is inhibited by 80%. The dotted line indicates equiactivity, i.e., an 80% inhibition of COX-1 (Warner et al., 1999).

Apart from their ability to inhibit cyclooxygenase-activity these drugs have other, less known idiosyncratic activities. Several NSAIDs have been reported to have anti-inflammatory activity independent of COX and prostaglandin synthesis inhibition e.g. ibuprofen and flurbiprofen, moreover, celecoxib has been reported to lose its anti-inflammatory efficacy at high doses (cf. Figure 1.12). These effects are mediated through alterations in transcription factors such as NF- κ B, and intracellular signalling kinases such as ERK (Niederberger et al., 2001; Tegeder, Pfeilschifter, & Geisslinger, 2001). Celecoxib was also shown to increase nuclear translocation of the glucocorticoid receptor (GR) increasing its binding to DNA, thus driving GR-mediated gene transcription, in association with p38 MAP kinase inhibition (Hu, Wang, Pace, Wu, & Miller, 2005). Moreover, both COX isozymes have been shown to decrease the secretion of ACTH in response to adrenergic-stimulation and thus decrease the associated release of corticosterone, also selective COX-2 inhibition with celecoxib in aged rats was shown to decrease corticosterone (Bugajski, Glod, Gadek-Michalska, & Bugajski, 2001; Casolini, Catalani, Zuena, & Angelucci, 2002).

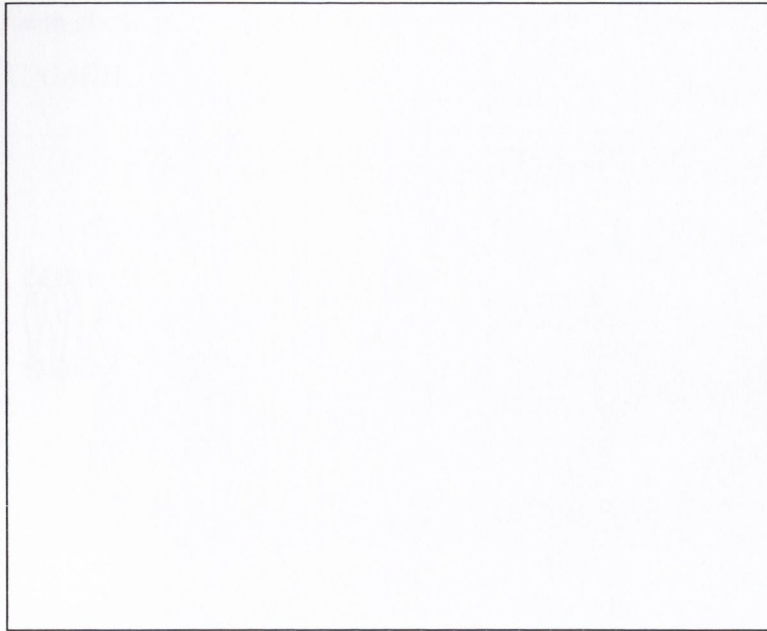


Figure 1.12 A possible mechanism by which celecoxib at high doses loses its anti-inflammatory activity via its activity on NF- κ B. Activation (+), inhibition (-), \downarrow reduction, \leftrightarrow no change (Niederberger et al., 2001).

1.1.4 ERK and intracellular signalling

ERKs (Extracellular signalling-Regulated Kinase) are serine/threonine kinase, whose targets include transcription factors, cytoskeletal proteins, regulatory enzymes and other kinases. Activation of ERK requires phosphorylation by MEK (MAPK/ERK), at two sites, a tyrosine and a threonine residue. This results in global and local conformational changes, with closure of the active site and exposure of the catalytic site (Cobb & Goldsmith, 1995).

The classic pathway for the activation of ERK requires activation and tyrosine autophosphorylation of growth factor receptor-tyrosine kinase. This leads to elevated levels of GTP-bound Ras, its active form (Ras usually exists in a GDP-bound inactive state); this can occur due to decreased GTPase activity or increased gyanyl nucleotide exchange factor activity. Ras-GTP then activates the protein kinase Raf, which in turn phosphorylates and activates MEK (reviewed by (Platenik, Kuramoto, & Yoneda, 2000; G. M. Thomas & Haganir, 2004) and see Figure 1.13). This pathway although originally associated with cell differentiation was also shown to occur in neurons in response to neurotrophic factors. Activation of ERK has multiple downstream effects including translocation to the nucleus (Boglari, Erhardt, Cooper, & Szeberenyi, 1998) and activation of transcription factors resulting in gene expression; this has been associated with the transition from STP to LTP (Davis & Laroche, 1998). NMDA receptor activation has also

been shown to initiate the MAP-kinase cascade in response to Ca^{2+} -entry and activation of CAMKII (Platenik et al., 2000).

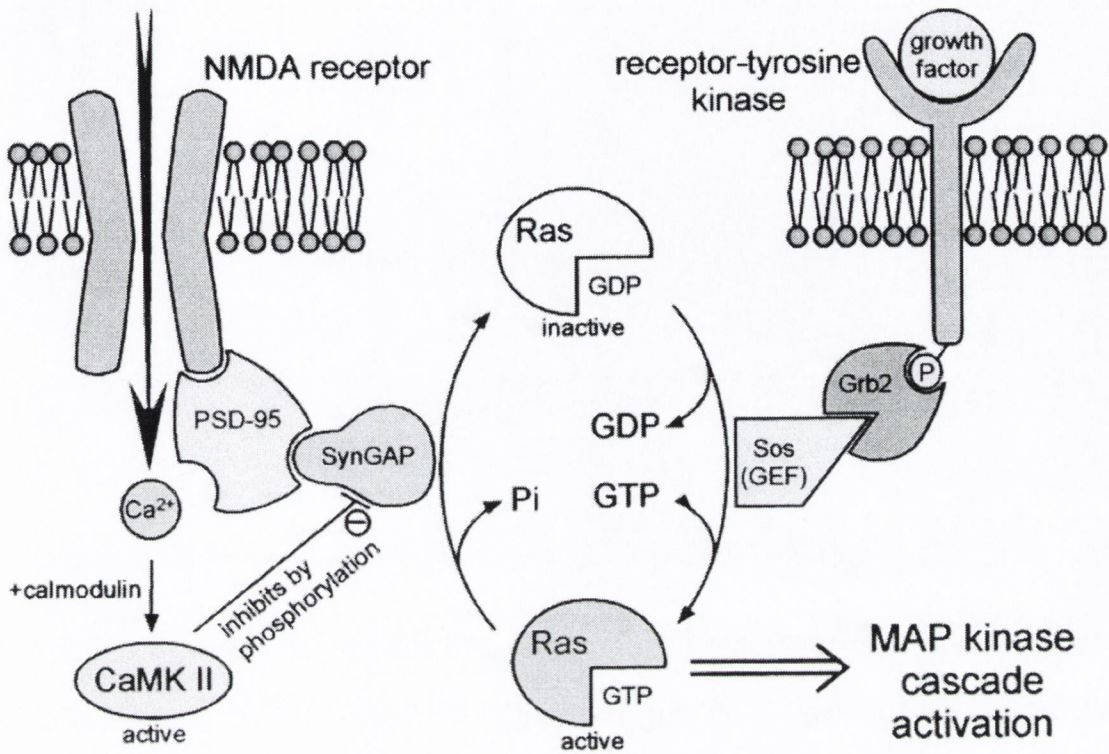


Figure 1.13 Activation of the MAP-kinase cascade in response to NMDA and growth factor receptor activation; taken from (Platenik et al., 2000).

The first report of a role for ERK in LTP was published by English & Sweatt in 1997 showing that ERK inhibition resulted in LTP impairment in the hippocampus (English & Sweatt, 1997). Furthermore, it was shown that in dentate gyrus tissue from rats that had either undergone training in the watermaze or LTP showed equivalent changes, whereby stimulated release of BDNF, TrkB-phosphorylation, ERK-phosphorylation and glutamate release were all increased (Gooney et al., 2002). This paper reported that exogenous BDNF increase TrkB- and ERK-phosphorylation, suggesting that BDNF is responsible for increase ERK-phosphorylation as a result of TrkB activation in response to learning processes. This activation of ERK by BDNF has been reported previously in cultured hippocampal neurons (Marsh et al., 1993). Most relevant to this thesis, ERK-phosphorylation has been implicated in the induction – but not the maintenance – of multiple forms of LTP, in particular HFS-LTP in the dentate gyrus (Coogan, O'Leary, & O'Connor, 1999).

1.1.5 Transcription factors

The expression of genes, for the proliferation, development, maturation and function of all cells, is under the control of nuclear proteins called transcription factors. When genes are expressed, they can be so in a rapid and transient manner (these have been called *immediately-early genes*) or with a lag (*delayed-response genes*). Some immediate-early genes (IEGs) are actually transcription factors that regulate the expression of the delayed-response genes. IEGs have been implicated in the transition from E-LTP to protein synthesis-dependent L-LTP.

Transcription factors have been classified by particular motifs in their protein structures, consisting mainly of α -helices and β -sheets, which enable the proteins to bind to the major and minor grooves of the DNA strands: 1) basic domain, 2) Helix-turn-helix 3) β -Scaffold factors with minor groove contacts 4) Zinc-finger and 5) other unspecified transcription factors. These categories can be further subdivided, for example, the basic domain factors are further classified by whether they contain a leucine-zipper motif, a helix-loop-helix motif, or a combination of these. The main transcription factors involved in hippocampal function are those containing basic domains (AP-1 and CREB), zinc-finger (glucocorticoid receptor) and β -scaffold factors (NF- κ B) (Hinoi, Balcar, Kuramoto, Nakamichi, & Yoneda, 2002). The following review will focus on c-Fos, a component of the dimeric transcription factor AP-1 and as an IEG, the regulation of its transcription in response to LTP induction.

c-Fos belongs to the family of immediate-early genes, and as such is rapidly transcribed by proteins already present in the cell, that is, new protein synthesis is not required and so their transcription is not blocked by protein synthesis inhibitors. It is often used as a marker of synaptic activity due to its rapid up-regulation; maximal expression is seen after 30 minutes to an hour after LTP induction (Davis & Laroche, 1998). Moreover, *c-Fos* mRNA is one of the most short-lived mammalian mRNAs, persisting only 30-45 minutes after the period of transcription has ended and is degraded rapidly upon arrival in the cytoplasm (Greenberg & Ziff, 1984; Schiavi et al., 1994). The c-Fos protein transcriptional activity is increased by phosphorylation by the c-Fos-regulating kinase, ERK and RSK (ribosomal S6 kinase) (X. C. Huang, Deng, & Sumners, 1998). Interestingly, c-Fos can act as a transrepressor of its own transcription i.e. c-Fos protein negatively feeds back on its own

transcription upon activation by ERK and RSK-mediated phosphorylation (R. H. Chen, Abate, & Blenis, 1993).

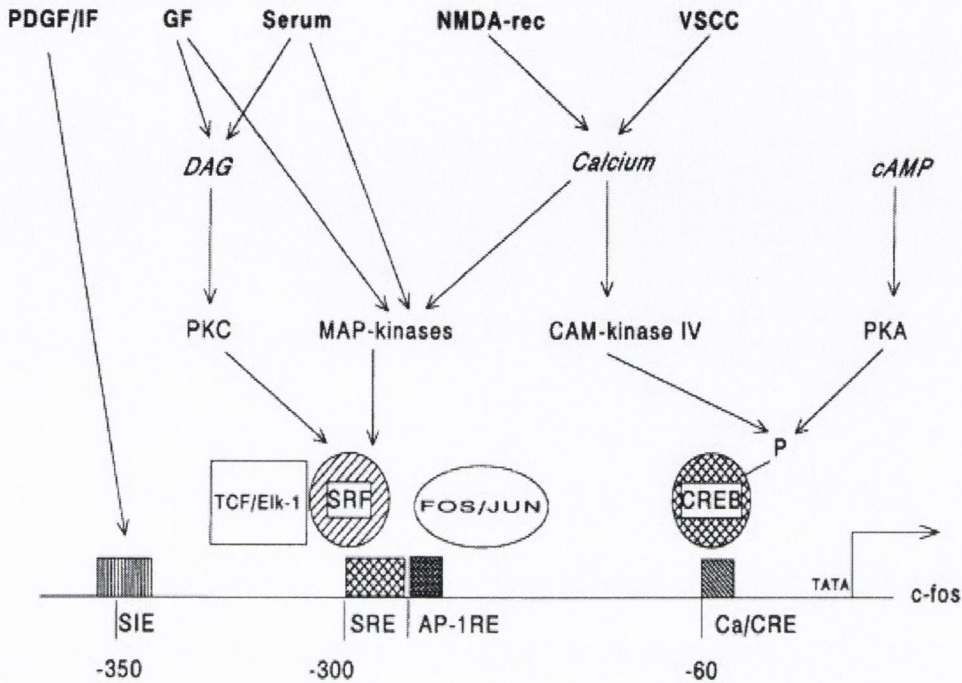


Figure 1.14 Link between NMDA receptor, MAP-kinase cascade and *c-Fos* transcription (Kovacs, 1998).

Several elements responsible for the regulation of the *c-Fos* gene are located in the 5' prime untranslated region: a cAMP-response element (CRE), a serum response element (SRE), and AP-1 site and a c-Sis-inducible element (SIE) (see Figure 1.14). These regulatory sequences interact with various transcription factors, for instance the ternary complex factor Elk-1, which is activated by ERK, interacts with the SRE and activated CREB binds to the CRE site, driving *c-Fos* transcription. However, all of the elements are highly interdependent and thus it is difficult to ascribe a particular element to a particular stimulus and associated pathway (Robertson et al., 1995). NMDA-driven transcription of *c-Fos* requires activation of the SRE by ERK phosphorylation of Elk-1; CRE activation is insufficient (Xia, Dudek, Miranti, & Greenberg, 1996) (reviewed by (Platenik et al., 2000)) and is dependent on an increase in $[Ca^{2+}]_i$ (Lerea, Butler, & McNamara, 1992).

1.1.6 Objectives of this thesis

Given the increase in prevalence and the devastating effects that all types of neuroinflammation can have on individuals and families it is pertinent that the role of the mediators of inflammation play in normal as well as pathological conditions be investigated. The author aims to define the isoform-specific roles of cyclooxygenase, and metabolites, in baseline synaptic transmission, short-term potentiation and a commonly used model of learning, long-term potentiation, *in vivo*. In association, the previously proposed relationship between LTP, BDNF and broad-spectrum COX inhibition (Shaw et al., 2003) will be investigated with respect to isoform selective antagonism. Moreover, the question of whether COX metabolites are involved in merely the induction of LTP or whether their actions carry over into the maintenance of LTP will be addressed.

As celecoxib is used therapeutically, two different concentrations will be compared to determine any dose dependency of the effects, and thus if there is any therapeutic relevance to the findings.

Temporal changes in intracellular signalling pathways will also be investigated downstream of LTP induction.

**Chapter 2 Cyclooxygenase: baseline synaptic
transmission and short-term
plasticity**

Chapter 2	Cyclooxygenase: baseline synaptic transmission and short-term plasticity	50
2.1	Introduction.....	52
2.2	Materials & methods.....	56
2.2.1	Animals.....	56
2.2.2	Materials	56
2.2.3	Pharmacological treatment schedules.....	56
2.2.4	Surgery.....	57
2.2.5	Input/output curves	58
2.2.6	Paired-pulse protocol.....	58
2.2.7	Bradford assay	59
2.2.8	BDNF ELISA	59
2.2.9	Analysis and statistics.....	60
2.3	Results.....	62
2.3.1	Input/output curves	62
2.3.1.1	Slope analysis	62
2.3.1.2	Population spike analysis.....	65
2.3.1.3	Excitability ratio	67
2.3.2	Paired-pulse ratio	69
2.3.3	BDNF concentration.....	71
2.3.3.1	Input/output curve BDNF	71
2.3.3.2	Paired-pulse BDNF.....	72
2.4	Discussion.....	74

2.1 *Introduction*

While searching for genes that were rapidly induced in response to seizure Yamagata and colleagues (1993), in a landmark paper, found elevated mRNA for the COX-2 isoform with similar kinetics to immediate early genes (IEG) upon stimulation. This isoform had only been recently described and shown to be distinct from COX-1 (D.A. Kujubu et al., 1991; Xie et al., 1991). Furthermore they found that COX-2 mRNA was present at basal levels prior to the induction of seizure. Thus in contrast to the periphery where unstimulated levels of COX-2 are undetectable in most tissues, it appeared that COX-2 had a function in basal synaptic activity. This hypothesis was investigated further and it was demonstrated that basal expression of COX-2 mRNA could be rapidly and reversibly decreased by NMDA receptor antagonism with MK801, in both mature and developing brains. Additionally, visual deafferentation by injection of tetrodotoxin (a Na⁺ channel blocker) into the eye also reduces COX-2 mRNA in the visual cortex, together indicating that the expression of this enzyme is under the regulation of homeostatic synaptic transmission in the brain (Yamagata et al., 1993). COX-2 mRNA and immunoreactivity (ir) showed widespread, yet discrete, expression throughout the CNS. This discreteness was apparent on many levels, regionally: highest concentrations were evident in forebrain structures, namely neocortex, allocortices, amygdala and hippocampus. Not all neurons in these regions were positive for COX-2, and within neurons COX-2 was not present in the nucleus but was in dendrites and dendritic spines (Breder, Dewitt, & Kraig, 1995; Kaufmann et al., 1996; Yamagata et al., 1993). These subpopulations of neurons positive for COX-2 were shown to co-localise with markers for excitatory neurons: glutamate, CAMKII and SMI-32, but not with markers of inhibitory GABAergic neurons (CaBP and PV) (Kaufmann et al., 1996). COX-2 mRNA and ir developmental expression coincide with activity-dependent synaptic remodelling. In the brains of COX-2 knockout mice, a compensatory upregulation of COX-1 has been reported which is not seen in any other tissue where COX-2 is constitutively expressed, providing further evidence for the functional importance of COX-2 in the brain (Zhang, Goorha, Raghov, & Ballou, 2002). In brief, COX-2 localisation to dendritic spines of excitatory neurons, with the rapid induction kinetic of an IEG, and sensitivity to NMDA receptor activation implicate COX-2 and its metabolites in basal and stimulated synaptic function.

Paired-pulse facilitation and depression are defined as the increase or decrease, respectively, in size of a second response relative to the first response to a pair of stimuli given in quick succession (less than 1000ms); these are forms of short-term plasticity. Paired-pulse depression (PPD) is characteristic of the medial perforant path (MPP) and is in fact used as a means of confirming electrode positioning (McNaughton, 1980). There are three phases of depression observed in the MPP; 1) a large depression at short inter-stimulus intervals (ISI), 2) 10-50ms, at intermediate intervals 50–200ms a reduction of this depression and 3) a sizeable depression at more delayed intervals >200 ms (DiScenna & Teyler, 1994). The size of the second EPSP relative to the first is determined by a delicate balance of two parallel but conflicting processes:

1. Facilitation of the second response due to residual Ca^{2+} in the presynaptic nerve terminals from the first action potential, resulting in increased release of neurotransmitter (Zucker, 1999; Zucker & Regehr, 2002).
2. Inhibition by inhibitory interneurons (Lømo, 1971b; E. I. Moser, 1996)

Fast inhibitory postsynaptic potentials (IPSP) mediated by GABA_A predominate in the first phase of depression but not in the long-latency, third phase (Albertson & Joy, 1987; Tuff, Racine, & Adamec, 1983). At about 25ms ISI the inhibitory interneurons themselves undergo inhibition, lasting for 200-350ms, relieving GABA_A inhibition resulting in the second phase of reduced depression (Brucato, Mott, Lewis, & Swartzwelder, 1995). There is conflicting evidence for the slower third phase of inhibition's dependence on GABA_B (Kahle & Cotman, 1993). Paired-pulse short-term plasticity, facilitation or depression, is a presynaptic phenomenon; synapses that undergo paired-pulse depression have a high probability of neurotransmitter release for the first response resulting in depleted neurotransmitter for the second. This type of short-term plasticity may be a mechanism of processing information as it enters the hippocampus via the perforant pathway (E. I. Moser, 1996).

Although COX-2 it has been localised to excitatory postsynaptic dendrites and dendritic spine, the metabolites of COX-2 activity are highly diffusible with the potential to diffuse intra- or extracellularly and act pre- or postsynaptically or even on non-neuronal targets such as glial cells (Bezzi et al., 1998; Bezzi & Volterra, 2001). By blocking the influence of GABA_A inhibition with bicuculline unmasking facilitation in the MPP – a protocol commonly used *in vitro* – Chen *et al* (2002) showed that the resultant PPF was not affected by selective COX-2 inhibition. Since PPF is a presynaptic phenomenon (Isaac et al., 1998;

Zucker & Regehr, 2002), Chen concluded that COX-2 metabolites do not act presynaptically. The range of ISIs employed was very narrow (80-100ms for maximal facilitation) and the use of bicuculline prevented the author from looking at alterations in PPD, which predominates in the MPP. Furthermore, they argued that since the rate and amplitude of miniature EPSPs (mEPSP), were unaffected by PGE₂, applied postsynaptically via the recording pipette, that PGE₂ did not function as a retrograde messenger modulating long-term synaptic plasticity, as proposed for its precursor arachidonic acid (J. H. Williams et al., 1989). Miniature EPSPs are a measure of the spontaneous release of presynaptic vesicles even when all action potentials have been eliminated with TTX (tetrodotoxin), a voltage gated sodium channel blocker. Changes in frequency of mEPSPs reflect changes in presynaptic transmitter secretion, while changes in mEPSP amplitude show modulation of postsynaptic response (Bouron, 2001); mEPSPs occur at low frequencies, reflecting the low probability of spontaneous vesicle release (Bouron, 2001).

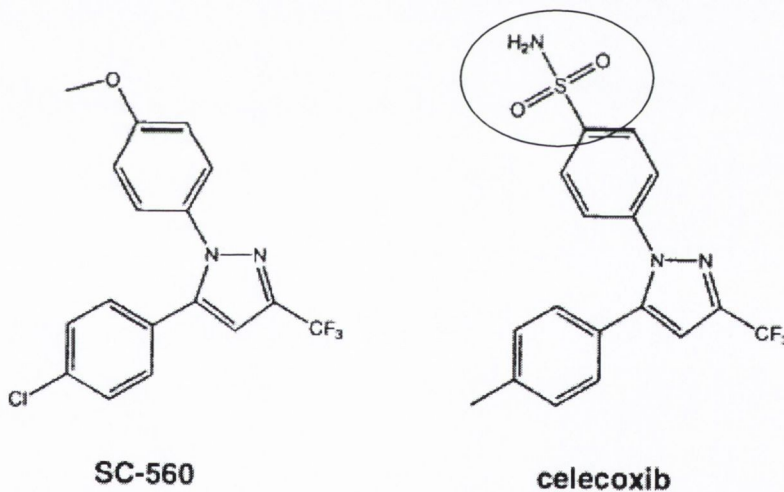


Figure 2.1 Chemical structures of Sc560 and celecoxib. Note the overall the structures are very similar except for the presence of a bulkier sulphonamide group (circled) on the celecoxib molecule that causes steric hindrance and prevents binding to the COX-1 isoform (C. J. Smith et al., 1998).

In the following experiments we employed two selective antagonists, Sc-560 (5-(4-chlorophenyl)-1-(4-methoxyphenyl)-3-trifluoromethylpyrazole) and celecoxib, for the COX-1 and -2 isoforms, respectively. The structures of these compounds are very similar (Figure 2.1), but the most notable difference is the bulky sulphonamide group on the celecoxib molecule, which confers its selectivity for COX-2 by to steric hindrance, fitting into a side-pocket in the COX-2 protein that is not present on the COX-1 isoform.

Pharmacokinetic analysis shows very similar volumes of distribution for both compounds (Teng, Abu-Mellal, & Davies, 2003), their high lipophilicity promoting their uptake by the brain. Sc-560 is a highly selective COX-1 inhibitor: COX-1 $IC_{50} = 0.009$ mM, COX-2 $IC_{50} = 6.3$ mM, while celecoxib is equally selective for COX-2: the IC_{50} of celecoxib for COX-1 = 15 mM and on COX-2 = 0.04 mM (C. J. Smith et al., 1998).

The effects of systemic administration of these pharmacological agents, on baseline synaptic transmission and paired-pulse depression, in the medial perforant path, were investigated. Furthermore, resultant changes in BDNF were quantified in the dentate gyrus tissue of both the stimulated and unstimulated hemispheres.

2.2 Materials & methods

Experiments were conducted in accordance with European Community directive, 86/609/EC, and the Cruelty to Animals Act, 1876 and followed local and international guidelines of good practice.

2.2.1 Animals

Male wistar rats (BioResources Unit, Trinity College, Dublin, Ireland) were triple housed and maintained on 12:12-light/dark cycles with food and water provided *ad lib*. The rats were randomly assigned to experimental groups and were a mean weight of 300-350g at the time of experiment. Thirty-seven rats were used in total for the following experiments.

2.2.2 Materials

Sc560 was purchased from Cayman Chemicals (Ann Harbour Mo., USA). Celecoxib (celebrex[®]) was obtained from Searle-Monsanto, Dublin. Dimethyl sulfoxide (DMSO), bovine serum albumin, urethane, Krebs-Ringer bicarbonate buffer powder and calcium chloride were purchased from Sigma. The micro concentric bipolar stimulating and monopolar recording, stainless steel electrodes were obtained from Harvard Apparatus LTD., Fircroft Way, Edenbridge, Kent TN8 6HE, UK. BDNF Emax[™] ImmunoAssay System was obtained from Promega UK LTD.

2.2.3 Pharmacological treatment schedules

Maximal concentrations of celecoxib in the rat brain have been reported to occur 1 hour after oral administration (Paulson et al., 2000), and celecoxib and Sc560 share very similar pharmacokinetic properties (Teng et al., 2003). Thus to allow sufficient time for the drugs to penetrate the blood-brain barrier, animals were injected i.p. with 35mg/kg celecoxib or 35mg/kg Sc560 or their vehicle 10% DMSO, 30 minutes pre-anaesthesia (approx. 1.5hrs pre-recording) and their effect on baseline transmission and the paired-pulse ratio of the medial perforant pathway were investigated.

2.2.4 Surgery

All rats were initially anaesthetised with sagatal (sodium pentobarbitone: 60mg/kg) and subsequently with urethane (ethyl carbamate: 1.5g/kg, i.p.) and mounted in a stereotactic holder upon loss of foot pedal reflex. Further injections of urethane were given to sustain anaesthesia throughout the experiment. An incision was made to visualise the skull.

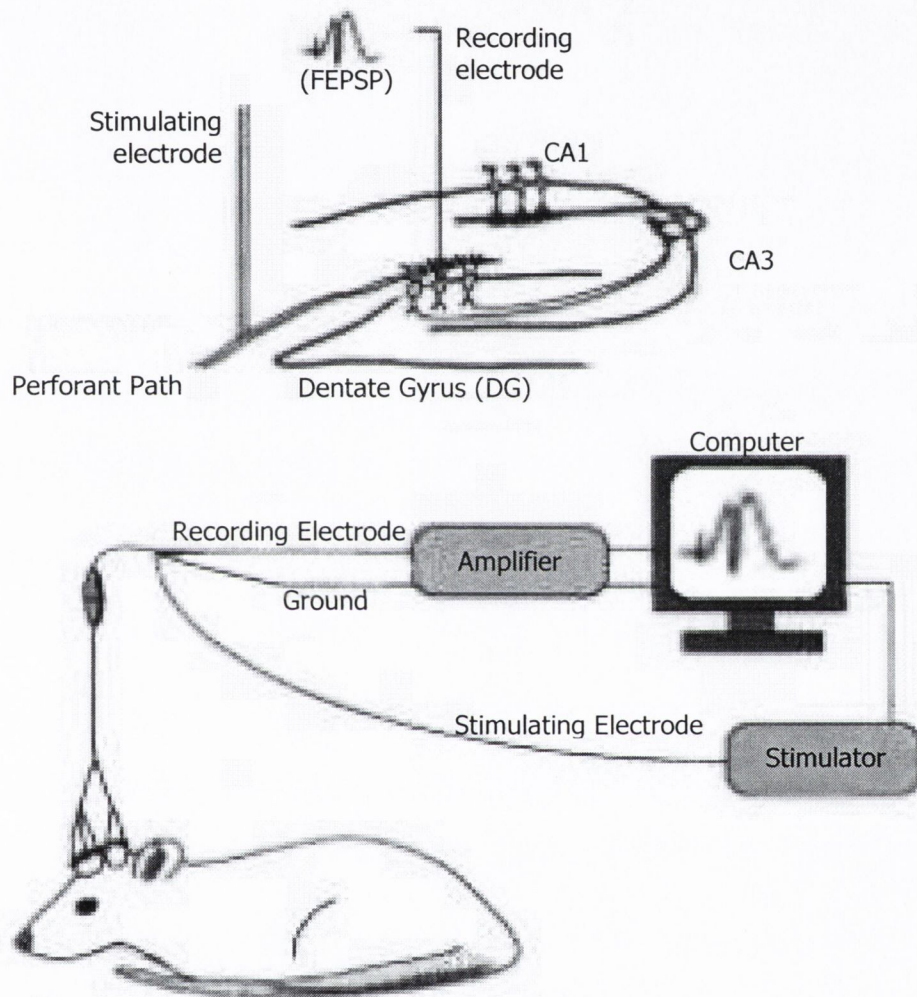


Figure 2.2 The upper diagram shows a representation of the hippocampal trisynaptic loop and the regions where the stimulating and recording electrodes were aimed. The lower diagram depicts the set up used to stimulate record and amplify evoked responses in the anaesthetised rat.

Stimulating electrodes were aimed at the angular bundle of the medial perforant path and the recording electrode at dentate gyrus. Electrode implantation sites were identified using stereotaxic coordinates, relative to bregma (Paxinos & Watson, 1996); recording and stimulating electrodes were positioned 3.9 mm posterior and 2.5 mm lateral to the midline and 8.1 mm posterior and 4.3 mm lateral to midline, respectively. Micro concentric bipolar

stimulating and monopolar recording, stainless steel electrodes were used. Signals were filtered between 0.1Hz and 1 KHz and then amplified (DAM-50 differential amplifier, World precision Instruments, Hertfordshire, UK). Recordings were digitised online using a PC connected to a CED-1401 *plus* interface (CED Cambridge, UK). Electrodes were slowly lowered to a depth of 2.5 mm; test pulses were administered during electrode positioning at 0.05Hz. The final depths were adjusted until maximal fEPSPs were obtained; fEPSP amplitudes were allowed to stabilize for 10mins.

2.2.5 Input/output curves

Input/output curves were constructed by varying the current between 0.01-5mA every three pulses incrementally. Slope and PSA (population spike amplitude) were taken as measures of changes in fEPSP and the average of each triplicate was calculated. All statistics are based on these averages.

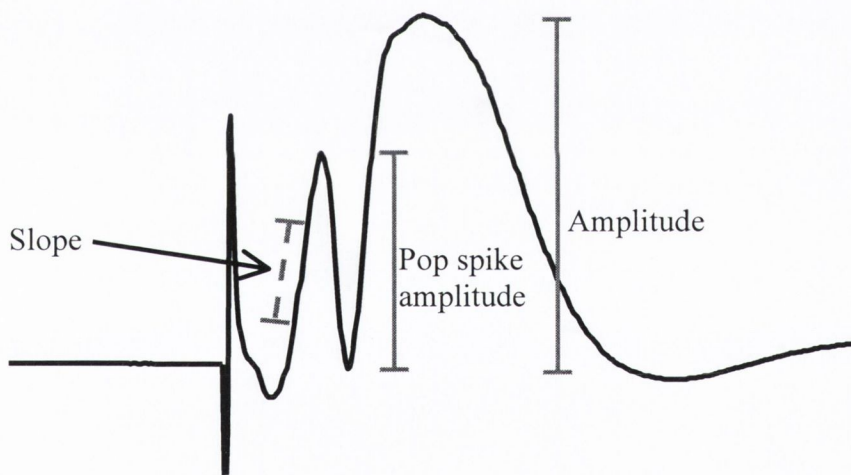


Figure 2.3 A typical field EPSP from stimulation of the medial perforant path recording in the dentate gyrus. The grey lines show how measurement of fEPSP slope, population spike amplitude (PSA) and amplitude of the fEPSP were made. All future analyses are based on these measurements.

2.2.6 Paired-pulse protocol

Pairs of stimuli were delivered every 20 sec with inter stimulus intervals (ISI) ranging from 10-1000 msec, with six repeats at each ISI. The first fEPSP and second fEPSP will be referred to as fEPSP1 and fEPSP2, respectively. The paired-pulse index (PPI) was

calculated by taking the average slope values of fEPSP1 for a given ISI and normalizing the average slope of fEPSP2 with respect to the latter.

Animals were euthanased immediately after recordings (approx. 2.5 hrs after celecoxib administration), the dentate gyrus from both stimulated and unstimulated hemispheres were dissected out and stored in 10% v/v DMSO/KREBS Ca^{2+} at -20°C for later analysis by ELISA for BDNF.

2.2.7 Bradford assay

To prepare the samples, dentate gyri were homogenised in ice-cold Krebs- Ca^{2+} 50 times. The protein concentration of tissue samples was calculated according to the method of Bradford (Bradford, 1976). The standard curve was prepared using a 1:1 serial dilution of bovine serum albumin (BSA) (1000 $\mu\text{g}/\text{ml}$ stock) with resultant concentrations ranging from 0 $\mu\text{g}/\text{ml}$ to 500 $\mu\text{g}/\text{ml}$ (N.B. the 1000 $\mu\text{g}/\text{ml}$ was not included in the calculation of the line of best fit for the standard curve). A 1 in 5 dilution of the Bio-Rad dye reagent was prepared in ddH₂O and filtered through whatmann paper. 10 μl of the standards and samples were added to the wells of a 96-well plate in triplicate to which 200 μl of the diluted dye reagent was added. Absorbance was read in a 96-well plate reader (Labsystems Multiscan RC with interface program Genesis Lite version 3.03) at a wavelength of 630 nm, following gentle agitation. The concentration of protein in samples was calculated with reference to the standard curve plotted from the absorbance of the BSA standards. Protein concentrations were expressed as mg protein/ml tissue homogenate.

2.2.8 BDNF ELISA

Protein was assessed and samples were diluted to give equal protein concentrations and stored at -80°C . Ninety-six well Nunc™ plates were coated with 100 μl anti-BDNF monoclonal antibody diluted (1:1000) in 0.025 M carbonate-bicarbonate buffer. Plates were covered, incubated overnight at 4°C and plates were subjected to interceding washes to remove excess antibody. Plates were blocked for non-specific binding for 1 hour at room temperature and washed (composition of wash buffer in mM: Tris-HCl, 20; NaCl, 150 containing 0.05% Tween (v/v); pH 7.6). Samples of dentate gyrus (50 μl), BDNF

standards (50 μ l; ranging from 0.0078 to 1 ng/ml) were added to the wells, which were covered, incubated for two hours at room temperature with shaking and incubation overnight at 4°C and washed. Aliquots (100 μ l) of anti-human BDNF pAb (diluted 1:500) were added to the wells, plates were incubated for 2h at room temperature and washed. Aliquots (100 μ l) of anti-IgY HRP (1:2000 dilution) were added to wells and incubated for 1h at room temperature. During this incubation, the enzyme substrate was removed from the refrigerator and allowed to come to room temperature. Plates were washed and 100 μ l of this substrate was added to the wells, incubated for approximately 15 minutes until a blue colour developed in the wells. The reaction was stopped by the addition of 100 μ l of 1N HCl acid to the wells. Plates were read a 450 nm in a 96-well plate reader (Labsystems Multiscan RC with interface program Genesis Lite version 3.03) and BDNF concentrations were estimated for the standard curve and expressed as pg/mg protein.

2.2.9 Analysis and statistics

The input/output curves for each animal were subjected to a non-linear regression curve fitting process (A. M. Brown, 2001) whereby the slope and PSA (Figure 2.3) averages were graphed against *log (current)* for that response, thus generating two curves for each animal. Equation 1 shows the generalised formula for a Boltzmann equation for a sigmoidal function.

$$y = \frac{1}{1 + \exp\left(\frac{V-x}{\text{Slope}}\right)}$$

Equation 1 where *y* is the dependent variable, *x* is the independent variable and *V* and *Slope* are the parameter values (A. M. Brown, 2001).

We applied a variation of this function to examine the saturation point (*R*_{max}) of the stimulus-response curve, slope factor (*S*) representing an index proportional to the slope of the curve and the stimulus intensity required to give half maximal response (*I*_h): $R_i = (R_{max} / (1 + \exp((I_h - I) / S)))$ where *R*_{*i*} is the magnitude of the response obtained at stimulus intensity (*I*) (Alvarez, Wiegert, Joels, & Krugers, 2002). These parameters generated by the solver function in *Excel* are obtained by iteration where the values of the parameters are changed by a small amount until the smallest value of *R*² is reached. Solver uses the “generalized reduced gradient” (GRG) method of iteration. This curve fitting process was applied to both the measurements of fEPSP slope, PSA and EPSP-spike (E-S) potentiation.

The parameters generated were analysed using a one-way ANOVA and subsequent Tukeys LSD post hoc test where a $p \leq 0.05$ was considered significant. The Welch statistic was reported where homogeneity of variance could not be assumed. Data were omitted when the R^2 (the index for goodness of fit of the sigmoidal curve to the data) was below 0.9.

A one-way ANOVA was used to analyse the between group effect of celecoxib on paired-pulse ratios at each inter-stimulus interval and a $p \leq 0.05$ was considered the threshold for significance.

2.3 Results

2.3.1 Input/output curves

The effect of treatment with either a selective COX-1 or a COX-2 antagonist compared to their vehicle (10% v/v DMSO) on the excitability of neurons in the medial perforant pathway was investigated. In field recordings of evoked potentials the slope of the response reflects the number of cells depolarising as a result of excitatory input and the amplitude of the population spike reflects the number of cells firing (Lømo, 1971a). The PSA additionally reflects the interaction between excitatory and inhibitory signals that arrive on the cell simultaneously (Marder & Buonomano, 2004). Thus at any given stimulus intensity it can be said that the greater the slope or population spike amplitude (PSA) the greater the excitability. In the following experiment, looking at excitability (using slope and PSA as an index of excitability) as a function of increasing current intensity, we used the parameters generated by a non-linear regression to identify any effects of pharmacological intervention. The results are presented below according to analysis of fEPSP slope, PSA and E-S (EPSP-Spike) curve (the E-S curve consists of a plot of PSA as a function of slope - (EPSP-Spike curve) and represents the ability of EPSPs to induce an action potential in the presence of inhibition).

2.3.1.1 Slope analysis

The question of whether isoform-specific inhibition of COX-1 and -2 alter baseline synaptic transmission was first addressed. There were no significant differences between any of the drug treatments for any of the parameters generated by the non-linear regression fitting of the Boltzmann equation: R_{\max} $F_{(2,17)} = 2.78$; $p > 0.05$, I_h $F_{(2,17)} = 0.273$; $p > 0.05$, Slope (note the Levene's test was significant thus homogeneity of variance could not be assumed and so the Welsh F statistic is reported) $F_{(2,7.57)} = 1.4$; $p > 0.05$. Descriptive statistics for the parameters generated by the regression analysis of fEPSP slope with respect to stimulus intensity are shown in Table 2.1.

	DMSO (n=6)			CXB (n=8)			Sc560 (n=6)		
	Rmax (mV/msec)	Ih (Log(μ A))	Slope	Rmax (mV/msec)	Ih (Log(μ A))	Slope	Rmax (mV/msec)	Ih (Log(μ A))	Slope
Mean	1.49	2.25	0.38	1.62	2.42	0.34	2.05	2.37	0.30
SEM	0.24	0.21	0.06	0.14	0.12	0.01	0.11	0.18	0.02
Std. Dev.	0.59	0.52	0.15	0.40	0.33	0.02	0.28	0.43	0.06

Table 2.1 Descriptive statistics for the parameters generated by curve fitting of the fEPSP slope values per stimulus intensity. Note Ih is log (current) required to give half max response due to transformation performed to fit data to Boltzmann curve.

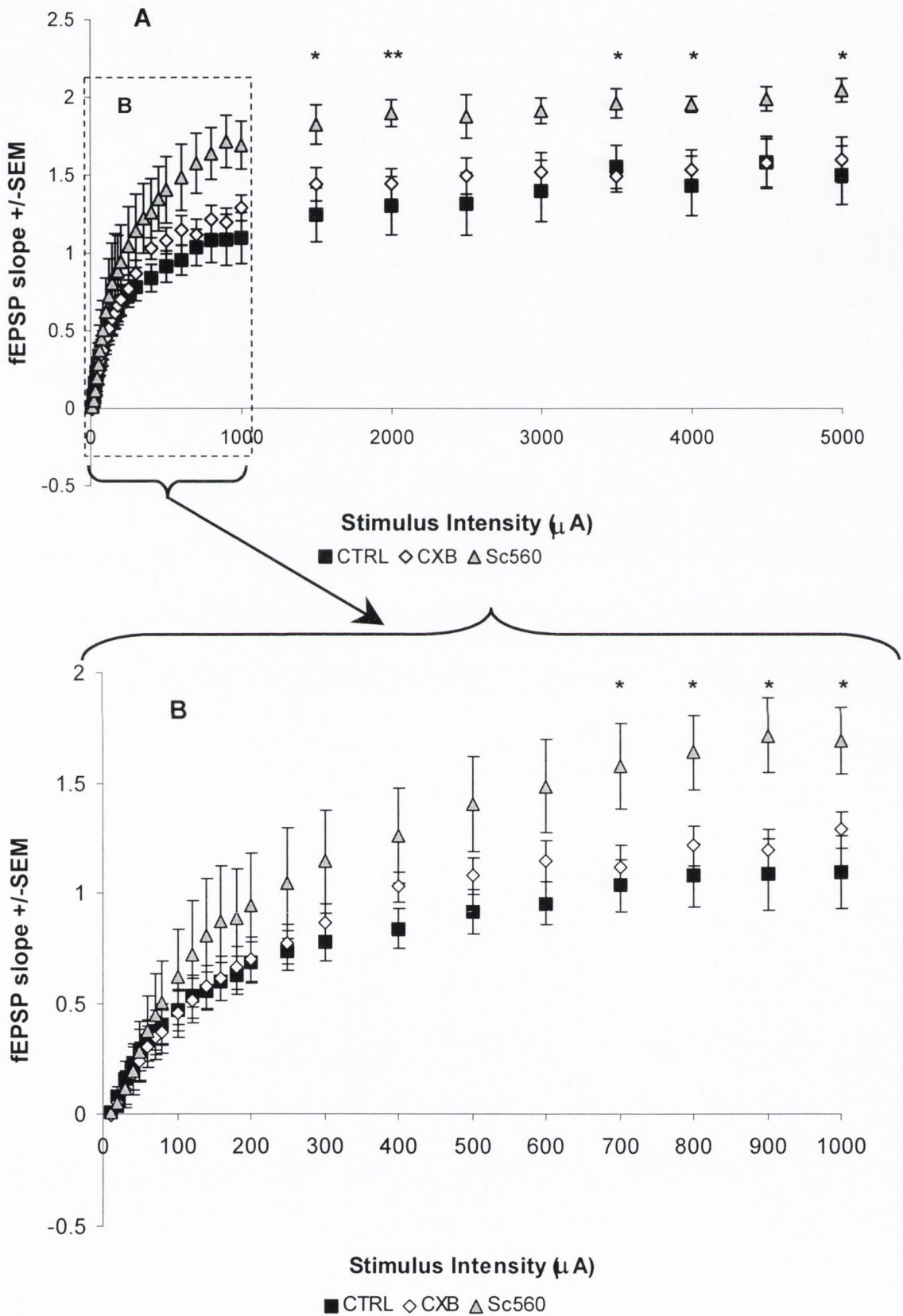


Figure 2.4 Input/output curves for the slope of fEPSP at each stimulus intensity applied: A) within the range 0-5000 μ A, B) expanding the early part of the graph to show the range 0-1000 μ A in more detail (CTRL v Sc560 * $p < 0.05$, ** $p < 0.01$).

Although the non-linear regression analysis of variance was not significant, arguing against a role for either COX isoform altering baseline synaptic transmission, a simple one-way ANOVA and subsequent Dunnett's post hoc 2-sided t-tests (used to compare treatment groups against a control), looking at the effect of selective COX inhibition on fEPSP slope at each stimulus intensity, revealed a significant increases in the size of the fEPSP slope as a result of COX-1 inhibition with Sc560 (represented by stars in Figure 2.4 A) and B)). These increases were evident at almost all stimulus intensities between 700-5000 μ A as shown in Table 2.2.

Intensity (μ A)	600	700*	800*	900*	1000*	1500*	2000**	2500	3000	3500*	4000*	4500	5000*
F statistic (df=2,19)	3.49	4.264	4.477	5.566	5.035	4.438	5.526	3.314	3.397	5.353	3.708	2.693	3.838
p-value	0.054	0.032	0.027	0.014	0.019	0.028	0.014	0.061	0.057	0.017	0.046	0.098	0.042

Table 2.2 The results from the one-way ANOVA showing the F-statistic and associated p-value for stimulus intensities between 600-5000 μ A. Using a Dunnett's 2-sided t-test post hoc, designed to compare test groups to a control, the origin of these differences was between vehicle control and Sc560, but not between control and celecoxib (CTRL v Sc560 * $p < 0.05$, ** $p < 0.01$).

2.3.1.2 Population spike analysis

Similarly, the parameters generated by the Boltzmann equation for PSA (as shown in Table 2.3) showed no significant differences between groups: R_{\max} $F_{(2,17)} = 1.37$; $p > 0.05$, I_h $F_{(2,17)} = 0.417$; $p > 0.05$, Slope $F_{(2,17)} = 1.607$; $p > 0.05$.

	DMSO (n=4)			CXB (n=4)			Sc560 (n=4)		
	Rmax mV	Ih Log(μ A)	Slope	Rmax mV	Ih Log(μ A)	Slope	Rmax mV	Ih Log(μ A)	Slope
Mean	0.80	2.64	0.16	0.54	2.94	0.14	0.99	2.90	0.11
SEM	0.38	0.13	0.06	0.13	0.10	0.03	0.17	0.11	0.03
Std. Dev.	0.75	0.26	0.12	0.34	0.26	0.07	0.41	0.27	0.06

Table 2.3 Descriptive statistics for the parameters generated by curve fitting of the fEPSP pop spike amplitude per stimulus intensity.

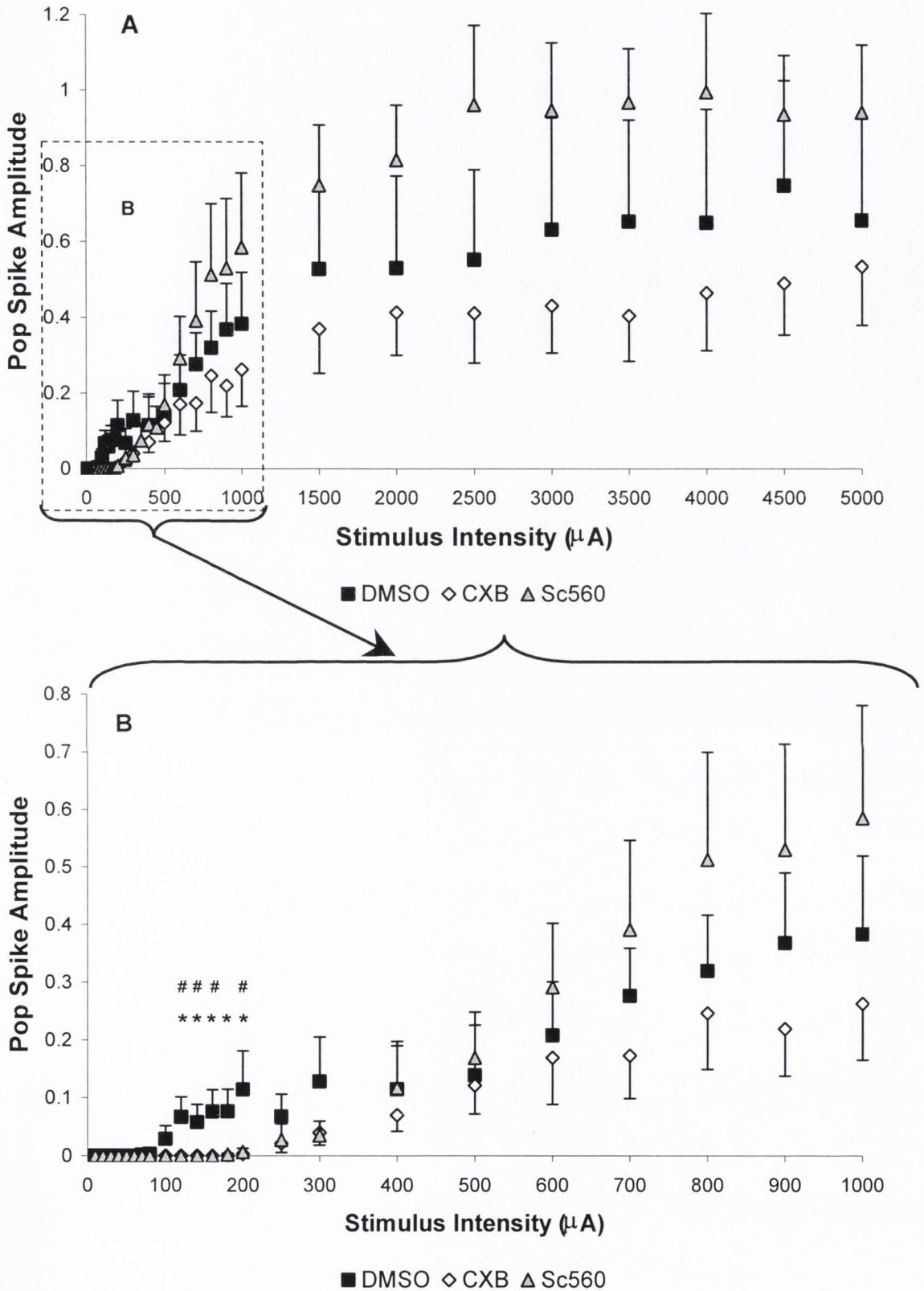


Figure 2.5 Population spike amplitude for current intensities ranging from A) 0-5000 μA and B) 0-1000 μA , for the three treatment groups vehicle, celecoxib and Sc560: # $p < 0.05$ Sc560 v CTRL, * $p < 0.05$ CXB v CTRL.

As for the fEPSP slope analysis, an alternative analysis with a one-way ANOVA and Dunnett's post hoc tests was performed to compare the groups at each individual stimulus intensity. Significances were only evident between 120-200 μ A, inclusive, whereby vehicle controls showed significantly more cell firing (as measured by PSA) compared to either CXB or Sc560 (Table 2.4).

Stimulus Intensity (μ A)	120 ^{#*}	140 ^{#*}	160 ^{#*}	180 [*]	200 ^{#*}
F-statistic	4.413	4.369	4.184	3.822	4.200
p-value	0.029	0.029	0.033	0.043	0.033

Table 2.4 One-way ANOVA results for PSA showing significant differences only in the range 120-200 μ A. Dunnett's t post hoc tests were used to compare drug treatment groups (CXB and Sc560) against controls: # $p < 0.05$ Sc560 v CTRL, * $p < 0.05$ CXB v CTRL.

2.3.1.3 Excitability ratio

As stated previously, the slope of the fEPSP is representative of the number of cells depolarising after a stimulus and the population-spike corresponds to the number of cells firing (Lømo, 1971a) and further reflects the interaction of excitation and inhibition which act on the cell at any one time (Marder & Buonomano, 2004). Thus an alternative measure of excitability is the ratio of cell depolarisation to firing, such that alterations to this ratio signify a change in the threshold for the cells to fire. Figure 2.6 shows the E-S (EPSP-Spike) curves for this relationship and the effects of selective COX inhibition compared to controls. The characteristic sigmoidal shape of these curves allows for the Boltzmann equation to be fitted as before and parameters R_{max} , I_h and Slope to be generated.

A one-way ANOVA showed no statistical differences in any of the generated parameters representative of the excitability ratio: R_{max} $F_{(2,13)}=1.280$; $p > 0.05$, I_h $F_{(2,13)}=0.71$; $p > 0.05$, slope $F_{(2,13)}=0.895$; $p > 0.05$; descriptive statistics for each parameter are displayed in Table 2.5.

	DMSO (n=4)			CXB (n=6)			Sc560 (n=6)		
	Rmax	Ih	Slope	Rmax	Ih	Slope	Rmax	Ih	Slope
Mean	0.56	2.64	0.14	0.36	2.80	0.10	0.52	2.87	0.10
SEM	0.13	0.19	0.04	0.08	0.11	0.01	0.10	0.11	0.03
Std. Dev.	0.26	0.37	0.08	0.19	0.27	0.02	0.23	0.27	0.07

Table 2.5 Descriptive statistics for the excitability ratio (i.e. PSA/slope fEPSP).

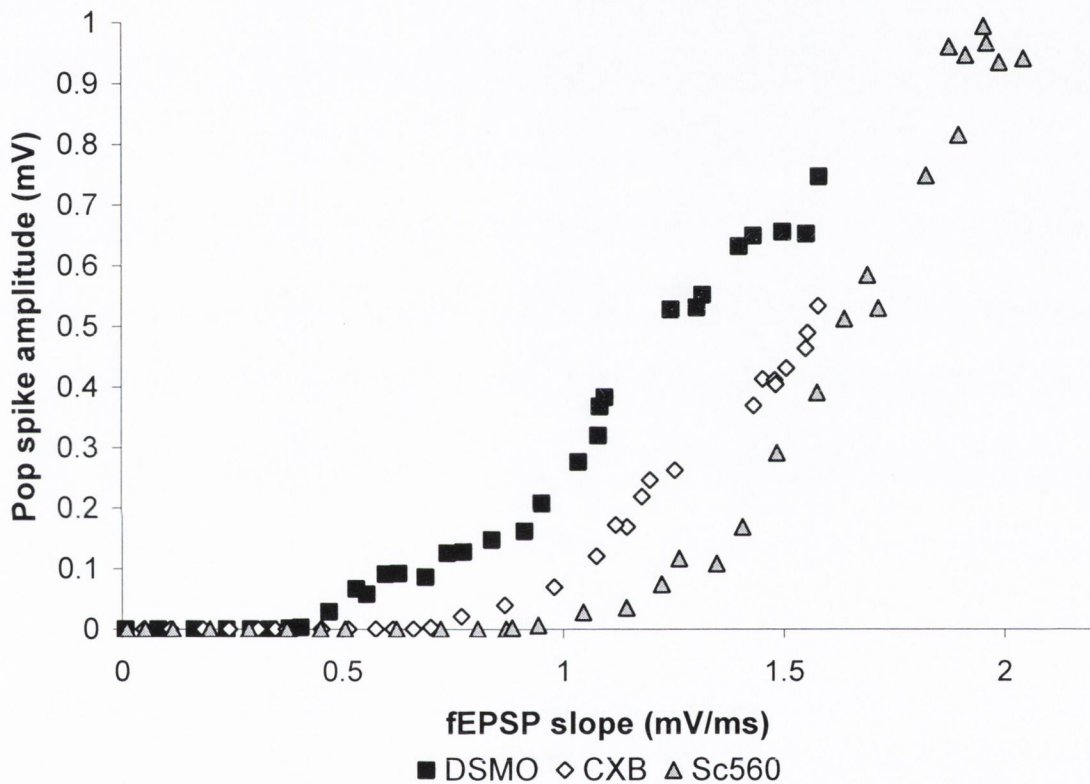


Figure 2.6 E-S curve showing the pattern of cell firing relative to cell depolarisation. The E-S curve for the control animals is shifted to the left relative to either COX-1 or COX-2 inhibitor treated animals implying that less depolarisation is required for the cell to fire i.e. they may be more excitable relative to the COX-1 and COX-2 inhibited animals.

Although there is no statistical effect of inhibition of COX-1 or COX-2 on the excitability ratio, from Figure 2.6 a shift to the right is evident in the amount of depolarisation required before the cells can fire in both drug treatments relative to controls. Furthermore, neither the controls nor the celecoxib treated group attain the same degree of excitability as the Sc560 treated group complimenting the findings from the one-way ANOVA in section 2.3.1.1 which showed greater depolarisation in the Sc560 treated group.

2.3.2 Paired-pulse ratio

Pairs of stimuli were delivered in close succession to the MPP and the characteristic triphasic pattern of depression was evident as described previously (DiScenna & Teyler, 1994). Independent samples t-tests showed that only at the shortest inter-stimulus interval, i.e. 10ms, was there a significant effect of COX-2 inhibition; $t_{10}=2.531$; $p<0.05$. COX-2 inhibition did not alter the PPR at any other inter-stimulus interval significantly.

	<i>ISI (ms)</i>	10	20	50	75	100	125	150	175	200
CTRL (n=5)	Mean	0.25	0.68	0.87	0.83	0.81	0.75	0.81	0.79	0.81
	Std. Dev.	0.25	0.26	0.19	0.10	0.09	0.19	0.14	0.12	0.13
	SEM	0.11	0.12	0.08	0.04	0.04	0.09	0.06	0.06	0.06
CXB (n=7)	Mean	0.52	0.79	0.84	0.90	0.88	0.88	0.87	0.87	0.86
	Std. Dev.	0.12	0.14	0.15	0.08	0.06	0.06	0.05	0.05	0.06
	SEM	0.04	0.05	0.06	0.03	0.02	0.02	0.02	0.02	0.02

...Continued

	<i>ISI (ms)</i>	250	300	400	500	600	750	800	1000
CTRL (n=5)	Mean	0.81	0.81	0.81	0.80	0.86	0.87	0.87	0.84
	Std. Dev.	0.14	0.13	0.11	0.09	0.05	0.06	0.04	0.07
	SEM	0.06	0.06	0.05	0.04	0.02	0.02	0.02	0.03
CXB (n=7)	Mean	0.85	0.85	0.88	0.88	0.87	0.89	0.87	0.96
	Std. Dev.	0.05	0.05	0.06	0.04	0.07	0.05	0.09	0.10
	SEM	0.02	0.02	0.02	0.02	0.03	0.02	0.04	0.03

Table 2.6 Descriptive statistics for the PPR at each ISI (ms) for control and celecoxib treated animals.

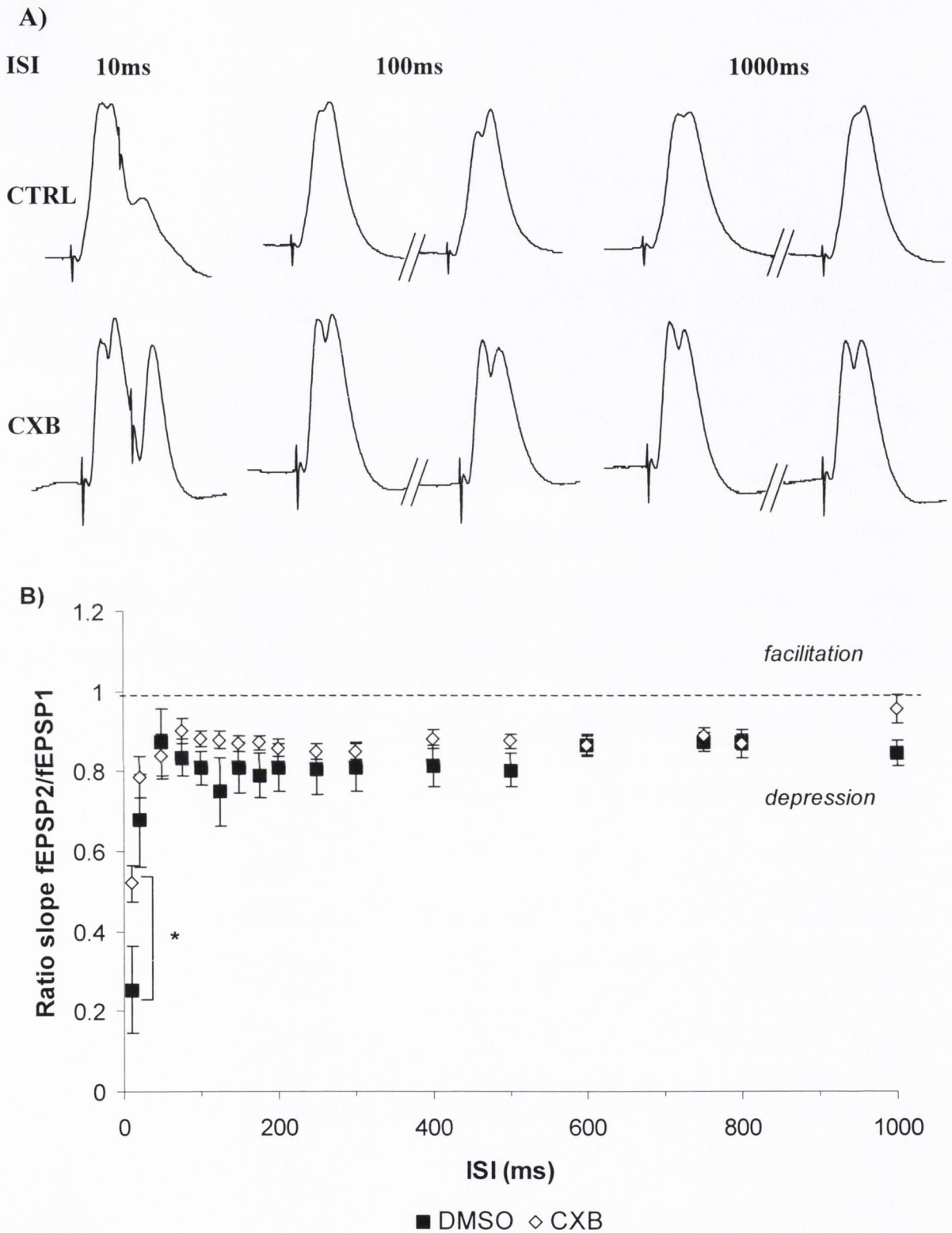


Figure 2.7 The paired-pulse ratio: **A)** representative fEPSPs for control and celecoxib treated rats for 10, 100 and 1000ms ISIs spanning all three phases of depression. **B)** Depicts the ratio of the slope of fEPSP2/fEPSP1 at various inter-stimulus intervals (ISI) within the range 10-1000ms; ratios <1 imply depression and >1 imply facilitation. Pre-treatment with celecoxib diminishes the degree of depression seen in the controls at 10ms ISI [evident in both **A)** and **B)**], but not at any other time latency.

2.3.3 BDNF analysis.

The BDNF content of the dentate gyrus tissue was quantified from both the input/output curves and the paired-pulse experiments by an enzyme-linked immunosorbent assay (ELISA). Results are expressed as a percentage of the concentration measured in unstimulated hemisphere, of the vehicle-treated control average for each experiment. A mixed-factorial ANOVA was used to investigate the effect of COX-2 inhibition (between-groups effect) and stimulation protocol (within-groups effect) for both the baseline and paired-pulse experiments.

2.3.3.1 Input/output curve BDNF

For the input/output curve experiment a significant difference was not evident between any of the conditions implying that neither COX-1 nor COX-2 inhibition, nor the experimental procedure of implanting electrodes and stimulation at 0.05Hz at various intensities between 0-5000mA, altered the concentration of BDNF (Figure 2.8): within-effect of hemisphere $F_{(1,14)}=0.015$; $p>0.05$, the interaction of hemisphere and celecoxib $F_{(1,14)}=0.304$; $p>0.05$ and the between-effect of drug $F_{(1,14)}=2.729$; $p>0.05$. Table 2.7 shows the percentage mean concentration of BDNF relative to unstimulated control tissue, for the input/output curve dentate gyri, and associated descriptive statistics.

DRUG		STIM	UNSTIM
CTRL (n=6)	Mean (%)	97.98	100.00
	SEM	12.34	2.01
	St. Dev	30.23	4.91
CXB (n=6)	Mean (%)	82.36	87.61
	SEM	3.02	4.36
	St. Dev	7.40	10.69
Sc560 (n=5)	Mean (%)	102.58	97.35
	SEM	9.41	4.59
	St. Dev	21.03	10.26

Table 2.7 Input/output Experiment: descriptive statistics for BDNF concentration in the dentate gyri of rats undergoing COX-1 (Sc560) or COX-2 inhibition (CXB), or vehicle control and baseline stimulation for input/output curve construction and their respective controls.

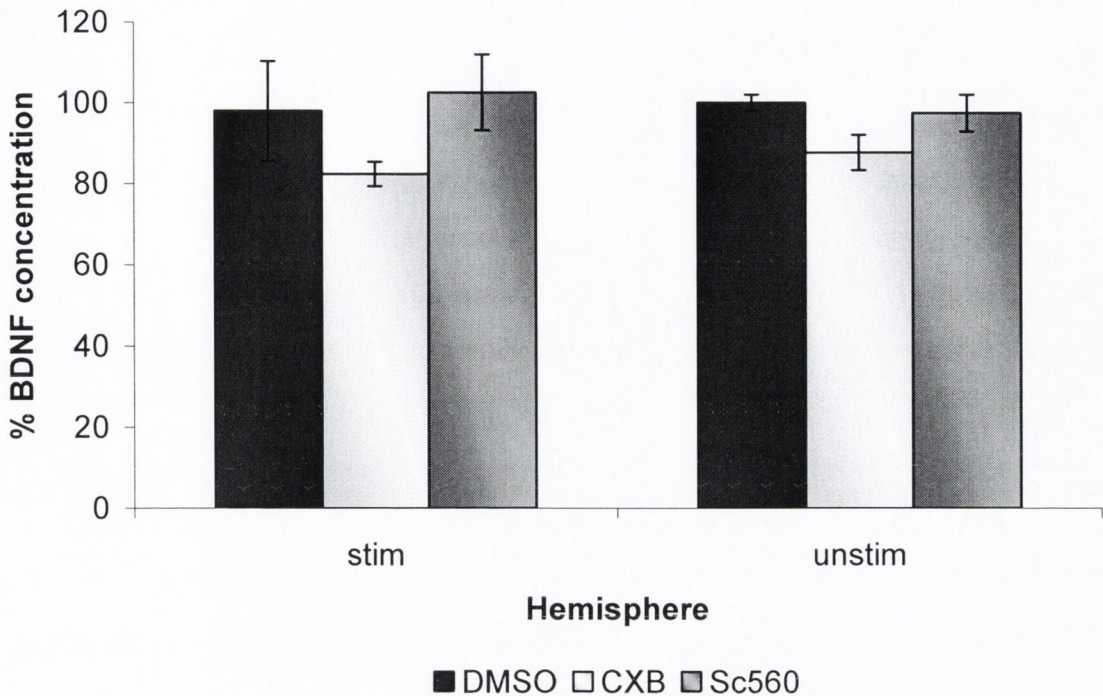


Figure 2.8 Input/output experiment: the percentage of BDNF relative to unstimulated control tissue in the dentate gyri \pm SEM. There are no significant differences between any of the conditions demonstrating that neither the administration of celecoxib nor Sc560, nor implanting electrodes and at 0.05Hz stimulating had any effect on BDNF concentration.

2.3.3.2 Paired-pulse BDNF

For the dentate gyri subjected to paired-pulse stimulation a significant interaction of celecoxib treatment and stimulation was evident: $F_{(1,10)}=6.016$; $p<0.05$. From Figure 2.9 this interaction can be interpreted as some alteration brought about by paired-pulse, e.g. an increase in intracellular, combined with celecoxib treatment resulting in an increase in BDNF concentration. There was neither an effect of drug ($F_{(1,10)}=0.303$; $p>0.05$) nor stimulation procedure ($F_{(1,10)}=0.562$; $p>0.05$) individually. Table 2.8 show the descriptive statistics for the percentage mean BDNF concentration for this tissue.

DRUG		STIM	UNSTIM
CTRL (n=6)	Mean (%)	93.34	100.00
	SEM	2.10	4.60
	St. Dev	5.14	11.27
CXB (n=6)	Mean (%)	110.66	98.12
	SEM	13.51	14.69
	St. Dev	33.09	35.98

Table 2.8 Paired-pulse experiment: descriptive statistics for the concentration of BDNF as a percentage of the unstimulated control hemisphere as a result of COX-2 inhibition and paired-pulse stimulation and their respective control conditions.

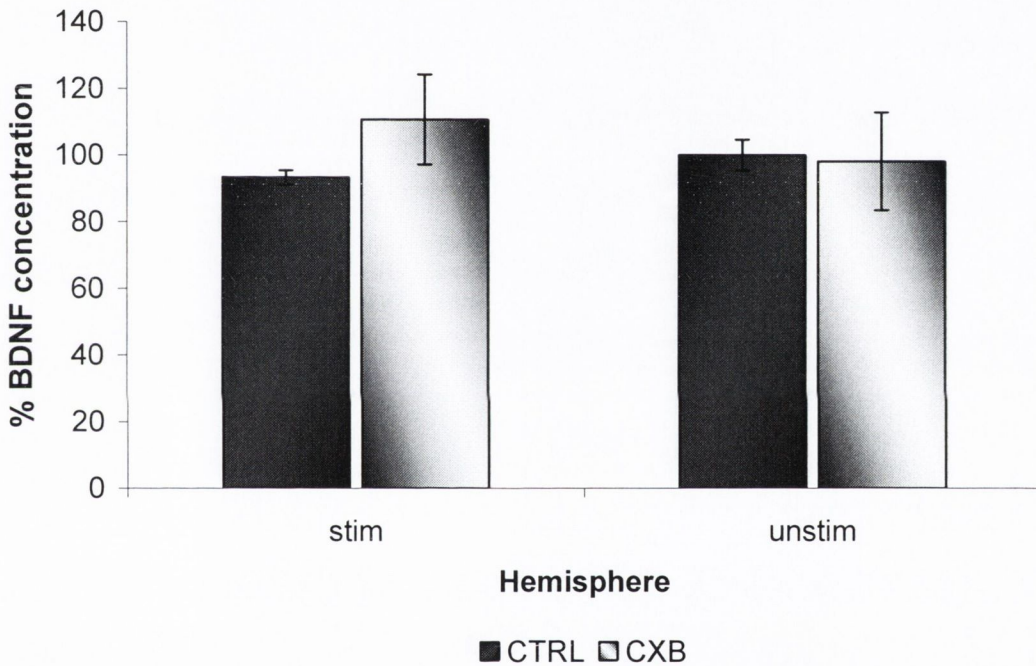


Figure 2.9 Paired-pulse experiment: BDNF concentration after paired-pulse stimulation. Although there was no individual effect of drug or stimulation on BDNF concentration in the dentate gyrus, there is a significant interaction of celecoxib treatment and stimulation ($p < 0.05$).

2.4 Discussion

In our preliminary investigations of the effects of isoform-specific inhibition of cyclooxygenase we found that baseline synaptic transmission was unaltered as measured by a non-linear regression analysis of fEPSP slope, PSA and E-S ratio. The purpose of the regression analysis was to standardize the interpretation of the data into homogeneous components that take into consideration all features of the curves – saturation point (Rmax), rate of increase in magnitude of fEPSP with respect to stimulus intensity (slope) and the stimulus intensity required to reach the half maximum response (I_h) – not just the size of the fEPSP. This holistic approach emphasizes the importance of the whole curve and the interdependence of its parts and revealed no significant differences between the curves. However, for completeness, a point-by-point analysis was also performed, which showed COX-1 inhibition resulted in increased maximum fEPSP slope at high stimulus intensities – 700-5000 μ A – but had no effect on PSA, intimating a potential division in the properties of COX-1 and -2 baseline synaptic transmission. A possible explanation for this difference could result from different prostaglandin profiles produced by the two enzymes (Brock, McNish, & Peters-Golden, 1999). Brock et al showed that in a cell with multiple prostaglandin synthases (peritoneal macrophage) that COX-1 activity produced PGI₂, TxA₂, PGD₂ and 12-HHT (12-hydroxyheptadecatrienoic acid), whereas COX-2 activity produced PGE₂ and PGI₂. It is important to note, for the LTP experiments that will follow in Chapter III, that neither COX inhibitor had an effect on the current required to achieve half maximal response and at low to intermediate stimulus intensities the magnitude of the fEPSP and PSA were equivalent in all groups, i.e. for the stimulus intensities that will be used to induce LTP.

The E-S curve is defined as: *a measure of the net ability of EPSPs to elicit action potentials in the presence of inhibition* (Marder & Buonomano, 2004). Thus the slight shift to the right observed in the E-S curves of both COX-1 and COX-2 inhibited animals could represent a shift in the balance of inhibition causing an increase in threshold to fire the cells i.e. action potential threshold (AP), which may be important for LTP induction. A similar result was reported by Chen et al. whereby COX-2 inhibition caused decreased membrane excitability, represented by a decrease in the number of AP recorded in response to high frequency stimulation (HFS) (C. Chen et al., 2002). In contrast, using indomethacin (a COX antagonist with a 2-order lower IC₅₀ for COX-1 inhibition than

COX-2) at a dose below the IC_{50} for COX-2, they showed no effect on AP production. Although based on very different protocols the fundamental finding of a decrease in excitability due COX-2 inhibition is the same but a discrepancy in the effect of COX-1 inhibition is evident.

We found that in the tissue analysis after baseline stimulation, BDNF concentration was unchanged as a result of either COX-1 or COX-2 inhibition. These findings are in agreement with similar results reported by Shaw *et al* (Shaw *et al.*, 2003) using broad-spectrum COX inhibition.

COX-2 inhibition resulted in a decrease in paired-pulse depression in the MPP. This effect was found only at very short latency ISI, <20 ms. Since this depression is reportedly $GABA_A$ mediated (Albertson & Joy, 1987; Tuff *et al.*, 1983) and reflects the probability of neurotransmitter (NT) release (Min, Asztely, Kokaia, & Kullmann, 1998) – the greater the probability of NT release for the first stimulus the greater the depression of the second response – it suggests that COX-2 inhibition at short latencies reduces the probability of NT release and/or reduces the inhibition imposed by GABA binding to postsynaptic $GABA_A$ receptors. The time-window at which COX-2 inhibition alters the PPR is also evincive of alteration in ion-channel opening, for example modulation of potassium (K^+) channel currents and cell after-hyperpolarisation. The modulatory effects of prostaglandins on ion channels have been well documented in sensory neurons, whereby membrane excitability is regulated by changes in ionic conductance. One study showed that COX-2 inhibition, with celecoxib, resulted in decrease glycine-induced ion currents (glycine is an inhibitory neurotransmitter, which hyperpolarises cells by Cl^- ion influx) and increase glutamate-induced ion currents, which agree with the pattern seen here (Shin *et al.*, 2003). The lack of effect at longer latencies is contraindicative of alterations in $GABA_B$ transmission and presynaptic calcium entry (Zucker, 1999; Zucker & Regehr, 2002).

The decrease in depression could also signify a shift in the balance between inhibition and facilitation (as discussed in the introduction) in favour of facilitation and increase intracellular Ca^{2+} concentration. In fact, celecoxib has been reported to impair Ca^{2+} -ATPase activity, an enzyme involved in the removal of Ca^{2+} back out of the cytoplasm, into intracellular stores in the endoplasmic reticulum, resulting in increased intracellular Ca^{2+} (Johnson, Hsu, Lin, Song, & Chen, 2002). However, if this were the case it would be

expected that the decrease in depression would manifest at all ISI not just at very short latencies. Since this inhibition of Ca^{2+} -ATPase is reportedly independent of celecoxib's effects on COX-2 it highlights the necessity to investigate whether the results are COX-2 mediated or epiphenomenal. Thus it will be subsequently investigated whether this impairment is due to a decrease in PGE2 concentration a metabolite of COX-2 activity, by injecting PGE2 into the hippocampus prior to paired-pulse. It is possible that a product of basal COX-2 enzymatic activity acts as a low pass filter, dampening down high-frequency stimuli (i.e. the PPD observed at high-frequency stimuli) preventing the development of epileptic activity; COX-2 inhibition results in a loss of this depression. Chen et al. have argued against a presynaptic locus for COX-2 inhibition on facilitation (C. Chen & Bazan, 2005a; C. Chen et al., 2002) however, inhibition was not addressed and further research need to be done.

An alternative substrate of COX-2 activity is the endocannabinoid 2-AG (2-arachidonoyl glycerol). 2-AG has been associated with a phenomenon called depolarization-induced suppression of inhibition (DSI) in which 2-AG is released in response to depolarisation and the associated increase in intracellular Ca^{2+} ; it can then bind to its receptor CB1 found on presynaptic inhibitory GABAergic neurons and decrease the release of GABA from presynaptic neurons. This ultimately results in disinhibition at the postsynaptic neuron. DSI is reported to have a delay to onset of ~1s and a half-life of approximately 20 seconds and is induced in response to prolonged depolarisation or repeated stimuli (as reviewed by (Alger, 2002)). COX-2 inhibition, which slows the metabolism of 2-AG, has been shown to prolong DSI in the hippocampus (Kim & Alger, 2004). Furthermore, DSI has been reported to cause an increase in PPF (Alger, 2002). The decrease in depression observed at 10ms ISI is too short a latency to implicate DSI as a mechanism and is not observed at any other ISI.

An association was demonstrated between the application of paired-pulse stimulation to the perforant pathway and celecoxib treatment, on the concentration of BDNF protein in the dentate gyrus tissue. Thus, some change in the postsynaptic neuron as a result of the application of paired stimuli, but not single stimuli – as this effect is not evident in the baseline tissue – cooperates with an effect of COX-2 inhibition to increase BDNF protein concentration. Such a mechanism will be considered in later chapters.

Given the diversity in potential effects of COX inhibition – e.g. a build-up of unmetabolised AA, spill-over into the LOX pathway, non-COX related activities of the pharmacological agents employed, the myriad of potential prostaglandins down-regulated – any interpretation at this point is fraught with complexity. However, the results from these experiments set a platform to further investigate the role of cyclooxygenase in synaptic function in particular with regard to long-term potentiation. Since COX-2 inhibition had no effect on baseline synaptic transmission or associated BDNF levels, any effects on LTP must be activity dependent.

**Chapter 3 The selective inhibition of COX-2 but
not COX-1 blocks the induction of
long-term potentiation**

Chapter 3	The selective inhibition of COX-2 but not COX-1 blocks the induction of long-term potentiation.....	78
3.1	Introduction.....	80
3.2	Materials & methods.....	82
3.2.1	Materials	82
3.2.2	Animals.....	82
3.2.3	Pharmacological treatment schedules.....	82
3.2.4	Surgery.....	83
3.2.5	Long-term potentiation protocol.....	83
3.2.6	Bradford assay	83
3.2.7	BDNF ELISA	83
3.2.8	Corticosterone measurement.....	83
3.2.9	Statistics.....	84
3.3	Results.....	85
3.3.1	Selective inhibition of the COXs and the effects on LTP & BDNF	85
3.3.1.1	Selective COX-2, but not COX-1 inhibition, blocks LTP induction.....	85
3.3.1.2	BDNF concentration is increased as a result celecoxib treatment.....	91
3.3.1.3	Blood plasma corticosterone was unaltered by COX-2 inhibition	94
3.3.2	COX-2 inhibition and baseline synaptic transmission at constant current ..	94
3.3.3	The effects of COX-2 inhibition on the maintenance of LTP and BDNF concentration in DG.....	96
3.3.3.1	The maintenance of LTP is not affected by COX-2 inhibition.....	96
3.3.3.2	BDNF was decreased as a result of COX-2 inhibition after HFS.	98
3.3.3.3	Blood plasma corticosterone was unaltered by COX-2 inhibition after the induction of LTP.....	99
3.4	Discussion.....	101
3.4.1	Isoform specificity and the block of LTP	101
3.4.2	The maintenance of LTP is not affected by COX-2 inhibition, although the concentration of BDNF is.....	104

3.1 Introduction

In 1988, the first papers implicating arachidonic acid or its metabolites in long-term potentiation were published (J.H. Williams & Bliss, 1988), and a plethora of similarly-themed papers from the same authors followed quickly (M. A. Lynch, Errington, & Bliss, 1989; J. H. Williams & Bliss, 1989; J. H. Williams et al., 1989). In summary, these papers showed that nordihydroguaiaretic acid (NDGA) – a drug which at low doses blocks lipoxygenase and at high doses blocks PLA2 – showed a dose-dependent inhibition of both Ca^{2+} - and HFS-induced LTP in CA1 and dentate gyrus, *in vitro* and *in vivo*, whereas indomethacin, a COX antagonist, had no effect. Furthermore, weak activation of the perforant path, when given in the presence of arachidonic acid, led to a slow-onset persistent potentiation, *in vitro* and *in vivo*. The induction of LTP is prompted by the entry of Ca^{2+} through NMDA receptors postsynaptically but there must be some presynaptic alteration for the LTP to be maintained. It was hypothesised that a signalling molecule released postsynaptically could act as a retrograde messenger to the presynaptic cell to cause greater neurotransmitter release. NMDA receptor activation had been shown to activate the arachidonic acid cascade (Dumuis et al., 1988) and arachidonic acid is a freely diffusible molecule and was thus proposed as a candidate. Thus, the conclusions drawn from the arachidonic acid/LTP experiments were that, since the COX antagonist indomethacin, and low-dose NDGA (which would only block lipoxygenase and not PLA2) had no effect on LTP, arachidonic acid and not COX or LOX metabolites must act as a retrograde messenger in LTP modulating the presynaptic response. A counter-argument was proposed by O'Dell et al pointing out that NDGA also blocked the production of nitric oxide (NO), another highly diffusible molecule that fitted more of the criteria for a retrograde messenger in LTP (O'Dell et al., 1991).

The subsequent discovery of the COX-2 isoform in 1991 (D.A. Kujubu et al., 1991; Xie et al., 1991), and the lack of efficacy of indomethacin as an inhibitor of COX-2, revealed a new dimension to the arachidonic acid/LTP story. This finding negated the conclusion that COX metabolites could be ruled out as retrograde messengers and the slow-onset of arachidonic acid-induced potentiation could represent the metabolism of arachidonic acid to its metabolites. In 1993, Yamagata et al showed that the induction of LTP stimulates the transcription of the COX-2 gene resulting in increased mRNA in dentate granule cells in an NMDA receptor-dependent manner since it can be blocked by MK801, an NMDA receptor

antagonist (Yamagata et al., 1993). The COX-2 gene was identified as an immediate early gene and was found to be rapidly upregulated in response to maximal electroconvulsive seizure (MECS) and also to high frequency stimulation (HFS). COX-2 mRNA levels were markedly increased 30 minutes after stimulation in both paradigms, peaking by 2-4hrs and, in the case of MECS, remaining elevated for up to 8hrs. This observed increase in COX-2 mRNA in response to electrical stimulation was extended to chemical induced seizure with the same temporal regulation and sensitivity to NMDA blockade reported, but COX-1 mRNA levels were unaltered (Adams, Collaco-Moraes, & de Belleruche, 1996). At the time of publication of the Yamagata paper there were no selective COX-2 antagonists available; the authors also found that pre-treatment with indomethacin had no effect on the induction of LTP. It was not until 2002 that direct evidence for the involvement of COX-2 in synaptic activity was presented (C. Chen et al., 2002). In this paper Chen *et al* demonstrated that COX-2 inhibition with either of two selective antagonists, NS398 or nimesulide, blocked LTP induction in the dentate gyrus, *in vitro*. Moreover, they reversed this block by putting PGE2 in the tissue bath prior to HFS. In the same year another *in vitro* experiment showed that COX-2 played a role in long-term depression that mirrored the effects seen with a p38 antagonist (Murray & O'Connor, 2003). Also, non-selective antagonism of COX-1 and COX-2 with ibuprofen was shown to block LTP *in vivo* and cause impairments in acquisition of the watermaze, a hippocampal dependent task (Shaw et al., 2003). These latter changes correlated with changes in the expression of both BDNF and PGE2.

As mentioned in Chapter I, LTP has been associated a temporal analysis of BDNF mRNA expression in response to LTP induction, in anaesthetised animals, showed maximal levels were expressed after 2 hrs (Bramham et al., 1996; Gooney & Lynch, 2001; Morimoto et al., 1998) and bilateral increase in BDNF mRNA were shown in response to unilateral LTP in unanaesthetised-animals after 6 hrs (Bramham et al., 1996). Gooney and Lynch showed that BDNF protein levels and KCl-stimulated release of BDNF were increased in tetanised dentate gyrus only 40 min post-HFS, with associated increases in phosphorylation of TrkB, ERK and CREB, and increased protein synthesis.

3.2 Materials & methods

Experiments were conducted in accordance with European Community directive, 86/609/EC, and the Cruelty to Animals Act, 1876 and followed local and international guidelines of good practice.

3.2.1 Materials

As described in Chapter II.

3.2.2 Animals

Male wistar rats (BioResources Unit, Trinity College, Dublin, Ireland) were triple housed and maintained on 12:12-light/dark cycles with food and water provided *ad lib*. The rats were randomly assigned to experimental groups and were a mean weight 300-350g at the time of experiment.

3.2.3 Pharmacological treatment schedules

Maximal concentrations of celecoxib in the rat brain have been reported to occur 1 hour after oral administration (Paulson et al., 2000); celecoxib and Sc560 share very similar pharmacokinetic properties (Teng et al., 2003). To allow sufficient time for the drugs to penetrate the blood-brain barrier, animals were injected i.p. with 28 mg/kg (low dose) or 35mg/kg (high dose) celecoxib, 35 mg/kg Sc560 or their vehicle 10% DMSO, 30 minutes pre-anaesthesia (i.e. 1.5 hours before HFS) and their effect on HFS of the medial perforant pathway were investigated. Alternatively, the animals were treated with 35 mg/kg celecoxib or its vehicle 10% DMSO 20mins post-HFS to study the effect of COX-2 blockade on the maintenance phase of LTP.

A further control was performed, whereby celecoxib was administered after anaesthesia and a stable baseline recording had been established to ensure that any immediate effects of COX-2 inhibition on the size of the fEPSP at constant current, which may have been missed with the I/O curve recordings, could be detected. Recordings were made for up to

an hour subsequent to celecoxib (or 10% DMSO vehicle control) administration and normalised to the first five minutes of the recordings.

3.2.4 Surgery

As described in Chapter II

3.2.5 Long-term potentiation protocol

LTP in the perforant path was induced, after a 10min baseline was recorded, by high frequency stimulation (HFS) consisting of three trains of stimuli of 250Hz for 200ms with a 30s inter-train interval. This protocol has been shown to induce saturated LTP in perforant path-granule cell synapses in anaesthetized rats (O'Donnell, Vereker, & Lynch, 2000). Stimulus intensity during HFS was maintained at that of baseline. Baseline stimulation was then resumed at a rate of 0.05Hz.

3.2.6 Bradford assay

As described in Chapter II.

3.2.7 BDNF ELISA

As described in Chapter II.

3.2.8 Corticosterone measurement

Corticosterone levels were measured by radioimmunoassay in trunk blood, which was collected after decapitation; serum was removed and stored at -20°C for subsequent analysis (DPC, USA; Shaw et al 2001). With this assay serum samples are assayed directly without preparation. Samples were thawed to room temperature and 50 µl of either serum or calibrator (ranging from 0 to 2000 ng/ml corticosterone) was added to the tubes precoated with rat corticosterone antibodies. ¹²⁵I rat corticosterone (100 ml) was added to every tube and incubated for 2 hrs at room temperature. The tubes were then decanted and

counted for 1min in a gamma counter. Concentrations were estimated from the calibrator standard curve and expressed as ng/ml of corticosterone.

3.2.9 Statistics

LTP experiments were analysed using two-way repeated measures ANOVAs with Newman-Keuls post hoc tests between groups. *A priori* planned comparisons were used in the one-way ANOVA to reduce the chances of a type II error. A p-value of 0.05 was considered as the threshold for a significant difference. All error-bars on plots represent \pm standard error of the mean (\pm SEM).

3.3 Results

3.3.1 Selective inhibition of the COXs and the effects on LTP & BDNF

3.3.1.1 Selective COX-2, but not COX-1 inhibition, blocks LTP induction.

We investigated the effects of pharmacological manipulations of the COX isozymes on the induction of long-term potentiation in the medial perforant path. We tested the hypotheses that:

- 1) Different COX inhibitors would interact with HFS to disrupt LTP compared to vehicle-treated controls and
- 2) Whether the dose of COX-2 antagonist would affect the degree of any impairment in LTP observed.

We found that pre-treating the rats with the selective COX-2 antagonist, celecoxib (35 mg/kg) (n=14), allowing time for drug absorption into the blood-stream and to cross the blood-brain barrier (Paulson et al., 2000), resulted in a complete block of LTP compared to vehicle treated animals (n=18) (Figure 3.1). In contrast, neither 28 mg/kg celecoxib (Figure 3.3) nor selective COX-1 inhibition with Sc58560 (35 mg/kg) (n=6), a structurally related compound to celecoxib, showed any such block of LTP (Figure 3.1).

A mixed-factorial ANOVA was performed to investigate the effects of HFS on baseline fEPSP slope compared with 60 seconds (post-tetanic potentiation, PTP), 30- and 60-minute time points, and the effect of pharmacological intervention. A significance of $p < 0.001$ for the Mauchly's test of sphericity required that the Greenhouse-Geisser test for within subject (i.e. repeated measures) effects be reported. There was a significant effect of HFS on the slope of the fEPSP $F_{(2,3,99,6)} = 18.22$; $p < 0.001$ and a significant interaction of the drug treatment with HFS, $F_{(6,9,99,6)} = 3.36$; $p < 0.01$. These results are reported with 100% and 95% power respectively. The between-subject test showed an overall effect of drug treatment on fEPSP slope, $F_{(3,43)} = 7.8$; $p < 0.001$ with 98.3% power. Newman-Keul post hoc tests indicated this effect arises from differences between 35 mg/kg celecoxib and all other groups; furthermore, there were no differences between Sc560, 28 mg/kg celecoxib and control.

DRUG	TIME	% Mean	SEM
DMSO (n=19)	BASELINE	100.23	0.22
	PTP	128.37	5.35
	25-30mins	121.95	2.63
	55-60mins	129.41	4.80
CXB 35mg/kg (n=14)	BASELINE	99.60	0.27
	PTP	110.58	4.30
	25-30mins	94.83	6.13
	55-60mins	96.43	6.31
SC560 (n=6)	BASELINE	100.00	0.00
	PTP	120.09	12.69
	25-30mins	118.05	4.58
	55-60mins	117.54	7.03
CXB 28mg/kg (n=10)	BASELINE	100.03	0.11
	PTP	122.30	6.21
	25-30mins	112.27	2.36
	55-60mins	123.31	4.77

Table 3.1 Descriptive statistics showing that selective COX-2 inhibition blocks the induction of LTP in a dose dependent manner: % mean fEPSP slope relative to their respective baselines.

To refine these results, to show at what time relative to HFS that the differences resulting from drug treatment were observed, one-way ANOVAs was performed at baseline, PTP, 30- and 60-minute time points. There was no significant effect of drug at baseline $F_{(3,45)}=1.56$; $p>0.05$ nor PTP $F_{(3,45)}=1.799$; $p>0.05$. At 30 minutes after HFS, however, the ANOVA was significant $F_{(3,45)}=9.04$; $p<0.0001$, and at 60 minutes $F_{(2,35)}=9.54$; $p<0.001$. Since in our first mixed-factorial ANOVA the only group different from control was the 35mg/kg celecoxib group, a planned *a priori* comparison in the one-way ANOVA was used to look at this difference and at what time relative to HFS it occurred taking into account that the ANOVA was not significant at baseline or PTP. This strategy revealed at 30- and 60-mins 35 mg/kg CXB significantly impaired LTP relative to control; $p<0.001$. Using a similar rationale we tested the second hypothesis that 28 mg/kg versus 35 mg/kg would differ; the planned comparisons showed a significant impairment at the higher dose at 30- and 60-mins post HFS ($p<0.01$ for both).

To summarise, therefore, we have found that COX-2 inhibition (35 mg/kg) resulted in a sustained block of LTP sixty minutes post-HFS, contrasting with the lack of effect of COX-1 inhibition (Figure 3.1). Furthermore, this block of LTP is dose-dependent, with the lesser dose of 28 mg/kg showing no impairment in LTP-induction relative to controls

(Figure 3.3). Figure 3.2 shows representative, non-averaged recordings from individual rats and although there is no statistical impairment in PTP observed between control and 35 mg/kg celecoxib in the ANOVA, our qualitative observations suggest some degree of impairment is present. This impairment might be more readily observed in the more controlled conditions available *in vitro* using a slice preparation.

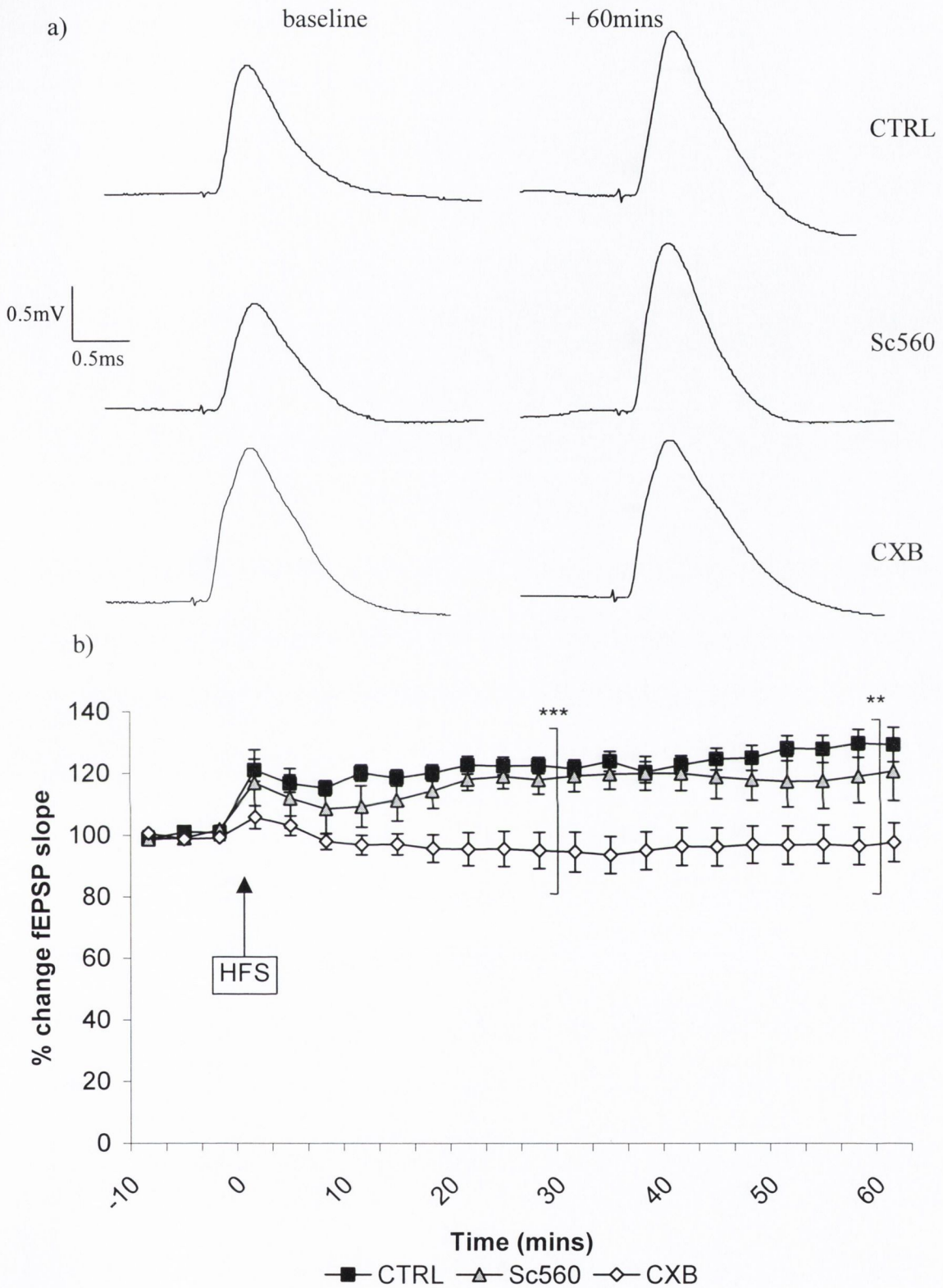


Figure 3.1 Effect of selective COX-1 and COX-2 inhibition on long-term potentiation. Selective COX-2 inhibition was obtained using celecoxib (CXB) and COX-1 with Sc560.

1a) Representative traces of fEPSPs recorded during baseline and 60mins post-HFS (as marked) for each treatment.

1b) Percent change in fEPSP slope relative to baseline \pm SEM (where error bars are not visible SEM is too small).

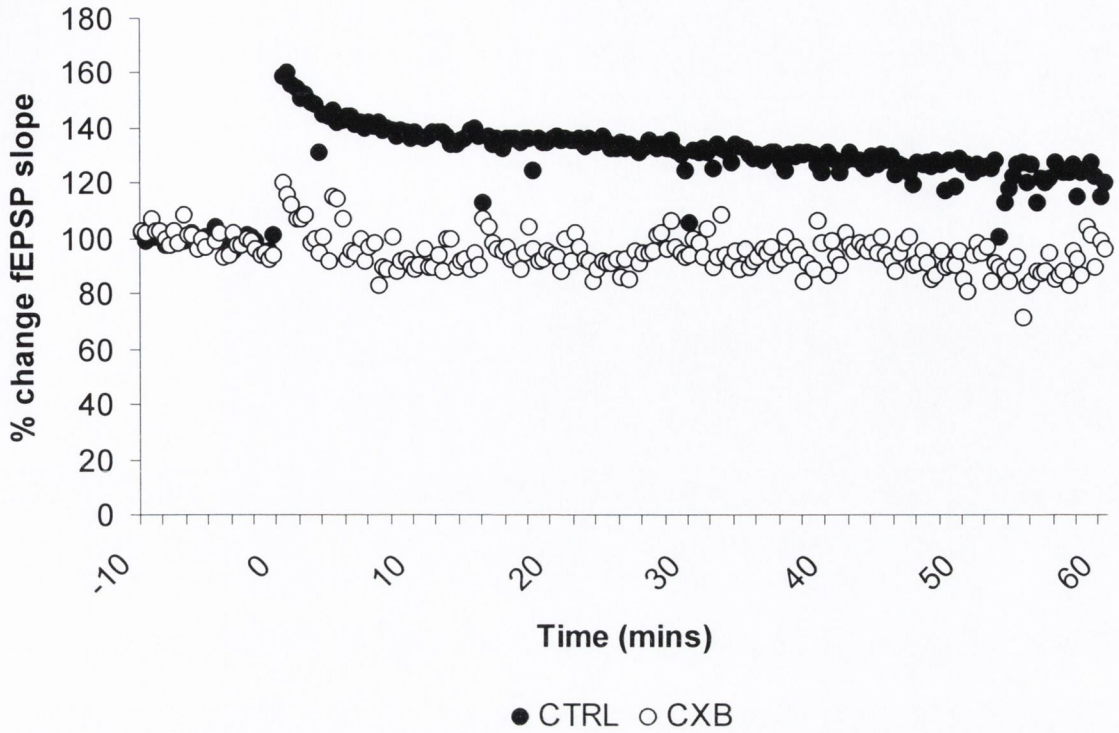


Figure 3.2 Representative non-averaged recordings from individual celecoxib and vehicle treated rats. Results are expressed as the percent change of the fEPSP slope relative to baseline for all stimuli. Note the impairment of a post-tetanic potentiation in the celecoxib (35 mg/kg) treated animal.

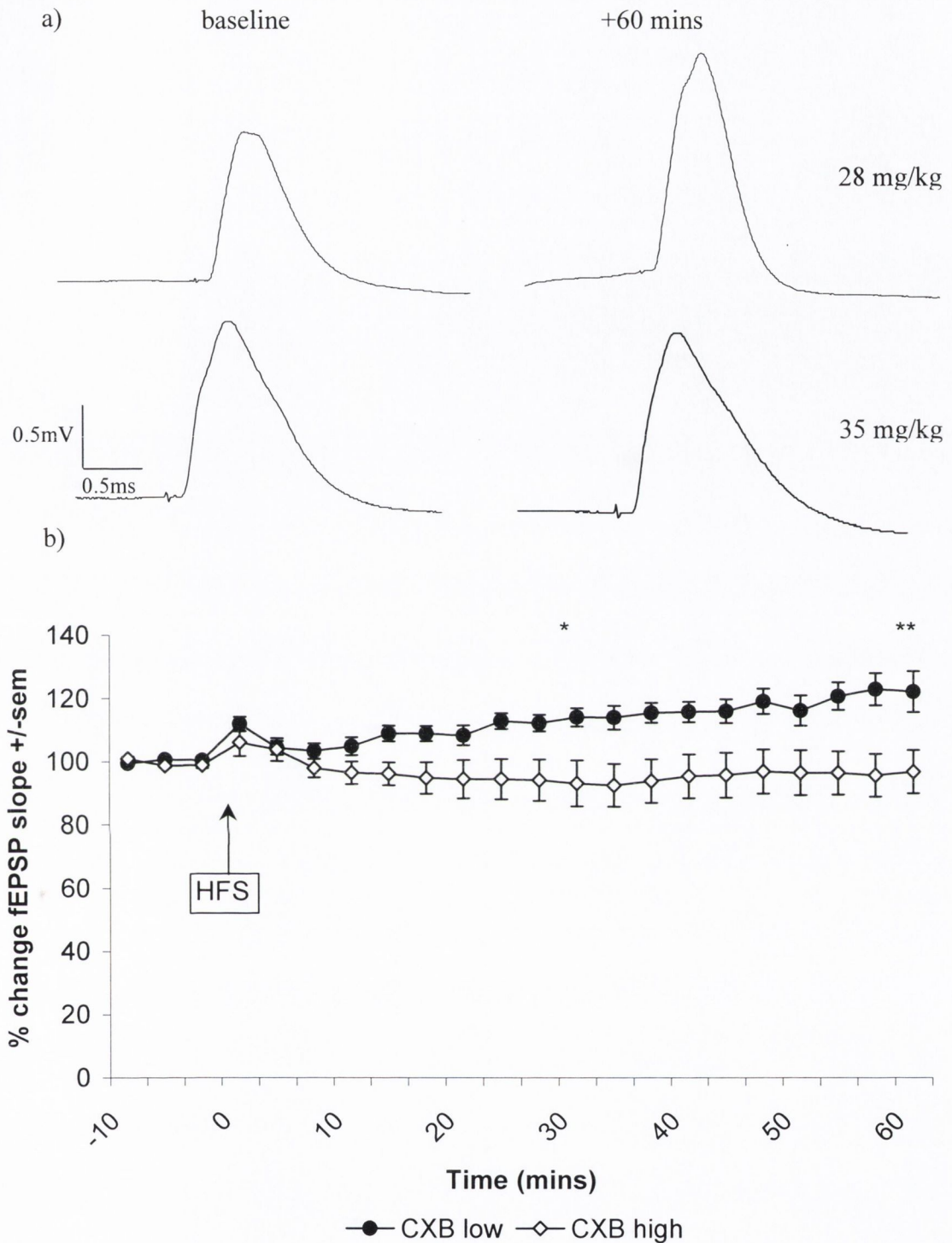


Figure 3.3 The block of LTP depends on the dose of celecoxib given to the rats. Either CXB low dose (28mg/kg) or CXB high dose (35mg/kg) was administered 30mins prior to anaesthesia.

- a) Representative traces of fEPSPs recorded during baseline and 60mins postHFS (as marked) for each treatment.
- b) Percent change in fEPSP slope relative to baseline \pm SEM (where error bars are not visible SEM is too small).

A binomial test was used to investigate whether COX-1 and COX-2 inhibition would alter the proportion of animals with successful LTP (defined as an increase of $\geq 20\%$, in either

amplitude or slope, of the fEPSP relative to baseline). The rate of success in the control, vehicle treated group (78.95%) was used as a measure of the test proportion to which the treatment groups were compared (SC560 66.67% and CXB 28.57%) (Figure 3.4). A highly significant decrease in the proportion of animals with $\geq 20\%$ in fEPSP was evident as a result of celecoxib, but no deficit resulted from Sc560.

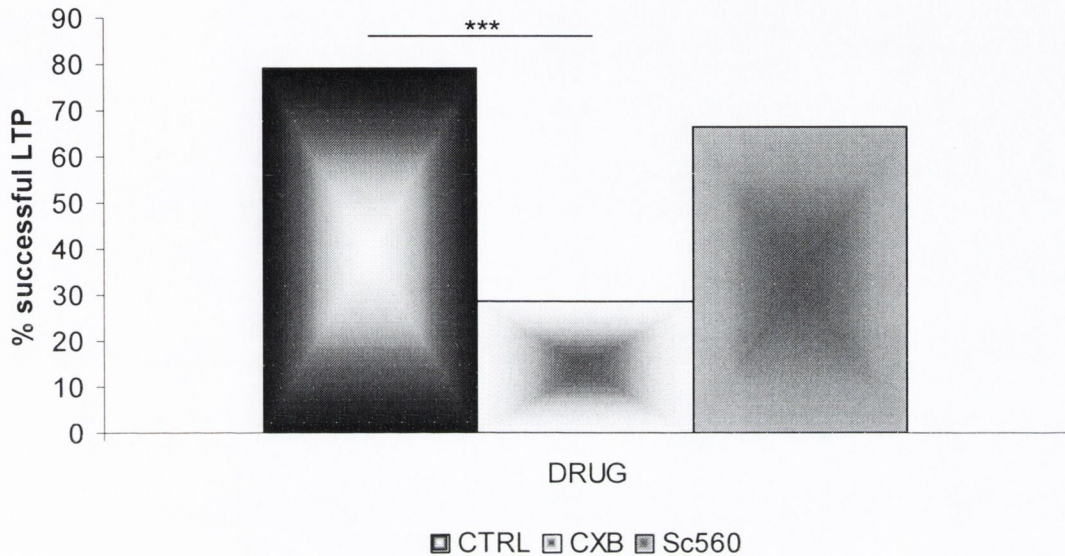


Figure 3.4 Percentage of animals with $\geq 20\%$ increase in fEPSP slope and/or amplitude after 25-30 minutes post HFS. A binomial test showed that the proportion of animals with LTP was greatly reduced by celecoxib treatment but not by Sc560.

3.3.1.2 BDNF concentration is increased as a result celecoxib treatment.

The dentate gyri from both the stimulated and contralateral, unstimulated hemispheres of the animals from the above experiment were dissected and measured for BDNF concentration by ELISA (Figure 3.5). Results are expressed as a percentage of the mean BDNF concentration in the vehicle-treated, unstimulated dentate gyri.

We tested the hypotheses that

1. HFS-induced LTP would trigger increases in ipsilateral BDNF concentration relative to contralateral, unstimulated controls,
2. Pharmacological intervention would alter BDNF relative to control and
3. That the dose of celecoxib systematically affects any changes that may be observed.

A two-way repeated measures ANOVA showed no within-group differences in the stimulated and unstimulated tissue, $F_{(1,43)}=1.0$; $p>0.05$ thus failing to reject the first hypothesis. However, the pharmacological interventions resulted in very significant changes in BDNF concentration, $F_{(3,43)}=5.01$; $p<0.01$. Newman-Keuls post hoc tests showed that 35 mg/kg CXB had significantly more BDNF than any of the other groups, and that neither the BDNF concentration in the dentate gyri of the Sc560 nor 28 mg/kg celecoxib was different from the control group. A one-way ANOVA found significant differences in BDNF concentration in the stimulated hemisphere only: $F_{(3,43)}=3.496$; $p<0.05$. To test the second and third hypotheses we used *a priori* planned comparison tests between CTRL v 35 mg/kg CXB and 28 mg/kg v 35 mg/kg CXB groups. Both comparisons were significant: the former was $p<0.05$ and the latter $p<0.01$. Thus, in summary, there were no differences between stimulated and unstimulated tissue, or as a result of treatment with the COX-1 inhibitor or low-dose CXB relative to controls. Conversely, the higher dose of celecoxib significantly increased the concentration of BDNF in the stimulated dentate relative to both the controls and lower dose celecoxib.

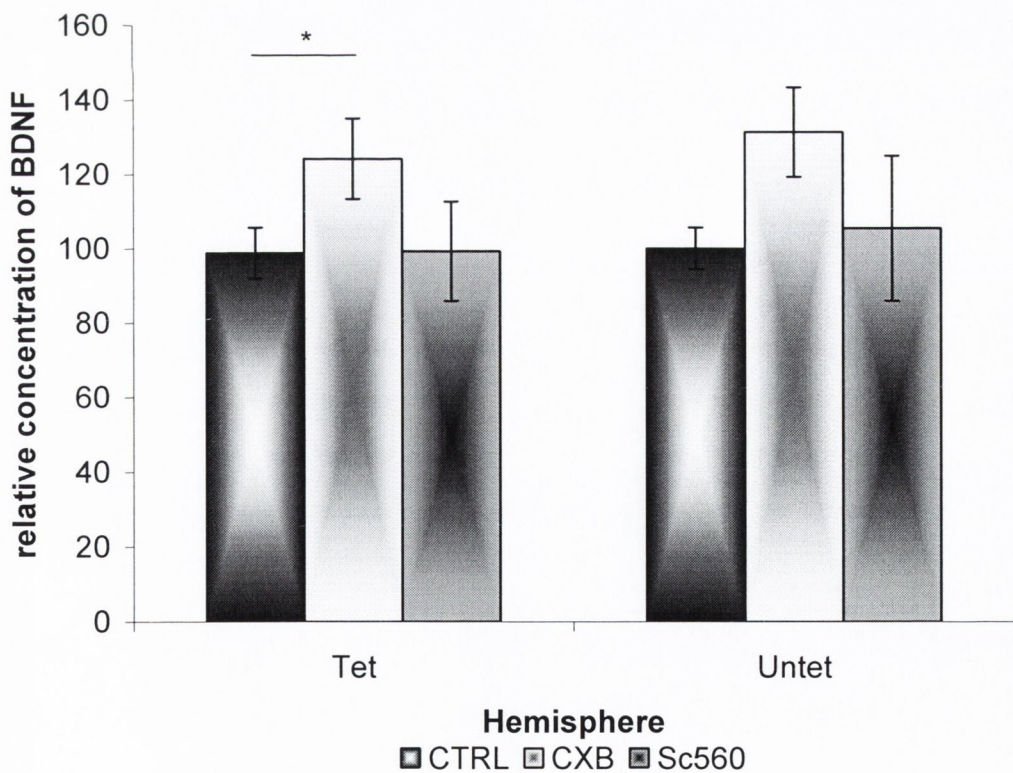


Figure 3.5 BDNF concentration was measured in the dentate gyrus of both stimulated and unstimulated hemispheres of each animal by ELISA and these concentrations are expressed as a percentage of the average untetanised, vehicle-treated control. Significantly more BDNF was measured in the celecoxib treated (35 mg/kg) animals than in the controls or Sc560 treated animals bilaterally.

DRUG	TISSUE	% Mean	SEM
CTRL (n=17)	Tet	96.28	6.79
	Untet	100.00	5.91
28mg/kg CXB (n=10)	Tet	82.39	9.0
	Untet	94.42	9.79
35mg/kg CXB (n=14)	Tet	125.40	11.58
	Untet	132.19	12.88
Sc560 (n=6)	Tet	99.27	13.39
	Untet	105.43	19.50

Table 3.2 Ipsi- and contralateral concentrations of BDNF after tetanic stimulation (tet). BDNF concentrations are expressed as a percentage of untetanised control concentration.

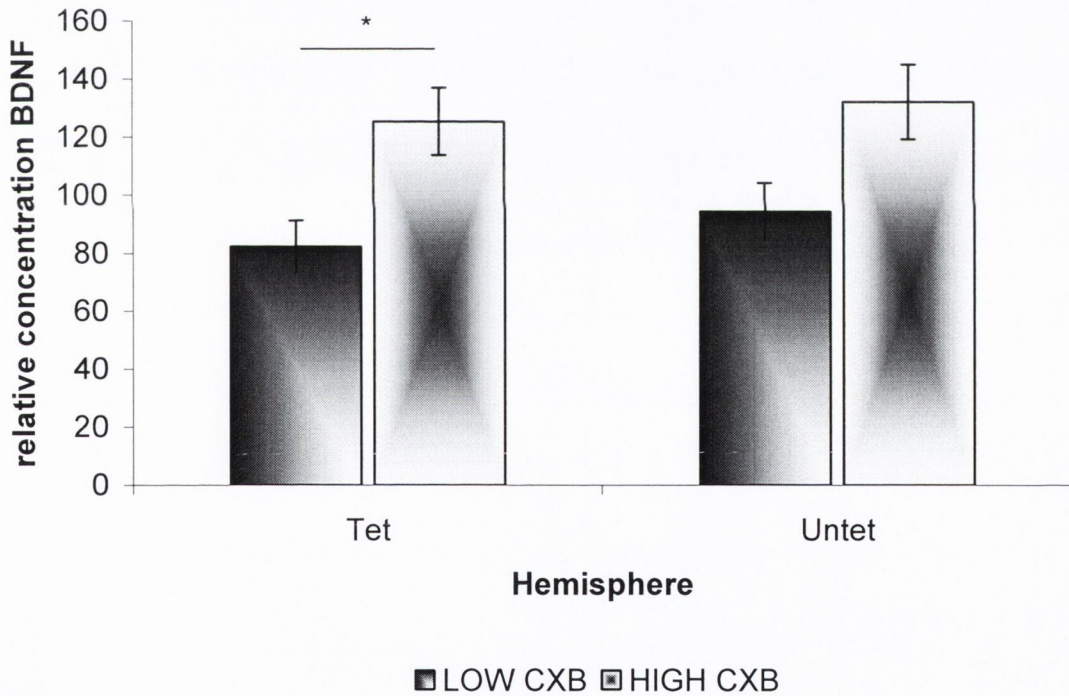


Figure 3.6 Significantly more BDNF was measured in the animals treated with the higher concentration of celecoxib (35mg/kg) compared to the lower dose of 28 mg/kg. Concentrations are expressed as a percentage of the BDNF concentration in the untetanised hemisphere of the vehicle-treated animals.

3.3.1.3 Blood plasma corticosterone was unaltered by COX-2 inhibition

Blood plasma corticosterone levels were measured in terminal bleed, trunk-blood samples taken immediately after the end of LTP recording. An independent samples t-test revealed no significant change in corticosterone as a result of treating the animals with celecoxib (CTRL: $n=7$, $\text{mean}=528.58\pm43.96$ ng/ml, CXB: $n=6$, 378.41 ± 89.95 ng/ml) $t_{(11)}=1.57$; $p>0.05$.

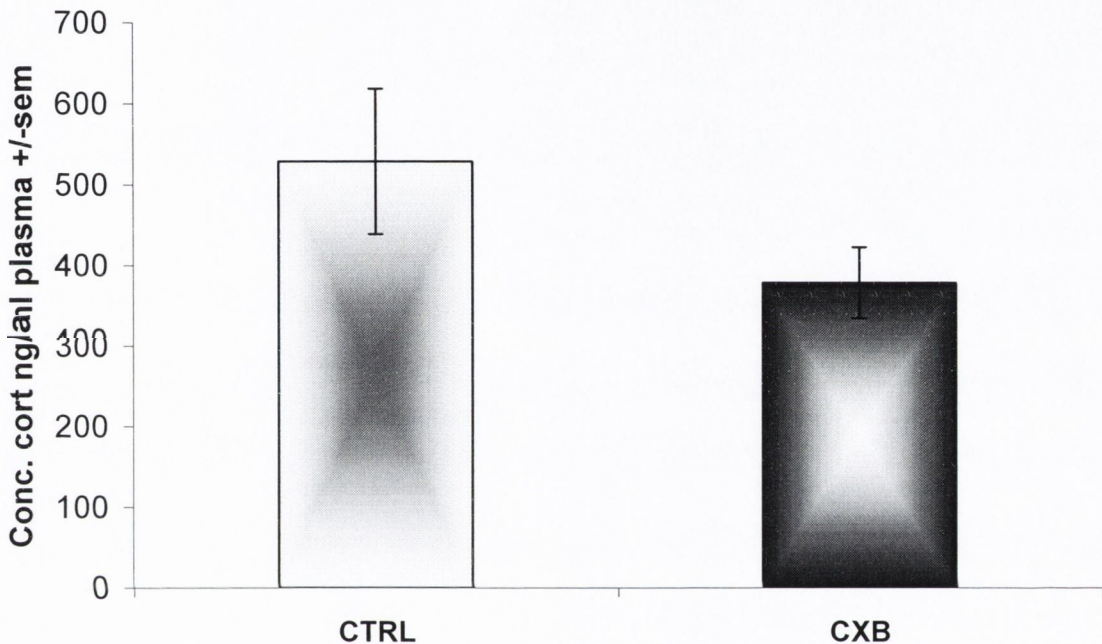


Figure 3.7 Blood plasma corticosterone was measured using radioimmunoassay as a control to ensure that celecoxib treatment (35 mg/kg) did not affect the corticosterone levels and thus impair LTP induction.

3.3.2 COX-2 inhibition and baseline synaptic transmission at constant current

In the above experiment the pharmacological agents were administered 30 minutes prior to anaesthesia, thus a minimum of an hour after the administration of celecoxib. Therefore, to ensure that celecoxib had no effect at shorter latencies, on baseline synaptic transmission, celecoxib was given after anaesthesia and the establishment of stable recordings. Upon injection baseline recording at a constant current were commenced. The fEPSP slope measured over an hour was normalised to the first five minutes of recording (Figure 3.8). A mixed-factorial ANOVA of the first five minutes and the last five minutes showed no effect of baseline recordings, $F_{(1,8)}=3.36$; $p>0.05$, nor an effect of celecoxib treatment,

$F_{(1,8)}=0.919$; $p>0.05$, nor an interactive effect of celecoxib and recording, $F_{(1,8)}=0.028$; $p>0.05$.

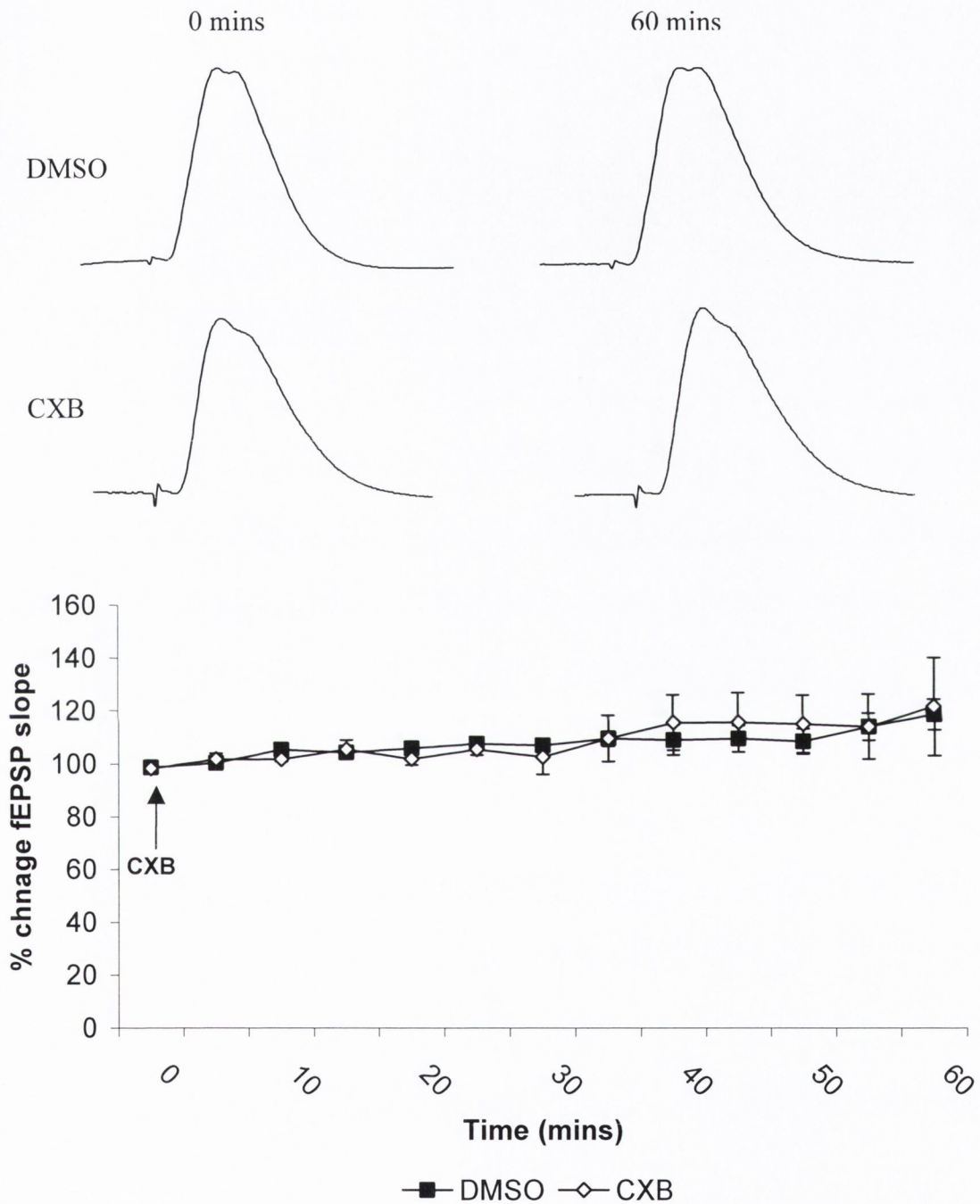


Figure 3.8 Recording made during the administration of celecoxib (CXB) or its vehicle remained constant up to an hour after administration when maximal concentrations of CXB are reported reached in the brain.

3.3.3 The effects of COX-2 inhibition on the maintenance of LTP and BDNF concentration in DG

3.3.3.1 The maintenance of LTP is not affected by COX-2 inhibition

In order to investigate if COX-2 inhibition would cause a degradation of previously established LTP, 20 minutes after the induction of LTP with 250hz HFS, we administered celecoxib (35 mg/kg) or vehicle (10% DMSO) and recorded for a further 70 minutes (a total of 90 minutes after HFS) (Figure 3.9).

DRUG	TIME	% Mean	SEM
CTRL (n=11)	BASELINE	100.59	0.26
	15-20mins	135.76	6.12
	85-90mins	148.94	12.60
CXB (n=10)	BASELINE	99.97	0.37
	15-20mins	126.10	4.00
	85-90mins	131.55	8.23

Table 3.3 Descriptive statistics for the injection of celecoxib (35mg/kg) or its vehicle after the induction of LTP.

A mixed-factorial ANOVA was used to compare the fEPSP slope of the CTRL and CXB treated animal at baseline, 15-20 minutes (immediately prior to CXB administration) and 85-90 minutes post-HFS (70 mins after CXB administration). The ANOVA showed an overall effect of HFS on the fEPSP slope $F_{(1,26,22,7)}=23.8$; $p<0.001$, implying that LTP was induced in both groups, but it failed to show any effect of celecoxib treatment $F_{(1,18)}=1.54$; $p>0.05$. Thus, the LTP induced by 250Hz HFS was unaffected by subsequent CXB treatment.

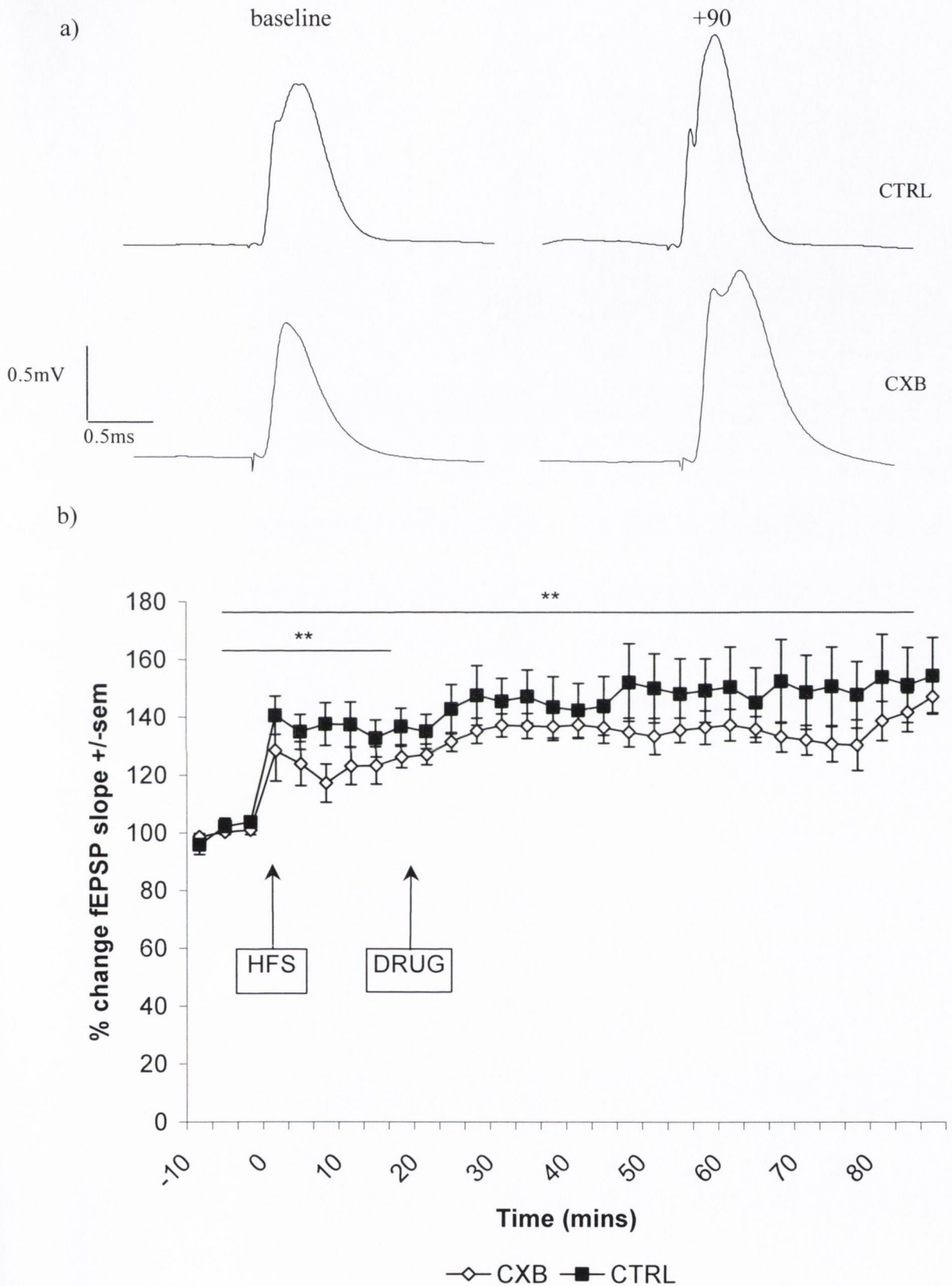


Figure 3.9 The injection of celecoxib (35 mg/kg) 20 minutes after the induction of LTP did not alter the maintenance phase of the LTP up to 90 minutes after its induction i.e. 70mins after the administration of celecoxib.

3.3.3.2 BDNF was decreased as a result of COX-2 inhibition after HFS.

We measured BDNF concentration in both the dentate gyri of these animals – whereby LTP was induced in one hemisphere and the other hemisphere was an unstimulated control. In contrast to the lack of effect of celecoxib on the maintenance of LTP we found that this manipulation resulted in a decrease in BDNF concentration. A mixed-factorial ANOVA, measuring within hemisphere differences and between drug treatment effects, showed no significant within-group differences in BDNF concentration as a result of inducing LTP in one hemisphere compared to the unstimulated control: $F_{(1,17)}=0.202$; $p>0.05$. However, injecting the animals with celecoxib after LTP had been induced resulted in significantly less BDNF: $F_{(1,17)}=7.451$; $p<0.05$. Independent t-tests showed that this effect stems from a difference between the celecoxib and control stimulated dentate gyri $t_{(17)}=2.34$, $p<0.05$.

DRUG	TISSUE	% Mean	SEM
DMSO (n=10)	Tet	114.84	13.99
	Untet	100.00	9.23
CXB (n=9)	Tet	75.09	8.86
	Untet	80.51	8.94

Table 3.4 Ipsi- and contralateral concentrations of BDNF after high frequency stimulation. BDNF concentrations are expressed as a percentage of unstimulated control concentration.

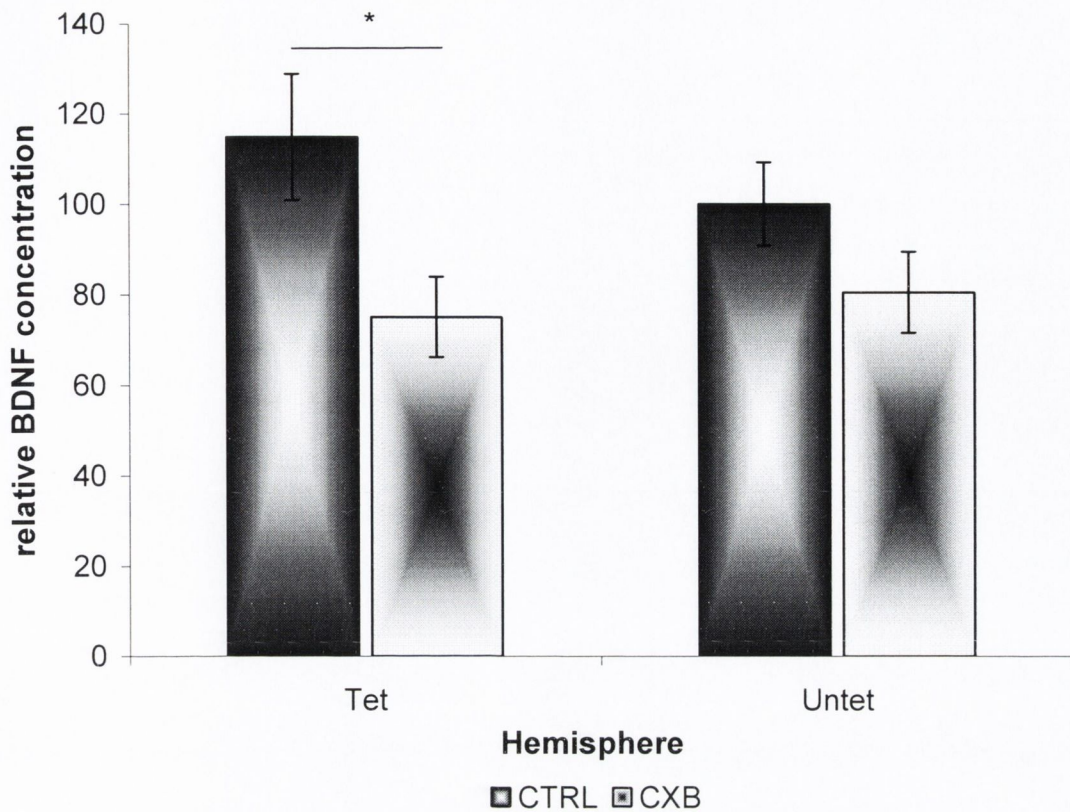


Figure 3.10 The concentration of BDNF, measured 90 minutes after LTP was induced by HFS, was dramatically decreased by injecting celecoxib (35 mg/kg) 20 minutes after HFS even though there was no effect on the degree of LTP. Concentrations are expressed as a percentage of the BDNF concentration in the unstimulated hemisphere of the vehicle treated animals.

3.3.3.3 Blood plasma corticosterone was unaltered by COX-2 inhibition after the induction of LTP

Blood plasma corticosterone levels were measured in terminal bleed, trunk-blood samples in the animals in the above experiment, taken immediately after the end of LTP recording. An independent samples t-test revealed no significant change in corticosterone as a result of treating the animals with celecoxib (CTRL: $n=5$, mean= 568.6 ± 26.2 ng/ml, CXB: $n=5$, 492.7 ± 38.6 ng/ml) $t_{(9)}=1.55$; $p>0.05$.

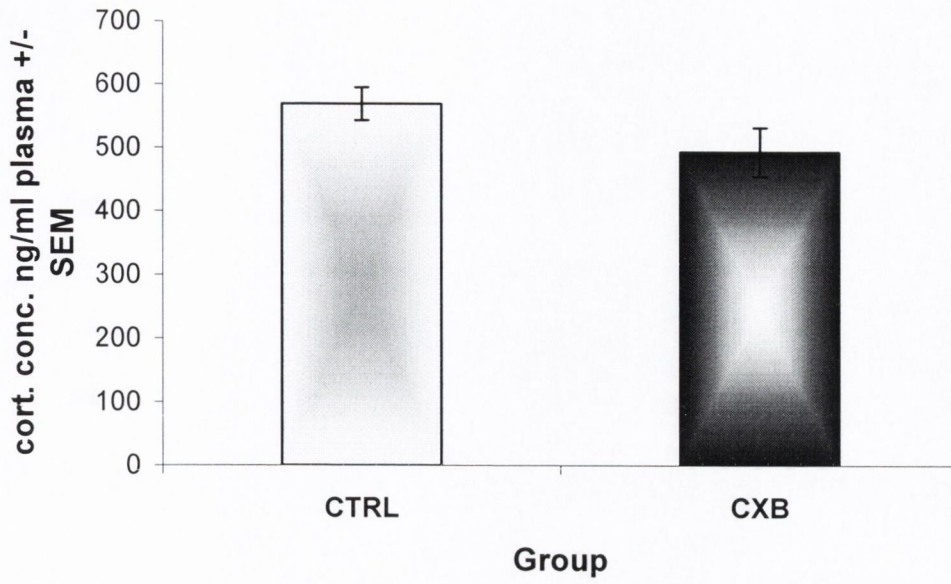


Figure 3.11 Blood plasma corticosterone was measured using radioimmunoassay as a control to ensure that celecoxib treatment (35 mg/kg) did not affect the corticosterone levels and thus impair LTP induction.

3.4 Discussion

3.4.1 Isoform specificity and the block of LTP

Selective COX-2 but not COX-1 inhibition successfully blocked the induction of LTP, in a dose-dependent manner and this impairment reveals itself immediately after HFS. Although COX-2 is an immediate early gene, and has been shown to be rapidly activated in response high frequency stimulation-induced NMDA receptor activation (Yamagata et al., 1993), it is obvious from the data presented here that a function for the basal activity of COX-2 in the induction of synaptic plasticity *in vivo* has been established.

Post-tetanic potentiation (the initial phase of increased response immediately after tetanus) is believed to occur as a result of residual Ca^{2+} in the presynaptic terminal resulting in an increase in probability of release of docked vesicles and hence neurotransmitter release (Zucker, 1999; Zucker & Regehr, 2002). An observation during experimentation was that PTP in COX-2 treated animals, while not significant, was markedly smaller, and suggests that PGE_2 could be involved in Ca^{2+} entry into the presynaptic cell.

Figure 3.1 demonstrates a disparity in function between COX-1 and -2 in the induction of LTP. Despite the fact that these isozymes have very similar structures, metabolise the same endogenous substrates, with very similar catalytic activity and kinetics, they appear to perform at least some unique physiological functions. Subtle differences, for instance in, sub-cellular localisation, co-localisation with phospholipases and downstream prostanoid synthases, and kinetic properties might explain these differences. The most obvious difference between the isoforms is in the regulation of the expression of their respective genes, which are even located on different chromosomes (W. L. Smith, Garavito, & DeWitt, 1996). In the periphery this results in the constitutive expression of COX-1 and the virtual absence of COX-2 until stimulated. However, in the CNS both enzymes are constitutively expressed; COX-1 is distributed in neurons throughout the brain (including the hippocampus), (Breder et al., 1992), while COX-2 is expressed in discrete populations of neurons most particularly in the hippocampus (Breder et al., 1995; Yamagata et al., 1993). Thus, both isozymes are expressed in the hippocampus. Moreover, differences in subcellular localisation are not drastic; COX-2 is more highly concentrated on the nuclear envelope (Morita et al., 1995) suggesting a link between it and a signal to the nucleus.

Furthermore, COX-2, but not COX-1, has been co-localised with cPLA2 (cleaves AA from phospholipids in the membrane) (Pardue, Rapoport, & Bosetti, 2003) and cPLA2 deficient mice show down regulation of COX-2 (Bosetti & Weerasinghe, 2003). Downstream of cyclooxygenase, mPGES2 (microsomal prostaglandin E synthase-2; converts PGH-2 from COX activity into PGE2) expression is attenuated in COX-2 deficient mice even with compensatory upregulation of COX-1 (Bosetti, Langenbach, & Weerasinghe, 2004). Since AA is highly diffusible within a cell, how could there be differences in its metabolism by the isozymes when both are expressed in the same cell? It has been shown that lower concentrations of AA are preferentially metabolised by COX-2 (W. L. Smith, DeWitt, & Garavito, 2000) and "*mPGES was functionally coupled with COX-2 in marked preference to COX-1, particularly when the supply of arachidonic acid was limited. Increased supply of arachidonic acid by explosive activation of cytosolic phospholipase A2 allowed mPGES to be coupled with COX-1*" (Murakami et al., 2000). Yermakova reported that COX-1 protein is localised to human hippocampal CA3, and CA4 neurons but not in the dentate gyrus (Yermakova, Rollins, Callahan, Rogers, & O'Banion, 1999). Thus it is feasible that the low levels of AA present prior to HFS are garnered by COX-2 to produce PGE2 via mPGES2 and that COX-1 inhibition does not interfere.

It is also noteworthy that the structural differences between the two isoforms, which have been identified with drug specificity, all facilitate a wider range of fatty acid substrates for COX-2 than for COX-1: eicosapentaenoic acid, α - and γ -linolenic acid, 2-AG amongst other (Vane, Bakhle, & Botting, 1998). Thus, the inequality between COX-1 and -2 in LTP could be independent of the production of PGs. Moreover, are they COX-dependent at all? Several COX-independent actions of NSAIDs, more especially celecoxib, have been reported. One such report showed that celecoxib, but not aspirin, ibuprofen, naproxen, rofecoxib, DuP697 or NS398, could inhibit endoplasmic reticulum Ca^{2+} -ATPase thus preventing the reuptake of Ca^{2+} release from intracellular store, leading to an increase in $[\text{Ca}^{2+}]_i$ (Johnson et al., 2002). This effect was shown in multiple cell types and to be concentration dependent. It is possible that the LTP impairment evident here results from disturbances in intracellular Ca^{2+} signalling (Behnisch & Reymann, 1995). Thus it is necessary to determine the cause of LTP impairment and in later experiment it will be investigated if direct replacement of PGE_2 , the principle metabolite of COX-2 activity (Brock et al., 1999), into the hippocampus is sufficient.

In contrast to previous reports of unilateral increases in BDNF protein in tissue where LTP had been induced by HFS (Gooney & Lynch, 2001), we found no significant difference between the unstimulated and stimulated hemisphere. The duration of the recording before the animal was sacrificed, 40 minutes versus 1-hour post-HFS, and the degree of LTP reported (approximately 140% compared to 125% above) should be taken into account. As discussed in this paper, elevations in BDNF mRNA are not evident until 2-6 hours after LTP induction (Bramham et al., 1996; Morimoto et al., 1998), suggesting the increase in protein does not depend on transcription. A further consideration is the lack of information regarding sensitivity of the BDNF antibody for pre-pro-, pro- and mature (m)BDNF provided by the Promega BDNF ELISA kit; if it detects only mBDNF then the results could represent cleavage of the pro-domains and not translation. Since we report no increase at 1-hour post-HFS we may have observed an acute phase of BDNF increase in E-LTP induction. Bi-lateral changes in BDNF mRNA have been reported as a result of unilateral LTP (Bramham et al., 1996) but this pattern does not manifest until 6 hours post-HFS.

Unexpectedly and in direct contradiction to the finding that ibuprofen results in a decrease in BDNF after HFS (Shaw et al., 2003), a significant increase in BDNF concentration was reported as a result of celecoxib treatment. This increase is activity-dependent since it is not evident in the concentration of BDNF measured in the baseline experiment in chapter II, furthermore, an interaction of celecoxib treatment and paired-pulse stimulation causing a small increase in BDNF. The different effects reported here and by Shaw et al. could simply be a result of the different stimulation protocols used to induce LTP (200Hz (Shaw et al., 2003) compared to 250Hz reported here) but one would expect that the stimulation protocol would affect both control and drug-treated groups equally. Alternatively, the effects of celecoxib on $[Ca^{2+}]_i$ reported above may result in increased BDNF expression (Sano, Nanba, Tabuchi, Tsuchiya, & Tsuda, 1996; Zafra, Lindholm, Castren, Hartikka, & Thoenen, 1992) but this does not explain the decrease as a result of ibuprofen treatment. Examination of the promoter region of the BDNF gene revealed a putative binding site for the calcium-activated transcription factor NF κ B, and NF κ B activation has been shown to be required for NMDA induced expression of BDNF (Marini et al., 2004). A non-cyclooxygenase activity of celecoxib is the activation of NF κ B at high doses (Niederberger

et al., 2001) whereas ibuprofen inactivates it directly, or indirectly by inhibition of IKK (Palayoor, Youmell, Calderwood, Coleman, & Price, 1999) (NF κ B exists in an inactive state bound to I κ B and, liberation and activation requires phosphorylation of I κ B by IKK). The results presented here also show dose dependence for the increase of BDNF concentration, since 28mg/kg did not increase BDNF. It could be suggested that the contradictory finding that ibuprofen decreases activity-dependent expression of BDNF as reported by Shaw et al. (Shaw et al., 2003) whereas celecoxib increases it are, in fact, coincidental to, and not necessary for the block of LTP and result from cyclooxygenase-independent action of the different cyclooxygenase inhibitors. This leads to the conclusion that the increase in BDNF concentration observed after exercise is also probably unrelated to the reverse of the block of LTP (Shaw et al., 2003) and could be a result of numerous genes being upregulated with exercise (Molteni, Ying, & Gomez-Pinilla, 2002).

The corticosterone levels in terminal blood were the same for both groups, which is an important control since glucocorticoids inhibit COX-2 expression (Yamagata et al., 1993). A second important control, where fEPSPs were recorded at constant current before and after COX-2 inhibition, was performed to ensure that the block of LTP was not as a result of baseline drift; a slow rising increase in the size of fEPSP as a result of COX-2 inhibition could occlude facilitation by HFS. No effect of COX-2 inhibition on the fEPSPs, recorded over an hour, was evident.

3.4.2 The maintenance of LTP is not affected by COX-2 inhibition, although the concentration of BDNF is

To test the hypothesis that COX-2 inhibition affects only the initial induction process and not the expression of LTP, 35 mg/kg celecoxib or its vehicle were injected 20 minutes after the successful induction of LTP (operationally defined at $\geq 20\%$ increase in fEPSP slope) and recorded up to 90 minutes after HFS. This approach did not alter the expression of LTP, thus confirming that basal COX-2 activity leading up to HFS is required for successful induction of LTP.

Given that LTP was not affected by post-HFS celecoxib, the discovery that BDNF concentration was decreased was unexpected. One consequence is that it shows the

increase observed as a result of celecoxib prior to HFS, depends on HFS for its expression. Further experiments are necessary to determine if this deficit in BDNF is functional regarding LTP maintenance and the expression of L-LTP, which has been shown to require BDNF. Kang et al. showed that scavenging of endogenous BDNF blocked L-LTP while leaving E-LTP intact, but most notable is the time dependence of this effect, that is, LTP was reversed between 30-60 min but not 70-100mins by BDNF scavenging (Kang, Welcher, Shelton, & Schuman, 1997). Thus our observation of decreased BDNF at 90 min may not be physiologically relevant. But this finding does suggest that COX-2 IEG up-regulation may modulate BDNF and the transition to L-LTP; experiments in unanaesthetised animals would allow sufficiently long recordings test this.

As mentioned a caveat must be noted in the measurement of BDNF using this ELISA in that it is not known whether the antibody used can differentiate between pre-pro-, pro-BDNF and mBDNF. Thus, interpretation of the functional relevance of the results is difficult. If the ELISA was definitively sensitive to mature BDNF then the changes in concentration could represent post-translational modification of immature pre-pro-BDNF. Likewise, if it was known that the assay detected all forms of BDNF then it could be concluded that the changes result from transcriptional regulation. Thus, to reach any conclusions about the causes of BDNF concentration alterations further, more sensitive experimentation is required (antibodies sensitive to immature and mature BDNF are available). BDNF will not be considered further in this thesis.

Chapter 4 Exogenous PGE₂ alleviates the block of LTP

Chapter 4	Exogenous PGE ₂ alleviates the block of LTP	106
4.1	Introduction.....	108
4.1.1	PGE ₂ and central effects	108
4.1.2	Intracellular signalling and LTP	111
4.2	Materials & methods.....	114
4.2.1	Materials	114
4.2.2	Surgery.....	114
4.2.3	Pharmacological treatment schedules.....	115
4.2.4	Stimulation and data acquisition.....	116
4.2.5	Western blotting.....	116
4.2.6	Statistics	117
4.3	Results.....	118
4.3.1	Input/output curves	118
4.3.2	Paired-pulse ratio	122
4.3.3	Occlusion of the COX-2-dependent block of LTP by intrahippocampal injection of PGE ₂	124
4.3.3.1	Baseline recordings during PGE ₂ -injection	124
4.3.3.2	PGE ₂ -injection before HFS reverses the COX-2-dependent LTP impairment: ERK-phosphorylation and c-Fos after 1 hour	125
4.3.3.3	PGE ₂ (132µM) treatment resulted in sustained LTP: no inter-hemispheric changes in ERK and c-Fos after 3 hours.....	134
4.4	Discussion.....	140
4.4.1	Baseline synaptic transmission, PPR and PGE ₂	140
4.4.1.1	Effects of PGE ₂ on I/O curves and baseline synaptic transmission	140
4.4.1.2	PPR and PGE ₂	141
4.4.2	Occlusion of the block of LTP by intrahippocampal injection of PGE ₂ ...	142

4.1 Introduction

Although we know celecoxib is a selective COX-2 inhibitor blocking the production of prostaglandins, it is important to rule out other consequent or non-specific actions, for instance a build-up of arachidonic acid no longer being metabolised by COX-2, altered endocannabinoid metabolism (Kim & Alger, 2004), stimulation of NFκB (Tegeeder et al., 2001), effects of celecoxib on intracellular Ca²⁺ stores (Johnson et al., 2002), among others. It has been reported that AA build-up from COX inhibition can lead to an increase of the stimulated release of glutamate (Dickie et al., 1994). AA has also been implicated with excitatory amino acid transporters (EAAT) altering the rate of glutamate reuptake out of the synaptic cleft back into the cell (Fairman, Sonders, Murdoch, & Amara, 1998; Volterra et al., 1992; Zerangue et al., 1995). The purpose of the following experiments is to determine the source of the deficits induced by COX-2 inhibition in both short-term and long-term plasticity. It will be investigated if exogenous replacement of PGE₂ is sufficient to overcome these deficits as shown in vitro by Chen et al (C. Chen et al., 2002) and the locus of changes within the cells of the dentate gyrus as regards signalling cascade and transcription factors.

4.1.1 PGE₂ and central effects

The focus of research regarding prostaglandins in synaptic function has been directed at their capability to modulate neuronal excitability in sensory neurons in all modalities of pain (mechanical, thermal, chemical) and their function in the induction of hyperalgesia (heightened sensitivity to repeated exposure to a painful stimulus). A rapidly growing body of literature has been published on the role of prostaglandins in the pain pathway via the dorsal root ganglion neurons (DRG) of the spinal cord, with respect to ion channels, and neurotransmitter release. There is one major similarity between the neurons of the DRG and the hippocampus; a phenomenon called ‘winding up’; when a certain frequency of stimulation is applied to the deep neurons of the dorsal horn their responses to even basal afferent stimulation can be augmented by up to 20-fold (Dickenson, 1995). PGE₂ can modulate this ‘winding up’ process by a number of different mechanisms – increased neurotransmitter release; alterations in ion channel opening in particular at a number of different K⁺-channels (see Table 4.1) – but what over shadows all this research is a lack of information on the specific EP receptors expressed and where in the neurons they are

localised. As discussed in the literature review, there are four EP receptor isoforms and several splice-variants of the EP₃ subtype, all of which are seven-transmembrane g-protein-coupled receptor. The intracellular cascade activated by PGE₂ depends on the isoform or splice variant it binds (see table 1.2). Up until very recently, a similar lack of information on EP receptor expression pattern was true of the hippocampal literature, except for reports on the virtual absence of EP₄ receptors (Takadera et al., 2004; Zhang & Rivest, 1999). Peimin Zhu in Nicolas Bazan's laboratory, profiled EP receptors in the hippocampus and reported them to be heterogeneously expressed in presynaptic, postsynaptic sites and soma (C. Chen & Bazan, 2005b; Zhu et al., 2005) (see literature review for synopsis of the main findings).

Ion	Channel	Tissue where PGE ₂ applied	Effects of PGE ₂	Pre vs. Post synaptic	EP receptor	Examples of functions	Reference
K ⁺	Calcium-dependent K ⁺ channel	Preoptic neurons of hypothalamus	↑NMDA-induced outward current and cell repolarisation thus ↓ firing rate POA neurons	Post-synaptic		Fever, hyperalgesia, immunosuppression	(Katafuchi, Duan, Take, & Yoshimura, 2005)
		Rat supraoptic neuron of hypothalamus	↓ in frequency of sIPSC ⇒ ↑ postsynaptic neuron excitability	Presynaptic	EP ₃	Fever, hyperalgesia, immunosuppression	(Ibrahim et al., 1999)
		Rat supraoptic neuron of hypothalamus	EP ₄ agonist excited postsynaptic neurons. EP ₃ agonist ↓ presynaptic sIPSCs.	Pre- and post-synaptic	EP ₃ EP ₄	Fever, hyperalgesia, immunosuppression	(Shibuya et al., 2002)
Cation	Inward Cation currents	Rat spinal dorsal horn neuron (<i>in vitro</i>)	↑ probability of action potential from subthreshold inputs.	Post-synaptic	EP ₂ -like	Nociception, hyperalgesia	(Baba, Kohno, Moore, & Woolf, 2001)
		Rat spinal dorsal horn neuron (<i>in vivo</i>)	↑ neuronal excitability during induction but not maintenance of inflammation using mechanical and chemical stimuli.			Nociception, hyperalgesia	(Vasquez et al., 2001)
Ca ²⁺	L-type Ca ²⁺ channel	Dorsal root ganglia (DRG) (chick embryo)	↑ Ca ²⁺ -entry into cells and release of Substance P. Delayed response thus probably indirect action via transduction cascade.	Presynaptic		Nociception, hyperalgesia	(Nicol, Klingberg, & Vasko, 1992)
K ⁺	Delayed rectifier-like I _k	DRG (Rat embryo)	↓ outward K ⁺ -current and 2-fold ↑ in the number of action potentials and is dependent on cAMP			Nociception, hyperalgesia	(Nicol, Vasko, & Evans, 1997), (Evans, Vasko, & Nicol, 1999)
Na ⁺	TTX-resistant Na ⁺ current	DRG	↑ rate of activation and inactivation of Na ⁺ channels in a cAMP dependent manner.			Nociception, hyperalgesia	(Gold, Reichling, Shuster, & Levine, 1996), (England, Bevan, & Docherty, 1996)
Cation	Inward Cation currents	NTS	Excites neurons by activating cation-channels. ↑ firing rate of neurons.			Temp. regulation, circulation	(Matsumura et al., 1993)
		Nucleus Tractus solitari (NTS)	↑ evoked and spontaneous release of glutamate (non-NMDAR sensitivity unaffected)	Presynaptic		Temp. regulation, circulation	(Sekiyama, Mizuta, Hori, & Kobayashi, 1995)
K ⁺ Ca ²⁺	Delayed rectifier I _k , VDCC	CA1 pyramidal neurons of the Hippocampus	↓ outward K ⁺ current causing ↑ membrane excitability. Inhibited Ca ²⁺ -currents.	Post-synaptic		Memory & learning, spatial navigation.	(C. Chen & Bazan, 2005a)
Ca ²⁺	VDCC	Rat melanotrophs of pituitary	Inhibition of Ca ²⁺ entry ↓ [Ca ²⁺] _i , thus ↓ spontaneous secretion of peptides	N/A	EP ₃	Neuro-immuno-endocrine	(Nagata et al., 2003)

Table 4.1 Effects of PGE₂ on cell excitability and ion channel modulation via the EP receptor subtype and/or second messenger system and possible consequences. VDCC = voltage dependent calcium channels, TTX = tetrodotoxin, I_k=potassium current. Intracellular signalling and LTP

4.1.2 Intracellular signalling and LTP

The activation of signalling cascades and IEG induction has been implicated in the progression for short-term to long-term strengthening of synapses (Davis & Laroche, 1998). In the experiments that follow the effects of intrahippocampal PGE₂-treatment will be investigated in relation to LTP induction and its ability to overcome the COX-2-dependent block of LTP; the associated changes in protein phosphorylation and IEG induction will also be examined.

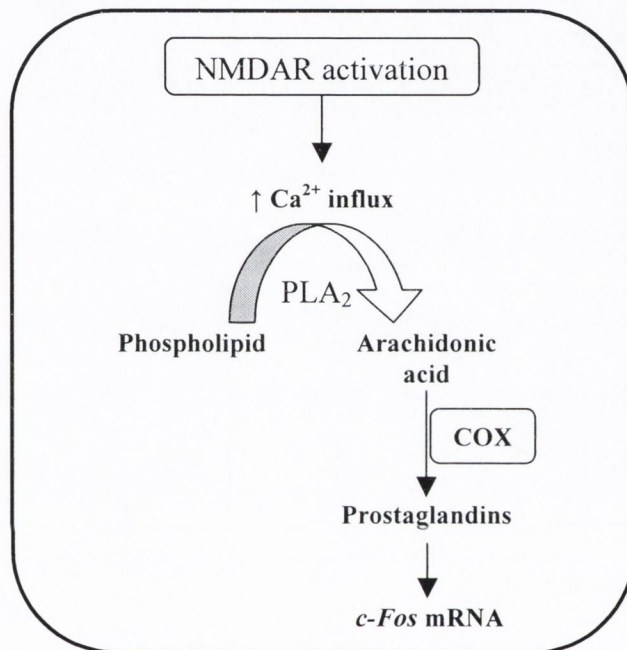


Figure 4.1 Schematic diagram of the intracellular signalling pathways involved in NMDA-mediated induction of *c-Fos* transcription in dentate gyrus neurons; adapted from (Lerea, Carlson, & McNamara, 1995).

A series of papers published by Lerea et al. culminated in a model of *c-Fos* transcription in dentate gyrus neurons in culture in response to NMDAR activation, which requires calcium influx and the formation of arachidonic acid metabolites (Figure 4.1) (Lerea et al., 1992; Lerea et al., 1995; Lerea et al., 1997; Lerea & McNamara, 1993). In the last paper of this series, it was shown that in order for *c-Fos* to be transcribed in response to NMDAR-activation, that PGF_{2α}, (but not PGE₂ or PGD₂), was necessary but not sufficient. The author hypothesised that Ca²⁺ entry through the NMDAR, in combination with PGF_{2α}, would lead to phosphorylation of a MAP kinase and thus promotion of *c-Fos* transcription, basing this supposition on paper which implicated PGF_{2α} in ERK activation. Similar papers have implicated PGE₂ in ERK activation (Fujino, Xu, & Regan, 2003; Krysan et al., 2005; Pozzi et al., 2004) and *c-Fos* induction (Lacroix, Vallieres, & Rivest, 1996), and thus we

have asked the question: if PGE₂ successfully reversed the COX-2-mediated block of LTP, would it result in ERK activation and an increase *c-Fos* expression? The tissue generated from the LTP experiment will be analysed by western blot for ERK, phospho-ERK, *c-Fos* and actin (as a control for equal-sample loading). Since the papers by Lerea et al. (Lerea et al., 1992; Lerea et al., 1995; Lerea et al., 1997; Lerea & McNamara, 1993) use a cell culture system whereby dentate gyrus neurons are treated with NMDA and prostaglandins, it will be interesting to see whether LTP will have an advantage over NMDA application with respect to *c-Fos* expression and to test the proposed ERK/*c-Fos* pathway.

An important methodological consideration for the following experiments is the extremely short half-life of PGE₂ and its catabolism in the brain. In the periphery, within one and a half minutes of injection of PGE₂ less than 5% is detectable in its undegraded form; it has an estimated half-life of only 15 seconds. The initial degradation products are biologically inactive (Bygdeman, 2003). The rate-limiting enzyme in the degradation of PGE₂ catabolism is 15-hydroxyprostaglandin dehydrogenase (15-PGDH) and is extensively detectable throughout the body with the exception of the brain (Anggard, Larsson, & Samuelsson, 1971; Nakano, Prancan, & Moore, 1972): note in Figure 4.2 the presence of almost 100% of ³H-PGE₁ in tissue homogenate from the rat brain. This is opportune for the following experiments ensuring that PGE₂ is not degraded before the completion of the experimental procedures.

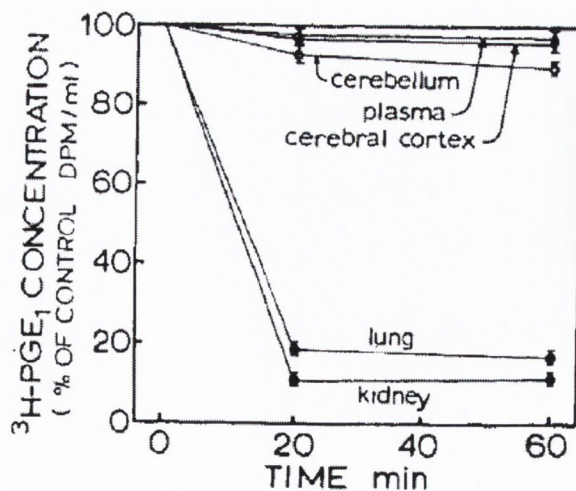


Figure 4.2 Metabolic degradation of PGE₁ in the rat plasma and tissue homogenate (Nakano et al., 1972).

Since selective COX-2 inhibition, without inflammatory insult, resulted in a block of LTP *in vivo* (see chapter III) it is logical that to restore the system to baseline that it should be sufficient to inject PGE₂ back into the hippocampus. In the following experiments, the role of PGE₂ in the dentate gyrus on baseline transmission, the paired-pulse ratio (PPR) and long-term potentiation will be investigated.

4.2 Materials & methods

4.2.1 Materials

A simultaneous electrode-cannula system obtained from Plastics One Inc. was used to record fEPSPs during the injection of PGE₂ into the hippocampus. A single syringe pump series 100 from Phymep, Paris, France in conjunction with a 10 μ L Hamilton syringe (Harvard Apparatus) was used to control volumes and flow rates precisely of the intrahippocampal injections. Anti-c-Fos (Ab-2) (4-17) Rabbit pAb was purchased from Calbiochem, Merck Biosciences. Phospho-ERK (E-4) Sc-7383 and ERK-2 Sc-1647 (used to measure total ERK) were purchased from Santa Cruz Biotechnology Inc. p-ERK (E-4) is recommended for detection of ERK 1 and ERK 2 phosphorylated at Tyr-204 and ERK 2 (D-2) is recommended for detection of ERK 2 p42 of rat origin by Western Blotting. Secondary anti-mouse IgG (whole molecule)-peroxidase and anti-rabbit were obtained from Sigma. Pierce West Dura Chemiluminescence supersignal[®] solution was purchased from Medical Supply Co. LTD., Dublin 15. Blots were stripped with reblot plus solution from Chemicon, Temecula, CA, USA. Mini-PROTEAN 3 Electrophoresis System by Biorad was used to do protein gel electrophoresis and a semi-dry electroblotter by Apollo Instrumentation was used for western blotting onto nitrocellulose. All chemicals for preparation of buffers and gels were purchased from Sigma Aldrich. The rats' body temperature was monitored with a Thermalert Model TH-8 Temperature Monitor from Bailey Instruments, 515 Victor Street, Saddle Brook, NJ 07662 and temperature was controlled with an instant heat pack from Heat Solutions (Harvard Apparatus).

4.2.2 Surgery

The anaesthesia and electrophysiological methods are as described in Chapter II for recording from the medial perforant pathway. Rectal temperature was monitored and maintained between 36-38°C. Intrahippocampal injection of PGE₂ did not result in any atypical fluctuations in body temperature. The electrode-cannula system, attached to a stereotaxic arm, was lowered slowly into the dorsal hippocampus until a positive-going fEPSP of maximum slope was obtained in the dentate hilus. The relative depths of the recording electrode, guide cannula and internal cannula were pre-cut by Plastics One Ltd. as specified in Messaoudi et al (Messaoudi et al., 1998): "*The final depth of the recording*

electrode ranged between 200 and 300 μm below the level of the maximum negative-going fEPSP sink recorded in the middle third of the dentate molecular layer. An inner ‘infusion’ cannula... (28 gauge)... then was inserted so that it protruded 300 μm below the end of the guide...(22 gauge). The tip of the infusion cannula was located in deep stratum lacunosum moleculare of field CA1, 700 μm above the hilar recording site and 300–400 mm above the medial perforant synapses.” To verify cannula placement dye was injected into the hippocampus of two animals, dissected out, frozen and sliced on a microtome.

4.2.3 Pharmacological treatment schedules

All animals were injected i.p. with 35 mg/kg celecoxib 30 minutes pre-anaesthesia. PGE₂ was diluted in DMSO and frozen in 10 μl aliquots. Aliquots were defrosted daily and diluted 0.5% or 1.0% v/v DMSO/0.9% Saline to give a final PGE₂ concentration of 66 μM or 132 μM respectively. In the following experiments, 1 μl of one or other PGE₂ solution was injected into the hippocampus at a rate of 5 μl/hour through an internal cannula, inserted through the guide-cannula previously cemented in place. This injection was given approx. 1.5hrs after celecoxib injection. The internal cannula was left in place for 2 min after the end of the injection to allow diffusion into the tissue and avoid suck-back into the cannula with its removal. Assuming a 200 ml hippocampal volume, 1 μL of the 66 μM solution would give an equivalent dose to that used *in vitro* by Chen et al (C. Chen et al., 2002). However, the drug concentration proximal to the infusion site is likely to be higher. It should be noted that upon implantation 4 animals showed epileptiform activity (two PGE₂ and two vehicle controls) and due to the potential for this activity to result in a subsequent facilitation of evoked responses and to induce immediate early gene expression the experiments were terminated and the data omitted from analysis.

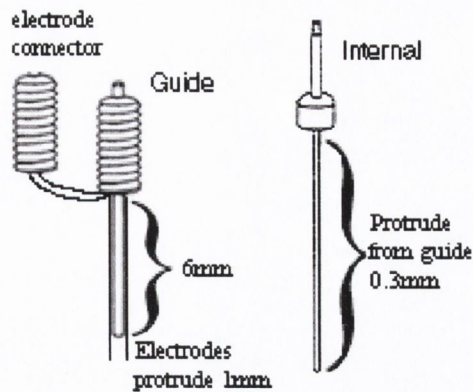


Figure 4.3 Diagram showing the simultaneous electrode-cannula system used to record fEPSP while injecting PGE₂.

4.2.4 Stimulation and data acquisition

As described in Chapters II and III. The calculations of the paired-pulse ratio are as described in Chapter II. Tetanus was induced ipsilateral to the delivery of PGE₂ fifteen minutes after the end of the injection, while the contralateral dentate was left untouched. The dorsal portion of both ipsi- and contralateral dentate gyri were dissected out and stored at -80°C for later analysis.

4.2.5 Western blotting

Tissue from both the ipsilateral and contralateral dorsal dentate gyri were homogenised in ice cold Krebs- Ca^{2+} and protein concentrations were calculated by the method of Bradford

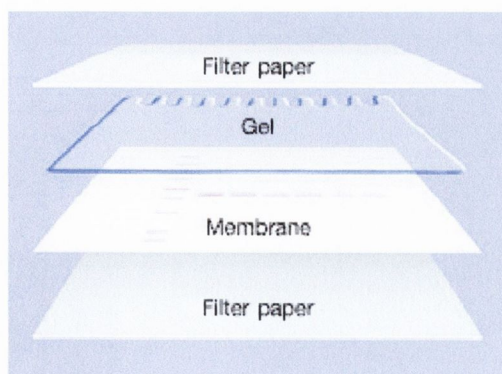


Figure 4.4 Transfer sandwich format for western blotting.

(Bradford, 1976) and diluted to give equal protein concentrations before being analysed by western blot (Laemmli, 1970; Towbin, Staehelin, & Gordon, 1979). Samples were diluted 1:1 in sample buffer (0.5 mM Tris-HCl, pH 6.8, 10% glycerol, 10% SDS, 5% β -mercaptoethanol, and 0.05% w/v bromophenol blue) and boiled for 2 min, and 10 μl aliquots were loaded onto 10% SDS gels. Proteins were separated by application

of a constant voltage of 200V for 35 min and then transferred onto nitrocellulose

membranes at a constant voltage of 225 mV for 75 mins. After blocking in Tris-buffered saline (TBS)-Tween 20 (150 mM NaCl, 50 mM Tris-HCl, and 0.05% v/v Tween 20, pH 7.4) containing bovine serum albumin (BSA) (5% w/v), membranes were washed in TBS-Tween 20 and incubated in anti-phospho-ERK [1:3000 in TBS-Tween 20 containing BSA (2%) for 2 hrs at room temperature. Membranes were washed and incubated in a horseradish peroxidase-conjugated anti-mouse [1:1000 in TBS-Tween 20 containing BSA (2% w/v)] for 1 hr at room temperature before being reacted with ECL solution, exposed to film for 8 seconds, and developed mechanically. Initial control experiments determined the optimal time of exposure to film, which was maintained throughout the experimental procedure. Protein bands were quantified using GelDoc-It imaging system and LabWorks™ Image acquisition and Analysis Software Version, 4.5.0 (Ultraviolet Product Ltd., Cambridge, UK) to yield a figure in arbitrary units that represented the density of the protein bands. To analyze the total ERK content of the samples, membranes were stripped of antibody by incubating in reblot plus solution, washed, and blocked in TBS-Tween 20 containing BSA (4% w/v). Membranes were washed in TBS-Tween 20 and incubated in anti-ERK [1:1000 in TBS-Tween 20 containing BSA (2% w/v)] for 2hrs min at room temperature and then washed and incubated in a horseradish peroxidase-linked anti-mouse IgG [1:1000 in TBS-Tween 20 containing BSA (2% w/v)] before being reacted with ECL solution. Blots were exposed to film for 8 seconds and developed, and protein bands were quantified as described above. The data represented below are the means of six animals per treatment group (n=6) with three replicated of each sample. Because there was no change in the levels of total-ERK, values of phosphorylated ERK (pERK) were normalized to the values of total-ERK. All values are further normalised to the concentration of actin per sample (a control measure of protein concentration known not to change with LTP).

4.2.6 Statistics

ANOVA and Student's t-test were used for statistical analysis. For the I/O curves experiment a repeated measures design was utilized whereby the stimulation protocol was performed before and after PGE₂ injection (or its vehicle 0.5% DMSO) to minimise variability and to look at the effect of the injection process on the recording of the fEPSPs. A mixed-factorial ANOVA, with current and pre- versus post-injection as the within-subject factors, and PGE₂ versus control as the between-subject factors was conducted.

4.3 Results

4.3.1 Input/output curves

Input/output curves were constructed to examine the effect of exogenous replacement of PGE₂ (66 μ M solution) by intrahippocampal injection, in the presence of the systemically administered COX-2 inhibitor, celecoxib. A repeated-measures design was used whereby input/output curves were performed before and after intrahippocampal PGE₂ injection (10 minutes were allowed after injection for baseline recordings to stabilise before starting the second I/O curve). As described in Chapter II, fEPSP slope is a measure of the number of cells depolarising, while the PSA represents the number of cell reaching threshold and firing. Figure 4.5 and Figure 4.6 show the changes in fEPSP slope and PSA, respectively, as a difference score of post- minus pre-injection; a positive score implies an increase in excitability and vice versa. No significant effect of applying PGE₂ to the tissue ($F_{(1,9)}=0.174$; $p>0.05$), nor any interaction of PGE₂ with current intensity ($F_{(31,279)}=0.22$; $p>0.05$) or of PGE₂ with the injection process itself ($F_{(1,279)}=0.001$; $p>0.05$), was reported by the mixed-factorial ANOVA performed on the slope data. However, there was a significant effect of injection irrespective of the solution ($F_{(1,279)}=5.687$; $p=0.041$); there was a slight decrease in the excitability of the tissue as a result of the experimental procedure, as measured by slope. These results were mirrored in the PSA analysis with neither a direct effect ($F_{(1,9)}=0.618$; $p>0.05$) nor any indirect interactions of PGE₂ treatment, however PSA was not affected by the injection process ($F_{(1,279)}=0.289$; $p>0.05$). Thus, PGE₂ does not alter neuronal excitability. This is also evident in E-S curve shown in Figure 4.7; the recordings made in the presence of PGE₂ show no alterations in the shape of their curves. The extraneous effect of the injection procedure was controlled for in subsequent experiments by continuing to inject the control animals with the vehicle solution.

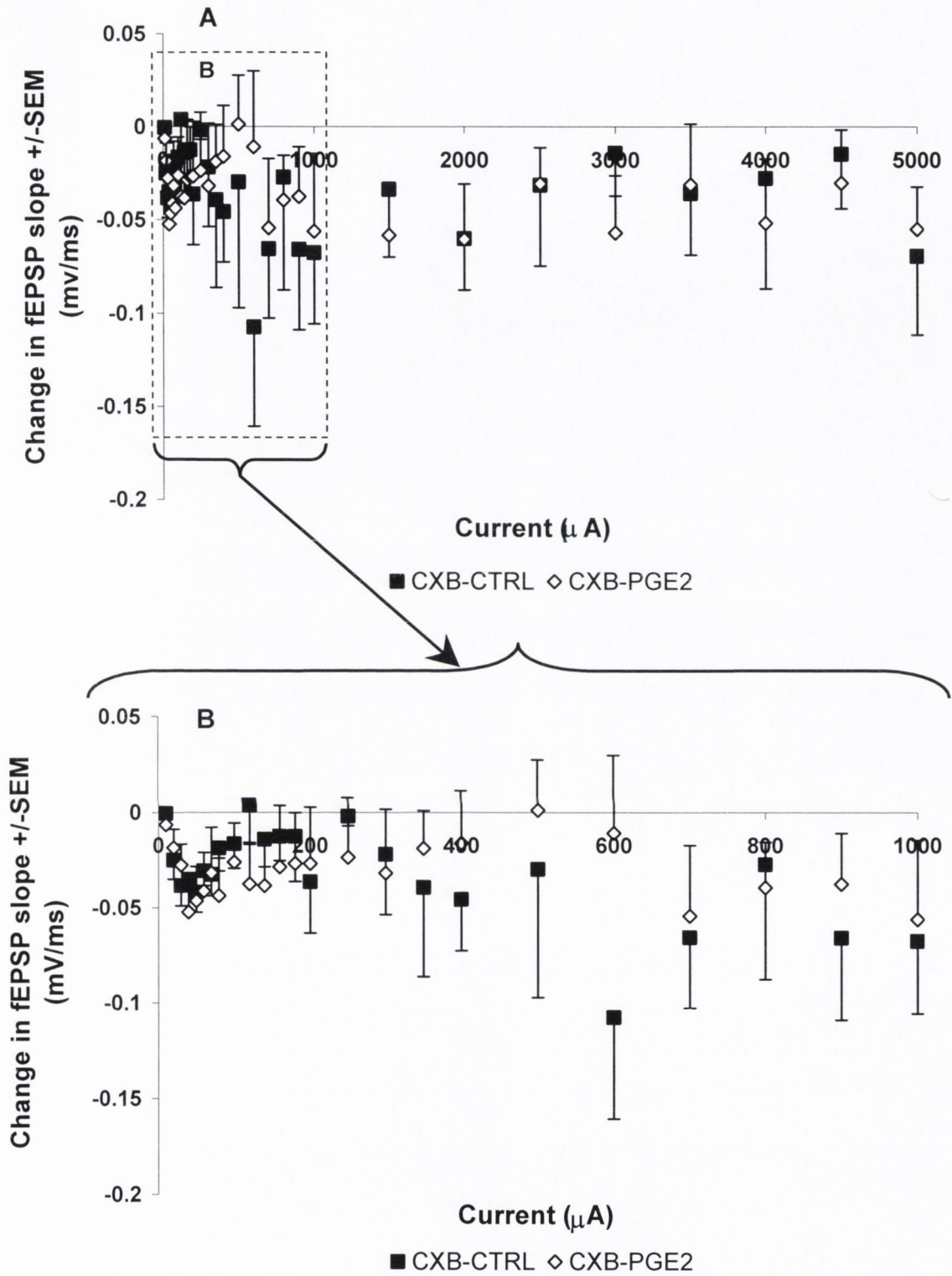


Figure 4.5 The change in fEPSP slope as a result of intra-hippocampal injection of PGE₂ across a range of stimulus intensities: A) 0-5000 μA, and B) 0-1000 μA.

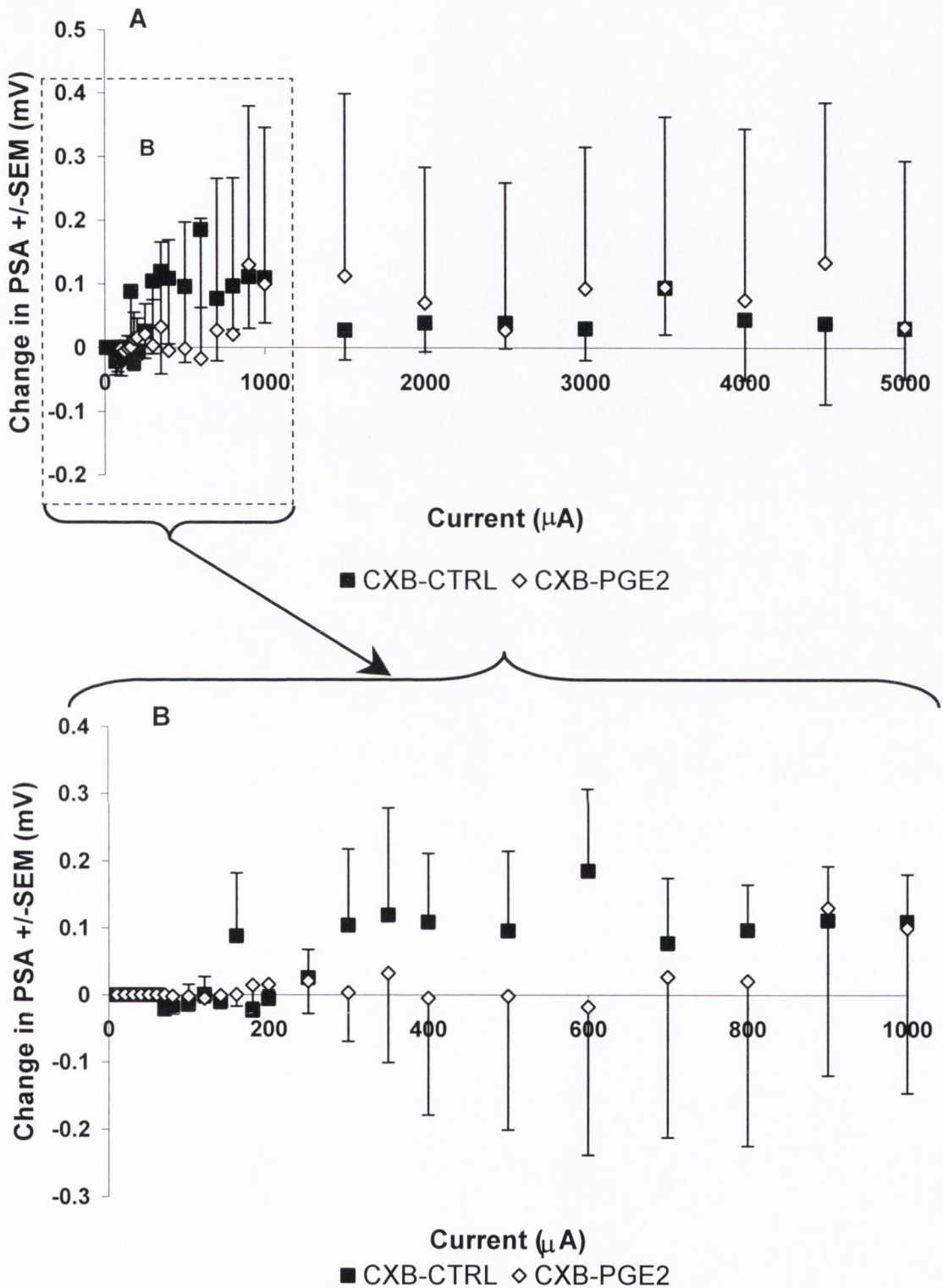


Figure 4.6 PGE₂ intra-hippocampal injection had no effect on input/output curves, recorded before and after the injection. The above graphs shows the change in PSA (pop spike amplitude) from pre-to-post PGE₂ in the range A) 0-5000 μA , and B) 0-1000 μA .

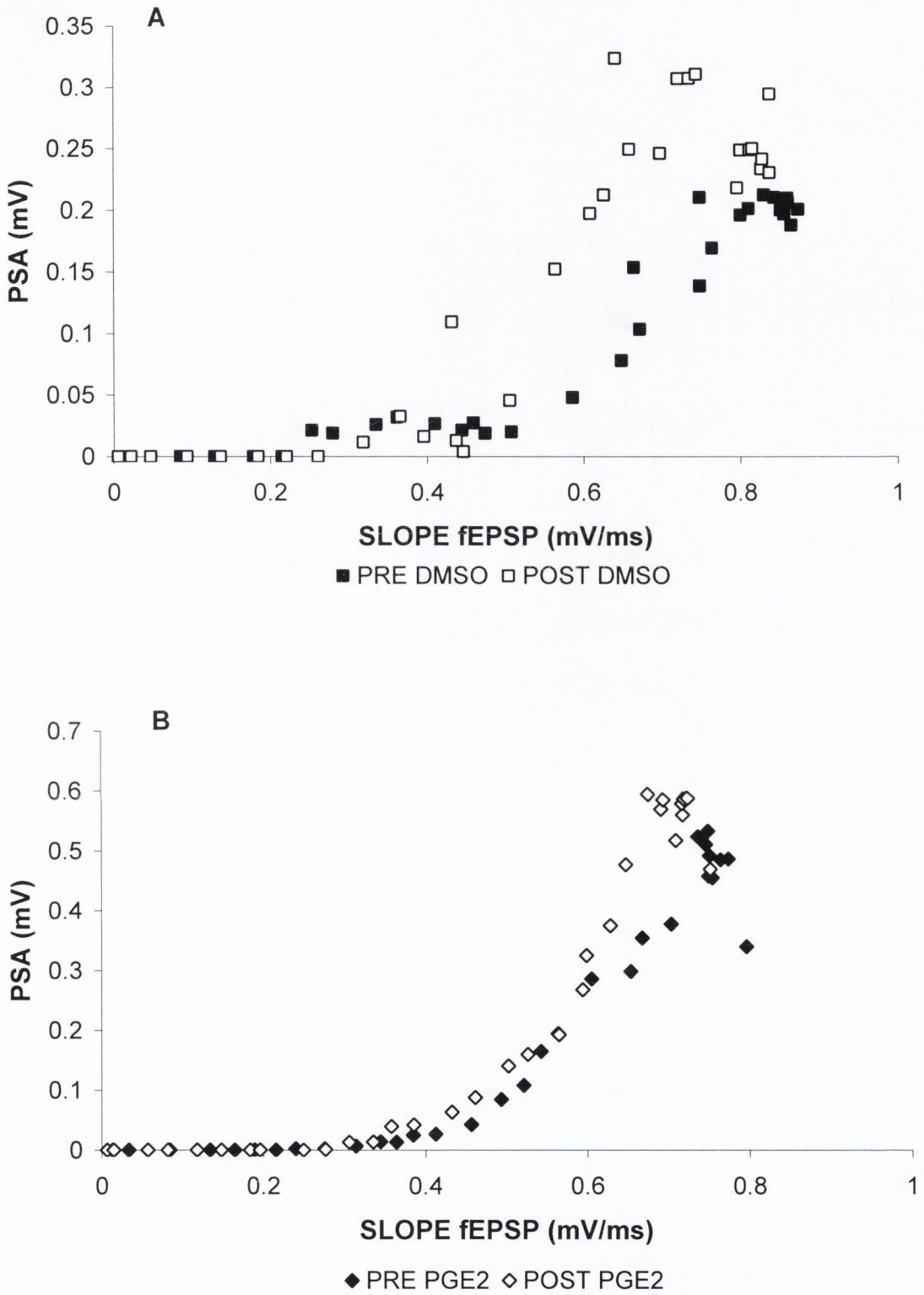


Figure 4.7 E-S curves for current intensities ranging from 0-5000 μ A, measured in systemic celecoxib treated animals, pre- and post-PGE₂ (66 μ M) (fig. B) or its vehicle (0.5%DMSO/saline) (fig. A) injected locally into the hippocampus. The curves are not obviously altered as a result of the injection process (fig. A) nor as a result of applying PGE₂ to the tissue (fig. B).

4.3.2 Paired-pulse ratio

COX-2 inhibition was shown to cause a loss of depression at very short latency ISI (10 ms) in the PPR. To confirm if this loss of depression was a result of decreased prostaglandin signalling from COX-2 inhibition, we injected PGE₂ into the hippocampus directly and recorded pairs of stimuli across the same range of ISIs as described in Chapter II. Figure 4.8 shows the resultant ratios at each ISI; independent t-tests showed no recovery of the depression evident in the absence of COX-2 inhibition. In contrast, however, there is a trend towards greater facilitation in the PGE₂ treated animals (evident in Table 4.2) reaching significance only at 250 ms ISI ($t_8 = -2.746$; $p < 0.05$).

DRUG	ISI (ms)	10	20	50	75	100	125	150	175	200
CXB-CTRL (n=5)	Mean	0.633	1.117	1.070	1.030	0.968	0.932	0.907	0.890	0.894
	SEM	0.083	0.127	0.090	0.055	0.058	0.039	0.033	0.043	0.034
	St. Dev	0.186	0.284	0.201	0.123	0.129	0.086	0.073	0.095	0.076
CXB-PGE ₂ (n=5)	Mean	0.575	1.220	1.220	1.156	1.142	1.117	1.046	1.159	0.995
	SEM	0.146	0.130	0.121	0.117	0.132	0.137	0.085	0.123	0.037
	St. Dev.	0.326	0.290	0.271	0.262	0.294	0.306	0.190	0.274	0.083
	t-test	0.343	1.022	-1.022	-0.977	1.212	1.297	1.531	2.067	2.00
	p-value	0.740	0.588	0.337	0.357	0.260	0.231	0.164	0.073	0.08

...continued

DRUG	ISI (ms)	250*	300	400	500	600	700	800	1000
CXB-CTRL (n=5)	Mean	0.894	0.881	0.895	0.894	0.895	0.899	0.886	0.913
	SEM	0.024	0.024	0.018	0.016	0.022	0.025	0.050	0.018
	St. Dev	0.055	0.054	0.040	0.035	0.050	0.056	0.111	0.040
CXB-PGE ₂ (n=5)	Mean	0.974	0.966	0.986	0.926	0.933	0.955	0.943	1.029
	SEM	0.016	0.031	0.044	0.043	0.033	0.029	0.022	0.054
	St. Dev.	0.037	0.070	0.097	0.096	0.073	0.066	0.050	0.120
	t-test	-2.746	-2.159	-1.935	-0.698	-0.962	-1.467	-1.052	-2.05
	p-value	0.025	0.063	0.089	0.505	0.364	0.181	0.324	0.07

Table 4.2 Descriptive statistics for the paired-pulse ratio calculated as the ratio of fEPSP2/fEPSP1. T-tests were performed to compare PPR for celecoxib-controls versus celecoxib-PGE₂ treated animals, at each stimulus intensity.

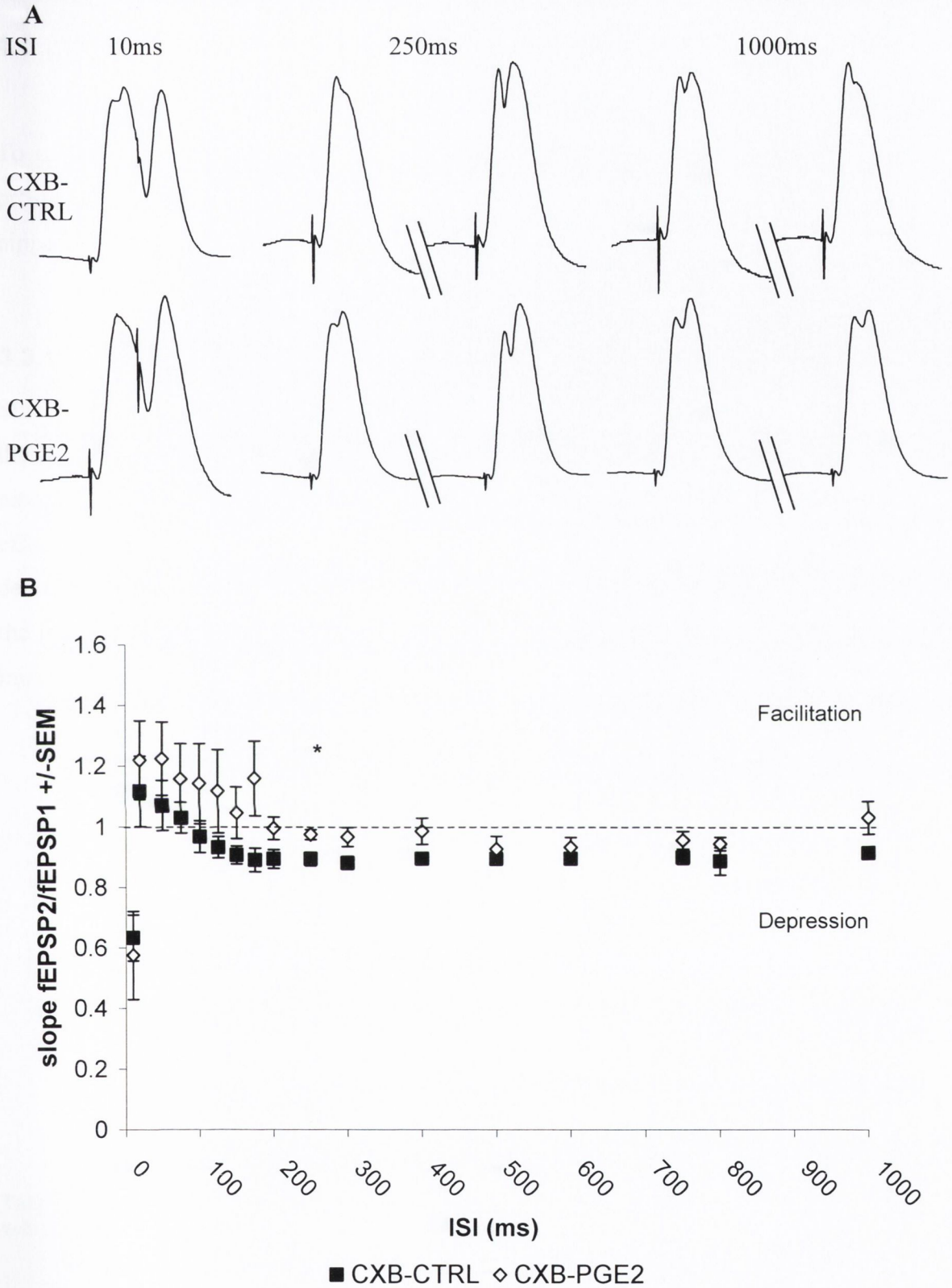


Figure 4.8 Effects of PGE₂ on the paired-pulse ratio in celecoxib treated animals. PGE₂ failed to restore the depression seen in the non-celecoxib treated animals (cf. Chapter II). **A**) Representative fEPSPs at 10, 250 and 1000ms. **B**) PPR calculated as slope fEPSP2/fEPSP1 ± SEM.

4.3.3 Occlusion of the COX-2-dependent block of LTP by intrahippocampal injection of PGE₂

To explore if the block of LTP by COX-2 inhibition resulted directly from a loss of a prostaglandin signal we attempted to replace this signal by injecting PGE₂ into the hippocampus of the anaesthetised, celecoxib-treated animal prior to inducing LTP.

4.3.3.1 Baseline recordings during PGE₂-injection

Since we found that PGE₂ injection had no effect on input/output curves – due possibly to the I/O curves taking too long a duration to record from the end of PGE₂ injection – we recorded fEPSPs before, during and after the PGE₂ injection to look for an immediate effect of PGE₂. We found that PGE₂ (n=6) injection resulted in a small but significant decrease in the fEPSP slope, relative to controls (n=3), up to ten minutes after the end of the injection. We analysed the differences in fEPSP at baseline, during the last minute of injection (-1) and 5-, 10- and 15-minutes after the end of injection

DRUG	Time (mins)	Mean (%)	SEM
CTRL (n=3)	BASELINE	100.00	0.00
	-1	104.62	2.68
	+5	108.53	4.05
	+10	105.34	2.86
	+15	105.19	4.06
PGE ₂ (n=6)	BASELINE	100.00	0.00
	-1	95.84	1.78
	+5	95.28	3.32
	+10	96.43	1.75
	+15	96.43	1.96

Table 4.3 The percentage change in fEPSP slope recorded during the injection of PGE₂ (0.66µM) or its vehicle (0.1% DMSO) into the hippocampus.

A two way repeated measures ANOVA showed no within effect across time: $F_{(4,28)}=0.322$; $p>0.05$, however, there was a significant interaction of time and drug injected; $F_{(4,28)}=3.426$; $p<0.05$, and a significant, between groups, effect of the injection of PGE₂ on fEPSP slope: $F_{(8,7)}=8.164$; $p<0.05$. A multivariate one-way ANOVA was used to deduce

any time point(s) at which PGE₂ injection had an effect, with significant differences showing by the end of injection (-1), 5- and 10- mins after ($p < 0.05$ for all) but by 15 mins there was no difference.

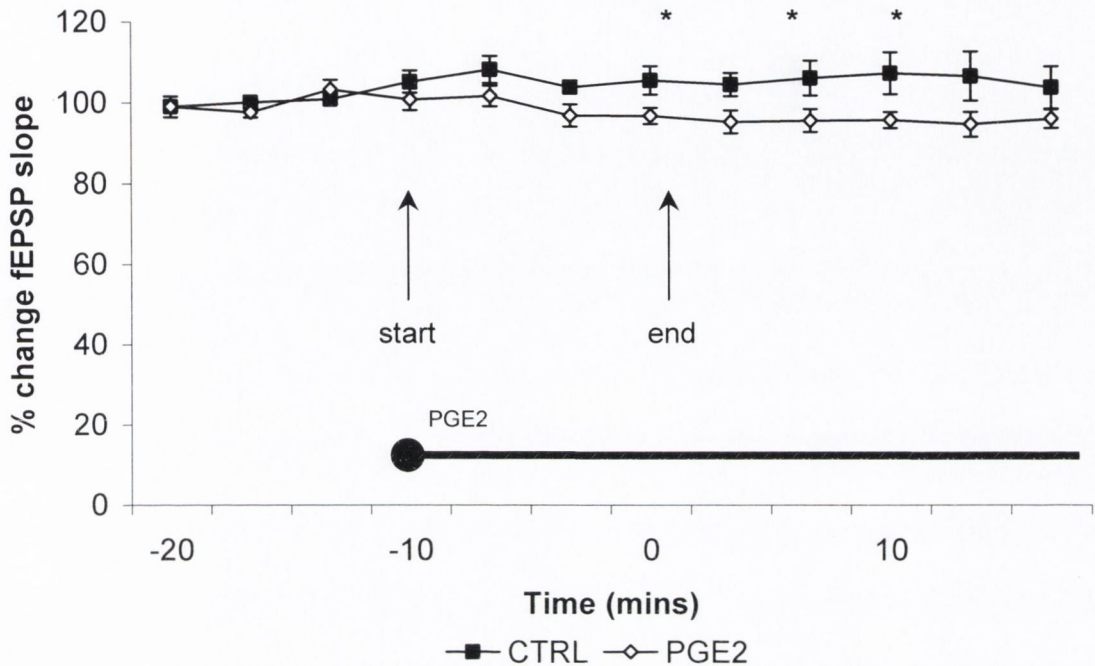


Figure 4.9 Baseline recording before, during and after the intrahippocampal injection of PGE₂ or its vehicle (0.1% DMSO/saline). All animals were treated with celecoxib 30mins prior to anaesthesia. The fEPSPs of the PGE₂ animals were significantly smaller than were those of the controls, immediately after injection and up ten minutes later. There was no observable difference by fifteen minutes after the end of injection.

4.3.3.2 PGE₂-injection before HFS reverses the COX-2-dependent LTP impairment: ERK-phosphorylation and c-Fos after 1 hour

A mixed-factorial ANOVA was performed, with tetanic stimulation as the within-factor – with four levels baseline, PTP, +30- and +60-mins – and PGE₂ injection compared to vehicle as the between-subjects factor, to determine if the injection of PGE₂ would prevent the block of LTP caused by COX-2 inhibition. A significance of $p < 0.001$ for Mauchly's test of sphericity required that the Greenhouse-Geisser test for within-subjects effects be reported. The effect of HFS was highly significant, $F_{(1,9,37.3)} = 15.574$; $p < 0.001$, in other words LTP was successfully induced, furthermore, the interactive effect of HFS and PGE₂ injection approached significance, $F_{(1,9,37.3)} = 3.325$; $p = 0.054$, suggesting PGE₂ cooperated with HFS to induce LTP compared to the vehicle treated animals. The between-subjects effect of injecting PGE₂ was also significant, $F_{(1,20)} = 7.013$; $p = 0.015$, with more than 70%

power. An independent t-test was performed to isolate the differences across the four time points (baseline, PTP, +30- and +60mins) due to PGE₂ compared to vehicle controls: baseline $t_{20}=0.434$; $p>0.05$, PTP $t_{20}=1.034$; $p>0.05$, +30-mins $t_{20}=2.375$; $p<0.05$, +60-mins $t_{20}=2.663$; $p<0.05$. Table 4.4 shows the descriptive statistics for the change in fEPSP slope as a percentage of their respective baselines, as a result of HFS after the application of PGE₂.

DRUG	TIME (mins)	MEAN (%)	SEM	Std. Dev
CXB-PGE2 (n=11)	BASELINE	100.16	0.17	0.57
	PTP	121.00	3.96	13.14
	30	118.15	3.28	10.88
	60	124.93	5.40	17.90
CXB-CTRL (n=11)	BASELINE	100.08	0.06	0.21
	PTP	115.62	3.37	11.18
	30	107.88	2.81	9.33
	60	107.84	3.47	11.51

Table 4.4 Descriptive statistics showing that intrahippocampal injection of PGE₂ curbs the block of LTP seen with CXB: mean fEPSP slope as a percentage of their respective baselines.

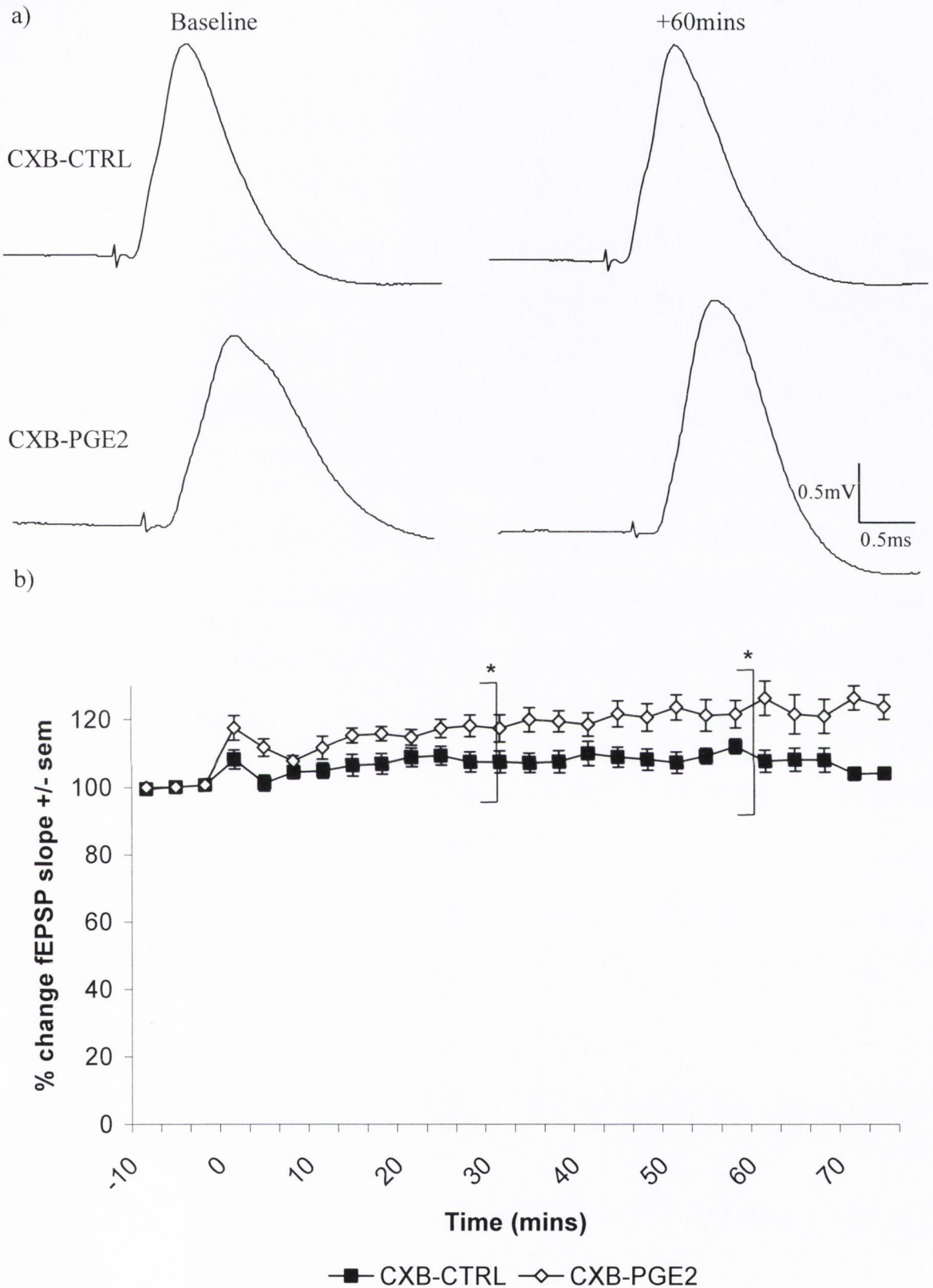


Figure 4.10 Exogenous replacement of PGE₂ prior to HFS assuages the deficit of LTP seen with COX-2 inhibition. Both groups were treated with celecoxib prior to anaesthesia and either PGE₂ or its vehicle (0.1% DMSO) was injected into the hippocampus 15mins prior to HFS.

Western blots were used to examine changes in protein concentration in the dentate gyrus in response to PGE₂ (66 μ M) injection and subsequent HFS, compared to vehicle-treated controls and their respective uninjected and unstimulated contralateral hemispheres. The proteins of interest were total-ERK, phosphorylated-ERK, c-Fos, and actin to control for equality of protein loading. Figure 4.11 show representative blots for each protein measured and Table 4.5 displays their descriptive statistics. Mixed-factorial ANOVAs were performed; the within-subjects factor was hemisphere and the between-subjects factor was PGE₂ vs. vehicle.

		CXB-CTRL (n=6)		CXB-PGE2 (n=6)	
Hemisphere		Mean \pm SEM	St. Dev	Mean \pm SEM	St. Dev
Tot-ERK	Tetanised	2.81 \pm 0.28	0.68	3.71 \pm 0.34	0.84
	Untetanised	2.74 \pm 0.02	0.49	2.98 \pm 0.32	0.78
p-ERK/tot-ERK	Tetanised	1.48 \pm 0.22	0.55	1.90 \pm 0.15	0.38
	Untetanised	1.08 \pm 0.05	0.11	1.14 \pm 0.11	0.26
c-Fos	Tetanised	1.29 \pm 0.21	0.52	1.41 \pm 0.19	0.48
	Untetanised	0.97 \pm 0.08	0.20	1.03 \pm 0.15	0.37

Table 4.5 Descriptive statistics for the densitometric measurement of tot-ERK, p-ERK/tot-ERK and c-Fos in both vehicle and PGE₂ injected brains, ipsi- (tetanised) and contralateral (untetanised) to HFS and injection (all concentration are expressed with respect to the quantity of actin present as a control for equal loading; arbitrary units).

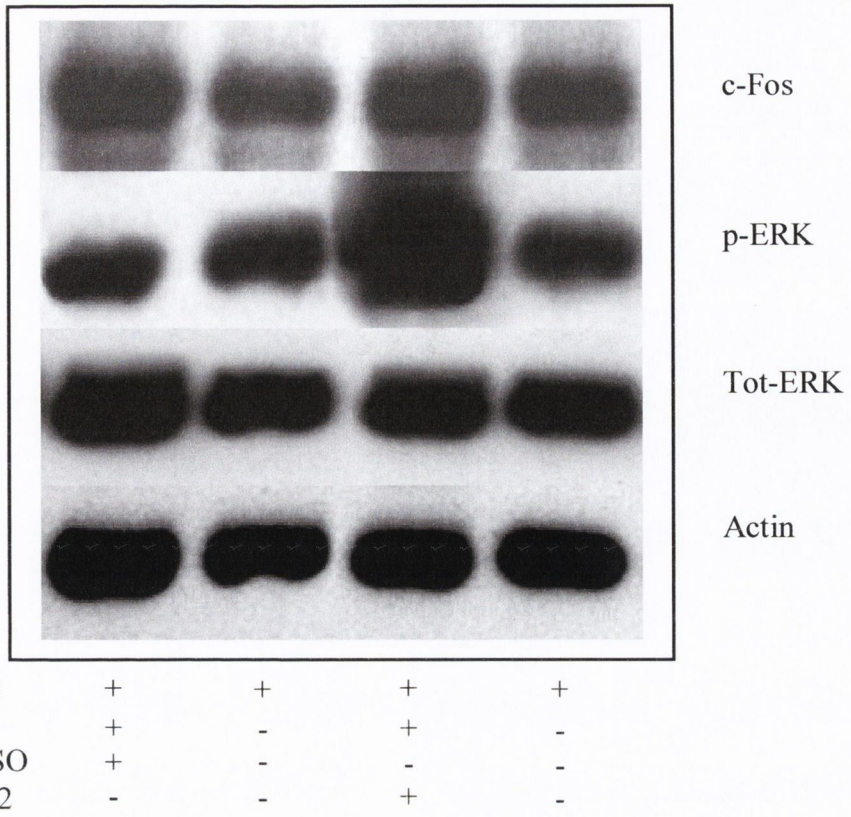


Figure 4.11 Protein expression measured in ipsi- and contralateral dentate gyri, 1 hour after the induction of LTP. All rats were injected i.p. with celecoxib prior to anaesthesia and then with either 1 μ l vehicle (0.1% DMSO) or PGE₂ ipsilateral to LTP induction, 15mins prior to HFS.

There were no significant differences reported for the concentration of tot-ERK in any of the conditions (Figure 4.12): hemisphere $F_{(1,10)}=2.758$, $p>0.05$, hemisphere-drug interaction $F_{(1,10)}=1.903$, drug $F_{(1,10)}=2.999$, $p>0.05$.

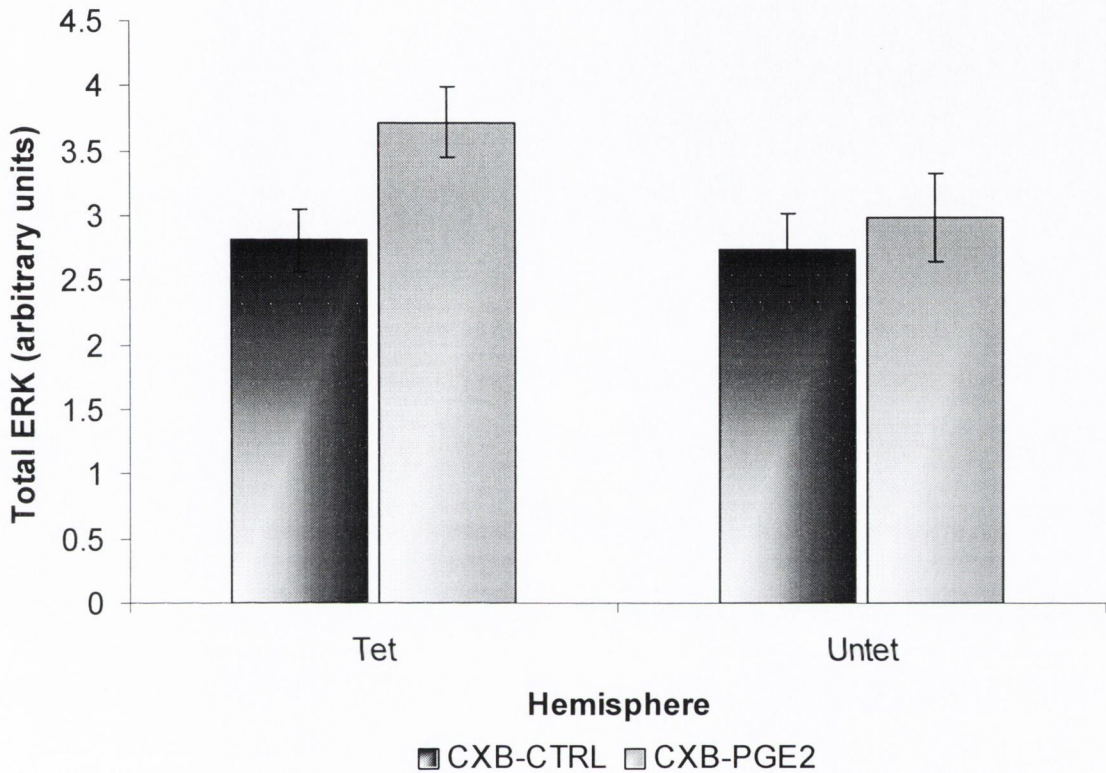


Figure 4.12 There was no significant difference in total-ERK concentration observed one hour after the application of HFS, in response to PGE₂ injection.

In contrast, the ANOVA performed on the ratio of p-ERK/tot-ERK identified a highly significant difference between hemispheres ($F_{(1,10)}=18.105$, $p<0.01$) but no other differences. Further analysis of this effect of hemisphere with paired t-tests, grouped according to treatment with PGE₂ or vehicle, showed a significant difference only in the PGE₂ treated animals ($t_5=4.295$, $p<0.01$) and not in the controls ($t_5=1.927$, $p>0.05$) (see Figure 4.13).

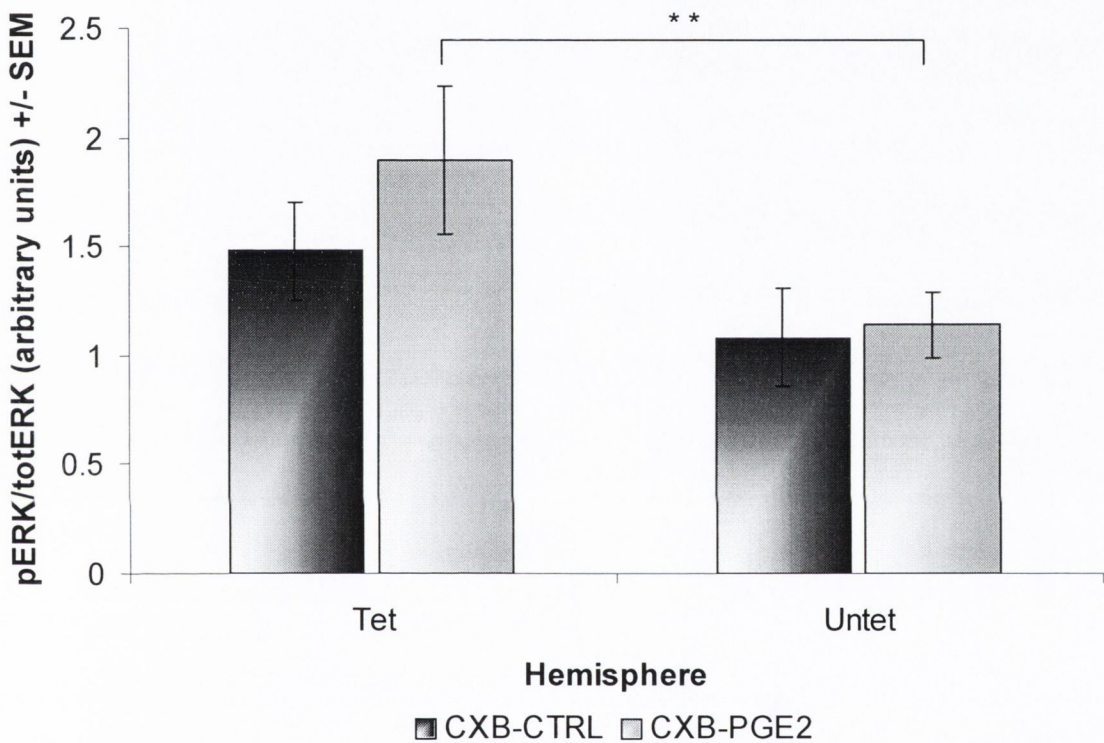


Figure 4.13 A significant increase in ERK phosphorylation was observed one hour after HFS in response to PGE₂ injection relative to the untetanised hemisphere. This increase was not seen in the control group.

The same strategy applied to the densitometric values obtained for c-fos revealed the same pattern as for p-ERK/tot-ERK; a significant effect of hemisphere was reported $F_{(1,10)}=8.106$; $p<0.05$, but neither a direct nor interactive significant effect of drug was shown. Paired t-tests again revealed a significant difference in the hemispheres of the PGE₂ treated animals ($t_5=2.742$; $p<0.05$), but not the controls ($t_5=1.563$; $p>0.05$) (Figure 4.14).

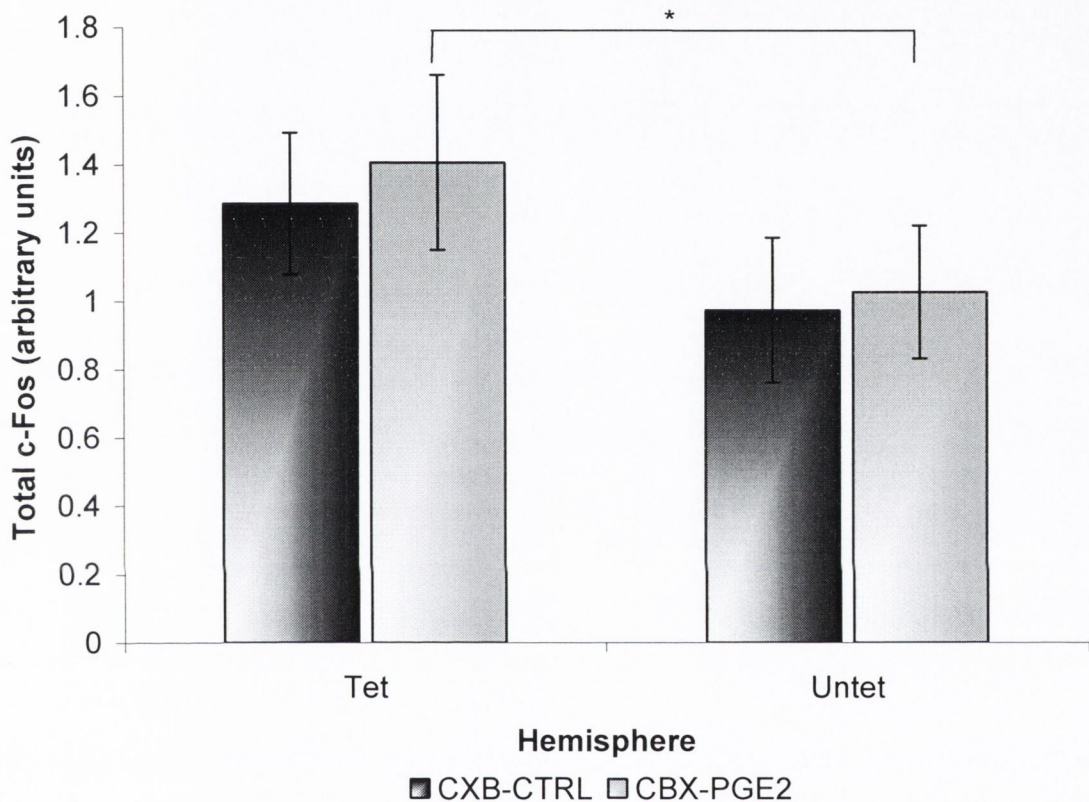


Figure 4.14 c-Fos protein was seen to be significantly upregulated only in the tetanised-PGE₂ treated animals relative to the contralateral untetanised hemisphere.

To investigate any relationship between the increases observed in ERK phosphorylation and c-Fos protein a series of correlations were performed. No significant correlations were reported between hemispheres, thus the amount of any of the proteins measured in the tetanised hemisphere was not related to that in the untetanised side, irrespective of PGE₂ or vehicle injection. In the same way, the concentration of c-Fos was not related to the tot-ERK concentration in either hemisphere, with or without PGE₂ injection being taken into account. However, there was a significant positive correlation between the phosphorylation of ERK and c-fos concentration in both the tetanised ($r=0.625$; $n=12$; $p<0.05$) and untetanised ($r=0.581$; $n=12$; $p<0.05$) hemispheres. These correlations are not significant

when the groups are divided according to PGE₂ vs. control but they are of the same magnitude.

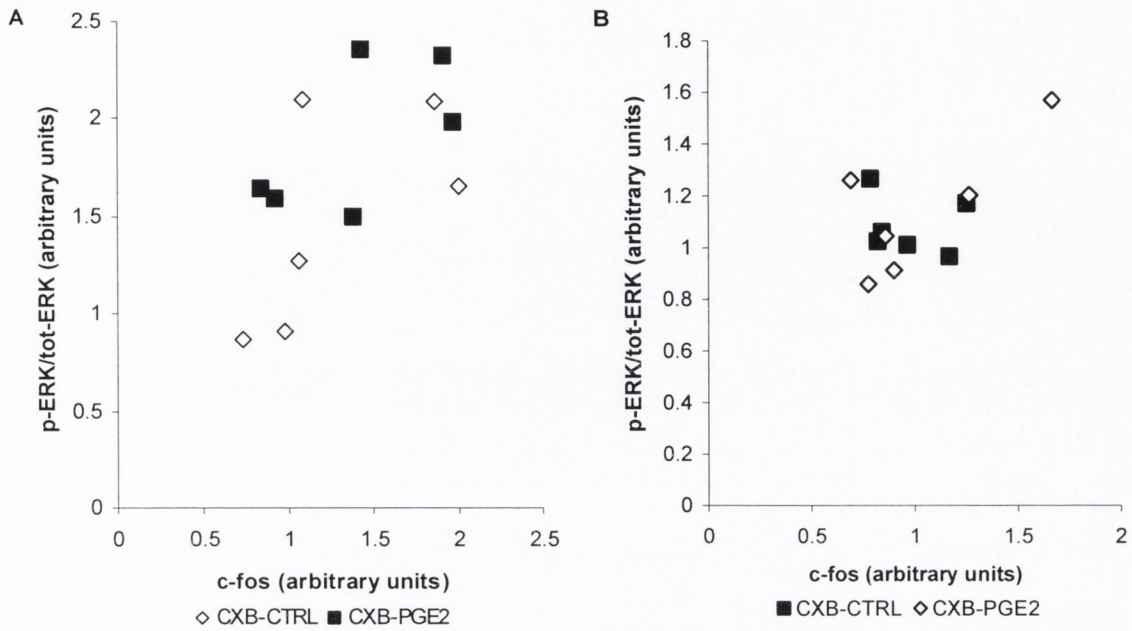


Figure 4.15 A significant positive correlation exists between the amount of phosphorylated ERK and the amount of c-fos present in the tetanised (fig A: $r=0.625$; $n=12$; $p<0.05$) and untetanised (fig B: $r=0.581$; $n=12$; $p<0.05$) tissue irrespective of whether it is control or PGE₂ treated.

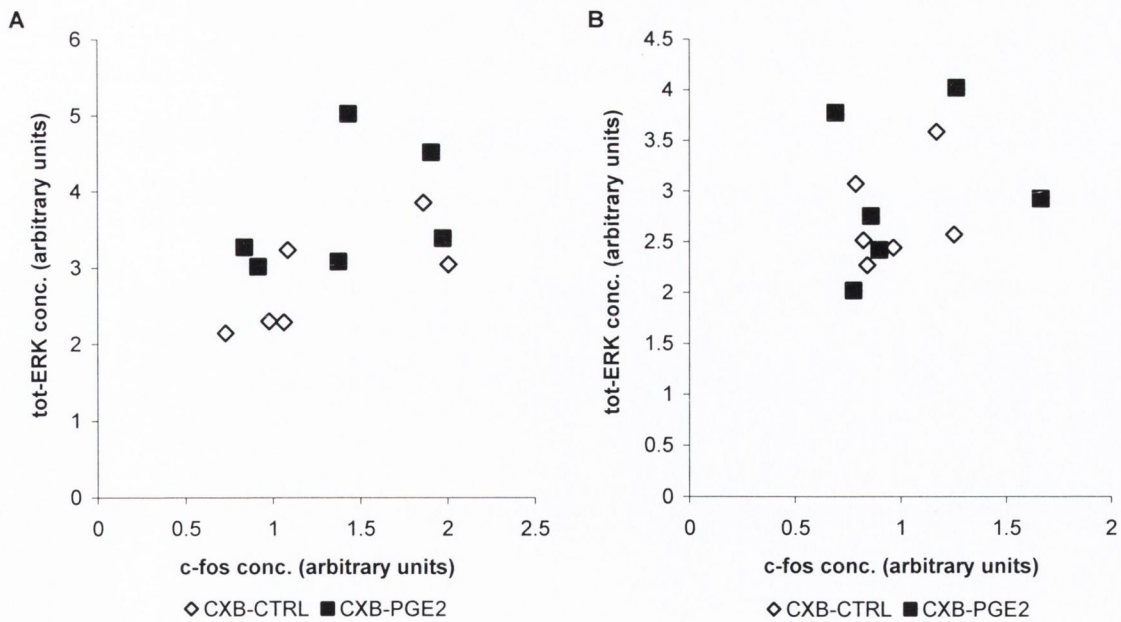


Figure 4.16 No significant correlation was reported for c-fos and tot-ERK concentrations measured at 1 hr post-HFS in either tetanised (fig A: $r=0.551$; $n=12$; $p>0.05$), or untetanised (fig B: $r=0.249$; $n=12$; $p>0.05$) hemispheres.

4.3.3.3 PGE₂ (132 μ M) treatment resulted in sustained LTP: no inter-hemispheric changes in ERK and c-Fos after 3 hours

The above experiment was repeated, recording for three hours and analysing the protein changes at that time point. To overcome the clearance of PGE₂ from the injection site the dose was doubled. A mixed-factorial ANOVA looking at the affect of HFS at 3 hours compared to baseline (within), and the effect of PGE₂ vs. vehicle control (between groups) was used to test the hypothesis that PGE₂ injection in the presence of tetanic stimulation would overcome the COX-2 inhibition-induced block of LTP lasting up to three hours; a highly significant effect of HFS was reported ($F_{(1,16)}=10.75$; $p<0.01$), showing LTP was successfully induced. There was also a significant effect of PGE₂ injection ($F_{(1,16)}=5.21$; $p<0.05$). Since there are only two groups, this intuitively translates into an interaction between HFS and PGE₂ injection, with the conclusion that LTP was successfully induced in the PGE₂ treated animals but not in the controls, at 180 mins. Paired t-tests between baseline and 180 minutes confirm that fEPSPs slope of PGE₂-treated animals at 180 mins are significantly bigger ($t_{(9)}=3.45$; $p<0.01$) but controls remained unchanged ($t_{(7)}=1.048$; $p>0.05$).

DRUG	BASELINE		180mins	
	Mean \pm SEM	Std. Dev.	Mean \pm SEM	Std. Dev.
CXB-CTRL (n=8)	100.00 \pm 0.00	.00018	105.30 \pm 5.06	14.31
CXB-PGE ₂ (n=10)	100.00 \pm 0.00	.00000	129.60 \pm 8.58	27.13

Table 4.6 The mean fEPSP slope (\pm SEM) 180mins after HFS expressed as a percentage of baseline for control and PGE₂ treated groups.

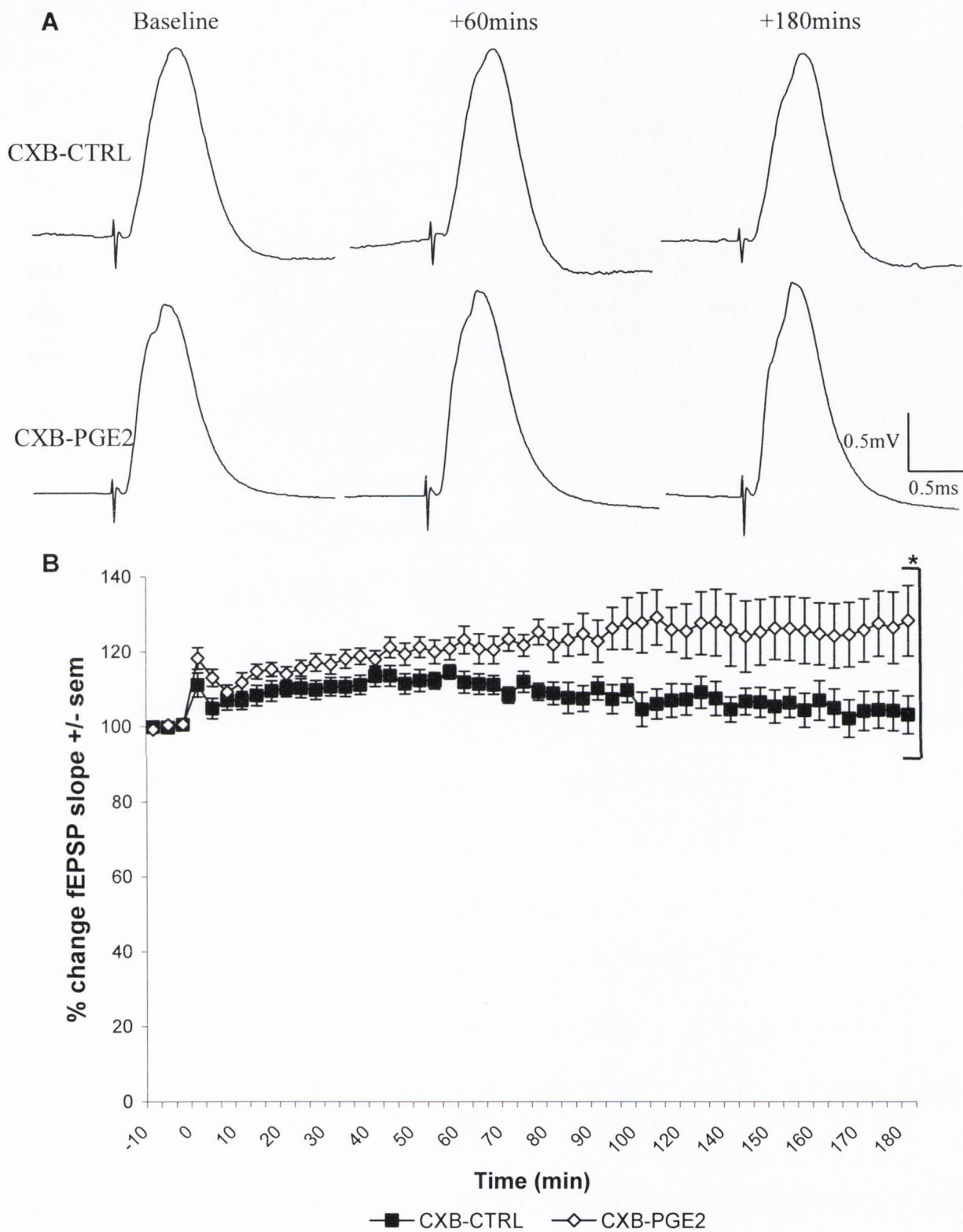


Figure 4.17 Long-term potentiation was successfully induced when PGE₂ (132 μ M) was exogenously replaced by intrahippocampal injection. Both groups were treated with celecoxib prior to anaesthesia and again four hours later (one $t_{1/2}$) to maintain the block of cyclooxygenase-2.

As before the concentration of total-ERK, c-fos and actin (as a control for equal loading of samples in the wells) but not phospho-ERK, was quantified by western analysis to look at protein changes three hours after HFS relative to the naïve hemisphere, as compared to 60 mins. Phospho-ERK was omitted since phosphorylation is a short latency event (Davis, Vanhoutte, Pages, Caboche, & Laroche, 2000). Mixed-factorial ANOVAs were performed as for the previous western blots: hemisphere as the within-subjects measure and PGE2 injection vs. vehicle control as the between-subjects measure. Figure 4.18 shows representative blots for c-Fos, tot-ERK and equal loading control, actin and Table 4.7 show their descriptive statistics.

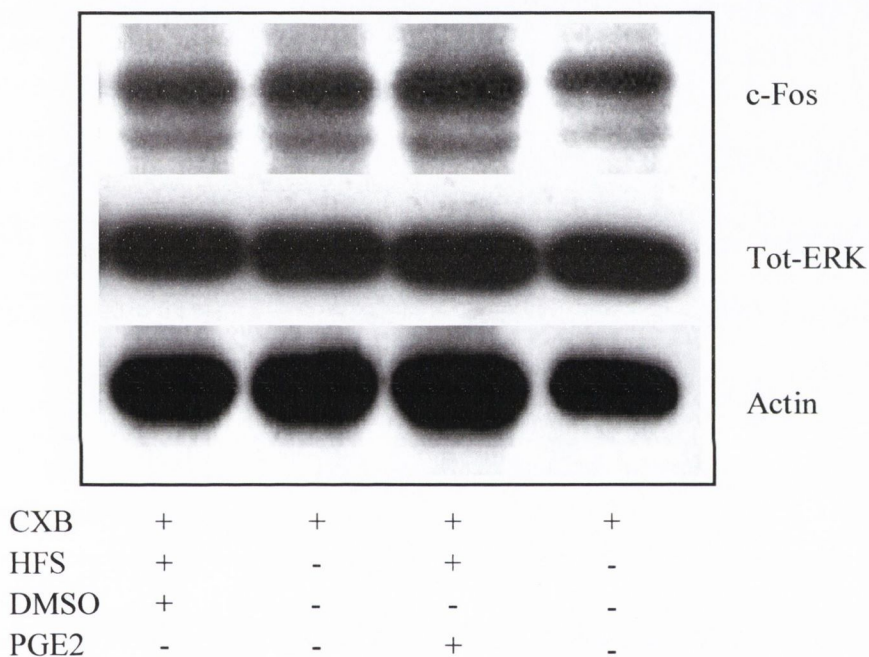


Figure 4.18 Representative blots from western analysis of dentate gyrus tissue three hours after HFS in the presence of intrahippocampal PGE₂ or its vehicle control or the respective naïve hemispheres.

		CXB-CTRL (n=6)		CXB-PGE2 (n=6)	
		Mean±SEM	Std. Dev.	Mean±SEM	Std. Dev.
Tot-ERK	Tetanised	1.67±0.08	0.19	1.64±0.11	0.27
	Untetanised	1.69±0.06	0.14	1.61±0.07	0.17
c-Fos	Tetanised	0.24±0.04	0.11	0.27±0.04	0.10
	Untetanised	0.28±0.02	0.06	0.28±0.03	0.09

Table 4.7 Descriptive statistics for the densitometric measurement of tot-ERK and c-Fos in both vehicle and PGE₂ (132µM) injected dentate gyri, ipsi- (tetanised) and contralateral (untetanised) to HFS and injection measured after three hours (all concentration are expressed with respect to the quantity of actin present as a control for equal loading; arbitrary units).

The ANOVA demonstrated that there was no significant difference in total-ERK concentration within the naïve versus manipulated hemispheres ($F_{(1,10)} = 0.00$; $p > 0.05$) nor between the vehicle control and PGE₂ treated animals ($F_{(1,10)} = 0.472$; $p > 0.05$). Moreover, there was no interaction of hemisphere and treatment group ($F_{(1,10)} = 0.115$; $p > 0.05$). A separate ANOVA testing changes in c-Fos similarly showed no difference in hemisphere ($F_{(1,10)} = 1.058$; $p > 0.05$), nor between drug treatment group ($F_{(1,10)} = 0.067$; $p > 0.05$) and finally no interactive effect of hemisphere and treatment group ($F_{(1,10)} = 0.413$; $p > 0.05$). These results are evident in Figure 4.19 and Figure 4.20.

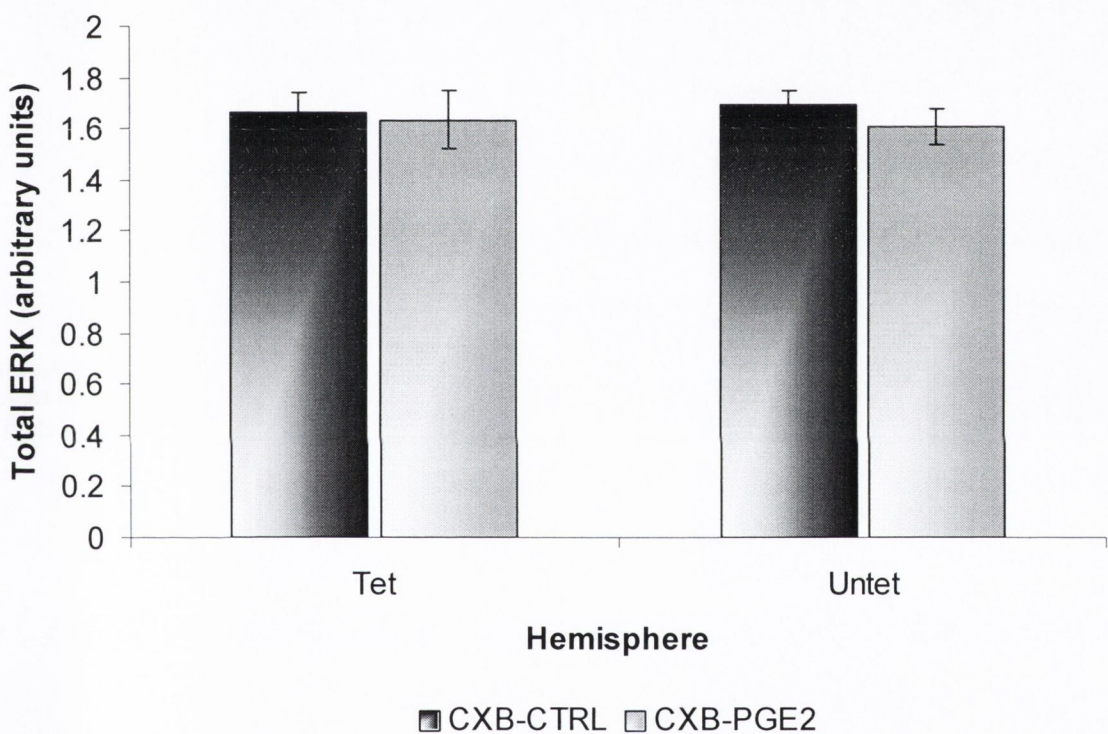


Figure 4.19 Densitometric analysis revealed no significant difference in the quantity of ERK-2, as a measure of total-ERK, three hours after HFS in response to PGE₂ injection while subjected to COX-2 antagonism with celecoxib (CXB).

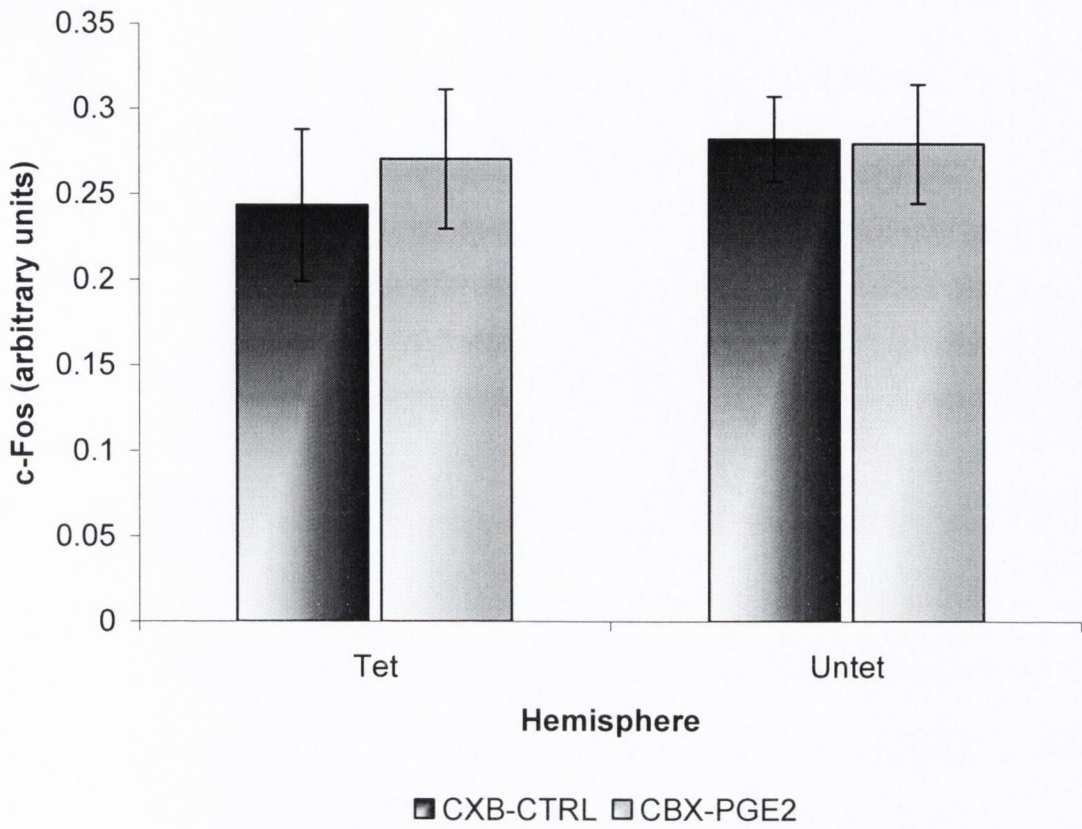


Figure 4.20 Densitometric analysis shows no significant difference in the quantity of c-Fos protein present in dentate gyrus three hours after HFS in response to PGE₂ intrahippocampal injection. All animals were injected with celecoxib prior to anaesthesia.

Correlations were performed to look at possible relationships that may exist between the concentration of total-ERK and c-fos in tetanised and untetanised tissue as evident in Figure 4.21. Without taking drug-treatment group into account a very strong and highly significant correlation of total-ERK and c-fos was reported in both the tetanised ($r=0.847$, $n=12$, $p<0.001$) and untetanised ($r=0.869$, $n=12$, $p<0.0001$) hemispheres. These correlations remained significant and are of the same magnitude when divided according to drug treatment group: CXB-CTRL tetanised tot-ERK vs. c-fos; $r=0.84$, $n=6$, $p<0.05$, CXB-PGE₂ tetanised tot-ERK vs. c-fos; $r=0.93$, $n=6$, $p<0.01$, CXB-CTRL untetanised tot-ERK vs. c-fos; $r=0.824$, $n=6$, $p<0.05$, CXB-PGE₂ untetanised tot-ERK vs. c-fos; $r=0.95$, $n=6$, $p<0.01$.

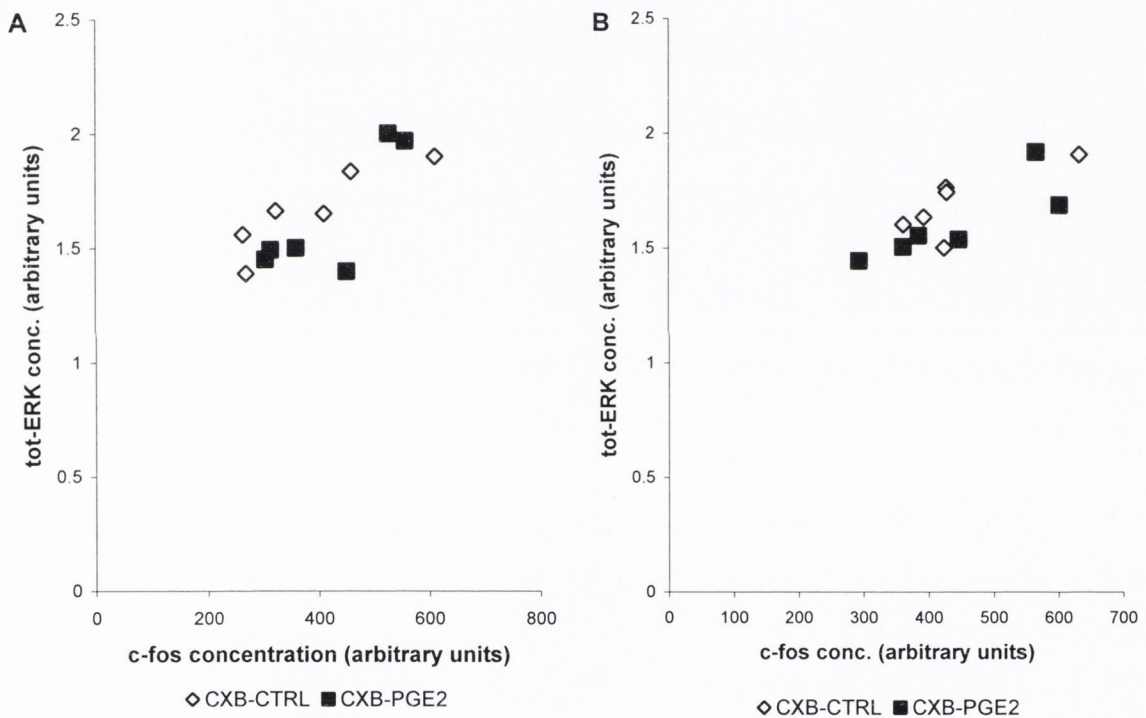


Figure 4.21 A very strong and highly significant correlation exists between the concentration of c-fos and total-ERK in both tetanised (fig A: $r=0.847$, $n=12$, $p<0.001$) and untetanised (fig B: $r=0.869$, $n=12$, $p<0.0001$) hemispheres.

4.4 Discussion

Direct application of PGE₂ to the hippocampus obviates interpretative problems of systemic COX-2 inhibition. Where it may be argued that systemic COX-2 inhibition could cause alterations to multiple possible CNS and peripheral sites, local application of exogenous PGE₂ confirms that the effects reported in previous chapters were in fact central, more specifically hippocampal in origin. This was the approach of the above experiments with the objective of explaining the changes observed with COX-2 inhibition.

4.4.1 Baseline synaptic transmission, PPR and PGE₂

4.4.1.1 Effects of PGE₂ on I/O curves and baseline synaptic transmission

Direct intrahippocampal injection of PGE₂ had no significant effect on neuronal excitability as measured by changes in fEPSP slope and PSA with varied current, before and after the injection. However, a significant effect of the injection process was apparent, resulting in a slight decrease in excitability. This is important to be aware of for extrapolation of results in this chapter to previous chapters.

Since the input/output curve takes ~30mins from beginning to end, with time needed for the recording to stabilise after intrahippocampal injection prior to recording, it is highly possible that short lived or rapidly induced effects on fEPSP size would be missed. Thus a continuous recording was made before during and after injection to look at short-lived effects. This approach revealed a significant, PGE₂-induced depression of the response in comparison to vehicle controls, which lasted only 15 minutes. This is in direct opposition to findings by Chen et al. who showed a facilitatory effect of PGE₂ application, which manifested itself immediately and maximised by 15 min of bath application of PGE₂ (C. Chen & Bazan, 2005a). However, there are significant methodological differences at play; Chen recorded from the Schaffer collateral, *in vitro*, without prior treatment with a COX-2 inhibitor. This is not the first time that such discrepancies have been reported. Sekiyama demonstrated a facilitation of EPSC size and a decrease in the number of failures in response to *in vitro* PGE₂ application to the nucleus tractus solitarii (Sekiyama et al., 1995), however, as discussed by this paper impairments in neurotransmitter release

(Belluzi et al., 1982) and inhibition of Ca²⁺ channels in sympathetic ganglion neurons (Ikeda, 1992) have been reported, reaching the conclusion that restricted expression of different EP receptor subtypes could be responsible. As discussed in the literature review each of the EP isoforms, and splice variants, result in different intracellular signalling cascades (c.f. table 1.1 taken from (Narumiya et al., 1999)). In brief EP₁ induces Ca²⁺ mobilization, EP₂ and EP₄ are coupled to stimulatory G-proteins whereas EP₃ is associated with inhibitory G-proteins resulting in a decrease in cAMP (Narumiya et al., 1999)). The sole paper, which examines EP₁₋₄ receptor expression in the hippocampus, does not delineate between the different sub-hippocampal structures (Zhu et al., 2005). Thus is possible that the short latency depression reported here and the long-lasting facilitation reported in the Schaffer collateral (C. Chen & Bazan, 2005a) could be mediated by different EP-receptor subtypes.

4.4.1.2 PPR and PGE₂

The decreased paired-pulse depression at very short latencies, observed as a result of COX-2 inhibition in Chapter II, was not restored by PGE₂ injection into the hippocampus; on the contrary, a facilitation of the ratio was evident in the PGE₂-treated animals, compared to controls. This leads to the conclusion that the decrement in PPD observed as a result of COX-2 inhibition was extraneous to the impaired PGE₂ production. Endocannabinoids have been shown to result in DSCI (depolarization-induced suppression of inhibition); activation of CB1 receptors by endocannabinoids, which are localized exclusively in GABAergic inhibitory interneurons, suppresses GABAergic synaptic transmission resulting in a response increase. COX-2 inhibition has been reported to result in decrease endocannabinoid metabolism and a resultant increase in DSI (Alger, 2002). Endocannabinoids, which are released from postsynaptic neurons, act as a retrograde signal to the presynaptic CB1 receptors (Kim & Alger, 2004).

As stated, paired-pulse stimulation in the presence of PGE₂ treatment resulted in a facilitation of the second response, only reaching significance at 200ms ISI. Paired-pulse facilitation is known to be a presynaptic phenomenon resulting from residual Ca²⁺ build-up from the first stimulus being carried over to the second response with a resultant increase in neurotransmitter release (Zucker, 1999; Zucker & Regehr, 2002). Such an effect of PGE₂ has been reported in other neurons, e.g. in the dorsal root ganglia PGE₂ results in

increased Ca²⁺ entry with a resultant increase in substance P release; moreover, a delay in the onset of this effect is indicative of an indirect mode of action (Nicol et al., 1992). The latency of the facilitation is coincidental with GABA_B autoinhibition which was shown to occur between 100-400ms and maximise at 200ms ISI (Mott, Xie, Wilson, Swartzwelder, & Lewis, 1993); if the effect was solely on Ca²⁺ channel then an equivalent facilitation would be expected across the board at all latencies, its manifestation as a progressive increase in significance between 175-400 ms ISI suggests a possible modulation of presynaptic GABA_B receptor and chloride ion channel opening.

The flip side of this argument is that the facilitation observed as a result of the application of paired-pulse protocol in the presence of PGE₂ is not representative of the endogenous actions of PGE₂. This maybe a concentration-dependent effect, with exogenous application of PGE₂ resulting in tissue concentrations in excess of the norm. Furthermore, as noted in the input/output curves, there are problems with comparisons made to experiments performed without intrahippocampal injection, i.e. comparing this paired-pulse data to that in Chapter II; with this said the paired-pulse response is facilitated here relative to its own control group. Given that only one t-test was significant out of 17 it is worth being conscious of the fact that this could be a chance event by definition of $p < 0.05$, and this interpretation – that PGE₂ had no effect on PPR – would agree with the fact that COX-2 inhibition had no effect at this ISI. Thus, this data weakly suggests a presynaptic locus for PGE₂ activity in the MPP, in contrast to the postsynaptic alteration in back-propagating action potentials proposed by Chen et al. (C. Chen et al., 2002).

4.4.2 Occlusion of the block of LTP by intrahippocampal injection of PGE₂

The demonstration that COX-2 inhibition only affected the induction and not the maintenance of LTP (Chapter III) suggests that PGE₂ is necessary only during HFS and in the initial minutes after induction. Thus it is not surprising that exogenous replacement of PGE₂ – the major metabolite of COX-2 activity - was sufficient to overcome the profound block of LTP due to COX-2 inhibition, ultimately confirming the deficit as PGE₂-dependent. The observation that the size of the post-tetanic potentiation in the COX-2 treated animals, while not significant, was markedly smaller, intimated that PGE₂ could be

involved in Ca²⁺ entry into the presynaptic cell (Zucker, 1999; Zucker & Regehr, 2002). Analysis of the effects of PGE₂ on the PTP measured immediately after HFS was not significant, thus it is unlikely that COX-2 inhibition on presynaptic Ca²⁺ is the main cause of the LTP deficit. Chen et al. argue also against a presynaptic site of action for PGE₂ in LTP, showing that PGE₂ can modulate back-propagation action potentials and postsynaptic membrane excitability (C. Chen et al., 2002). Evidence for EP receptors in both pre- and postsynaptic neurons in the hippocampus (Zhu et al., 2005) and the fact that LTP in the MPP has been associated with both pre- and postsynaptic alterations (Bliss & Collingridge, 1993) does allow scope for presynaptic effects of PGE₂ in LTP. More research is needed to further define PGE₂'s role in hippocampal LTP.

In association with successful induction of LTP, a significant increase in ERK-phosphorylation (independent of total ERK concentration in the samples) and immunological detection of c-Fos was detected in the dentate gyrus of the tetanised, PGE₂-treated hemispheres. Furthermore, a positive correlation between phosphorylated-ERK and the expression of c-fos was also established. The increase in c-Fos expression disagrees with the findings of Lerea et al. (Lerea et al., 1997), showing that PGE₂ in association with NMDAR activation failed to increase *c-Fos* mRNA, in comparison to PGF_{2α}. The experimental protocols used by Lerea and in the above experiments, are very different, for instance LTP induction activates more than just NMDAR e.g. BDNF induced activation of ERK-phosphorylation (Gooney et al., 2002; Ying et al., 2002). An alternative effect on the presynaptic terminus, could involve the proposed synergism between mGluR receptor activation and AA resulting in increased glutamate release, which is occluded by LTP induction (McGahon & Lynch, 1994, , 1996). Thus it appears that LTP induction and downstream ERK phosphorylation requires more than NMDAR activation and PGE₂. The correlation between ERK-phosphorylation and c-Fos concentration suggest that the two events are related, a pathway which has been described before (Xia et al., 1996).

The lack of correlation between tot-ERK and c-Fos measured at 1 hr postHFS and the change to a highly significant correlation at 3 hr postHFS could be interpreted as an indication of a transition from E-LTP to protein synthesis-dependent L-LTP. There is no significant increase in expression of ERK but this is to be expected since ERK is not increased in the cell bodies until 24 hr after stimulation (K. L. Thomas, Laroche, Errington, Bliss, & Hunt, 1994).

It should be noted that increases in c-Fos are not due to seizure activity induced as a result of cannula implantation, PGE₂ injection or HFS application since any animals which showed the characteristic decrease in the EPSP associated with seizure and after-discharge were omitted from both LTP calculation and western blot analysis.

Prolongation of LTP in the dentate gyrus *in vivo* was shown to be blocked by protein synthesis inhibitors in several laboratories (Krug et al., 1984; Otani, Marshall, Tate, Goddard, & Abraham, 1989). Curiously, however, it was found to be mRNA synthesis-independent, since actinomycin D, an inhibitor of mRNA synthesis had no effect up to 3 hours post-tetanus (Frey, Frey, Schollmeier, & Krug, 1996; Otani et al., 1989). This finding suggests that protein synthesis during this time window does not require *de novo* mRNA synthesis (discussed by (Kelly, Mullany, & Lynch, 2000)). Thus the increase in concentration of c-Fos observed after 1 hour in the stimulated hemisphere of the PGE₂ treated animals may be from previously formed mRNA transcripts.

Identifying the induction of c-fos is like finding a jigsaw piece, without knowing where it fits into the puzzle. Finding how it fits in is not a simple task since AP-1 dimers incorporating c-fos may inhibit, as well as stimulate gene induction depending on the other half of the dimer; c-fos/c-jun has been shown to be stimulatory, while c-fos/junB is mostly inhibitory (Schuttle et al., 1989; Sheng & Greenberg, 1990). However, the data presented here add strength the association between NMDA receptor activation and PGE₂ in LTP induction, and the necessity for both to result in downstream phosphorylation and activation of ERK, and ensuing c-Fos transcription.

Chapter 5 Summary & conclusions

Chapter 5	Summary & conclusions	145
5.1	Introduction.....	147
5.2	Summary of results	147
5.2.1	Chapter II: Baseline synaptic transmission and short-term plasticity.....	147
5.2.2	Chapter III: Cyclooxygenase and synaptic plasticity	148
5.2.3	Chapter IV: Exogenous PGE ₂ alleviates the block of LTP	149
5.3	Discussion & conclusions.....	151
5.3.1	COX-2 inhibition and LTP induction: effects on BDNF.....	151
5.3.2	COX-2 inhibition and exogenous PGE ₂	152
5.3.3	COX, PGE ₂ & memory.....	154
5.3.4	COX and neuroinflammation.....	155

5.1 Introduction

The role of the cyclooxygenase isoforms 1 & 2, in synaptic transmission and plasticity, were investigated *in vivo*, using pharmacological, electrophysiological and immunological techniques. Cyclooxygenase-2 has been implicated in synaptic plasticity for a number of reasons: its localisation to dendrites and dendritic spine of excitatory neurons most notably in the hippocampus (Kaufmann et al., 1996), the demonstration that it is upregulated in response to ECT and HFS with the expression pattern of an IEG (Yamagata et al., 1993), selective COX-2 but not COX-1 inhibition *in vitro* was shown to significantly impair but not block the induction of LTP in the dentate gyrus (C. Chen et al., 2002). Furthermore, COX-2 inhibition has been implicated in learning and memory: systemic COX-2 but not COX-1 inhibition immediately after learning impairs spatial memory in the watermaze (Teather et al., 2002), intrahippocampal infusion of the COX-2 inhibitor celecoxib impaired acquisition of the watermaze (Rall et al., 2003). This research group has also shown associations between learning impairments in the watermaze and LTP induction in the dentate gyrus as a result of BSCI (broad-spectrum COX inhibition) and that prior exercise could reverse these deficits by a putative BDNF dependent method, whereby the BDNF deficit reported in BSCI animals was occluded as a result of a period of prior exercise (Shaw et al., 2003). This thesis aims to build upon and advance this evidence.

5.2 Summary of results

5.2.1 Chapter II: Baseline synaptic transmission and short-term plasticity

- Using a regression analysis neither COX-2 nor COX-1 inhibition resulted in changes in baseline synaptic transmission, however, a facilitation of the fEPSP slope at high stimulus intensities was observed with COX-1 inhibition.
- A shift to the right in the E-S curves as a result of COX-1 and COX-2 inhibition suggests a slight increase in the threshold before the cell fires.
- BDNF concentration was not altered as a result of either selective COX inhibitor and low frequency stimulation.

- COX-2 inhibition affected PPR at only very short latency ISI (10 ms) suggesting a decrease in GABA transmission or alteration in ion channel opening.
- COX-2 inhibition interacted with paired-pulse stimulation causing an increase in BDNF concentration.

5.2.2 Chapter III: Cyclooxygenase and synaptic plasticity

- Selective antagonism of COX-2, but not COX-1, resulted in an immediate impairment in the induction of LTP. This block of LTP was dose dependent within a very narrow range – 35 mg/kg compared to 28 mg/kg. This block of LTP was reflected in the percentage of animals showing successful LTP; CXB treated animals showed significantly less animals with more than 20% increase in fEPSP slope compared to controls and COX-1 treated group. A depression of the PTP was apparent during recording of the 35 mg/kg CXB treated group, although it was non-significant according to the ANOVA.
- A significant increase in the concentration of BDNF was shown in response to 35 mg/kg celecoxib in the tetanised dentate gyrus but not in the untetanised side, relative to the controls and to the 28mg/kg celecoxib treated animals. Thus tetanic stimulation in association with 35 mg/kg CXB was responsible for a significant increase in BDNF.

What was not observed however was an increase in the BDNF in the tetanised DG compared to the untetanised hemisphere. This is contrast to a previous report of significant unilateral BDNF increase observed at only 40mins (Gooney & Lynch, 2001).

- Corticosterone levels in trunk blood samples, taken at the end of LTP recording, were not affected by celecoxib treatment either before or after LTP induction. Glucocorticoids can down regulate the expression of COX-2 activity thus we measured corticosterone to ensure that the block of LTP was a direct result of COX-2 inhibition by celecoxib.
- Celecoxib treatment showed no effect on fEPSP slope recorded over the course of an hour from the time of CXB injection. This was done to ensure that a drift in the baseline response, due to CXB treatment, did not obscure the potential increase in response as a result of HFS and thus concluding that the block of LTP was just due to it being masked.

- The block of LTP by COX-2 inhibition shows a temporal specificity, in that CXB treatment after successful induction of LTP had no effect up to 90 minutes after HFS.
- Even in the absence of an effect on LTP maintenance, we found CXB treatment resulted in a highly significant decrease, or more likely, impairment in the increase in BDNF concentration as a result of LTP induction.

5.2.3 Chapter IV: Exogenous PGE₂ alleviates the block of LTP

- PGE₂ intrahippocampal injection, in the presence of systemic CXB, did not affect the input/output curve. Using a repeated measures design, an effect of the injection process itself was apparent.
- PGE₂ significantly increased the paired-pulse ratio at 200ms ISI.
- Recordings of fEPSPs before, during and after PGE₂ injection showed that it resulted in a small but significant depression compared to vehicle injection in the control animals.
- Exogenous replacement of PGE₂, in the presence of 35mg/kg CXB, was sufficient to occlude the block of LTP, confirming that the original effect was COX-2-mediated via its metabolite, PGE₂. The LTP in the PGE₂-treated groups was sustained up to 3 hrs after HF stimulation. PGE₂ had no significant effect on PTP.
- A significant increase in ERK phosphorylation, relative to tot-ERK present in the tissue, was quantified at 60 min after HFS as a result of PGE₂ treatment and tetanus. Similarly, there was a significant increase in c-Fos expression in the tetanised PGE₂ treated dentate gyri compared to unstimulated controls. Tot-ERK concentration was unchanged.

A significant positive correlation between ERK phosphorylation and c-Fos at 1 hr post-HFS was calculated but not between tot-ERK and c-Fos. The positive correlation suggests the ERK-phosphorylation is involved in the regulation of c-Fos expression.

- By three hours however, c-Fos protein had returned to baseline levels and again total-ERK was not significantly altered. However, a highly significant correlation between ERK and c-Fos was calculated. This suggests that since ERK is a late

response gene – as compared to c-Fos being an IEG – it would suggest that c-Fos was involved in ERK expression and a shift from E-LTP to L-LTP was occurring.

5.3 *Discussion & conclusions*

5.3.1 **COX-2 inhibition and LTP induction: effects on BDNF**

The aim of this thesis was to investigate the role of cyclooxygenase and its metabolites in synaptic transmission and long-term potentiation, a model of how the brain stores memory (Bliss & Collingridge, 1993). The results presented in the preceding chapters demonstrate that synaptic plasticity, in the form of HFS-LTP, is modulated by a metabolite of COX-2 activity, but not the activity of COX-1, moreover that this modulation is mediated by PGE₂ the principle metabolite of COX-2 activity. The lack of effect of COX-2 inhibition on both the input/output curves and recordings at constant current show that the impairment of LTP induction was not a result of impairments in baseline synaptic transmission and thus must be activity-dependent.

Since BDNF concentration was elevated in association with pre-HFS celecoxib treatment, we have shown that the deficit in BDNF associated with BSCI and LTP impairment (Shaw et al., 2003) is epiphenomenal and that it is probably mediated by non-COX activities of the drugs used (Tegeger et al., 2001), e.g. NFκB is activated by celecoxib but inhibited by ibuprofen treatment. In the absence of specific antagonist of NFκB to confirm these findings (several indirect and non-selective drugs are under examination in treatments for cancer (Li, Withoff, & Verma, 2005)), selective COX-2 antagonists without activity at NFκB could be used, for example NS398 (Tegeger et al., 2001). An alternative explanation could involve celecoxib's ability to inactivate Ca²⁺-ATPase on endoplasmic reticulum, preventing the reuptake of Ca²⁺ out of the cytoplasm back into intracellular store (Johnson et al., 2002). This has also been identified as a celecoxib specific effect and dose dependent. But for the fact that celecoxib upregulation of BDNF was only evident at high doses, 35 mg/kg- but not 28 mg/kg (the highest human dose used is 800mg/day and estimating average weight at 80 kg gives a dose of 10 mg/kg), this increase in BDNF could be an important neuroprotective action of celecoxib.

Further to the COX-2-dependent block of LTP we showed that the maintenance of LTP was not affected by COX-2 inhibition, there was however, a deficit in the BDNF concentration as a result of COX-2 inhibition and tetanic stimulation. This suggests a role for COX-2 metabolites in the regulation of BDNF expression; BDNF is required for L-

LTP (Kang et al., 1997). The chronic implantation of electrodes and the recording of L-LTP under the influence of COX-2 inhibition would be ideal for determining L-LTP effects.

5.3.2 COX-2 inhibition and exogenous PGE₂

Although celecoxib is selective for the COX-2 isoform of the cyclooxygenases it has several COX-independent actions as mentioned above. Furthermore, given the added side-pocket on COX-2 isozyme compared to COX-1, the range of substrates it can metabolise is more extensive. In addition, when COX-2 metabolic activity is antagonised the substrates released by synaptic activity that would normally be metabolised by COX-2, can build-up and their own biological activities can alter synaptic function themselves e.g. AA (Nishizaki, Matsuoka, Nomura, Enikolopov, & Sumikawa, 1999; Nishizaki, Nomura, Matsuoka, Enikolopov, & Sumikawa, 1999; J. H. Williams et al., 1989). Thus it was important to confirm the origin of the deficit and the most obvious place to start was with its most abundant metabolite, PGE₂ (Brock et al., 1999). In these experiments we found that directly replacing PGE₂ was absolutely sufficient to reverse the impairment in LTP induction as discussed, lasting up to three hours after HFS. Examination of the effects of PGE₂ on baseline synaptic transmission showed no significant changes thus PGE₂ modulated activity dependent synaptic changes in the MPP. This is in contrast to results in the Schaffer collateral *in vitro* which showed that PGE₂ mediated a facilitation independent of tetanic stimulation i.e. the facilitation was activity independent (C. Chen & Bazan, 2005a). Feinmark et al. describe four criteria required to define a molecule as a mediator of long-term synaptic plasticity 1) the molecule must be present in the neurons of interest and activated during the induction of plasticity, 2) inhibition of this molecule must block the plasticity, 3) exogenous application of the molecule must induce activity independent plasticity and 4) this plasticity should prevent plasticity induced by subsequent synaptic activity. It was not demonstrated by Chen et al. whether the facilitation was occluded by tetanic stimulation, thus it cannot be concluded whether PGE₂ mediates or simply modulates synaptic plasticity (Feinmark et al., 2003). In the MPP-dentate gyrus pathway PGE₂ would appear to only modulate synaptic plasticity.

Western blot analysis of the dentate gyrus tissue at 1 hour and 3 hours post-HFS showed a time dependent pattern of expression of c-Fos – an immediate early gene used as a marker

of synaptic activity due to its rapid induction – as a result of PGE₂ injection into the hippocampus. A significant increase in ERK-phosphorylation was also demonstrated and was significantly correlated with the c-Fos expression, suggesting that ERK-phosphorylation lead to c-Fos expression. These changes were only evident at 1-hour but not 3-hours after HFS. Furthermore, although no differences in c-Fos or ERK concentration were observed at 3 hours post-HFS a highly significant correlation was evident suggesting ERK expression (a late-response gene) was related to the expression of the transcription factor c-Fos and could be interpreted as a transition from E-LTP to protein synthesis dependent L-LTP. Thus PGE₂ is required to induce activity-dependent LTP, with successful transition to L-LTP

In a review of the LTP literature Sanes and Lichtman pointed out that in *in vitro* slice experiment alteration in slice viability due to anoxia, the effects of temperature at which recording are made, perfusion rates or sprouting of spines due to the slicing procedure itself could be critical to results (Sanes & Lichtman, 1999). Thus we have used an *in vivo* technique to verify the finding of Chen et al. (C. Chen & Bazan, 2005a; C. Chen et al., 2002) and as discussed above found similar results regarding the role of COX-2 and PGE₂ in LTP induction. However, discrepancies are also apparent in that Chen et al. argued against any presynaptic effects of COX-2 inhibition, in contrast we reported changes in the paired-pulse ratio at short latencies and that PGE₂ showed a facilitation of the PPR at 200ms ISI. Furthermore, we did not show a similar facilitation in the MPP as demonstrated in the Schaffer collateral (C. Chen & Bazan, 2005a).

The findings presented above show different isoforms of cyclooxygenase have different functions in the hippocampus (changes in I/O curve and differential inhibition of LTP induction with Sc560 compared to celecoxib treatment) and that some of these effects are mediated by PGE₂ (LTP induction), while others may be artefacts of non-COX-2 activities of celecoxib (BDNF increases in association with LTP and celecoxib treatment) and yet other may be mediated by other COX-2 activity (decrease in PPD in celecoxib treated animals).

While no resolution has been reached regarding the locus of the effects of COX-2 mediated inhibition of LTP (pre- or postsynaptic or astrocytes), Figure 5.1 gives some indication as to the complexity of this debate. But most importantly it may be more the case that all of

these effects are important and isolation of one effect will not negate the involvement of the other. The isolation of EP receptors both pre- and postsynaptically and in astrocytes in the hippocampus reinforces this possibility (Zhu et al., 2005).

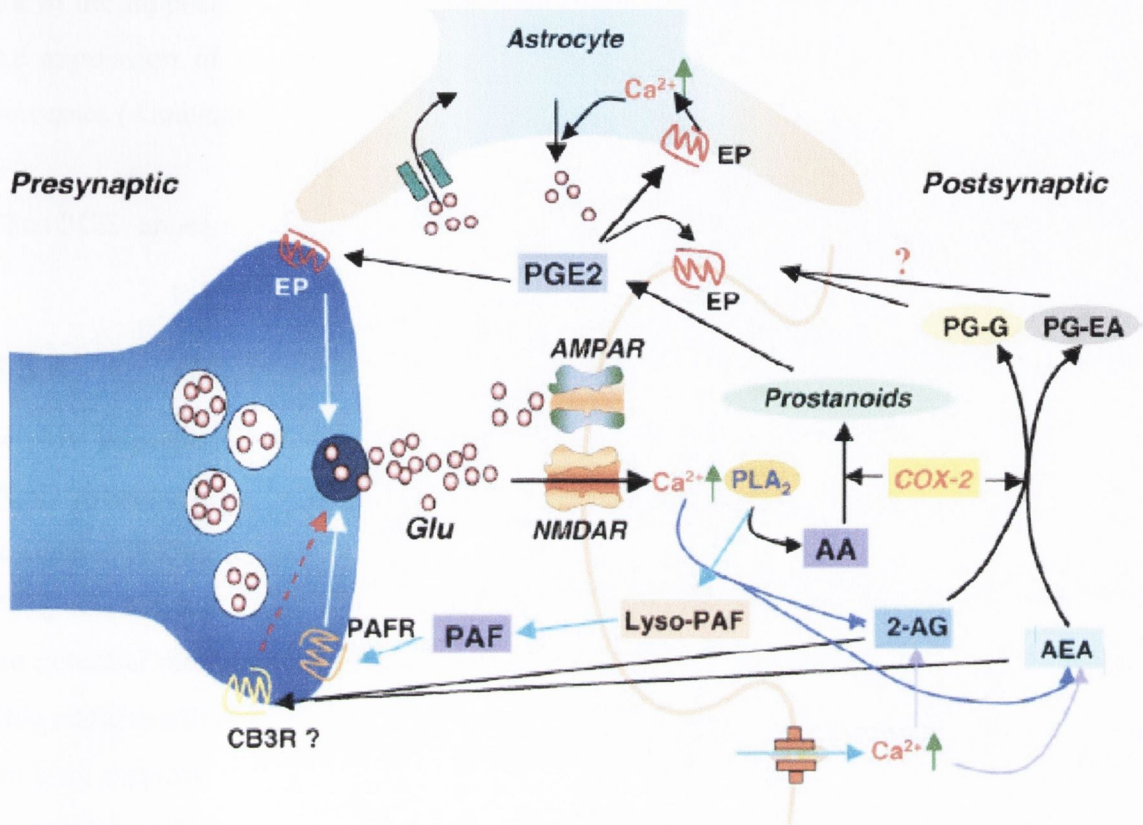


Figure 5.1 Hypothetical scheme illustrating lipids in synaptic signalling. Taken from (C. Chen & Bazan, 2005b)

5.3.3 COX, PGE₂ & memory

The data presented in this thesis confirm PGE₂ can modulate LTP induction in the hippocampus *in vivo* and since LTP has been proposed as a model of how the brain stores memory by changing synaptic weights (Bliss & Collingridge, 1993) this implicates COX-2 and PGE₂ in memory and learning. Behavioural correlates of these experiments have also shown similar results (Holscher, 1995a, , 1995b; Rall et al., 2003; Teather, Packard, & Bazan, 2001).

Prostaglandin E₂ has been shown to stimulate neurogenesis in the dentate gyrus of adult rats (Uchida et al., 2002). This is one of the few areas in the brain where new progenitor cells are made, however, their function is not completely understood. The fact that

enriched environment increases the rate of neurogenesis was successfully exploited to show a role for these newborn neurons in long-term recognition memory (Bruehl-Jungerman, Laroche, & Rampon, 2005). Furthermore, in the developing preoptic area, but not in the hippocampus, estradiol induced synthesis of PGE₂ has been shown to augment the expression of the dendritic spine protein spinophilin and the density of spine-like processes (Amateau & McCarthy, 2002).

Thus PGE₂ appears to have multiple roles in learning and memory.

5.3.4 COX and neuroinflammation

In vitro experiments by Chen *et al* showed that incubation of hippocampal slices with PGE₂ caused a lasting facilitation of evoked responses in the Schaffer-collateral (C. Chen & Bazan, 2005a). This facilitation was more pronounced when endogenous production of PGE₂ was blocked with NS398, a COX-2 inhibitor. This implies that basal levels of PGE₂ are potential modulators of synaptic efficacy and plasticity but higher concentrations had little additive effect on this facilitation. IL-1 β has been shown to induced impairments in a working memory task, as a result of elevated PGE₂ in the rat hippocampus, which can be reversed by COX-2 inhibition. They confirmed by intra-hippocampal injection of PGE₂ that this impairment was indeed due to excess PGE₂, the consequent impairment being concentration dependent (Matsumoto, Yamaguchi, Watanabe, & Yamamoto, 2004). These findings suggest a multi-tiered functionality for PGE₂ in the hippocampus and possibly all of the CNS. This has been proposed previously by Shaw whereby PGE₂ at low levels of expression is important for normal synaptic function, moderate stimulation of PGE₂ (HFS, learning etc) augments the activation state of neurons as in synaptic plasticity, and high-level stimulation (LPS, seizure etc) results in damage and cell death from excitotoxicity (Shaw, 2001). A model of this multi-tiered system is shown in Figure 5.2. The findings presented in this thesis have added to this model by showing that COX-2 inhibition is responsible for the impairment of LTP in a PGE₂ dependent manner. Thus while many neurological and neuroinflammatory disease have implicated elevations in COX-2 activity, most notably Alzheimer's disease (Minghetti, 2004) it is important to keep in mind that not all of this activity is harmful.

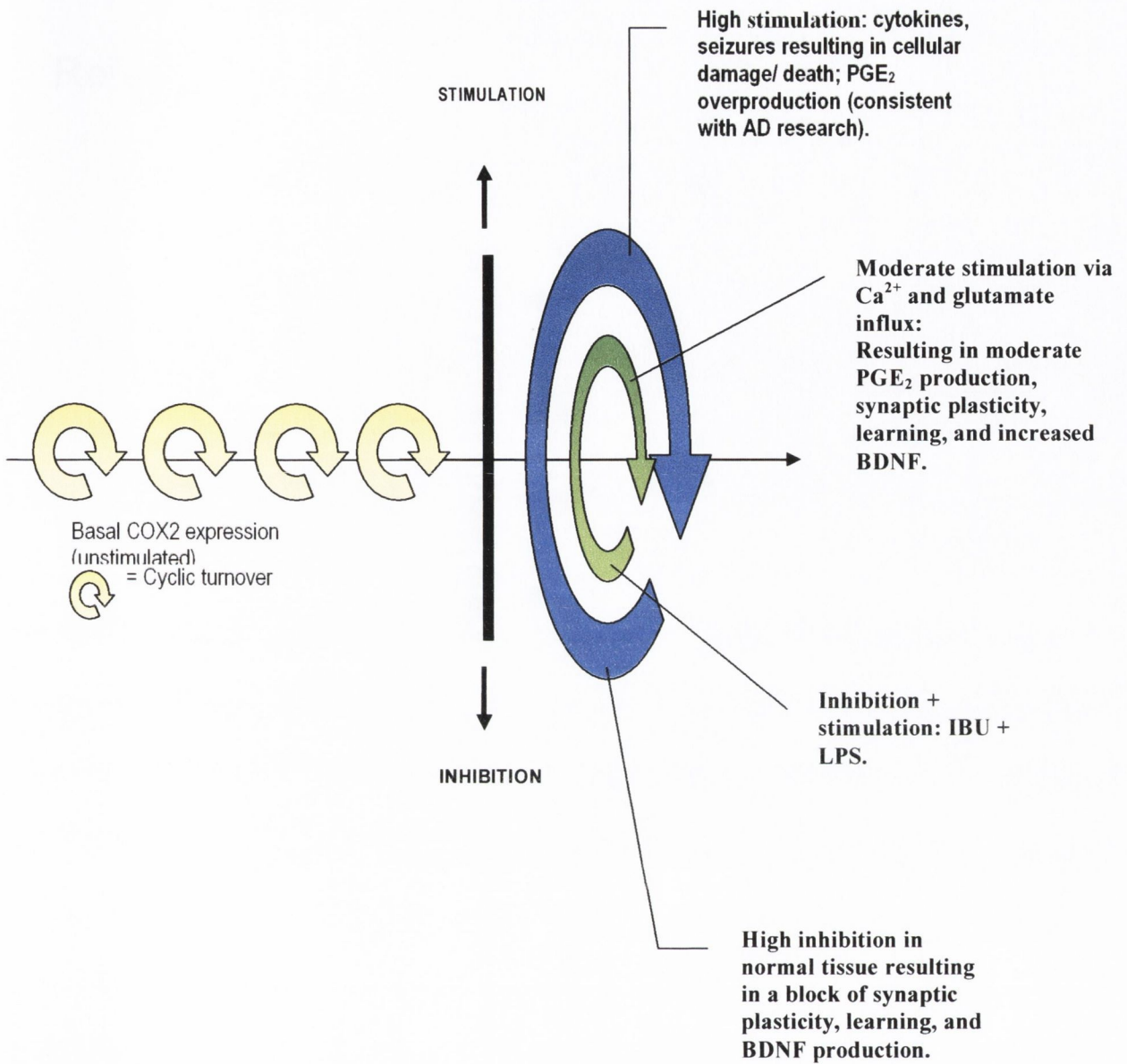


Figure 5.2 A hypothetical model for the regulation of COX2 during varying degrees of stimulation and inhibition (Shaw, 2001).

References

- Adams, J., Collaco-Moraes, Y., & de Bellerocche, J. (1996). Cyclooxygenase-2 in cerebral cortex: an intracellular response to synaptic excitation. *Journal of Neurochemistry*, *66*, 6-13.
- Ajmone-Cat, M. A., Iosif, R. E., Ekdahl, C. T., Kokaia, Z., Minghetti, L., & Lindvall, O. (2006). Prostaglandin E(2) and BDNF levels in rat hippocampus are negatively correlated with status epilepticus severity: No impact on survival of seizure-generated neurons. *Neurobiol Dis*.
- Alberts, B., Bray, D., Lewis, J., Raff, M., Roberts, K., & Watson, J. D. (1994a). Cell Signalling. In *Molecular Biology of the Cell* (3rd ed., pp. 744-748). New York: Garland Publishing, Inc.
- Alberts, B., Bray, D., Lewis, J., Raff, M., Roberts, K., & Watson, J. D. (1994b). Small Molecules, Energy, and Biosynthesis. In *Molecular Biology of the Cell* (3rd ed., pp. 41-88). New York: Garland Publishing, Inc.
- Albertson, T. E., & Joy, R. M. (1987). Increased inhibition in dentate gyrus granule cells following exposure to GABA-uptake blockers. *Brain Res*, *435*(1-2), 283-292.
- Alvarez, D. N., Wiegert, M., Joels, M., & Krugers, H. J. (2002). Corticosterone and stress reduce synaptic potentiation in mouse hippocampal slices with mild stimulation. *Neuroscience*, *115*(4), 1119-1126.
- Alger, B. E. (2002). Retrograde signaling in the regulation of synaptic transmission: focus on endocannabinoids. *Prog Neurobiol*, *68*(4), 247-286.
- Amateau, S. K., & McCarthy, M. M. (2002). A novel mechanism of dendritic spine plasticity involving estradiol induction of prostaglandin-E2. *J Neurosci*, *22*(19), 8586-8596.
- Andersen, P. (2003). A prelude to long-term potentiation. *Philos Trans R Soc Lond B Biol Sci*, *358*(1432), 613-615.
- Anggard, E., Larsson, C., & Samuelsson, B. (1971). The distribution of 15-hydroxy prostaglandin dehydrogenase and prostaglandin-delta 13-reductase in tissues of the swine. *Acta Physiol Scand*, *81*(3), 396-404.
- Asztely, F., Kokaia, M., Olofsson, K., Ortegren, U., & Lindvall, O. (2000). Afferent-specific modulation of short-term synaptic plasticity by neurotrophins in dentate gyrus. *Eur J Neurosci*, *12*(2), 662-669.
- Baba, H., Kohno, T., Moore, K. A., & Woolf, C. J. (2001). Direct activation of rat spinal dorsal horn neurons by prostaglandin E2. *J Neurosci*, *21*(5), 1750-1756.

- Balkowiec, A., & Katz, D. M. (2002). Cellular mechanisms regulating activity-dependent release of native brain-derived neurotrophic factor from hippocampal neurons. *J Neurosci*, *22*(23), 10399-10407.
- Bannerman, D. M., Rawlins, J. N., McHugh, S. B., Deacon, R. M., Yee, B. K., Bast, T., et al. (2004). Regional dissociations within the hippocampus--memory and anxiety. *Neurosci Biobehav Rev*, *28*(3), 273-283.
- Barde, Y. A., Edgar, D., & Thoenen, H. (1982). Purification of a new neurotrophic factor from mammalian brain. *Embo J*, *1*(5), 549-553.
- Bazan, N. G. (2003). Synaptic lipid signaling: significance of polyunsaturated fatty acids and platelet-activating factor. *J Lipid Res*, *44*(12), 2221-2233.
- Bazan, N. G., & Flower, R. J. (2002). Medicine: lipid signals in pain control. *Nature*, *420*(6912), 135-138.
- Behnisch, T., & Reymann, K. G. (1995). Thapsigargin blocks long-term potentiation induced by weak, but not strong tetanisation in rat hippocampal CA1 neurons. *Neurosci Lett*, *192*(3), 185-188.
- Belluzi, O., Biondi, C., Borasio, P. G., Capuzzo, A., Ferretti, M. E., Trevisani, A., et al. (1982). Electrophysiological evidence for a PGE₂-mediated presynaptic control of acetylcholine output in the guinea-pig superior cervical ganglion. *Brain Res*, *236*, 383-391.
- Bezzi, P., Carmignoto, G., Pasti, L., Vesce, S., Rossi, D., Rizzini, B. L., et al. (1998). Prostaglandins stimulate calcium-dependent glutamate release in astrocytes. *Nature*, *391*(6664), 281-285.
- Bezzi, P., & Volterra, A. (2001). A neuron-glia signalling network in the active brain. *Curr Opin Neurobiol*, *11*(3), 387-394.
- Bliss, T. V., & Collingridge, G. L. (1993). A synaptic model of memory: long-term potentiation in the hippocampus. *Nature*, *361*(6407), 31-39.
- Bliss, T. V., & Lomo, T. (1973). Long-lasting potentiation of synaptic transmission in the dentate area of the anaesthetized rabbit following stimulation of the perforant path. *J Physiol*, *232*(2), 331-356.
- Boglari, G., Erhardt, P., Cooper, G. M., & Szeberenyi, J. (1998). Intact Ras function is required for sustained activation and nuclear translocation of extracellular signal-regulated kinases in nerve growth factor-stimulated PC12 cells. *Eur J Cell Biol*, *75*(1), 54-58.

- Bosetti, F., Langenbach, R., & Weerasinghe, G. R. (2004). Prostaglandin E2 and microsomal prostaglandin E synthase-2 expression are decreased in the cyclooxygenase-2-deficient mouse brain despite compensatory induction of cyclooxygenase-1 and Ca²⁺-dependent phospholipase A2. *J Neurochem*, *91*(6), 1389-1397.
- Bosetti, F., & Weerasinghe, G. R. (2003). The expression of brain cyclooxygenase-2 is down-regulated in the cytosolic phospholipase A2 knockout mouse. *J Neurochem*, *87*(6), 1471-1477.
- Bouron, A. (2001). Modulation of spontaneous quantal release of neurotransmitters in the hippocampus. *Progress in Neurobiology*, *63*(6), 613-635.
- Bradford, M. M. (1976). A rapid and sensitive method for the quantitation of microgram quantities of protein utilizing the principle of protein-dye binding. *Anal Biochem*, *72*, 248-254.
- Bramham, C. R., & Messaoudi, E. (2005). BDNF function in adult synaptic plasticity: The synaptic consolidation hypothesis. *Prog Neurobiol*, *76*(2), 99-125.
- Bramham, C. R., Southard, T., Sarvey, J. M., Herkenham, M., & Brady, L. S. (1996). Unilateral LTP triggers bilateral increases in hippocampal neurotrophin and trk receptor mRNA expression in behaving rats: evidence for interhemispheric communication. *J Comp Neurol*, *368*(3), 371-382.
- Breder, C. D., Dewitt, D., & Kraig, R. P. (1995). Characterization of inducible cyclooxygenase in rat brain. *J Comp Neurol*, *355*(2), 296-315.
- Breder, C. D., Smith, W. L., Raz, A., Masferrer, J. L., Seibert, K., Needleman, P., et al. (1992). The distribution and characterisation of cyclooxygenase-like immunoreactivity in the ovine brain. *Journal of comparative neurology*, *322*, 409-438.
- Breyer, R. M., Bagdassarian, C. K., Myers, S. A., & Breyer, M. D. (2001). Prostanoid receptors: subtypes and signaling. *Annu Rev Pharmacol Toxicol*, *41*, 661-690.
- Brock, T. G., McNish, R. W., & Peters-Golden, M. (1999). Arachidonic acid is preferentially metabolized by cyclooxygenase-2 to prostacyclin and prostaglandin E2. *J Biol Chem*, *274*(17), 11660-11666.
- Brown, A. M. (2001). A step-by-step guide to non-linear regression analysis of experimental data using a Microsoft Excel spreadsheet. *Computer Methods and Programs in Biomedicine*, *65*(3), 191-200.

- Brown, T. H., & Zador, A. M. (1990). Hippocampus. In G. M. Shepherd (Ed.), *The Synaptic Organisation of the Brain* (3rd ed., pp. 346-388). New York: Oxford University Press, Inc.,.
- Brucato, F. H., Mott, D. D., Lewis, D. V., & Swartzwelder, H. S. (1995). GABAB receptors modulate synaptically-evoked responses in the rat dentate gyrus, in vivo. *Brain Res*, 677(2), 326-332.
- Bruel-Jungerman, E., Laroche, S., & Rampon, C. (2005). New neurons in the dentate gyrus are involved in the expression of enhanced long-term memory following environmental enrichment. *Eur J Neurosci*, 21(2), 513-521.
- Brun, V. H., Ytterbo, K., Morris, R. G., Moser, M. B., & Moser, E. I. (2001). Retrograde amnesia for spatial memory induced by NMDA receptor-mediated long-term potentiation. *J Neurosci*, 21(1), 356-362.
- Bugajski, J., Glod, R., Gadek-Michalska, A., & Bugajski, A. J. (2001). Involvement of constitutive (COX-1) and inducible cyclooxygenase (COX-2) in the adrenergic-induced ACTH and corticosterone secretion. *J Physiol Pharmacol*, 52(4 Pt 2), 795-809.
- Bygdeman, M. (2003). Pharmacokinetics of prostaglandins. *Best Practice & Research Clinical Obstetrics & Gynaecology*, 17(5), 707-716.
- Casolini, P., Catalani, A., Zuena, A. R., & Angelucci, L. (2002). Inhibition of COX-2 reduces the age-dependent increase of hippocampal inflammatory markers, corticosterone secretion, and behavioral impairments in the rat. *J Neurosci Res*, 68(3), 337-343.
- Chandrasekharan, N. V., Dai, H., Roos, K. L. T., Evanson, N. K., Tomsik, J., Elton, T. S., et al. (2002). From the Cover: COX-3, a cyclooxygenase-1 variant inhibited by acetaminophen and other analgesic/antipyretic drugs: Cloning, structure, and expression. *PNAS*, 99(21), 13926-13931.
- Chen, C., & Bazan, N. G. (2005a). Endogenous PGE2 regulates membrane excitability and synaptic transmission in hippocampal CA1 pyramidal neurons. *J Neurophysiol*, 93(2), 929-941.
- Chen, C., & Bazan, N. G. (2005b). Lipid signaling: sleep, synaptic plasticity, and neuroprotection. *Prostaglandins Other Lipid Mediat*, 77(1-4), 65-76.
- Chen, C., Magee, J. C., & Bazan, N. G. (2002). Cyclooxygenase-2 regulates prostaglandin E2 signaling in hippocampal long-term synaptic plasticity. *J Neurophysiol*, 87(6), 2851-2857.

- Chen, R. H., Abate, C., & Blenis, J. (1993). Phosphorylation of the c-Fos transrepression domain by mitogen-activated protein kinase and 90-kDa ribosomal S6 kinase. *Proc Natl Acad Sci U S A*, *90*(23), 10952-10956.
- Chen, W., Pawelek, T. R., & Kulmacz, R. J. (1999). Hydroperoxide Dependence and Cooperative Cyclooxygenase Kinetics in Prostaglandin H Synthase-1 and -2. *J. Biol. Chem.*, *274*(29), 20301-20306.
- Cobb, M. H., & Goldsmith, E. J. (1995). How MAP Kinases Are Regulated. *J. Biol. Chem.*, *270*(25), 14843-14846.
- Collingridge, G. L., Kehl, S. J., & McLennan, H. (1983). Excitatory amino acids in synaptic transmission in the Scaffer collateral-commissural pathway of the rat hippocampus. *Journal of Physiology*, *334*, 33-46.
- Coogan, A. N., O'Leary, D. M., & O'Connor, J. J. (1999). P42/44 MAP Kinase Inhibitor PD98059 Attenuates Multiple Forms of Synaptic Plasticity in Rat Dentate Gyrus In Vitro. *J Neurophysiol*, *81*(1), 103-110.
- Cooper, S. J. (2005). Donald O. Hebb's synapse and learning rule: a history and commentary. *Neurosci Biobehav Rev*, *28*(8), 851-874.
- Corkin, S., Amaral, D. G., Gonzalez, R. G., Johnson, K. A., & Hyman, B. T. (1997). H. M.'s Medial Temporal Lobe Lesion: Findings from Magnetic Resonance Imaging. *J. Neurosci.*, *17*(10), 3964-3979.
- Craver, C. F. (2003). The making of a memory mechanism. *J Hist Biol*, *36*(1), 153-195.
- Cunha, R. A., Almeida, T., & Ribeiro, J. A. (2000). Modification by arachidonic acid of extracellular adenosine metabolism and neuromodulatory action in the rat hippocampus. *J Biol Chem*, *275*(48), 37572-37581.
- Dannhardt, G., & Kiefer, W. (2001). Cyclooxygenase inhibitors - current status and future prospects. *Eur J Med Chem*(36), 109-126.
- Davis, S., & Laroche, S. (1998). A molecular biological approach to synaptic plasticity and learning. *C R Acad Sci III*, *321*(2-3), 97-107.
- Davis, S., Vanhoutte, P., Pages, C., Caboche, J., & Laroche, S. (2000). The MAPK/ERK Cascade Targets Both Elk-1 and cAMP Response Element-Binding Protein to Control Long-Term Potentiation-Dependent Gene Expression in the Dentate Gyrus In Vivo. *J. Neurosci.*, *20*(12), 4563-4572.
- Desmond, N. L., & Levy, W. B. (1988). Synaptic interface surface area increases with long-term potentiation in the hippocampal dentate gyrus. *Brain Research*, *453*, 308-314.

- Dickenson, A. H. (1995). Spinal cord pharmacology of pain. *Br. J. Anaesth.*, 75(2), 193-200.
- Dickie, B. G., Stevens, J. A., & Davies, J. A. (1994). Effects of cyclo-oxygenase inhibition upon glutamate release from rat cerebellum. *NeuroReport*, 5(4), 393-396.
- DiScenna, P. G., & Teyler, T. J. (1994). Development of inhibitory and excitatory synaptic transmission in the rat dentate gyrus. *Hippocampus*, 4(5), 569-576.
- Doyere, V., Srebro, B., & Laroche, S. (1997). Heterosynaptic LTD and depotentiation in the medial perforant path of the dentate gyrus in the freely moving rat. *J Neurophysiol*, 77(2), 571-578.
- Dumuis, A., Pin, J. P., Oomagari, K., Sebben, M., & Bockaert, J. (1990). Arachidonic acid released from striatal neurons by joint stimulation of ionotropic and metabotropic quisqualate receptors. *Nature*, 347(6289), 182-184.
- Dumuis, A., Sebben, M., Haynes, L., Pin, J. P., & Bockaert, J. (1988). NMDA receptors activate the arachidonic acid cascade system in striatal neurons. *Nature*, 336(6194), 68-70.
- England, S., Bevan, S., & Docherty, R. J. (1996). PGE2 modulates the tetrodotoxin-resistant sodium current in neonatal rat dorsal root ganglion neurones via the cyclic AMP-protein kinase A cascade. *J Physiol*, 495 (Pt 2), 429-440.
- English, J. D., & Sweatt, J. D. (1997). A requirement for the mitogen-activated protein kinase cascade in hippocampal long term potentiation. *J Biol Chem*, 272(31), 19103-19106.
- Evans, A. R., Vasko, M. R., & Nicol, G. D. (1999). The cAMP transduction cascade mediates the PGE2-induced inhibition of potassium currents in rat sensory neurones. *J Physiol*, 516 (Pt 1), 163-178.
- Fairman, W. A., Sonders, M. S., Murdoch, G. H., & Amara, S. G. (1998). Arachidonic acid elicits a substrate-gated proton current associated with the glutamate transporter EAAT4. *Nature Neuroscience*, 1(2), 105-113.
- Feinmark, S. J., Begum, R., Tsvetkov, E., Goussakov, I., Funk, C. D., Siegelbaum, S. A., et al. (2003). 12-lipoxygenase metabolites of arachidonic acid mediate metabotropic glutamate receptor-dependent long-term depression at hippocampal CA3-CA1 synapses. *J Neurosci*, 23(36), 11427-11435.
- Fifkova, E., & Vanharraveld, A. (1977). Long-lasting morphological changes in dendritic spines of dentate granular area following stimulation of the entorhinal cortex. *Journal of Neurocytology*, 6, 211-230.

- Frey, U., Frey, S., Schollmeier, F., & Krug, M. (1996). Influence of actinomycin D, a RNA synthesis inhibitor, on long-term potentiation in rat hippocampal neurons in vivo and invitro. *J Physiol [Lond]*, *490*, 703-711.
- Friedman, W. J., Larkfors, L., Ayer-LeLievre, C., Ebendal, T., Olson, L., & Persson, H. (1990). Regulation of beta-nerve growth factor expression by inflammatory mediators in hippocampal cultures. *J Neurosci Res*, *27*(3), 374-382.
- Fujino, H., Xu, W., & Regan, J. W. (2003). Prostaglandin E2 induced functional expression of early growth response factor-1 by EP4, but not EP2, prostanoid receptors via the phosphatidylinositol 3-kinase and extracellular signal-regulated kinases. *J Biol Chem*, *278*(14), 12151-12156.
- Fuster, J. M. (1997). Network Memory. *Trends in Neuroscience*, *20*, 451-459.
- Gartner, A., & Staiger, V. (2002). Neurotrophin secretion from hippocampal neurons evoked by long-term-potential-inducing electrical stimulation patterns. *Proc Natl Acad Sci U S A*, *99*(9), 6386-6391.
- Gierse, J. K., Koboldt, C. M., Walker, M. C., Seibert, K., & Isakson, P. C. (1999). Kinetic basis for selective inhibition of cyclo-oxygenases. *Biochem J*, *339* (Pt 3), 607-614.
- Gold, M. S., Reichling, D. B., Shuster, M. J., & Levine, J. D. (1996). Hyperalgesic agents increase a tetrodotoxin-resistant Na⁺ current in nociceptors. *Proc Natl Acad Sci U S A*, *93*(3), 1108-1112.
- Gooney, M., & Lynch, M. A. (2001). Long-term potentiation in the dentate gyrus of the rat hippocampus is accompanied by brain-derived neurotrophic factor-induced activation of TrkB. *Journal of neurochemistry*, *77*, 1198-1207.
- Gooney, M., Shaw, K., Kelly, A., O'Mara, S. M., & Lynch, M. A. (2002). Long-term potentiation and spatial learning are associated with increased phosphorylation of TrkB and extracellular signal-regulated kinase (ERK) in the dentate gyrus: evidence for a role for brain-derived neurotrophic factor. *Behav Neurosci*, *116*(3), 455-463.
- Greenberg, M. E., & Ziff, E. B. (1984). Stimulation of 3T3 cells induces transcription of the c-fos proto-oncogene. *Nature*, *311*(5985), 433-438.
- Hallbook, F., Ibanez, C. F., & Persson, H. (1991). Evolutionary studies of the nerve growth factor family reveal a novel member abundantly expressed in *Xenopus* ovary. *Neuron*, *6*(5), 845-858.

- Hata, A. N., & Breyer, R. M. (2004). Pharmacology and signaling of prostaglandin receptors: multiple roles in inflammation and immune modulation. *Pharmacol Ther*, *103*(2), 147-166.
- Hebb, D. O. (1949). *The organization of behaviour: a neuropsychological theory*. New York: Wiley.
- Hinoi, E., Balcar, V. J., Kuramoto, N., Nakamichi, N., & Yoneda, Y. (2002). Nuclear transcription factors in the hippocampus. *Progress in Neurobiology*, *68*(2), 145-165.
- Hohn, A., Leibrock, J., Bailey, K., & Barde, Y. A. (1990). Identification and characterization of a novel member of the nerve growth factor/brain-derived neurotrophic factor family. *Nature*, *344*(6264), 339-341.
- Holscher, C. (1995a). Inhibitors of cyclooxygenases produce amnesia for a passive avoidance task in the chick. *Eur J Neurosci*, *7*(6), 1360-1365.
- Holscher, C. (1995b). Prostaglandins play a role in memory consolidation in the chick. *European Journal of Pharmacology*, *294*(1), 253-259.
- Hu, F., Wang, X., Pace, T. W., Wu, H., & Miller, A. H. (2005). Inhibition of COX-2 by celecoxib enhances glucocorticoid receptor function. *Mol Psychiatry*, *10*(5), 426-428.
- Huang, E. J., & Reichardt, L. F. (2001). Neurotrophins: roles in neuronal development and function. *Annu Rev Neurosci*, *24*, 677-736.
- Huang, X. C., Deng, T., & Sumners, C. (1998). Angiotensin II stimulates activation of Fos-regulating kinase and c-Jun NH2-terminal kinase in neuronal cultures from rat brain. *Endocrinology*, *139*(1), 245-251.
- Ibrahim, N., Shibuya, I., Kabashima, N., Sutarmo, S. V., Ueta, Y., & Yamashita, H. (1999). Prostaglandin E2 inhibits spontaneous inhibitory postsynaptic currents in rat supraoptic neurones via presynaptic EP receptors. *J Neuroendocrinol*, *11*(11), 879-886.
- Ikeda, S. R. (1992). Prostaglandin modulation of calcium channels in rat sympathetic neurones is mediated by guanine nucleotide binding proteins. *J. Physiol*, *458*, 339-359.
- Insausti, R., Amaral, D. G., & Cowan, W. M. (1987). The entorhinal cortex of the monkey: II. Cortical afferents. *J Comp Neurol*, *264*(3), 356-395.
- Isaac, J. T., Luthi, A., Palmer, M. J., Anderson, W. W., Benke, T. A., & Collingridge, G. L. (1998). An investigation of the expression mechanism of LTP of AMPA

- receptor-mediated synaptic transmission at hippocampal CA1 synapses using failures analysis and dendritic recordings. *Neuropharmacology*, 37(10-11), 1399-1410.
- Jakobsson, P. J., Thoren, S., Morgenstern, R., & Samuelsson, B. (1999). Identification of human prostaglandin E synthase: a microsomal, glutathione-dependent, inducible enzyme, constituting a potential novel drug target. *Proc Natl Acad Sci U S A*, 96(13), 7220-7225.
- Jeffery, K. J. (1995). Paradoxical enhancement of long-term potentiation in poor-learning rats at low test stimulus intensities. *Exp Brain Res*, 104(1), 55-69.
- Johnson, A. J., Hsu, A. L., Lin, H. P., Song, X., & Chen, C. S. (2002). The cyclooxygenase-2 inhibitor celecoxib perturbs intracellular calcium by inhibiting endoplasmic reticulum Ca²⁺-ATPases: a plausible link with its anti-tumour effect and cardiovascular risks. *Biochem J*, 366(Pt 3), 831-837.
- Kahle, J. S., & Cotman, C. W. (1993). L-2-amino-4-phosphonobutanoic acid and 1S,3R-1-aminocyclopentane-1,3-dicarboxylic acid reduce paired-pulse depression recorded from medial perforant path in the dentate gyrus of rat hippocampal slices. *J Pharmacol Exp Ther*, 266(1), 207-215.
- Kang, H., & Schumann, E. M. (1995). Long-lasting neurotrophin-induced enhancement of synaptic transmission in the adult hippocampus. *Science*, 267, 1658-1662.
- Kang, H., Welcher, A. A., Shelton, D., & Schuman, E. M. (1997). Neurotrophins and time: different roles for TrkB signaling in hippocampal long-term potentiation. *Neuron*, 19(3), 653-664.
- Katafuchi, T., Duan, S., Take, S., & Yoshimura, M. (2005). Modulation of glutamate-induced outward current by prostaglandin E(2) in rat dissociated preoptic neurons. *Brain Res*, 1037(1-2), 180-186.
- Kaufmann, W. E., Andreasson, K. I., Isakson, P. C., & Worley, P. F. (1997). Cyclooxygenases and the central nervous system. *Prostaglandins*, 54(3), 601-624.
- Kaufmann, W. E., Worley, P. F., Pegg, J., Bremer, M., & Isakson, P. (1996). COX-2, a synaptically induced enzyme, is expressed by excitatory neurons at postsynaptic sites in rat cerebral cortex. *Proc Natl Acad Sci U S A*, 93(6), 2317-2321.
- Kelly, A., Mullany, P. M., & Lynch, M. A. (2000). Protein synthesis in entorhinal cortex and long-term potentiation in dentate gyrus. *Hippocampus*, 10(4), 431-437.
- Kesslak, J. P., So, V., Choi, J., Cotman, C. W., & Gomez-Pinilla, F. (1998). Learning upregulates brain-derived neurotrophic factor messenger ribonucleic acid: a

- mechanism to facilitate encoding and circuit maintenance? *Behav Neurosci*, 112(4), 1012-1019.
- Kim, J., & Alger, B. E. (2004). Inhibition of cyclooxygenase-2 potentiates retrograde endocannabinoid effects in hippocampus. *Nat Neurosci*, 7(7), 697-698.
- Korte, M., Carroll, P., Wolf, E., Brem, G., Thoenen, H., & Bonhoeffer, T. (1995). Hippocampal long-term potentiation is impaired in mice lacking brain-derived neurotrophic factor. *Proc Natl Acad Sci U S A*, 92(19), 8856-8860.
- Kovacs, K. J. (1998). Invited review c-Fos as a transcription factor: a stressful (re)view from a functional map. *Neurochemistry International*, 33(4), 287-297.
- Kraemer, S. A., Meade, E. A., & DeWitt, D. L. (1992). Prostaglandin endoperoxide synthase gene structure: identification of the transcriptional start site and 5'-flanking regulatory sequences. *Arch Biochem Biophys.*, 293(2), 391-400.
- Krug, M., Lossner, B., & Otto, T. (1984). Anisomycin blocks the late phase of long-term potentiation in the dentate gyrus of free moving rats. *Brain Research Bulletin*, 13, 39-42.
- Krysan, K., Reckamp, K. L., Dalwadi, H., Sharma, S., Rozengurt, E., Dohadwala, M., et al. (2005). Prostaglandin E2 activates mitogen-activated protein kinase/Erk pathway signaling and cell proliferation in non-small cell lung cancer cells in an epidermal growth factor receptor-independent manner. *Cancer Res*, 65(14), 6275-6281.
- Kujubu, D. A., Fletcher, B. S., Varnum, B. C., Lim, R. W., & Herschman, H. R. (1991). TIS10, a phorbol ester tumor promoter-inducible mRNA from Swiss 3T3 cells, encodes a novel prostaglandin synthase/cyclooxygenase homologue. *J. Biol. Chem.*, 266(20), 12866-12872.
- Kujubu, D. A., Reddy, S. T., Fletcher, B. S., & Herschman, H. R. (1993). Expression of the protein product of the prostaglandin synthase-2/TIS10 gene in mitogen-stimulated Swiss 3T3 cells. *J Biol Chem*, 268(8), 5425-5430.
- Kurumbail, R. G., Stevens, A. M., Gierse, J. K., McDonald, J. J., Stegeman, R. A., Pak, J. Y., et al. (1996). Structural basis for selective inhibition of cyclooxygenase-2 by anti-inflammatory agents. *Nature*, 384(6610), 644-648.
- Lacroix, S., Vallieres, L., & Rivest, S. (1996). C-fos mRNA pattern and corticotropin-releasing factor neuronal activity throughout the brain of rats injected centrally with a prostaglandin of E2 type. *Journal of Neuroimmunology*, 70(2), 163-179.
- Laemmli, U. K. (1970). Cleavage of structural proteins during the assembly of the head of bacteriophage T4. *Nature*, 227(5259), 680-685.

- Lavenex, P., & Amaral, D. G. (2000). Hippocampal-neocortical interaction: a hierarchy of association. *Hippocampus*, *10*, 420-430.
- Lerea, L. S., Butler, L. S., & McNamara, J. O. (1992). NMDA and non-NMDA receptor-mediated increase of c-fos mRNA in dentate gyrus neurons involves calcium influx via different routes. *J Neurosci*, *12*(8), 2973-2981.
- Lerea, L. S., Carlson, N. G., & McNamara, J. O. (1995). N-methyl-D-aspartate receptors activate transcription of c-fos and NGFI-A by distinct phospholipase A2-requiring intracellular signaling pathways. *Mol Pharmacol*, *47*(6), 1119-1125.
- Lerea, L. S., Carlson, N. G., Simonato, M., Morrow, J. D., Roberts, J. L., & McNamara, J. O. (1997). Prostaglandin F2alpha is required for NMDA receptor-mediated induction of c-fos mRNA in dentate gyrus neurons. *J Neurosci*, *17*(1), 117-124.
- Lerea, L. S., & McNamara, J. O. (1993). Ionotropic glutamate receptor subtypes activate c-fos transcription by distinct calcium-requiring intracellular signaling pathways. *Neuron*, *10*(1), 31-41.
- Lessmann, V., Gottmann, K., & Heumann, R. (1994). BDNF and NT-4/5 enhance glutamatergic synaptic transmission in cultures hippocampal neurones. *NeuroReport*, *6*, 21-25.
- Levi-Montalcini, R. (1987). The nerve growth factor: thirty-five years later. *Embo J*, *6*(5), 1145-1154.
- Levine, E. S., Dreyfus, C. F., Black, I. B., & Plummer, M. R. (1995). Brain-derived neurotrophic factor rapidly enhances synaptic transmission in hippocampal neurons via postsynaptic tyrosine kinase receptors. *Proc. Natl. Acad. Sci. U.S.A.*, *92*, 8074-8077.
- Li, Q., Withoff, S., & Verma, I. M. (2005). Inflammation-associated cancer: NF-kappaB is the lynchpin. *Trends Immunol*, *26*(6), 318-325.
- Lohof, A. M., Ip, N. Y., & Poo, M. M. (1993). Potentiation of developing neuromuscular synapses by the neurotrophins NT-3 and BDNF. *Nature*, *363*, 350-353.
- Lømo, T. (1971a). Patterns of activation in a monosynaptic cortical pathway: The perforant path input to the dentate area of the hippocampal formation. *Experimental Brain Research*, *12*(1), 18 - 45.
- Lømo, T. (1971b). Potentiation of monosynaptic EPSPs in the perforant path-dentate granule cell synapse. *Experimental Brain Research*, *12*(1), 46 - 63.
- Lu, B. (2003a). BDNF and Activity-Dependent Synaptic Modulation. *Learn. Mem.*, *10*(2), 86-98.

- Lu, B. (2003b). Pro-region of neurotrophins: role in synaptic modulation. *Neuron*, *39*(5), 735-738.
- Lynch, G., Larson, J., Kelso, S., Barrionuevo, G., & Schottler, F. (1983). Intracellular injections of EGTA block induction of hippocampal long-term potentiation. *Nature*, *305*(5936), 719-721.
- Lynch, M. A. (2004). Long-term potentiation and memory. *Physiol Rev*, *84*(1), 87-136.
- Lynch, M. A., Errington, M. L., & Bliss, T. V. P. (1989). Nordihydroguaiaretic acid blocks the synaptic component of long-term potentiation and the associated increases in the release of glutamate and arachidonate: an in vivo study in the dentate gyrus of the rat. *Neuroscience*, *30*, 693-701.
- Magee, J. C., & Johnston, D. (1997). A synaptically controlled, associative signal for hebbian plasticity in hippocampal neurons. *Science* (Vol. 275, pp. 209): American Association for the Advancement of Science.
- Malenka, R. C., Kauer, J. A., Perkel, D. J., Mauk, M. D., Kelly, P. T., Nicoll, R. A., et al. (1989). An essential role for postsynaptic calmodulin and protein kinase activity in long-term potentiation. *Nature*, *340*, 554-557.
- Malenka, R. C., Kauer, J. A., Zucker, R. S., & Nicoll, R. A. (1988). Postsynaptic calcium is sufficient for potentiation of hippocampal synaptic transmission. *Science*, *242*(4875), 81-84.
- Malenka, R. C., & Nicoll, R. A. (1999). Long-term potentiation - a decade of progress. *Science*, *285*, 1870-1874.
- Malinow, R., Schulman, H., & Tsien, R. W. (1989). Inhibition of postsynaptic PKC and CaMKII blocks induction but not expression of LTP. *Science*, *245*, 862-866.
- Marder, C. P., & Buonomano, D. V. (2004). Timing and balance of inhibition enhance the effect of long-term potentiation on cell firing. *J Neurosci*, *24*(40), 8873-8884.
- Marini, A. M., Jiang, X., Wu, X., Tian, F., Zhu, D., Okagaki, P., et al. (2004). Role of brain-derived neurotrophic factor and NF-kappaB in neuronal plasticity and survival: From genes to phenotype. *Restor Neurol Neurosci*, *22*(2), 121-130.
- Marsh, H. N., Scholz, W. K., Lamballe, F., Klein, R., Nanduri, V., Barbacid, M., et al. (1993). Signal transduction events mediated by the BDNF receptor gp 145trkB in primary hippocampal pyramidal cell culture. *J Neurosci*, *13*(10), 4281-4292.
- Martin, S. J., & Morris, R. G. M. (2002). New life in an old idea: The synaptic plasticity and memory hypothesis revisited. *Hippocampus*, *12*, 609-636.

- Masferrer, J. L., Zweifel, B. S., Manning, P. T., Hauser, S. D., Leahy, K. M., Smith, W. G., et al. (1994). Selective inhibition of inducible cyclooxygenase 2 in vivo is antiinflammatory and nonulcerogenic. *Proc Natl Acad Sci U S A*, *91*(8), 3228-3232.
- Matsumoto, Y., Yamaguchi, T., Watanabe, S., & Yamamoto, T. (2004). Involvement of arachidonic acid cascade in working memory impairment induced by interleukin-1 beta. *Neuropharmacology*, *46*(8), 1195-1200.
- Matsumura, K., Watanabe, Y., Imai-Matsumura, K., Connolly, M., Koyama, Y., & Onoe, H. (1992). Mapping of prostaglandin E2 binding sites in rat brain using quantitative autoradiography. *Brain Res*, *581*(2), 292-298.
- Matsumura, K., Watanabe, Y., Onoe, H., Watanabe, Y., Tanaka, S., Shiraki, T., et al. (1993). Prostaglandin E2 excites neurons of the nucleus tractus solitarius by activating cation channels. *Brain Res*, *626*(1-2), 343-346.
- McGahon, B., & Lynch, M. A. (1994). A study of the synergism between metabotropic glutamate receptor activation and arachidonic acid in the rat hippocampus. *Neuroreport*, *5*(17), 2353-2357.
- McGahon, B., & Lynch, M. A. (1996). The synergism between ACPD and arachidonic acid on glutamate release in hippocampus is age-dependent. *Eur J Pharmacol*, *309*(3), 323-326.
- McNaughton, B. L. (1980). Evidence for two physiologically distinct perforant pathways to the fascia dentata. *Brain Res*, *199*(1), 1-19.
- McNaughton, B. L., Barnes, C. A., Rao, G., Baldwin, J., & Rasmussen, M. (1986). Long-term enhancement of hippocampal synaptic transmission and the acquisition of spatial information. *J Neurosci*, *6*(2), 563-571.
- Messaoudi, E., Bardsen, K., Srebro, B., & Bramham, C. R. (1998). Acute intrahippocampal infusion of BDNF induces lasting potentiation of synaptic transmission in the rat dentate gyrus. *J Neurophysiol*, *79*(1), 496-499.
- Miller, R. R., & Matzel, L. D. (2000). Memory involves far more than 'consolidation'. *Nat Rev Neurosci*, *1*(3), 214-216.
- Milner, B., Squire, L. R., & Kandel, E. R. (1998). Cognitive neuroscience and the study of memory. *Neuron*, *20*(3), 445-468.
- Min, M. Y., Asztely, F., Kokaia, M., & Kullmann, D. M. (1998). Long-term potentiation and dual-component quantal signaling in the dentate gyrus. *Proc Natl Acad Sci U S A*, *95*(8), 4702-4707.

- Minghetti, L. (2004). Cyclooxygenase-2 (COX-2) in inflammatory and degenerative brain diseases. *J Neuropathol Exp Neurol*, 63(9), 901-910.
- Molteni, R., Ying, Z., & Gomez-Pinilla, F. (2002). Differential effects of acute and chronic exercise on plasticity-related genes in the rat hippocampus revealed by microarray. *European Journal of Neuroscience*, 16, 1107-1116.
- Morimoto, K., Sato, K., Sato, S., Yamada, N., & Hayabara, T. (1998). Time-dependent changes in neurotrophic factor mRNA expression after kindling and long-term potentiation in rats. *Brain Res Bull*, 45(6), 599-605.
- Morita, I., Schindler, M., Regier, M. K., Otto, J. C., Hori, T., DeWitt, D. L., et al. (1995). Different Intracellular Locations for Prostaglandin Endoperoxide H Synthase-1 and -2. *J. Biol. Chem.*, 270(18), 10902-10908.
- Morris, R. G. M., Anderson, E., Lynch, G. S., & Baudry, M. (1986). Selective impairment of learning and blockade of long-term potentiation by an N-methyl-D-aspartate receptor antagonist AP5. *Nature*, 319, 774-776.
- Moscovitch, M., & Nadel, L. (1998). Consolidation and the hippocampal complex revisited: in defense of the multiple-trace model. *Curr Opin Neurobiol*, 8(2), 297-300.
- Moscovitch, M., Rosenbaum, R. S., Gilboa, A., Addis, D. R., Westmacott, R., Grady, C., et al. (2005). Functional neuroanatomy of remote episodic, semantic and spatial memory: a unified account based on multiple trace theory. *J Anat*, 207(1), 35-66.
- Moser, E., Moser, M. B., & Andersen, P. (1993). Spatial learning impairment parallels the magnitude of dorsal hippocampal lesions, but is hardly present following ventral lesions. *J Neurosci*, 13(9), 3916-3925.
- Moser, E. I. (1995). Learning-related changes in hippocampal field potentials. *Behav Brain Res*, 71(1-2), 11-18.
- Moser, E. I. (1996). Altered inhibition of dentate granule cells during spatial learning in an exploration task. *J Neurosci*, 16(3), 1247-1259.
- Moser, E. I., & Moser, M. B. (1999). Is learning blocked by saturation of synaptic weights in the hippocampus? *Neurosci Biobehav Rev*, 23(5), 661-672.
- Moser, M. B., & Moser, E. I. (1998). Functional differentiation in the hippocampus. *Hippocampus*, 8(6), 608-619.
- Moser, M. B., Moser, E. I., Forrest, E., Andersen, P., & Morris, R. G. (1995). Spatial learning with a minilab in the dorsal hippocampus. *Proc Natl Acad Sci U S A*, 92(21), 9697-9701.

- Mott, D. D., Xie, C. W., Wilson, W. A., Swartzwelder, H. S., & Lewis, D. V. (1993). GABAB autoreceptors mediate activity-dependent disinhibition and enhance signal transmission in the dentate gyrus. *J Neurophysiol*, *69*(3), 674-691.
- Murakami, M., & Kudo, I. (2004). Recent advances in molecular biology and physiology of the prostaglandin E2-biosynthetic pathway. *Prog Lipid Res*, *43*(1), 3-35.
- Murakami, M., Naraba, H., Tanioka, T., Semmyo, N., Nakatani, Y., Kojima, F., et al. (2000). Regulation of prostaglandin E2 biosynthesis by inducible membrane-associated prostaglandin E2 synthase that acts in concert with cyclooxygenase-2. *J Biol. Chem.*, *275*(42), 32783-32792.
- Murray, H. J., & O'Connor, J. J. (2003). A role for COX-2 and p38 mitogen activated protein kinase in long-term depression in the rat dentate gyrus in vitro. *Neuropharmacology*, *44*(3), 374-380.
- Nader, K., Schafe, G. E., & Le Doux, J. E. (2000). Fear memories require protein synthesis in the amygdala for reconsolidation after retrieval. *Nature*, *406*(6797), 722-726.
- Nagata, T., Harayama, N., Sasaki, N., Inoue, M., Tanaka, K., Toyohira, Y., et al. (2003). Mechanisms of cytosolic Ca²⁺ suppression by prostaglandin E2 receptors in rat melanotrophs. *J Neuroendocrinol*, *15*(1), 33-41.
- Nakano, J., Prancan, A. V., & Moore, S. E. (1972). Metabolism of prostaglandin E 1 in the cerebral cortex and cerebellum of the dog and rat. *Brain Res*, *39*(2), 545-548.
- Narumiya, S., Sugimoto, Y., & Ushikubi, F. (1999). Prostanoid receptors: structures, properties, and functions. *Physiol Rev*, *79*(4), 1193-1226.
- Nicol, G. D., Klingberg, D. K., & Vasko, M. R. (1992). Prostaglandin E2 increases calcium conductance and stimulates release of substance P in avian sensory neurons. *J Neurosci*, *12*(5), 1917-1927.
- Nicol, G. D., Vasko, M. R., & Evans, A. R. (1997). Prostaglandins suppress an outward potassium current in embryonic rat sensory neurons. *J Neurophysiol*, *77*(1), 167-176.
- Nicoll, R. A., & Malenka, R. C. (1995). Contrasting properties of two forms of long-term potentiation in the hippocampus. *Nature*, *377*, 115-118.
- Niederberger, E., Tegeder, I., Vetter, G., Schmidtko, A., Schmidt, H., Euchenhofer, C., et al. (2001). Celecoxib loses its anti-inflammatory efficacy at high doses through activation of NF-kappaB. *Faseb J*, *15*(9), 1622-1624.

- Nishizaki, T., Matsuoka, T., Nomura, T., Enikolopov, G., & Sumikawa, K. (1999). Arachidonic acid potentiates currents through Ca²⁺-permeable AMPA receptors by interacting with a CaMKII pathway. *Brain Res Mol Brain Res*, *67*(1), 184-189.
- Nishizaki, T., Nomura, T., Matsuoka, T., Enikolopov, G., & Sumikawa, K. (1999). Arachidonic acid induces a long-lasting facilitation of hippocampal synaptic transmission by modulating PKC activity and nicotinic ACh receptors. *Brain Res Mol Brain Res*, *69*(2), 263-272.
- Nowak, L., Bregestovski, P., Ascher, P., Herbert, A., & Prochiantz, A. (1984). Magnesium gates glutamate-activated channels in mouse central neurones. *Nature*, *307*, 462-465.
- O'Dell, T. J., Hawkins, R. D., Kandel, E. R., & Arancio, O. (1991). Test of the roles of two diffusible substances in long-term potentiation: Evidence for nitric oxide as a possible early retrograde messenger. *Proc. Natl. Acad. Sci. USA*, *88*, 11285-11289.
- O'Donnell, E., Vereker, E., & Lynch, M. A. (2000). Age-related impairment in LTP is accompanied by enhanced activity of stress-activated protein kinases: analysis of underlying mechanisms. *Eur J Neurosci*, *12*(1), 345-352.
- Otani, S., Marshall, C. J., Tate, W. P., Goddard, G. V., & Abraham, W. C. (1989). Maintenance of long-term potentiation in rat dentate gyrus requires protein synthesis but not messenger RNA synthesis immediately post-tetanzation. *Neuroscience*, *28*, 519-526.
- Palayoor, S. T., Youmell, M. Y., Calderwood, S. K., Coleman, C. N., & Price, B. D. (1999). Constitutive activation of IkappaB kinase alpha and NF-kappaB in prostate cancer cells is inhibited by ibuprofen. *Oncogene*, *18*, 7389-7394.
- Pang, P. T., Teng, H. K., Zaitsev, E., Woo, N. T., Sakata, K., Zhen, S., et al. (2004). Cleavage of proBDNF by tPA/Plasmin Is Essential for Long-Term Hippocampal Plasticity. *Science*, *306*(5695), 487-491.
- Pardue, S., Rapoport, S. I., & Bosetti, F. (2003). Co-localization of cytosolic phospholipase A2 and cyclooxygenase-2 in Rhesus monkey cerebellum. *Molecular Brain Research*, *116*(1-2), 106-114.
- Patterson, S. L., Abel, T., Deuel, T. A., Martin, K. C., Rose, J. C., & Kandel, E. R. (1996). Recombinant BDNF rescues deficits in basal synaptic transmission and hippocampal LTP in BDNF knockout mice. *Neuron*, *16*(6), 1137-1145.

- Paulson, S. K., Zhang, J. Y., Breau, A. P., Hribar, J. D., Liu, N. W., Jessen, S. M., et al. (2000). Pharmacokinetics, tissue distribution, metabolism, and excretion of celecoxib in rats. *Drug Metab Dispos*, 28(5), 514-521.
- Penfield, W., & Milner, B. (1958). Memory deficit produced by bilateral lesions in the hippocampal zone. *AMA Arch Neurol Psychiatry*, 79(5), 475-497.
- Piomelli, D., Shapiro, E., Feinmark, S. J., & Schwartz, J. H. (1987). Metabolites of arachidonic acid in the nervous system of *Aplysia*: possible mediators of synaptic modulation. *J Neurosci*, 7(11), 3675-3686.
- Platenik, J., Kuramoto, N., & Yoneda, Y. (2000). Molecular mechanisms associated with long-term consolidation of the NMDA signals. *Life Sciences*, 67(4), 335-364.
- Pozzi, A., Yan, X., Macias-Perez, I., Wei, S., Hata, A. N., Breyer, R. M., et al. (2004). Colon carcinoma cell growth is associated with prostaglandin E2/EP4 receptor-evoked ERK activation. *J Biol Chem*, 279(28), 29797-29804.
- Quan, N., Whiteside, M., & Herkenham, M. (1998). Cyclooxygenase-2 expression in rat brain after peripheral injection of lipopolysaccharide. *Brain Research*, 802, 189-197.
- Rall, J. M., Mach, S. A., & Dash, P. K. (2003). Intrahippocampal infusion of a cyclooxygenase-2 inhibitor attenuates memory acquisition in rats. *Brain Research*, 968(2), 273-276.
- Robertson, L. M., Kerppola, T. K., Vendrell, M., Luk, D., Smeyne, R. J., Bocchiaro, C., et al. (1995). Regulation of c-fos expression in transgenic mice requires multiple interdependent transcription control elements. *Neuron*, 14(2), 241-252.
- Rodriguez de Turco, E. B., Tang, W., Topham, M. K., Sakane, F., Marcheselli, V. L., Chen, C., et al. (2001). Diacylglycerol kinase epsilon regulates seizure susceptibility and long-term potentiation through arachidonoyl- inositol lipid signaling. *Proc Natl Acad Sci U S A*, 98(8), 4740-4745.
- Rongo, C. (2002). A fresh look at the role of CaMKII in hippocampal synaptic plasticity and memory. *Bioessays*, 24(3), 223-233.
- Sales, K. J., & Jabbour, H. N. (2003). Cyclooxygenase enzymes and prostaglandins in reproductive tract physiology and pathology. *Prostaglandins Other Lipid Mediat*, 71(3-4), 97-117.
- Sanes, J. R., & Lichtman, J. W. (1999). Can molecules explain long-term potentiation? *Nat Neurosci*, 2(7), 597-604.

- Sano, K., Nanba, H., Tabuchi, A., Tsuchiya, T., & Tsuda, M. (1996). BDNF gene can be activated by Ca²⁺ signals without involvement of de novo AP-1 synthesis. *Biochem Biophys Res Commun*, 229(3), 788-793.
- Sara, S. J. (2000). Retrieval and reconsolidation: toward a neurobiology of remembering. *Learn Mem*, 7(2), 73-84.
- Schiavi, S. C., Wellington, C. L., Shyu, A. B., Chen, C. Y., Greenberg, M. E., & Belasco, J. G. (1994). Multiple elements in the c-fos protein-coding region facilitate mRNA deadenylation and decay by a mechanism coupled to translation. *J Biol Chem*, 269(5), 3441-3448.
- Schuttle, J., Viallet, J., Nau, M., Segal, S., Fedorko, J., & Minna, J. (1989). jun-B inhibits and c-fos stimulates the transforming and trans-activating activities of c-jun. *Cell*, 59, 987-997.
- Scoville, W. B., & Milner, B. (1957). Loss of recent memory after bilateral hippocampal lesions. *J Neurochem*, 20(1), 11-21.
- Segal, M. (2005). Dendritic spines and long-term plasticity. *Nat Rev Neurosci*, 6(4), 277-284.
- Sekiyama, N., Mizuta, S., Hori, A., & Kobayashi, S. (1995). Prostaglandin E2 facilitates excitatory synaptic transmission in the nucleus tractus solitarius of rats. *Neurosci Lett*, 188(2), 101-104.
- Shaw, K. N. (2001). *Molecular and cellular mechanisms underlying signal transduction in the hippocampal formation: the role of brain-derived neurotrophic factor*. Unpublished PhD, University of Dublin, Trinity College, Dublin.
- Shaw, K. N., Commins, S., & O'Mara, S. M. (2003). Deficits in spatial learning and synaptic plasticity induced by the rapid and competitive broad-spectrum cyclooxygenase inhibitor ibuprofen are reversed by increasing endogenous brain-derived neurotrophic factor. *17*(11), p. 2438.
- Sheng, M., & Greenberg, M. E. (1990). The regulation and function of c-fos and other immediate early genes in the nervous system. *Neuron*, 4, 477-485.
- Shibuya, I., Setiadji, S. V., Ibrahim, N., Harayama, N., Maruyama, T., Ueta, Y., et al. (2002). Involvement of postsynaptic EP4 and presynaptic EP3 receptors in actions of prostaglandin E2 in rat supraoptic neurones. *J Neuroendocrinol*, 14(1), 64-72.
- Shimamura, A. P. (2002). Relational Binding Theory and the Role of Consolidation in Memory Retrieval. In L. R. a. S. Squire, D.L. (Ed.), *Neuropsychology of Memory* (3rd ed., pp. 61-72). New York: The Guilford Press.

- Shimizu, T., & Wolfe, L. S. (1990). Arachidonic acid cascade and signal transduction. *J Neurochem*, *55*(1), 1-15.
- Shin, M. C., Jang, M. H., Chang, H. K., Kim, Y. J., Kim, E. H., & Kim, C. J. (2003). Modulation of cyclooxygenase-2 on glycine- and glutamate-induced ion currents in rat periaqueductal gray neurons. *Brain Res Bull*, *59*(4), 251-256.
- Silva, A. J., Paylor, R., Wehner, J. M., & Tonegawa, S. (1992). Impaired spatial learning in alpha-calcium-calmodulin kinase II mutant mice. *Science*, *257*, 206-211.
- Silva, A. J., Stevens, C. F., Tonegawa, S., & Wang, Y. (1992). Deficient hippocampal long-term potentiation in alpha-calcium-calmodulin kinase II mutant mice. *Science*, *257*, 201-206.
- Smith, C. J., Zhang, Y., Koboldt, C. M., Muhammad, J., Zweifel, B. S., Shaffer, A., et al. (1998). Pharmacological analysis of cyclooxygenase-1 in inflammation. *PNAS*, *95*(22), 13313-13318.
- Smith, W. L., DeWitt, D. L., & Garavito, R. M. (2000). Cyclooxygenase: structural, cellular, and molecular biology. *Annual Review of Biochemistry*, *69*, 145-182.
- Smith, W. L., Garavito, R. M., & DeWitt, D. L. (1996). Prostaglandin Endoperoxide H Synthases (Cyclooxygenases)-1 and -2. *J. Biol. Chem.*, *271*(52), 33157-33160.
- Squire, L. R. (1992). Memory and the hippocampus: a synthesis from findings with rats, monkeys, and humans. *Psychol Rev*, *99*(2), 195-231.
- Squire, L. R., & Alvarez, P. (1995). Retrograde amnesia and memory consolidation: a neurobiological perspective. *Curr Opin Neurobiol*, *5*(2), 169-177.
- Squire, L. R., Stark, C. E., & Clark, R. E. (2004). The medial temporal lobe. *Annu Rev Neurosci*, *27*, 279-306.
- Stanton, P. K., & Sarvey, J. M. (1984). Blockade of long-term potentiation in rat hippocampal CA1 region by inhibitors of protein synthesis. *Journal of Neuroscience*, *4*, 3080-3088.
- Steffenach, H. A., Witter, M., Moser, M. B., & Moser, E. I. (2005). Spatial memory in the rat requires the dorsolateral band of the entorhinal cortex. *Neuron*, *45*(2), 301-313.
- Swinney, D. C., Mak, A. Y., Barnett, J., & Ramesha, C. S. (1997). Differential Allosteric Regulation of Prostaglandin H Synthase 1 and 2 by Arachidonic Acid. *J. Biol. Chem.*, *272*(19), 12393-12398.
- Takadera, T., Shiraishi, Y., & Ohyashiki, T. (2004). Prostaglandin E2 induced caspase-dependent apoptosis possibly through activation of EP2 receptors in cultured hippocampal neurons. *Neurochem Int*, *45*(5), 713-719.

- Teather, L. A., Packard, M. G., & Bazan, N. G. (2001). Differential Interaction of Platelet-Activating Factor and NMDA Receptor Function in Hippocampal and Dorsal Striatal Memory Processes. *Neurobiology of Learning and Memory*, 75(3), 310-324.
- Teather, L. A., Packard, M. G., & Bazan, N. G. (2002). Post-Training Cyclooxygenase-2 (COX-2) Inhibition Impairs Memory Consolidation. *Learn. Mem.*, 9(1), 41-47.
- Tegeder, I., Pfeilschifter, J., & Geisslinger, G. (2001). Cyclooxygenase-independent actions of cyclooxygenase inhibitors. *FASEB J.*, 15(12), 2057-2072.
- Teng, X. W., Abu-Mellal, A. K., & Davies, N. M. (2003). Formulation dependent pharmacokinetics, bioavailability and renal toxicity of a selective cyclooxygenase-1 inhibitor SC-560 in the rat. *J Pharm Pharm Sci*, 6(2), 205-210.
- Thomas, G. M., & Huganir, R. L. (2004). MAPK cascade signalling and synaptic plasticity. *Nat Rev Neurosci*, 5(3), 173-183.
- Thomas, K. L., Laroche, S., Errington, M. L., Bliss, T. V., & Hunt, S. P. (1994). Spatial and temporal changes in signal transduction pathways during LTP. *Neuron*, 13(3), 737-745.
- Towbin, H., Staehelin, T., & Gordon, J. (1979). Electrophoretic transfer of proteins from polyacrylamide gels to nitrocellulose sheets: procedure and some applications. *Proc Natl Acad Sci U S A*, 76(9), 4350-4354.
- Toyomoto, M., Ohta, M., Okumura, K., Yano, H., Matsumoto, K., Inoue, S., et al. (2004). Prostaglandins are powerful inducers of NGF and BDNF production in mouse astrocyte cultures. *FEBS Letters*, 562(1-3), 211-215.
- Tuff, L. P., Racine, R. J., & Adamec, R. (1983). The effects of kindling on GABA-mediated inhibition in the dentate gyrus of the rat. I. Paired-pulse depression. *Brain Res*, 277(1), 79-90.
- Uchida, K., Kumihashi, K., Kurosawa, S., Kobayashi, T., Itoi, K., & Machida, T. (2002). Stimulatory effects of prostaglandin E2 on neurogenesis in the dentate gyrus of the adult rat. *Zoolog Sci*, 19(11), 1211-1216.
- Vane, J. R. (1971). Inhibition of prostaglandin synthesis as a mechanism of action for aspirin-like drugs. *Nat New Biol*, 231(25), 232-235.
- Vane, J. R., Bakhle, Y. S., & Botting, R. M. (1998). Cyclooxygenase 1 and 2. *Annual Review of Pharmacology and Toxicology*, 38(1), 97-120.
- Vasquez, E., Bar, K. J., Ebersberger, A., Klein, B., Vanegas, H., & Schaible, H. G. (2001). Spinal Prostaglandins Are Involved in the Development But Not the Maintenance

- of Inflammation-Induced Spinal Hyperexcitability. *J. Neurosci.*, 21(22), 9001-9008.
- Vicario-Abejon, C., Owens, D., McKay, R., & Segal, M. (2002). Role of neurotrophins in central synapse formation and stabilization. *Nat Rev Neurosci*, 3(12), 965-974.
- Volterra, A., Trotti, D., Cassutti, P., Tromba, C., Galimberti, R., Lecchi, P., et al. (1992). A role for the arachidonic acid cascade in fast synaptic modulation: ion channels and transmitter uptake systems as target proteins. *Adv Exp Med Biol*, 318, 147-158.
- Warner, T. D., Giuliano, F., Vojnovic, I., Bukasa, A., Mitchell, J. A., & Vane, J. R. (1999). Nonsteroid drug selectivities for cyclo-oxygenase-1 rather than cyclo-oxygenase-2 are associated with human gastrointestinal toxicity: a full in vitro analysis. *Proc Natl Acad Sci U S A*, 96(13), 7563-7568.
- Williams, J. H., & Bliss, T. V. P. (1988). Induction but not maintenance of calcium-induced long-term potentiation in dentate gyrus and area CA1 of the hippocampal slice is blocked by nordihydroguaiaretic acid. *Neuroscience Letters*, 88, 81-85.
- Williams, J. H., & Bliss, T. V. P. (1989). An in vitro study of the effect of lipoxygenase and cyclo-oxygenase inhibitors of arachidonic acid on the induction and maintenance of long-term potentiation in the hippocampus. *Neuroscience Letters*, 107(1-3), 301-306.
- Williams, J. H., Errington, M. L., Lynch, M. A., & Bliss, T. V. (1989). Arachidonic acid induces a long-term activity-dependent enhancement of synaptic transmission in the hippocampus. *Nature*, 341(6244), 739-742.
- Xia, Z., Dudek, H., Miranti, C. K., & Greenberg, M. E. (1996). Calcium influx via the NMDA receptor induces immediate early gene transcription by a MAP kinase/ERK-dependent mechanism. *J Neurosci*, 16(17), 5425-5436.
- Xie, W., Chipman, J. G., Robertson, D. L., Erikson, R. L., & Simmons, D. L. (1991). Expression of a Mitogen-Responsive Gene Encoding Prostaglandin Synthase is Regulated by mRNA Splicing. *PNAS*, 88(7), 2692-2696.
- Xu, L., Anwyl, R., & Rowan, M. J. (1998). Spatial exploration induces a persistent reversal of long-term potentiation in rat hippocampus. *Nature*, 394, 891-894.
- Yamagata, K., Andreasson, K. I., Kaufmann, W. E., Barnes, C. A., & Worley, P. F. (1993). Expression of a mitogen-inducible cyclooxygenase in brain neurons: regulation by synaptic activity and glucocorticoids. *Neuron*, 11(2), 371-386.
- Yermakova, A. V., Rollins, J., Callahan, L. M., Rogers, J., & O'Banion, M. K. (1999). Cyclooxygenase-1 in human Alzheimer and control brain: quantitative analysis of

- expression by microglia and CA3 hippocampal neurons. *J Neuropathol Exp Neurol*, 58(11), 1135-1146.
- Ying, S. W., Futter, M., Rosenblum, K., Webber, M. J., Hunt, S. P., Bliss, T. V., et al. (2002). Brain-derived neurotrophic factor induces long-term potentiation in intact adult hippocampus: requirement for ERK activation coupled to CREB and upregulation of Arc synthesis. *J Neurosci*, 22(5), 1532-1540.
- Zador, A., Koch, C., & Brown, T. H. (1990). Biophysical model of a Hebbian synapse. *Proceedings of the National Academy of Science, U.S.A.*, 87(16), 6718-6722.
- Zafra, F., Lindholm, D., Castren, E., Hartikka, J., & Thoenen, H. (1992). Regulation of brain-derived neurotrophic factor and nerve growth factor mRNA in primary cultures of hippocampal neurons and astrocytes. *J Neurosci*, 12(12), 4793-4799.
- Zerangue, N., Arriza, J. L., Amara, S. G., & Kavanaugh, M. P. (1995). Differential Modulation of Human Glutamate Transporter Subtypes by Arachidonic Acid. *J Biol. Chem.*, 270(12), 6433-6435.
- Zhang, J., Goorha, S., Raghov, R., & Ballou, L. R. (2002). The tissue-specific, compensatory expression of cyclooxygenase-1 and -2 in transgenic mice. *Prostaglandins and other lipid mediators*, 67, 121-135.
- Zhang, J., & Rivest, S. (1999). Distribution, regulation and colocalization of the genes encoding the EP2- and EP4-PGE2 receptors in the rat brain and neuronal responses to systemic inflammation. *Eur J Neurosci*, 11(8), 2651-2668.
- Zhu, P., Genc, A., Zhang, X., Zhang, J., Bazan, N. G., & Chen, C. (2005). Heterogeneous expression and regulation of hippocampal prostaglandin E2 receptors. *J Neurosci Res*, 81(6), 817-826.
- Zola-Morgan, S., Squire, L. R., D.G., A., & Suzuki, W. A. (1989). Lesions of the perirhinal and parahippocampal cortex that spare the amygdala and hippocampal formation produce severe memory impairment. *Journal of Neuroscience*, 9, 4355-4370.
- Zola S.M., S. L. R. (2000). The Medial Temporal Lobe and th Hippocampus. In C. Tulving E., F.I.M. (Ed.), *The Oxford Handbook of Memory* (pp. 485-450).
- Zucker, R. S. (1999). Calcium- and activity-dependent synaptic plasticity. *Curr Opin Neurobiol*, 9(3), 305-313.
- Zucker, R. S., & Regehr, W. G. (2002). Short-term synaptic plasticity. *Annu Rev Physiol*, 64, 355-405.

Chapter 6 Appendix 1

	Ri	Boltzmann	Upper CI	Lower CI
1	0	= $(R_{max}/(1+EXP((Ih-A2)/Slope)))$	=C2+CI	=C2-CI
1.30102	0.01302	= $(R_{max}/(1+EXP((Ih-A3)/Slope)))$	=C3+CI	=C3-CI
1.47712	0.03255	= $(R_{max}/(1+EXP((Ih-A4)/Slope)))$	=C4+CI	=C4-CI
1.60205	0.17903	= $(R_{max}/(1+EXP((Ih-A5)/Slope)))$	=C5+CI	=C5-CI
1.69897	0.20833	= $(R_{max}/(1+EXP((Ih-A6)/Slope)))$	=C6+CI	=C6-CI
1.77815	0.25146	= $(R_{max}/(1+EXP((Ih-A7)/Slope)))$	=C7+CI	=C7-CI
1.84509	0.39062	= $(R_{max}/(1+EXP((Ih-A8)/Slope)))$	=C8+CI	=C8-CI
1.90308	0.36133	= $(R_{max}/(1+EXP((Ih-A9)/Slope)))$	=C9+CI	=C9-CI
2	0.45572	= $(R_{max}/(1+EXP((Ih-A10)/Slope)))$	=C10+CI	=C10-CI
2.07918	0.73568	= $(R_{max}/(1+EXP((Ih-A11)/Slope)))$	=C11+CI	=C11-CI
2.14612	0.68359	= $(R_{max}/(1+EXP((Ih-A12)/Slope)))$	=C12+CI	=C12-CI
2.20411	0.87239	= $(R_{max}/(1+EXP((Ih-A13)/Slope)))$	=C13+CI	=C13-CI
2.25527	1.02213	= $(R_{max}/(1+EXP((Ih-A14)/Slope)))$	=C14+CI	=C14-CI
2.30102	1.32812	= $(R_{max}/(1+EXP((Ih-A15)/Slope)))$	=C15+CI	=C15-CI
2.39794	1.55599	= $(R_{max}/(1+EXP((Ih-A16)/Slope)))$	=C16+CI	=C16-CI
2.47712	1.81152	= $(R_{max}/(1+EXP((Ih-A17)/Slope)))$	=C17+CI	=C17-CI
2.60205	1.98567	= $(R_{max}/(1+EXP((Ih-A18)/Slope)))$	=C18+CI	=C18-CI
2.69897	2.44791	= $(R_{max}/(1+EXP((Ih-A19)/Slope)))$	=C19+CI	=C19-CI
2.77815	2.50651	= $(R_{max}/(1+EXP((Ih-A20)/Slope)))$	=C20+CI	=C20-CI
2.84509	2.72460	= $(R_{max}/(1+EXP((Ih-A21)/Slope)))$	=C21+CI	=C21-CI
2.90308	2.77343	= $(R_{max}/(1+EXP((Ih-A22)/Slope)))$	=C22+CI	=C22-CI
2.95424	3.1543	= $(R_{max}/(1+EXP((Ih-A23)/Slope)))$	=C23+CI	=C23-CI
3	2.95573	= $(R_{max}/(1+EXP((Ih-A24)/Slope)))$	=C24+CI	=C24-CI
3.17609	3.51562	= $(R_{max}/(1+EXP((Ih-A25)/Slope)))$	=C25+CI	=C25-CI
3.30102	3.54167	= $(R_{max}/(1+EXP((Ih-A26)/Slope)))$	=C26+CI	=C26-CI
3.39794	3.71093	= $(R_{max}/(1+EXP((Ih-A27)/Slope)))$	=C27+CI	=C27-CI

Rmax	3.90736953092135
Ih	2.56736631958057
Slope	0.31320924846365
Mean of Y	=AVERAGE(B2:B32)
df	=COUNT(B2:B32)-COUNT(G1:G3)
SE of Y	=SQRT(SUM((B2:B32-C2:C32)^2)/df) =1-SUM((B2:B32-C2:C32)^2)/SUM((B2:B32-Mean_of_y)^2)
R^2	
Critical t	=TINV(0.05,df)
CI	=Critical_t*SE_of_Y

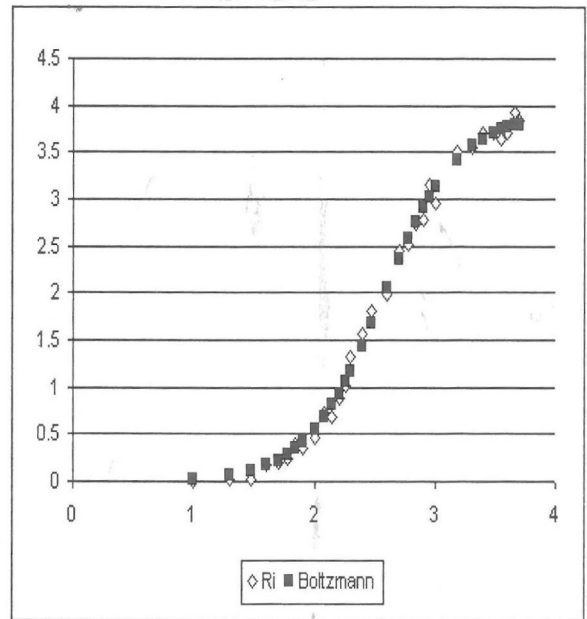


Figure 1 Example of spreadsheet for the fitting of a Boltzmann equation to an input/output curve and generation of parameters for statistical analysis. The above table illustrates the spreadsheet template with the formulas used in the fitting protocol are displayed. R_{max} , I_h and slope are generated by iteration by the solver function under the Tools menu.

Figure 1 shows the spreadsheet used to fit the curve, where the labels are as follows:

I	Log(current) i.e. independent variable
Ri	Response with respect to current (I) i.e. dependent variable
Boltzmann	Equation describing the Boltzmann function
Upper/Lower CI	Upper and lower confidence limits (95%) of fit
R_{max}	The maximal response at which the curve saturates
Slope	The rate of change of response with respect to current.
Mean of y	Mean of all the responses
df	Degrees of freedom = # responses - # parameters
SE of y	Standard error of the mean of the responses

R^2 Index of goodness of fit.

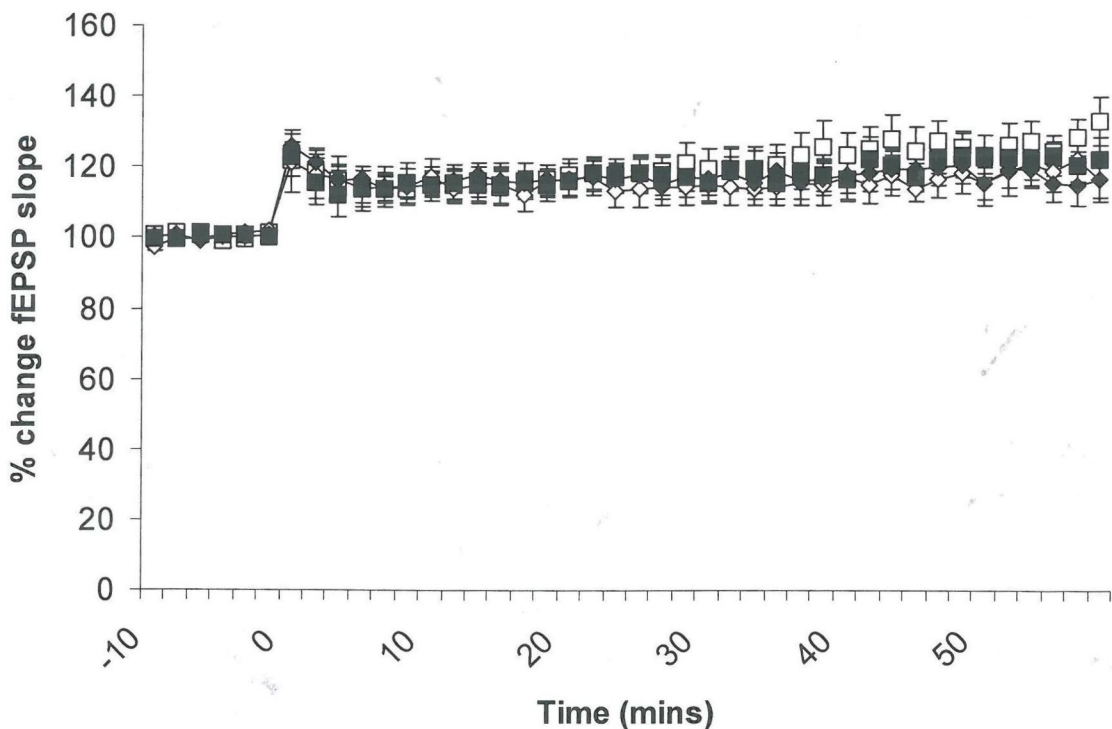
Critical t t value corresponding to $\alpha=0.05$

The SE of the Y, R^2 and CI are automatically calculated.

Appendix 2

An attempt was made to recreate the experiment by Shaw et al (Shaw et al., 2003), whereby the block of LTP induced by non-selective COX inhibition with ibuprofen, was reverted by five days prior exercise. However, in this version a selective COX-2 antagonist was used. This attempt failed for a number of reasons:

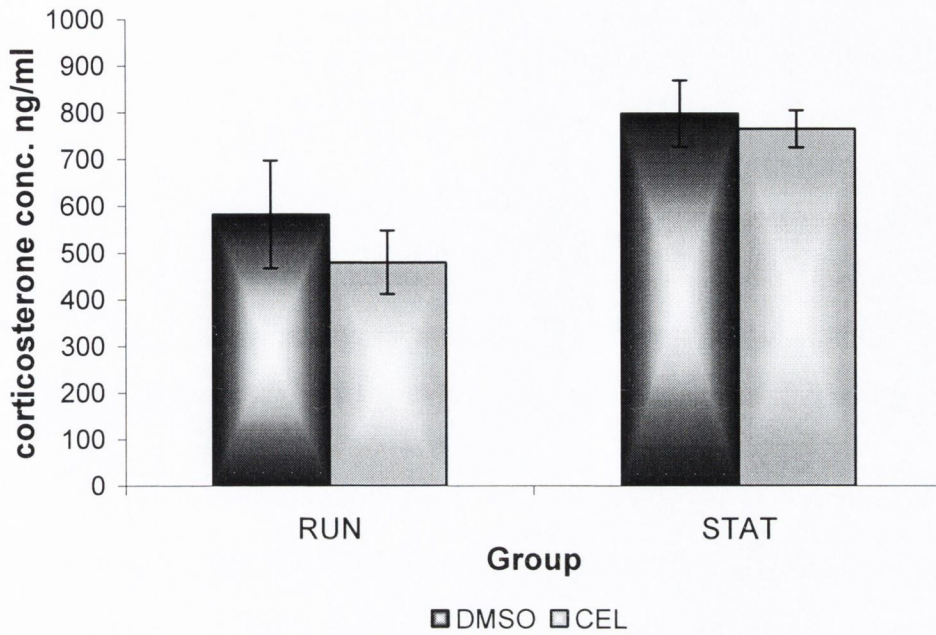
- 1) As discussed in chapter III the block of LTP by the COX-2 inhibitor celecoxib is dose dependent. Unwittingly, a change in source of the celecoxib in this experiment, resulted in a 28mg/kg dose of the drug being used, which has now been shown to be insufficient to block LTP induction successfully. Note in the figure below that neither 28mg/kg celecoxib resulted in LTP inhibition nor running result in LTP facilitation.



□ RUN CXB ◇ RUN DMSO ■ SED CXB ◆ SED DMSO

- 2) Plasma corticosterone levels measured from trunk blood revealed highly elevated levels in the control condition for running, whereby animals were placed in the running wheels but they were held in the stationary position. Although the animals could see each other through Perspex, and were acclimatised to the wheel before

the experiment was commenced, the elevation in the corticosterone levels indicate increased stress levels.



- 3) Measurement of the BDNF levels in all animals, celecoxib sedentary and exercised, vehicle-control sedentary and exercised, after electrophysiological recordings revealed no significant difference.

